INSTITUTES FOR ENVIRONMENTAL RESEARCH
Institute for Telecommunication Sciences and Aeronomy
Boulder, Colorado
July 1967

Conjugate Point Symposium

June 13-16, 1967 Boulder, Colorado

Arranged by:

HIGH ALTITUDE OBSERVATORY of NCAR &

INSTITUTE for TELECOMMUNICATION

SCIENCES and AERONOMY of ESSA

Volume 2
Session III

Technical Memorandum IERTM-ITSA 72

U.S. DEPARTMENT OF COMMERCE / ENVIRONMENTAL SCIENCE SERVICES ADMINISTRATION

U.S. DEPARTMENT OF COMMERCE
ENVIRONMENTAL SCIENCE SERVICES ADMINISTRATION
INSTITUTES FOR ENVIRONMENTAL RESEARCH

Institutes for Environmental Research Technical Memorandum-ITSA 72

CONJUGATE POINT SYMPOSIUM
JUNE 13-16, 1967
BOULDER, COLORADO

ARRANGED BY
High Altitude Observatory of NCAR
and
Institute for Telecommunication Sciences and Aeronomy

INSTITUTE FOR TELECOMMUNICATION SCIENCES AND AERONOMY
TECHNICAL MEMORANDUM NO. 72

BOULDER, COLORADO
JULY 1967

Foreword

The Conjugate Point Symposium was held at Boulder, Colorado, during June 13-16, 1967. The symposium concerned upper atmospheric phenomena whose manifestations uniquely identify pairs of northern and southern hemisphere locations at the earth's surface which are connected by the earth's field lines. The papers presented at the meeting were divided among four sessions: Luminosity, Ionosphere and Particle Precipitation, EM and HM Guided Waves, and Geomagnetic Field and Magnetosphere.

This Technical Memorandum is a reproduction of the papers submitted by the speakers. In a few cases only the abstract is available. The pages are numbered for the session and paper order with some changes from the original order to improve continuity. The reproduction in this Memorandum does not constitute formal publication; it is done as a service to the attendees and the symposium sponsors. Primary responsibility for the technical content of this document must rest, of course, with the individual authors and their organizations. Readers should refer to these papers as presentations to the Conjugate Point Symposium.

W. H. Campbell

S. Matsushita

It contains the papers given at the third session.

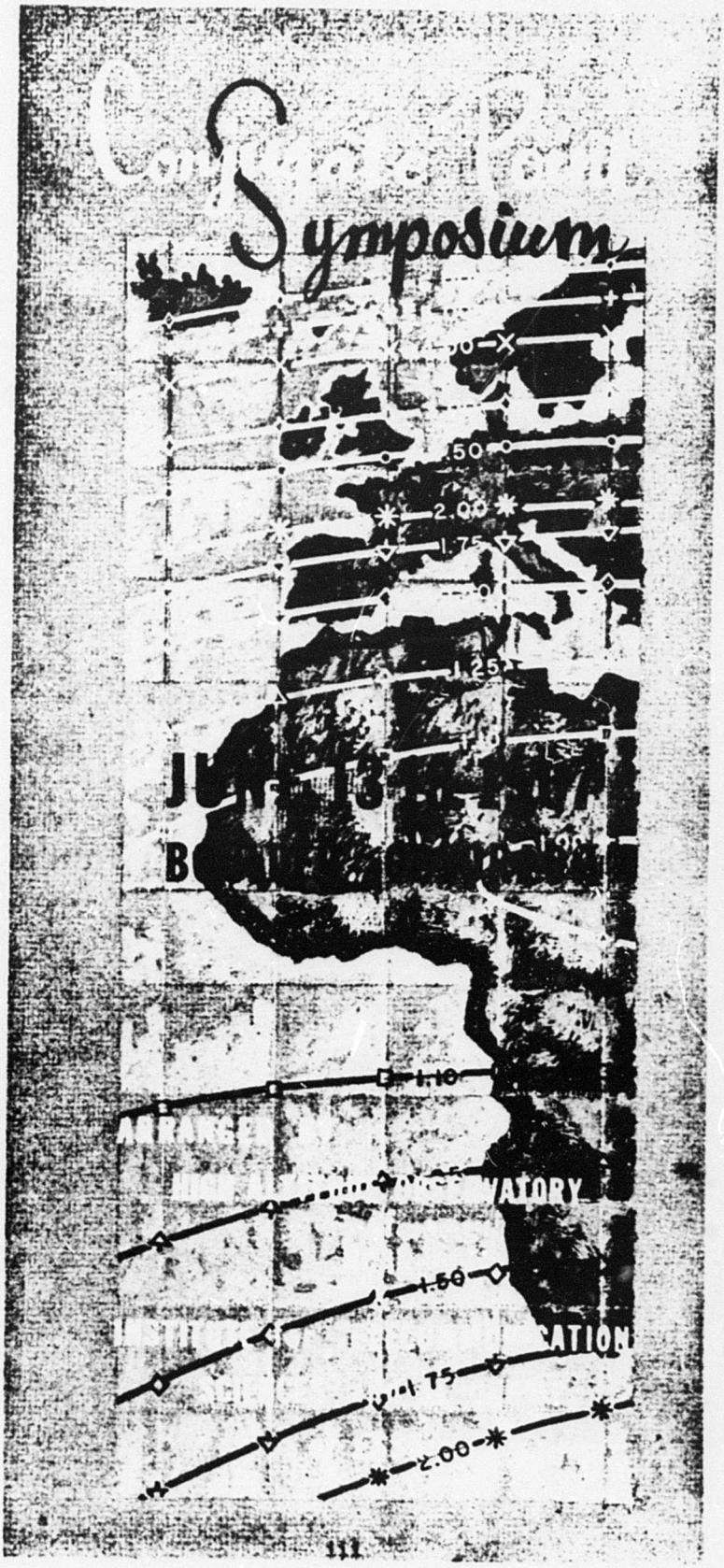
Symposium
.50
2.00
1.75
1.25
1.10
1.50
1.75
2.00

SPONSORING ORGANIZATIONS

INTERNATIONAL ASSOCIATION OF GEOMAGNETISM AND AERONOMY

AMERICAN GEOPHYSICAL UNION

AIR FORCE CAMBRIDGE RESEARCH LABORATORIES

OFFICE OF NAVAL RESEARCH

REPRESENTATIVES OF SUPPORTING ORGANIZATIONS

ITSA C. G. LITTLE

NCAR W. O. ROBERTS

HAO J. W. FIROR

AGU W. E. SMITH

IAGA L. ALLDREDGE

ONR A. SHOSTAK

AFCRL E. J. CHERNOSKY

TECHNICAL PROGRAM COMMITTEE

W. H. Campbell	ESSA--Institute for Telecommunication Sciences and Aeronomy
S. Matsushita	NCAR--High Altitude Observatory

LOCAL ARRANGEMENTS COMMITTEE

K. Armstrong	NBS--Technical Information Office
A. T. Scott	National Center for Atmospheric Research
R. L. Haynes	University Housing Office

SECRETARY

S. J. Guiraud	Institute for Telecommunication Sciences and Aeronomy

TREASURER

J M. Quinn	Institute for Telecommunication Sciences and Aeronomy

ADVISORY COMMITTEE

L. R. Alldredge	R. W. Knecht	J. G. Roederer
D. K. Bailey	K.-I. Maeda	S. Ruttenberg
E. J. Chernosky	K. Mather	A. H. Shapley
A. J. Dessler	M. G. Morgan	A. Shostak
J. W. Firor	T. Nagata	S. Silver
R. R. Heer, Jr.	T. Obayashi	F. Singer
R. A. Helliwell	M. A. Pomerantz	E. K. Smith
J. P. Heppner	G. C. Reid	W. E. Smith
J. A. Jacobs	F. E. Roach	M. Sugiura
A. G. Jean		E. H. Vestine

Y. Kato, Special Representative for Nippon Gakujutus Kaigi

Contents

I. LUMINOSITY — F. E. Roach, Chairman

Paper No.		
1.	Conjugate Effects in Aurora	M. H. Rees
2.	Photometric Observations of Auroras	G. J. Romick
3.	Conjugate Optical Measurements: Total Night Hours Possible for One Year	E. Marovich
4.	Characteristics of Auroral Brightness Flucutations	G. G. Shepherd
5.	The Conjugacy of Optical Auroras	A. E. Belon and K. B. Mather
6.	Photometric Observations at Auroral Zone Conjugate Points	M. D. Watson A. J. Spitz
7.	Photometry of [OI] λ5577 and λ6300 on a Six-Minute Time Scale Within the Southern Auroral Zone	M. A. Gordon
8.	Conjugate Observation of Lyman Alpha Auroras from an Orbiting Satellite	M. A. Clark and P. H. Metzger
9.	Twilight Helium 10,830 Å Emission and Conjugate Point Photoelectrons	B. A. Tinsley
10.	Midlatitude Auroral Spectra	K. C. Clark and R. J. Hoch
11.	Temperature Profile of the Daytime Atmosphere from Rocket Spectral Data	M. Ahmed

II. IONOSPHERE AND PARTICLE PRECIPITATION — R. W. Knecht and G. C. Reid, Chairmen

1.	Most Recent Studies of Low Latitude Effects Due to Conjugate Location Heating	H. C. Carlson
2.	Solar Cycle Variation of Conjugate Photoelectron Flux Onset Timing Deduced from 6300 Å and T_e Observations	H. C. Carlson and G. M. Weill

3.	Presunrise Heating of the Ionosphere at Arecibo due to Conjugate Point Photoelectrons	M. W. Kwei and J. S. Nisbet
4.	Photoelectron Escape from the Ionosphere and Fluxes in the Conjugate Hemisphere	J. S. Nisbet
5.	A Possible Evidence of Ionospheric Heating by Photoelectrons from the Sunlit Magnetic Conjugate Ionosphere	L. Liszka
6.	Ionospheric F2 Behavior at Conjugate Places in Low Latitutes	S. Matsushita
7.	Conjugate F - Region Enhancement Related to the South Atlantic Magnetic Anomaly	C. P. Pike, J. R. Herman and G. J. Gassmann
8.	A Suggested Conjugate Point Dependence for Intense Temperate Latitude Sporadic E	E. K. Smith
9.	A Statistical Study of D- and E- Region Effects at Conjugate Stations in High Latitudes	V. Agy
10.	Scintillation Observations at Medium Latitude Geomagnetically Conjugate Stations	K. C. Yeh, D. Simonich, J. Mawdsley and G. F. Preddey
11.	Review of Conjugate-Point Observations of Ionospheric Disturbances	G. C. Reid
12.	The "Winter Anomaly" in the Midlatitude D-Region, A Conjugate Phenomenon?	B. N. Maehlum
13.	Average Behaviour of High-Latitude Disturbance Phenomena	N. Brice
14.	The Correlation of Auroral Radio Absorption between Conjugate Points	J. K. Hargreaves and W. L. Ecklund
15.	Conjugate and Spatial Properties of Auroral Absorption: Preliminary Results from Space Riometers at Great Whale River and Byrd	J. K. Hargreaves

16. The Time Distribution of Small Absorption Events at High Latitude Conjugate Locations — P. R. Satterblom, A. J. Masley and R. E. Santina

17. Balloon Observations of Electron Precipitation in Conjugate Regions of the Auroral Zone — R. R. Brown

18. Non-Conjugate Aspects of Recent Polar Cap Absorption Events — H. H. Sauer

19. Some Quantitative Aspects of Particle Precipitation Events Observed by Ionospheric Forward Scattering — D. K. Bailey

20. Cosmic Ray Intensity Variations in the Polar Regions — M. A. Pomerantz

III. EM AND HM GUIDED WAVES — R. A. Helliwell and N. M. Brice, Chairmen

1. Rapid Geomagnetic Field Variations Observed at Conjugate Locations — W. H. Campbell

2. Pi Events — J. A. Jacobs

3. Conjugate Observations of the pi 1 Micropulsation Event of May 25, 1964 — R. G. Green

4. Relation of Correlated Magnetic Micropulsations and Electron Precipitation to the Auroral Substorm — R. L. McPherron, G. K. Parks and F. Coroniti

5. Polarization Analysis of Natural and Artificially Induced Geomagnetic Micropulsations — R. A. Fowler and B. J. Kotick

6. Frequency Analysis of the Geomagnetic Micropulsations Observed at the Magnetic Equator — Y. Kato

7. Simultaneity of Pc 3 Micropulsations at Conjugate Points — A. C. Fraser-Smith

8. The Behavior of Magnetospheric Proton Densities Derived from Pearl Dispersion Measurements — H. B. Liemohn, J. F. Kenney and H. B. Knaflich

9. Recent Investigation on Hydromagnetic Emissions — T. Watanabe

10. Diffusion Processes Influenced by Conjugate-Point Wave Phenomena — J. M. Cornwall

11. Measurement and Interpretation of ULF and VLF Power Spectra — J. F. Kenney, H. B. Knaflich and H. B. Liemohn

12. EM and HM Guided Waves in the Earth's Atmosphere — N. Brice

13. Selected Problems in Wave-Particle Interaction, from Conjugate Point Observations — R. M. Gallet

14. Polar Emissions — L. Owren

15. Recent Research on the Magnetospheric Plasmapause — D. L. Carpenter

16. Whistler Propagation in Magnetospheric Ducts — R. L. Smith and J. J. Angerami

17. Waveguidance in the Magnetosphere Along Field-Aligned Irregularities — N. Gothard

18. Conjugate HF Ducting — J. A. Thomas

19. Medium-Frequency Conjugate Echoes Observed on Topside-Sounder Data — D. B. Muldrew

20. Propagation Characteristics of the Equatorial Ionosphere as Measured Between Magnetically Conjugate Points at VHF — E. D. Bowen

IV. GEOMAGNETIC FIELDS AND THE MAGNETOSPHERE — C. P. Sonett, Chairman

1. General Remarks on Conjugate Point Phenomena — J. G. Roederer

2. Calculations of High-Latitude Conjugate Points in a Model Magnetosphere — G. D. Mead

3. Geomagnetic Euler Potentials — D. Stern

4. The Role of the Main Geomagnetic Field in Locating Conjugate Points — J. C. Cain

5. World Maps of Conjugate Coordinates and L Contours — W. H. Campbell and S. Matsushita

6. Magnetosphere Inflation Energy for Four Storms in 1965 — L. J. Cahill

7.	Some Problems on Magnetospheric Tail	T. Obayashi
8.	Irrotational Current Systems with Conjugate Source-Sink Pairs	R. N. DeWitt
9.	Polar Storms and Ring Currents	S.-I. Akasofu
10.	Polar Magnetic Substorms in the Conjugate Areas	C.-I. Meng and S.-I. Akasofu
11.	Transverse Geomagnetic Disturbances in the Auroral Oval	A. J. Zmuda
12.	Morphology of Elementary Magnetospheric Substorms	N. Brice
13.	Spatial Extent of Geomagnetic Events at the Byrd Conjugate Point	J. K. Walker
	Simultaneous Magnetic Field Variations at the Earth's Surface and at Synchronous, Equatorial Distance	
14.	Bay-Associated Events	W. D. Cummings and P. J. Coleman, Jr.
15.	Magnetic Storms	P. J. Coleman, Jr. and W. D. Cummings
16.	Magnetospheric Wave Modes Observed on Explorer 33	D. S. Colburn, R. G. Currie and C. P. Sonett
17.	Gross Local Time Particle Asymmetries at the Synchronous Orbit Altitude	J. W. Freeman, Jr. and J. J. Maguire
18.	Conjugate Effects on Energy Electrons between the Equator at 6.6 R_e and the Auroral Zone Part 1	T. W. Lezniak R. L. Arnoldy, G. K. Parks and J. R. Winckler
19.	Conjugate Effects on Energy Electrons between the Equator at 6.6 R_e and the Auroral Zone Part 2	G. K. Parks, R. L. Arnoldy, T. W. Lezniak and J. R. Winckler

20. Ion Spectrometer Observations of the Plasmapause; Evidence of Fine Structure — H. A. Taylor, Jr., H. C. Brinton and M. W. Pharo

21. The Solar Proton Events of August 28 and September 2, 1966 — C. O. Bostrom, J. W. Kohl and A. J. Zmuda

22. Examination of Storm Time Outer Zone Electron Intensity Changes at 1100 Kilometers — J. F. Arens and D. J. Williams

Rapid Geomagnetic Field Variations Observed at Conjugate Locations

by

W. H. Campbell

Institute for Telecommunication Sciences and Aeronomy
Environmental Science Services Administration
Boulder, Colorado

1. Introduction

This paper reviews the observational evidence for the earth field line dependence of rapid geomagnetic field variations in the frequency range from 4.0 to 0.002 c/s. In the literature of geomagneticians the "micropulsations" have been referred to using the letters p for "pulsation" followed by t, c, g, or p for the amplitude trace characteristics of "transient", "continuous", "giant" (Ann. IGY, 1959) or "pearl" (Sucksdorff, 1936) appearance. In 1963 an international committee (Gen. Assem. IUGG, 1963) recommended a pi and pc system of naming for the field fluctuations, using i to indicate an irregular pattern and c a regular mainly continuous appearance of the amplitude trace. A suffix 1 to 5 is proportional to the pulsation period (fig. 1).

This later naming will provide an order for presenting the topic of this paper. The pi will be given first, then the pc following from lower to higher frequencies. The review will emphasize the important characteristics of the micropulsations which have been observed simultaneously at comparable earth field locations in opposite hemispheres (Campbell and Matsushita, 1967). Table 1 summarizes the station locations of the authors whose work is discussed herein. A review of the general properties of geomagnetic pulsations has been given by Campbell (1967b). With a focus upon the phenomena, there will be no attempt to evaluate priority of first observations.

2. Pulsations with Irregular Forms

This class of pulsations has frequency components spread through the entire range of 4.0 to 0.002 c/s. They are known to be closely related in occurrence and amplitude to auroral zone, disturbed ionospheric contions. It is usually difficult to indicate a distinct separation between the lower pi frequencies and types which typically occur simultaneously with the rapid variations such as the magnetic disturbances of SSC (storm sudden commencement), positive and negative bays, SI (sudden impulses), etc.

Figure 2 illustrates for College, Alaska, and Macquarie Island some of the similarities and difference observed in pi 1 amplitude records on December 28, 1961 (Campbell et al., 1962). The top two records have a pass-band for oscillations between 30 sec and 5 sec period, the lower two records for 5 sec to 1 sec period. Note the missing higher frequencies at College at the first burst of the event and the similar onset times for both major activity peaks.

Figure 3 illustrates a pi 1 event at the Great Whale-Byrd conjugate stations on 3 August 1963. In this presentation, the pulsation events appear as impulsive, vertical darkening of the chart. The bursts of activity are often simultaneous but some non-conjugate behavior is evident even though these stations are in closer conjugacy than College-Macquarie. A station 100 km away from an E-region line-current location would sense only about a 30% signal amplitude reduction; exact conjugacy of sites would not seem to be a necessary requirement in data acquisition for such phenomena. Difference in the occurrence of the vertical bands of activity in figure 3 should be ascribed to a large but brief, changed location in the earth's field lines connecting the two sites or to an asymmetry of the auroral particle precipitation between the two hemispheres. Often the spectral records show horizontal regions of enhanced or faded signal level. Since these are usually band-like, at similar frequencies for many impulsive bursts at one station but differing at conjugate stations (figure 3), resonant transmission or selective absorption at ionospheric heights is probably responsible.

Mather and Wescott (1962) compared earth current records for pi events occurring at Cold Bay in the Aleutian Islands and Oamaru in New Zealand. The major disturbances on the two station records occurred simultaneously, had similar duration, and usually showed peak for peak correspondence. Other Alaskan stations generally were disturbed at the same time but failed to be correlated in the detailed variations. Figure 4 shows the similarity of amplitude changes at the two sites for an event on April 2, 1962. Mather and Wescott (1962) interpreted the relative loss of shorter period pi flucutations at Cold Bay due to the unique ground conductivity at that site.

A series of papers concerning micropulsation studies at Great Whale River and Byrd Station have been published by the Canadian research groups at Pacific Naval Laboratory and the University of British Columbia. Lokken et al.(1961, 1962), Yanagihara (1963), Wright (1964), Jacobs (1964), Lokken (1964) and Wright and Lokken (1965) presented conjugate data obtained in January 1961. Jacobs and Wright (1965) added to the analysis the conjugate events for the year from February 1963 to February 1964. In their comparison of Byrd pi events with those at Canadian stations, Great Whale River proved to be best correlated. At times, though, it seemed that a Byrd pi burst corresponded best with Ft. Churchill data. The field line location was thought to flucutate enough that occasionally the two stations were not at all conjugate. Using 72 selected events with good timing, Jacobs and Wright (1965) found two groups of 26 and 29 cases when one station led the other by an average of 1.1 min and one group of 17 cases with zero time difference.

In figure 5, the 5-min average amplitudes at six world stations are displayed for a brief period of pi activity in November 1963. The disturbance starting about 1800 UT on 7 November probably reached from Sweden to Alaska across Siberia. Northern Canada seemed to catch most of the activity at 0200 on November 8. The pulsations starting near 0520 UT were spread over the western hemisphere and extended to low latitude. The conjugate stations of Great Whale River-Byrd exhibited a correlation coefficient of 0.7 for 5-min scalings of the data during the period of

figure 5; other pairs of stations gave much lower coefficients. In one hemisphere, great differences in the amplitude changes for pi typically occur at distances of 1000 km and disappear for 200 km separation. The conjugate region may be within such dimensions. The distribution of activity for pi events in figure 5 is quite similar to the regions of ionospheric absorption of cosmic noise with which the pi are clearly related (Campbell and Leinbach, 1961).

Equatorial locations sometimes have been called "self conjugate". In a study of the long-period irregular fluctuations which are most numerous during daytime hours, Onwumechilli and Ogbuehi (1962) reported that about 90% of the events at Ibadan, Nigeria, could be identified at other observatories along the equator and within the auroral zone. Wescott and Mather's (1965c) results for long period variations at San Juan, Puerto, Rico, and Trelew, Argentina, near conjugate locations with L of about 1.4, were in agreement with the Nigerian study. The close association of the amplitude of the fluctuations with the strength of the equatorial Sq current system implies that the field variations are actually changes in Sq communicated to the equatorial regions from the higher latitudes.

The longer-period irregular variations were compared for College and Little America by Ahmed and Scott (1955). Activity at conjugate locations in middle and auroral latitudes were more recently reported in a series of papers by Wescott (1961, 1962), Wescott and Mather (1963, 1965a, b) and Brown, Barcus, and Parsons (1965). Between Cold Bay, Alaska, and Oamaru, New Zealand, activity correlation was about the same or slightly poorer than auroral zone pairs. Macquarie Island records compared best with Alaskan stations at Healy and Kotzebue. The region of coherence of signals in Alaska was elongated along the line of constant L about 350 km E-W and 120 km N-S. There was a seasonal change in the relative amplitude of the field disturbance variations such that the southern station was more active in the December solstice months and the northern station more active in the June solstice months. It appears that ionospheric conductivity and currents play an important role in the conjugate occurrence region and amplitudes for these auroral zone field variations.

Irregular field fluctuations seen on magnetometers at Shepherd Bay, Canada, and Scott Base, Antarctica, both within the auroral zone, exhibited their greatest similarity during the nighttime hours, a secondary maximum of moderate correlation about midday, and usually dissimilar behavior between the two maxima (Wescott and Mather, 1963). One interpretation of figure 6 is that during the midday hours Sq-like currents carry the variations in from the auroral zones whereas at nighttime either the high latitude field lines are connected and/or the auroral magnetic disturbance, associated with particle precipitation, is spread over a broader region.

Magnetic storm sudden commencements (SSC) and magnetic field, sudden impulses (SI) are typically associated with pi type pulsations in the auroral zone (Campbell and Matsushita, 1962). More than 50% of SSC's are associated with pulsations of 2.5 to 10 minutes period (Sugiura and Wilson, 1961). For that reason some results of three studies of SSC and SI phenomena are mentioned here.

The SSC's are rapid changes in the geomagnetic field which last about 1 to 6 minutes, breaking a quiet period of recording, and occur at the beginning of a magnetic storm. Sugiura and Wilson (1961) and Nagata et al. (1966) found that conjugately located auroral stations have SSC's with similar appearance, occurrence frequency and polarization vectors showing elliptic counterclockwise rotation (viewed along the field line) from 22 h to 10 h local geomagnetic time. In this feature the SSC behaves like pc 5 pulsations. The relative sizes of the SSC's at Reykjavik, Iceland, and Syowa, Antarctica, seemed to indicate slightly larger amplitudes in the winter hemisphere. Sato (1962) gave excellent examples of the concurrent ionospheric absorption effects associated with the SSC simultaneously occurring in Alaska and Antarctica.

The SI's are sudden, world-wide changes in the magnetic field, much like the SSC's but not followed by a magnetic storm. The general conjugate features were the same as that reported above for the SSC.

Longer period continous pulsations of the pc 4-5 variety are often seen within the pi 2 spectra. Figure 7 illustrates that type of conjugate pi micropulsation received on ITSA recorders at Great Whale River and Byrd Station. Three aspects of this figure should be pointed out. There is a good agreement in the occurrence time for most of these pi bursts. Saito (1967) used an interesting photographic technique for displaying this coincident spectral pattern. A higher frequency portion of activity between 08 h and 09 h UT is missing at Great Whale River whereas a higher frequency portion between 09 and 10 UT is absent at Byrd. There is a well developed pc 4-5 in the early hours of the event that becomes the major micropulsation activity after 10 h UT.

There are a few reports of the behavior of the long period, damped oscillation type pulsations (pt) at conjugate locales. Some aspects of these may place them in the transitory region between pi pc pulsation types or miniature version of the SI mentioned earlier. Saito's (1961) hodographs of the pt disturbance vector in the horizontal plane showed a northern hemisphere convergence into a region lying along the auroral zone near the local midnight meridian while vectors in the southern hemisphere diverged from the approximate conjugate point. Jacobs and Wright (1965) show one example of a large 4 to 5 min period pt observed simultaneously at Great Whale River and Byrd (figure 8).

3. Continuous Pulsations with Periods of One to Ten Minutes

The long period continuous pulsations, pc 4-5 generally have large amplitudes reaching, at times, to several hundred gammas. They occur principally in the auroral latitudes in periods of high solar-terrestrial activity. The forms are quite sinusoidal, often damped, and the duration ranges from a few minutes to several hours. Many events have harmonic structure. The spectra in figure 7 from 1015 to 1200 h UT is typical of the detailed, fine structure coincidence found at conjugately located high latitude stations.

The reports by Sugiura (1961) on the conjugate College-Macquarie pair of stations, by Nagata et al. (1963, 1966) and Kokubun and Nagata (1965)

on the Reykjavik-Syowa stations pointed to the correspondence of such pulsations at conjugate locations and their hydromagnetic-wave-like behavior. The signals seemed not unlike the magnetic impulses of SCMS (Wilson and Sugiura, 1961) with the disturbance vector rotation sense invariant along the whole line of force in space; a counterclockwise direction (fig. 9) in the horizontal field vector, H, during the morning (looking into the northern hemisphere) and reversed in the afternoon with a transition about 11 h local time. The main axis of the polarization was almost perpendicular to the direction of the main geomagnetic force. Correlation coefficients between successive maxima and minima were about 0.8. Amplitudes were close to the same value at the two stations but amplitudes of the morning pulsations were appreciably larger than the afternoon variety. Frequency spectra show usually one but often two discrete peaks. The pulsations were ascribed to hydromagnetic waves, resonating with the eigen-oscillation of the geomagnetic field line and excited by the arrival of the solar wind.

Ahmed and Scott (1955) found pc 4-5 with similar occurrence and period at College and Little America. Wescott and Mather (1965b) mention pc 4-5 events observed at the Cold Bay-Oamaru station pair. Jacobs and Wright (1965) and Saito (1967) published some similar pc 4-5 events at the Great Whale-Byrd station pair.

Recently Wilson (1966) reexamined some of the College-Macquarie data and concluded that ionospheric current systems were induced by the circularly polarized standing hydromagnetic waves on the field lines. He ascribed differences in signal appearance at near conjugate locations to the position of the observing station relative to the terminal point of the oscillating field line. His model seemed to leave unexplained the interrelationship of the pc 4-5 with ionospheric absorption (Sato, 1964, 1965), auroral radar reflection (Kaneda et al., 1964) and precipitating auroral electrons (Anger et al., 1963, and Barcus and Rosenberg, 1965).

Sato's (1964, 1965) study used the data from a world network of stations. He found most pulsations in Antarctica to be a local phenomenon with occurrence maxima different in each area and phases not coincident

between stations. Figure 10 illustrates the amplitude and phase similarity of the pulsations he studied at the conjugate College-Macquarie pair of stations. The correspondence with concurrent riometer measured ionospheric absorption led Sato to the conclusion that most high latitude pulsations of this type are caused by currents arising from the high latitude, particle bombardment of the ionosphere.

4. Pulsations with 5 to 50 sec Period

Mather et al. (1964) studied an active period in April 1962 during which pulsations with about 40 sec period occurred at Cold Bay and Oamaru. The signal's behavior is rather like that expected of pc 4 type pulsations. The amplitude and the periods were somewhat shorter during the daytime. There was some tendency to slightly longer periods at the time of auroral disturbance onset. Figure 11 is an example of their study on the direction of rotation of the disturbance vector for the two stations. Four of their ten simultaneous conjugate disturbances maintained exactly the same phase relationship with oppositely rotating vectors. The polarization sense was uniform at night, counterclockwise (looking into the ground) at Cold Bay and clockwise at Oamaru. The rotation pattern was more irregular during the day but generally reversed to the nighttime behavior. The earth-sun line division of the sense change seemed at variance with the results of Wilson and Sugiura (1961) and Nagata et al. (1963) for the longer period variations.

The true pc 2-3 pulsations are typically a daytime phenomena with longer periods at midday and amplitudes proportional to the K_p index of world wide geomagnetic disturbance. The signals usually stay under 1 gamma in size and maximize in the auroral region. Examples of simultaneous high latitude appearance of these pulsations have been published by Lokken et al. (1962) for Victoria and Byrd, by Campbell (1963) for College and Macquarie (fig. 11), and by Jacobs and Wright (1965) for Great Whale and Byrd.

At low latitudes Kato and Okuda (1956) reported similar 30 to 50 sec pulsations at Japan and Ceylon. Schlumberger and Kunetz (1946) reported a possible reversal of signal polarization between France and Madagascar for these signals.

The pc 2-3 are the most poorly studied pc group of pulsations. The polarization sense and major direction of the horizontal disturbance vector undergoes a regular diurnal variation at most latitudes (Terada, 1917; Kawamura et al., 1961) which can account for some of the hemispherical differences reported. The peak for peak identification at conjugate stations does exclude the local ionospheric resonance as a generative model.

5. Regular Pulsations in the 1 sec Period Range

The pc 1 pulsations occur principally in the band from 0.15 to 3.5 c/s. They usually have a rising frequency structure but variations have been observed. The average frequency and emission-recurrence period seem to be linearly related. Bursts of activity typically last about one-half hour; the general disturbance level may be as long as twelve hours. The averaged diurnal variation in mid-frequencies is similar at all world locations: minima of about .4 or .5 c/s occur from 1400 to 1800 hours local time and maxima of about .9 or 1.0 c/s occur from 0100 to 0500 hours local time. The occurrences are usually near the local noon hours at auroral latitude stations and they shift into the morning to predawn hours at middle and low latitudes.

At times the events are found simultaneously at widely spaced stations over a hemisphere of the earth (Tepley et al., 1965; Kenney and Knaflich, 1967). The usual case, however, is for a rather local appearance of the events. This is evidenced in the unique local occurrence maxima as a function of latitude and in the local-time diurnal variation of mid-frequency for the events. Campbell and Stiltner (1965) and Campbell (1967a) demonstrated the conjugate station similarity of these two characteristics. They placed the typical range for coherent signal to be under 1000 km in the high latitudes. In contrast, Borsoukov and Ponsot (1964) found phase coherence at 1100 km. Campbell and Stiltner (1965) only found significant correlation coefficients for data from stations conjugately located. Figure 13 shows the cross-correlation for joint sampling periods at College-Macquarie, Great Whale-Byrd, Baie St. Paul (Quebec)-Eights. The highest

correlation was obtained from this last pair. These stations were not only nearest to computed conjugacy but closer to each other in local time and at lower L values than the other two pairs.

Figure 14 is an example of the spectra of pc 1 events received at conjugate locations. In addition to the last two references a number of authors have published examples of conjugate pc 1 signals. Dawson (1965) discussed occurrence and similar average frequency changes at College and Macquarie. Lokken et al. (1963), Yanagihara (1963), and Wright and Lokken (1965) presented examples of concurrent events at the Great Whale-Byrd pair of stations. The data received at Kerguelen and Sogra or Borok appeared in publications of Borsoukov and Ponsot (1964), Laurent et al. (1964), Troitskaya et al. (1964), Gendrin and Troitskaya (1965), Lacourly et al. (1965), Loran et al. (1965), Matveyeva and Troitskaya (1965) and Gendrin et al. (1966). Schlicht (1963) reported some similarities in the records taken at Chambon-la-Foret and Garchy, France, and at Hermanus, South Africa. The pc 1 at the near conjugate locations of Kauai and Tongatapu have been presented by Tepley (1964, 1965, 1966).

A number of unique features have come to light in the conjugate studies which should give insight into the magnetospheric propagation characteristics and separate out the local ionospheric effects on the signal recorded. At conjugate stations with greatly differing geographic longitude, the average occurrence and diurnal changes in mid-frequency are best matched at the two sites when a common field-line time is assumed (Campbell and Stiltner, 1965). Some of the gross appearance of the signal is immediately evident in viewing such examples as figure 14. There is often a general activity recurrence pattern of about one-half or one hour. The general envelope of the event is often similar at the two stations, for example in the early hours of figure 14. These features and the horizontal "streaking" of signal enhancement and disappearance must not be dependent upon the transient ionospheric conditions which vary independently in opposite hemispheres.

In figure 15 we see the several surprising results of the study by Gendrin et al. (1966). The polarization sense is unique with respect to a field line connecting the stations throughout an identifiable family of

a pc 1 events. However, as the figure shows, both senses are observed. Theoretical models seem to predict a left-hand polarized (looking into the northern hemisphere), Alfven-mode of field guided propagation in the magnetosphere. The results of this figure must modify that assumption or introduce increased importance to propagation processes within the ionosphere.

The interlacing of pc 1 fine structure has been demonstrated by several independent researchers. Figure 15 also illustrates this alternation between the two hemispheres. Lokken et al. (1963) and Yanagihara (1963), examining Great Whale River and Byrd Station records, found a few remarkable cases when the amplitude envelope of activity alternated in the northern and southern auroral zones with the maxima of activity at one station occurring midway between the maxima at the other. Tepley's (1964) studies in the Pacific area indicated that emissions observed simultaneously in the same hemisphere were simultaneous within an accuracy of ± 12 seconds whereas emissions observed at Kauai and Tongatapu, at near conjugate locations, had structural elements displaced in time by one-half the fine structure periodicity. He also observed occasional doubling of the fine structure repetition frequency at middle and low latitude stations. Borscukov and Ponsot (1964) calculated correlation coefficients and autocorrelation functions for simultaneous pc 1 events. They found no time differences greater than 0.1 sec between Borok and Lovozero, a distance of about 1100 km; the oscillations were in phase. The authors found no phase coherence between the conjugate regions of Borok and Kerguelen for the individual oscillations. Figure 16 shows the correlation function for various time shifts between the envelopes of activity received alternately in the two hemispheres. The figure indicates that the signals appeared at Kerguelen about 70 sec after its appearance at Borok whereas the repetition period was 120 sec. Gendrin and Troitskaya (1965) point out that this discrepancy may be due to some heating between overlapping emissions. Wentworth et al. (1966) reported that for Pacific stations in the northern hemisphere the pc 1 seem to penetrate the ionosphere at high latitudes and propagate equatorward with an average apparent velocity of about 900 km/sec. They interpreted such propagation time as responsible for the difference from exact 180° phase shift measured for signals received in opposite hemispheres.

Apparent attenuation of the ionosphere upon pc 1 signals was investigated by Campbell (1967). Studying the 0.5 to 1.0 c/s pc 1 emissions at the conjugately located stations he selected Northern summer solstice times when the ionosphere was dark over Eights, Antarctica, but cycle normally over Baie St. Paul, Canada. Table 2 indicates that the signal level was reduced under the daytime ionosphere. At the higher frequencies and with more disturbed (higher K_p) ionospheric conditions greater attenuation was found. Slight changes in seasonal occurrence and signal frequency were shown to be consistent with the estimated attenuation. The signal amplitude reduction was matched to theoretical expectations by the assumption of Alfven to modified-Alfven mode coupling of the propagated signal in the ionosphere.

Several features of the pc 1 now seem quite evident. The phenomenon is of magnetospheric origin. It is field guided into high latitude stations without appreciable ionospheric attenuation. The signals may travel to lower latitudes in other ducted modes. There are still numerous unexplained characteristics of the form of these pc 1 events which cannot be ascribed to local anomalies.

6. Acknowledgements

A portion of this study was made possible by funds from the Advanced Research Projects Agency under contract 183. The ITSA Antarctic work reported in this paper has had the continued support of the National Science Foundation under grant GA 147. The Canadian National Research Council was extremely helpful to ITSA in assisting the studies at Baie St. Paul and Great Whale River. Macquarie Island measurements were made possible through the kindness of the ANARE Office of the Australian Department of External Affairs.

References

Ahmed, J. J., and W. E. Scott (1955), Time relationship of small magnetic disturbances in Arctic and Antarctic, J. Geophys. Res. 60, 147-154.

Ann. IGY, II (1959), Symposium on geomagnetics and telluric rapid variations, 668-709.

Anger, C. D., J. R. Barcus, R. R. Brown, and D. S. Evans (1963), Long-period pulsations in electron precipitation associated with hydromagnetic waves in the auroral zone, J. Geophys. Res. 68, 3306-3310.

Barcus, J. R., and T. J. Rosenberg (1965), Observation on the spatial structure of pulsating electron precipitation accompanying low frequency hydromagnetic disturbances in the auroral zone, J. Geophys. Res. 70, 1707-1716.

Borsoukov, A. M., and C. Ponsot (1964), Characteristics essentiales de la structure des oscillations en perles dans les regions geomagnetiquement conjuguees, Ann. Geophys. 20, 473-479.

Brown, R. R., J. R. Barcus, and N. R. Parsons (1965), Balloon observations of auroral zone x-rays in conjugate regions, J. Geophys. Res. 70, 2579-2598.

Brown, R. R., and J. R. Barcus (1965), Balloon observations of auroral zone x-rays in conjugate regions, 2. Microbursts and pulsations, J. Geophys. Res. 70, 2599-2612.

Campbell, W. H. (1963), Natural electromagnetic field fluctuations in the 3.0 to 0.02-cps range, Proc. IEEE 51, 1337-1342.

Campbell, W. H. (1965), A review of seven studies of geomagnetic pulsations associated with auroral zone disturbance phenomena, paper 28, Proceedings Symp. ULF Fields, August 1964, NBS Report 8815, 1-41.

Campbell, W. H. (1966), A review of the equatorial studies of rapid fluctuations in the earth's magnetic field, Annales Geophys. 22, 492-501.

Campbell, W. H. (1967a), Low attenuation of hydromagnetic waves in the ionosphere and implied characteristics in the magnetosphere for pc 1 events, J. Geophys. Res. 72, 3429-3445.

Campbell, W. H. (1967b), Geomagnetic pulsations, Physics of Geomagnetic Phenomena, ed. S. Matsushita and W. H. Campbell (Academic Press, New York).

Campbell, W. H., and H. Leinbach (1961), Ionospheric absorption at times of auroral and magnetic pulsations, J. Geophys. Res. 66, 25-34.

Campbell, W. H., and S. Matsushita (1962), Auroral-zone geomagnetic micropulsations with periods of 5 to 30 seconds, J. Geophys. Res. 67, 555-573.

Campbell, W. H., and S. Matsushita (1967), World maps of conjugate coordinates and L contours, J. Geophys. Res. 72, 3518-3521.

Campbell, W. H., J. H. Pope, and M. D. Littlefield (1962), Problems regarding geomagnetic micropulsations at conjugate field locations on the earth's surface, paper 47, Geomag. Aeron. Section, AGU Meeting, Stanford, California, Dec. 29, 1962.

Campbell, W. H., and E. C. Stilwner (1965), Some characteristics of geomagnetic pulsations at frequencies near 1 c/s, Radio Sci. 69D, 1117-1132.

Dawson, J. A. (1965), Geomagnetic micropulsations with emphasis placed on the properties and interpretation of pearls, Ph.D. Thesis, University of Alaska, Phys. Dept., 120 pgs.

Gen. Assembly of IUGG, XIII, Berkeley (1963), IAGA Resolution No. 13.

Gendrin, R., S. Lacourly, M. Gokhberg, O. Malevskaya, and V. A. Troitskaya (1966), Polarisation des oscillations hydromagnetiques de type pc 1 observe en deux stations geomagnetiquement conjuguees, Annales de Geophys. 22, 329-337.

Gendrin, R. E., and V. A. Troitskaya (1965), Preliminary results of a micropulsation experiment at conjugate points, Radio Sci. 69D, 1107-1116.

Jacobs, J. A. (1964), Micropulsations of the electromagnetic field in the frequency range 0.1-10 cps, Natural Electromagnetic Phenomena Below 30 kc/s, ed. D. F. Bleil (Plenum Press, New York).

Jacobs, J. A., and C. S. Wright (1965), Geomagnetic micropulsation results from Byrd Station and Great Whale River, Can. J. Phys. 43, 2099-2122.

Kaneda, E., S. Kokubun, T. Oguti, and T. Nagata (1964), Auroral radar echoes associated with pc 5, Rept. Ionos. Space Res. Japan 18, 165-172.

Kato, Y., and M. Okuda (1956), The effect of the solar eclipse on the rapid pulsation of the earth's magnetic fields, Sci. Rept. Tohoku Univ., Ser. 5, Geophys. 7, 37-41.

Kawamura, M., K. Kuwusu, H. Oshima, and K. Yanagihara (1961), On the geomagnetic pulsation pc-(I), World-wide distribution of the horizontal disturbing vector, Mem. Kakioka Magn. Obs. Suppl. 10, 7-13.

Kenney, J. F., and H. B. Knaflich (1967), A systematic study of structural micropulsations, J. Geophys. Res. 72, 2857-2869.

Kokubun, S., and T. Nagata (1965), Geomagnetic pulsation pc 5 in and near the auroral zones, Rept. Ionos. Space Res. Japan 19, 158-176.

Lacourly, S., R. Gendrin, and P. Leflock (1965), Relations d'amplitude des oscillations hydromagnetiques recues en deux points conjuguees de haute latitudes, Ann. Geophys. 21, 467-468.

Laurent, G., M. Panthenier, C. Ponsot, L. N. Baranski, N. B. Kazak and E. T. Mateeva (1964), Ann. Geophys. 20, 503-505.

Lokken, J. E. (1964), Instrumentation for receiving electromagnetic noise below 3,000 cps, Natural Electromagnetic Phenomena Below 30 kc/s, ed. D. F. Bleil (Plenum Press, New York).

Lokken, J. E., J. A. Shand, C. S. Wright, L. H. Martin, N. M. Brice, and R. A. Helliwell (1961), Stanford-Pacific Naval Laboratory Conjugate Point Experiment, Nature 192, 319-321.

Lokken, J. E., J. A. Shand, and C. S. Wright (1962), A note on the classification of geomagnetic signals below 30 cycles per second, Can. J. Phys. 40, 1000-1009.

Lokken, J. E., J. A. Shand, and C. S. Wright (1963), Some characteristics of electromagnetic background signals in the vicinity of one cycle per second, J. Geophys. Res. 68, 789-794.

Loran, J., C. Ponsot, M. Potenie, L. N. Baranskiy, B. N. Kazak, and E. T. Matveyeva (1965), Some characteristics of magnetic pc-1 pulsation in magnetically conjugate regions (Borok-Kerguelen, February 1964), Geomag. Aeron. 5, 499-501.

Mather, K. B., E. J. Gauss, and G. R. Cresswell (1964), Diurnal variations in the power spectrum and polarization of telluric currents at conjugate points, L = 2.6, Australian J. Physics 17, 373-388.

Mather, K. B., and E. M. Wescott (1962), Telluric currents at geomagnetically conjugate stations in the Aleutian Islands and New Zealand, J. Geophys. Res. 67, 4825-4831.

Matveyeva, E. T., and V. A. Troitskaya (1965), General patterns of pearl-type pulsations, Geomag. Aeron. 5, 1078-1084.

Nagata, T., S. Kokubun, and T. Iijima (1963), Geomagnetically conjugate relationships of giant pulsations at Syowa Base, Antarctica, and Reykjavik, Iceland, J. Geophys. Res. 68, 4621-4625.

Nagata, T., S. Kokubun, and T. Iijima (1966), Geomagnetically conjugate relationship of polar disturbances--particularly the distinct geomagnetic conjugacy between Syowa station in Antarctica and Reykjavik in Iceland, JARE Scientific Repts. Aeronomy, Series A, No. 3, 1-64.

Onwumechilli, A., and P. O. Ogbuehi (1962), Fluctuations in the geomagnetic horizontal field, J. Atmos. Terr. Phys. 24, 173-190.

Saito, T. (1961), Oscillations of geomagnetic field with progress of pt type pulsation, Sci. Rept. Tohoku Univ., Ser. 5, Geophys. 13, 53-61.

Saito, T. (1967), Some characteristics of the dynamic spectrum of long-period geomagnetic pulsations, J. Geophys. Res. 72.

Sato, T. (1962), Structures of sudden commencements of geomagnetic storms and giant pulsations in high latitudes, Rept. Ionos. Space Res. Japan 16, 295-333.

Sato, T. (1964), Geomagnetic giant pulsations in the Antarctic, Sci. Rept. 12, Antarctic Research and Data Analysis, AVCO Corp. Tech. Rept. RAD-TR-64-8, 1-52.

Sato, T. (1965), Long period geomagnetic oscillations in southern high latitudes, Geomagn. Aeronomy 4, Antarctic Ser., Ed. A. H. Waynick, Am. Geophys. Union, Washington, D. C., 173-188.

Schlicht, R. (1963), Micropulsations de Periodes Comprises entre 0.5 et 6 s Observees dans les Regions de Hautes et Mayennes Latitudes, Annales de Geophysique 19, 347-355.

Schlumberger, M., and G. Kunetz (1946), Variations rapides simultanes du champ tellurique en France et a Madagascar, Compt. Rend. 223, 551-553.

Sucksdorff, E. (1936), Occurrences of rapid micropulsations at Sodankyla during 1932 to 1935, Terres. Magn. Atmos. Elect. 41, 337-344.

Sugiura, M. (1961), Evidence of low-frequency hydromagnetic waves in the exosphere, J. Geophys. Res. 66, 4087-4095.

Tepley, L. R. (1964), Low-latitude observations of fine structured hydromagnetic emissions, J. Geophys. Res. 69, 2273-2290.

Tepley, L. R. (1965), Regular oscillations near 1 c/s observed at middle and low latitudes, Radio Sci. 69D, 1089-1105.

Tepley, L. R. (1966), Recent investigations of hydromagnetic emissions, Part I, Experimental Observations, J. Geomag. Geoelect. 18, 227-256.

Tepley, L. R., and K. D. Admundsen (1965), Observations of continuous sub ELF emissions in the frequency range 0.2-1.0 c/s, J. Geophys. Res. 70, 234-239.

Tepley, L. R., R. R. Heacock, and B. J. Fraser (1965), Hydromagnetic emissions (pc 1) observed simultaneously in the auroral zone and at low latitudes, J. Geophys. Res. 70, 2720-2725.

Terada, T. (1917), On rapid periodic variations of terrestrial magnetism, J. College Sci., Tokyo Imperial Univ. 37, Art 9, 1-85.

Troitskaya, V. A., R. Gendrin, and R. Stefant (1964), Observations en points conjuguees de moyenne latitude des emissions hydromagnetiques strucurees, Compt. Rend. Acad. Sci. 259, 1175-1178.

Wentworth, R. C., L. Tepley, K. D. Admundsen, and R. R. Heacock (1966), Intra- and interhemisphere differences in occurrence times of hydromagnetic emissions, J. Geophys. Res. 71, 1492-1498.

Wescott, E. M. (1961), Magnetic variations at conjugate points, J. Geophys. Res. 66, 1789-1792.

Wescott, E. M. (1962), Magnetic variations during periods of auroras at geomagnetically conjugate points, J. Geophys. Res. 67, 1353-1355.

Wescott, E. M., and K. B. Mather (1963), Diurnal effects in magnetic conjugacy at very high latitude, Nature 197, 1259-1261.

Wescott, E. M., and K. B. Mather (1965a), Magnetic conjugacy from L = 6 to L = 1.4, 1. Auroral Zone: Conjugate Area, Seasonal Variations, and Magnetic Coherence, J. Geophys. Res. 70, 29-42.

Wescott, E. M., and K. B. Mather (1965b), Magnetic conjugacy from L = 6 to L = 1.4, 2. Midlatitude Conjugacy, J. Geophys. Res. 70, 43-47.

Wescott, E. M., and K. B. Mather (1965c), Magnetic conjugacy from L = 6 to L = 1.4, 3. Low Latitude Conjugacy, J. Geophys. Res. 70, 49-51.

Yanagihara, K. (1963), Geomagnetic micropulsation with periods from 0.03 to 10 seconds in the auroral zones with special reference to conjugate points studies, J. Geophys. Res. 68, 3383-3397.

Wilson, C. R. (1966), Conjugate three dimensional polarization of high latitude micropulsations from a hydromagnetic wave-ionospheric current model, J. Geophys. Res. 71, 3233-3249.

Wilson, C. R., and M. Sugiura (1961), Hydromagnetic interpretation of sudden commencements of magnetic storms, J. Geophys. Res. 66, 4097-4111.

Wright, C. S. (1964), Micropulsations at near conjugate stations in the auroral zones and their association with other ionospheric phenomena, Natural Electromagnetic Phenomena Below 30 kc/s., ed. D. F. Bleil (Plenum Press, New York), 287-318.

Wright, C. S., and J. E. Lokken (1965), Geomagnetic micropulsations in the auroral zones, Canadian J. Phys. 43, 1373-1387.

Table 1

Coordinates and L parameters of Near Conjugate Stations*

Stations	Geographic Coordinates		Conjugate Coordinates		L Parameters
	Lat.°	Long.°	Lat.°	Long.°	
San Juan, Puerto Rico	18.43N	66.00W	47.2S	63.7W	1.5
Trelew, Argentina	43.20S	65.30W	14.6N	66.7W	1.4
Chambon-la-Foret, France	48.02N	2.27E	38.7S	22.1E	2.1
Garchy, France	47.30N	3.07E	37.4S	21.8E	2.1
Hermanus, South Africa	34.42S	19.22E	45.3N	2.3E	1.9
Cold Bay, Alaska	55.27N	162.87W	45.2S	170.9E	2.7
Oamaru, New Zealand	44.99S	170.97E	55.1N	163.0W	2.7
Borok, USSR	58.03N	38.33E	45.5S	60.1E	2.9
Sogra, USSR	62.80N	46.25E	49.0S	71.1E	3.7
Lovozero, USSR	67.99N	35.08E	55.8S	71.8E	5.2
Kerguelen Island	49.35S	70.27E	62.9N	45.2E	3.7
Baie St. Paul, Canada	47.37N	70.55W	75.5S	78.4W	4.0
Eights, Antarctica	75.23S	77.17W	47.1N	70.4W	4.0
College, Alaska	64.85N	147.83W	56.8S	168.4E	5.5
Kotzebue, Alaska	66.88N	162.60W	54.4S	160.1E	5.3
Healy, Alaska	63.85N	119.00W	66.0S	178.9E	8.7
Macquarie Island	54.50S	158.95E	67.6N	163.6W	5.4
Little America, Antarctica	78.39S	163.56W	62.6N	89.3W	13.4
Reykjavik, Iceland	64.13N	21.78W	69.5S	39.5E	6.3
Syowa, Antarctica	69.03S	39.60E	64.2N	21.0W	6.3
Great Whale River, Canada	55.33N	77.83W	80.3S	117.2W	7.0
Byrd Station, Antarctica	79.98S	120.02W	55.4N	79.5W	7.2
Shepherd Bay, Canada	68.75N	93.75W	76.7S	167.8E	28.6
Scott Base, Antarctica	77.85S	166.75E	69.5N	91.4W	33.0

*Computations for November 1966 and 100 km altitude above station (Campbell and Matsushita, 1967).

Table 2

Average Amplitude Ratio (Quebec/Eights) for Dark Ionosphere at Eights and Daylight at Quebec (Campbell, 1967).

	Frequency c/s	
Kp index	0.5	1.0
0 to 1+	.70	.49
2- to 2+	.59	.45
3- to 3+	.53	.19

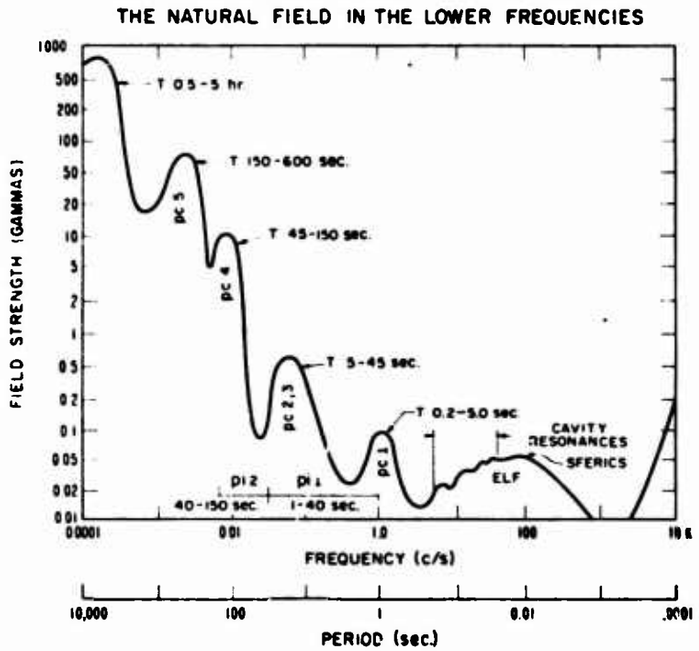

Figure 1. Amplitude levels of signals to be expected in the lower frequency range The period range for pc and pi classification is noted (Campbell, 1966)

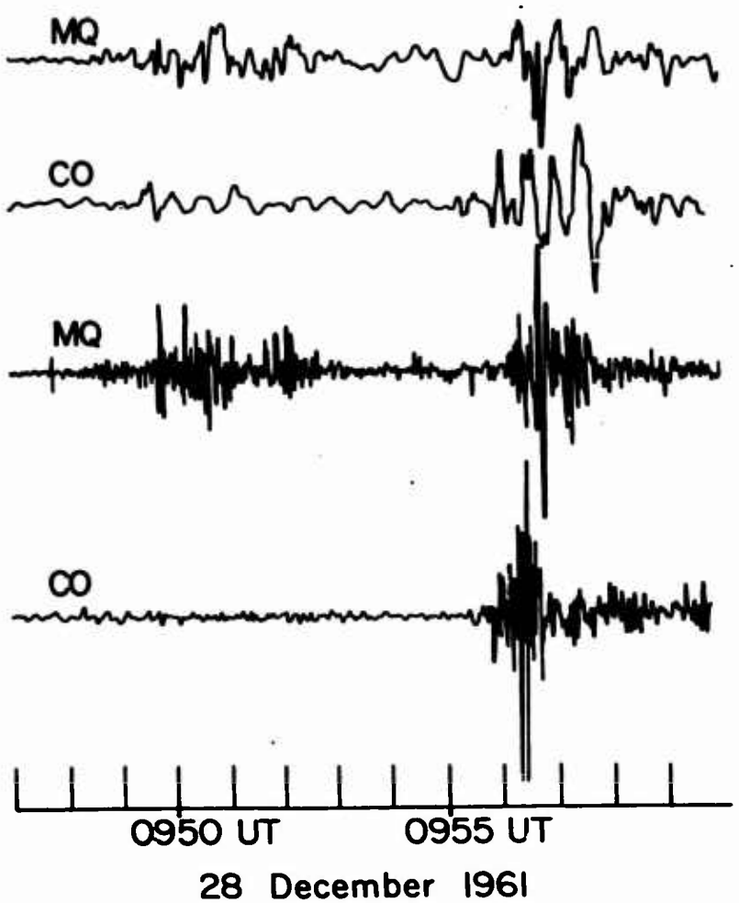

Figure 2. Simultaneous pi event at Macquarie Island (MQ) and College, Alaska (CO) on December 28, 1961. The upper two traces are for the 5 to 30 sec period band and the lower two traces are for the 1 to 5 sec period band (Campbell et al., 1962).

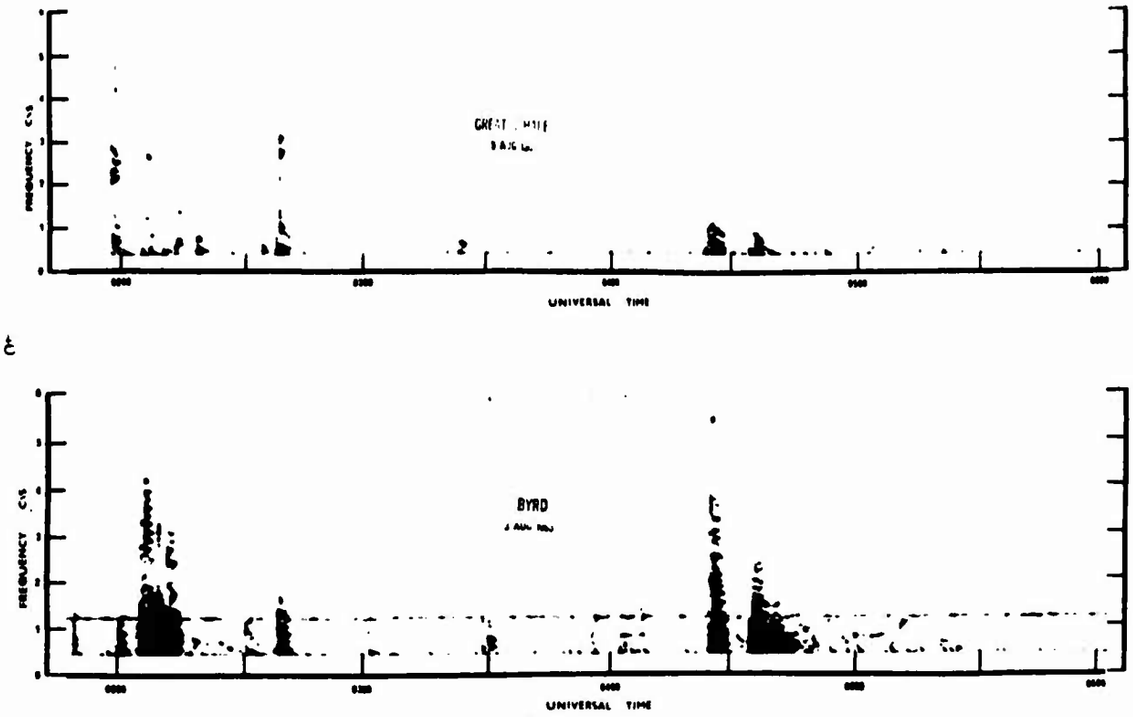

Figure 3. Sonagraph spectral display of conjugate behavior of pi signals at Great Whale River and Byrd on August 3, 1963 (Campbell, 1965).

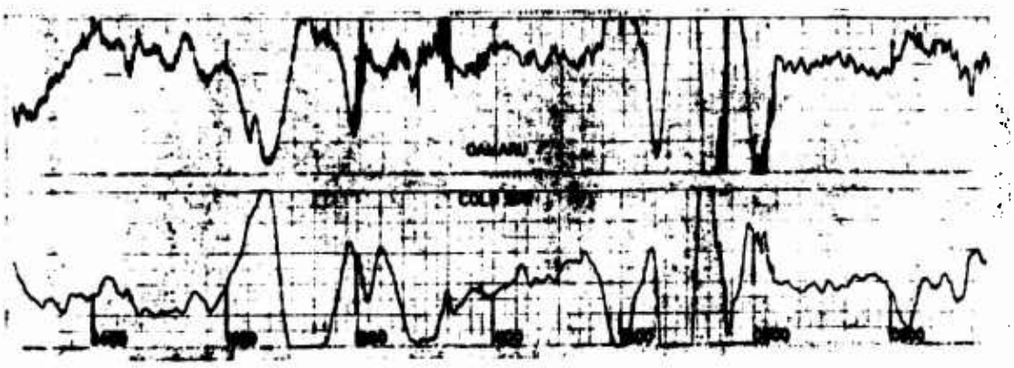

Figure 4. Telluric current charts for April 7, 1962, at Cold Bay, Alaska, and Oamaru, New Zealand (Mather and Wescott, 1962).

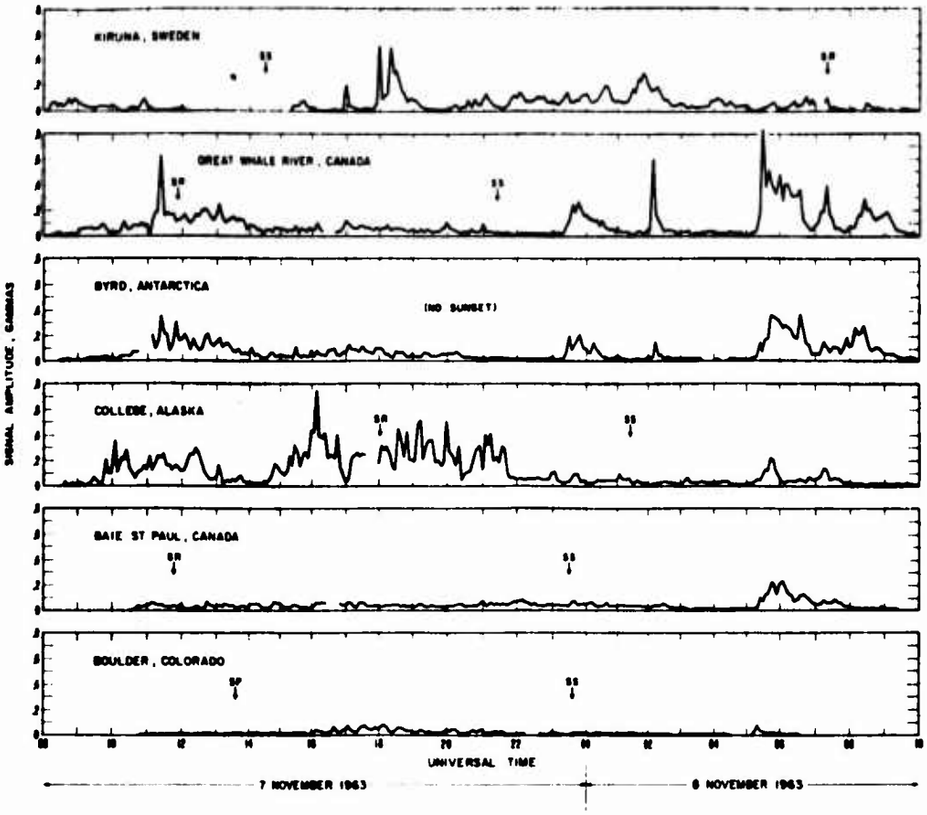

Figure 5. Pi activity at six world stations on 7 and 8 November 1963. Local sunrise (SR) and sunset (SS) times are indicated (Campbell, 1965).

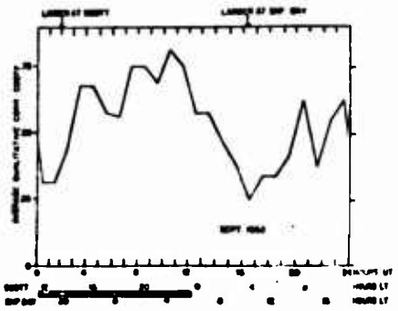

Figure 6. Variation of correlation between Shepherd Bay and Scott Base magnetic disturbances. The shading refers to the local night. (Wescott and Mather, 1963).

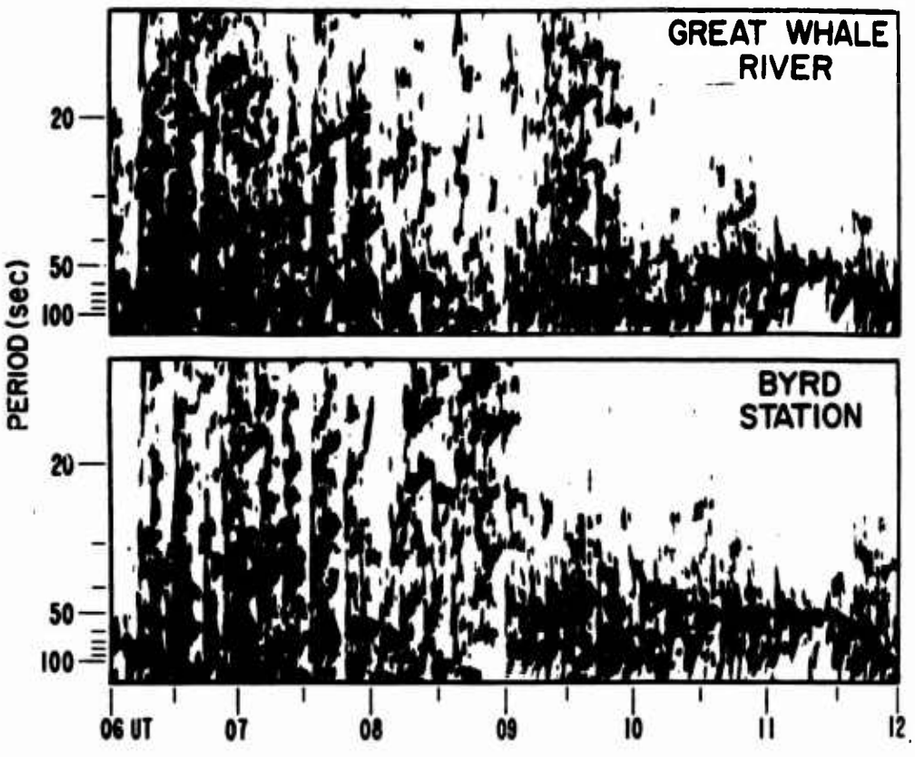

Figure 7. Spectra of simultaneous disturbance at Great Whale River and Byrd Station on September 22, 1965. The early hours show a pi 1-2 event; later in the day a pc 4-5 develops.

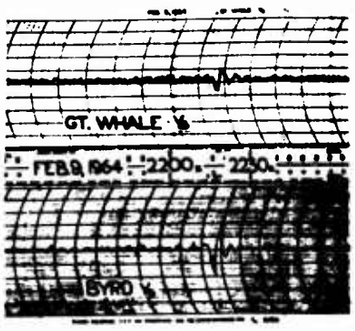

Figure 8. A pt event recorded at Great Whale River and Byrd on February 9, 1964 (Jacobs and Wright, 1965).

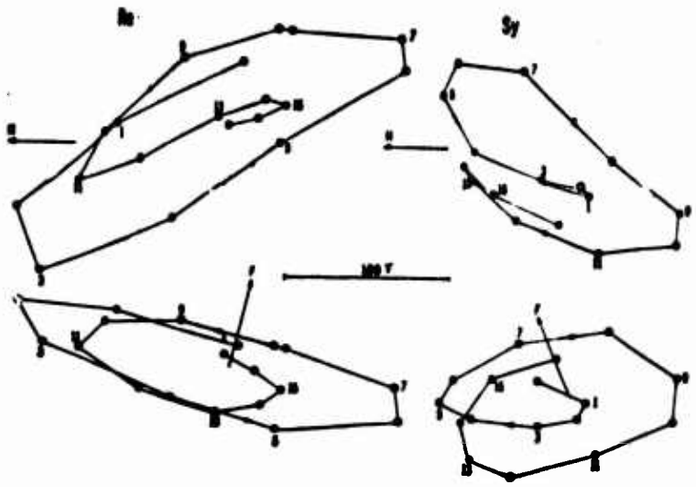

Figure 9. Example of locus of rotating vectors for the morning pulsations in the horizontal plane (top) and in the magnetic plane (bottom) observed at Reykjavik (Re) and Syowa (Sy) at 0655 to 0705 UT on Setpember 18, 1959 (Nagata et al., 1963).

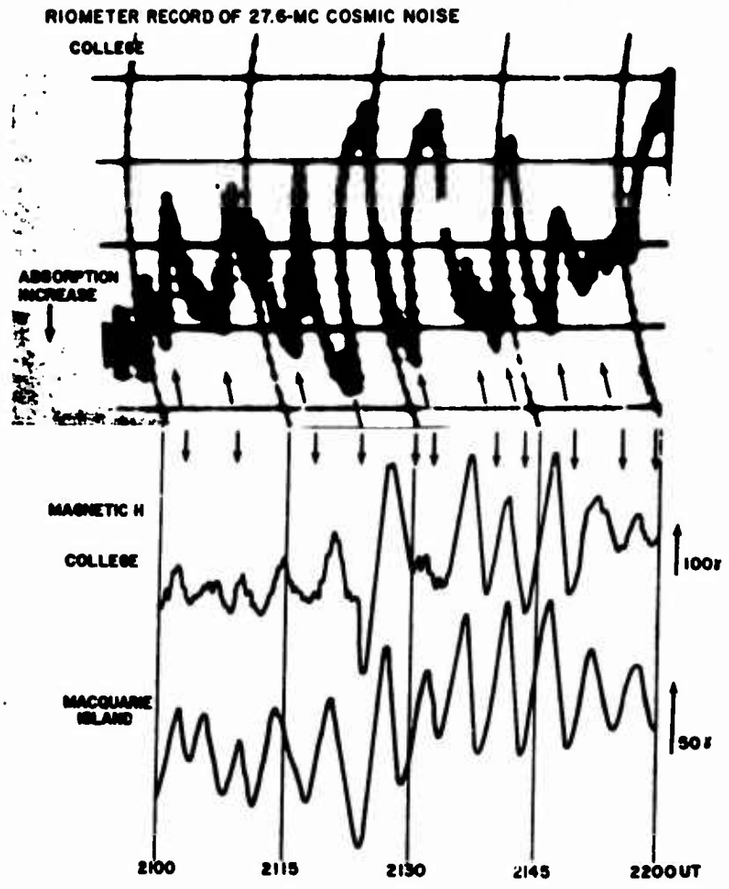

Figure 10. Simultaneous pc 5 magnetic field pulsations at College and Macquarie Island on 19 March 1958. Concurrent ionospheric absorption measured with the College Riometer is shown on a similar time scale at the top (Sato, 1965).

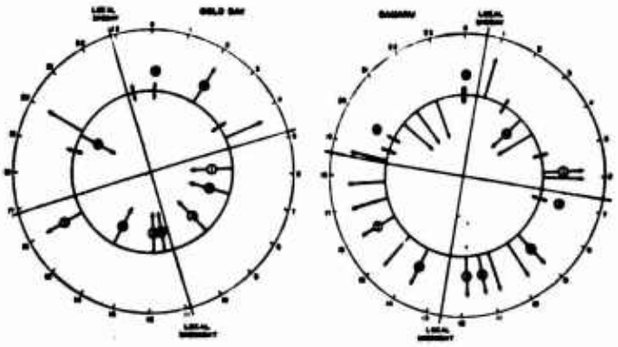

Figure 11. Polarization of 40 sec pulsations received at Cold Bay and Oamaru for a 24 hr period on 11-12 April 1967. Radial arrows drawn from the reference circle denote the direction of rotation at various times throughout the day. Long arrows directed outward denote clockwise rotation; directed inward, counterclockwise. Short bi-directional arrows mean both sense or linear polarization were present with no preferred direction (Mather et al., 1964).

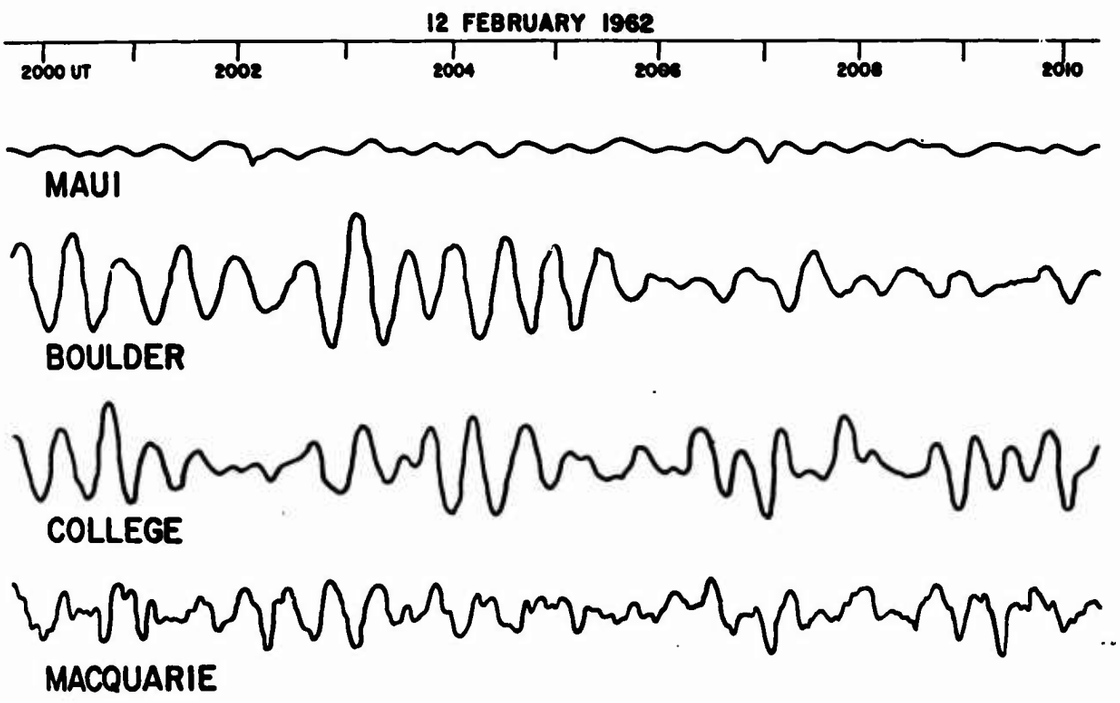

Figure 12. A pc 2-3 event recorded simultaneously along the Pacific Ocean region on 12 February 1962 (Campbell, 1963).

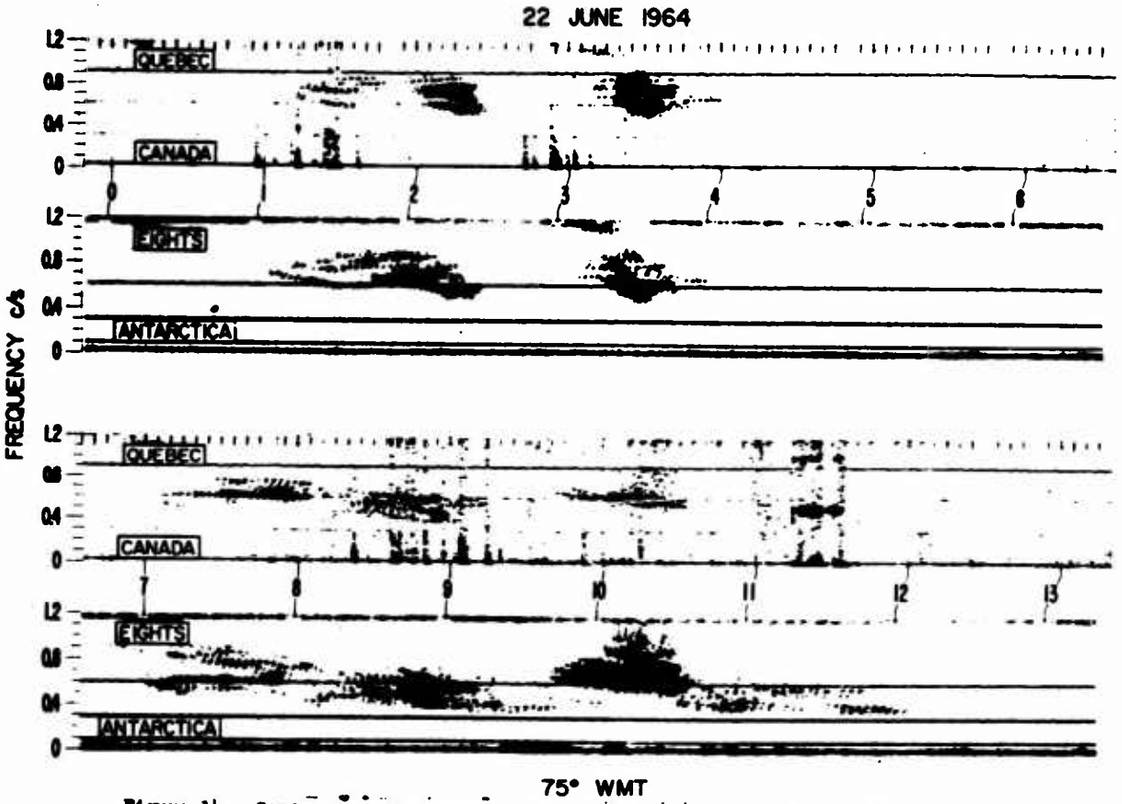

Figure 14. Conjugate pc 1 events at Baie St. Paul, Quebec, and Eights, Antarctica, on June 22, 1964 (Campbell, 1967a).

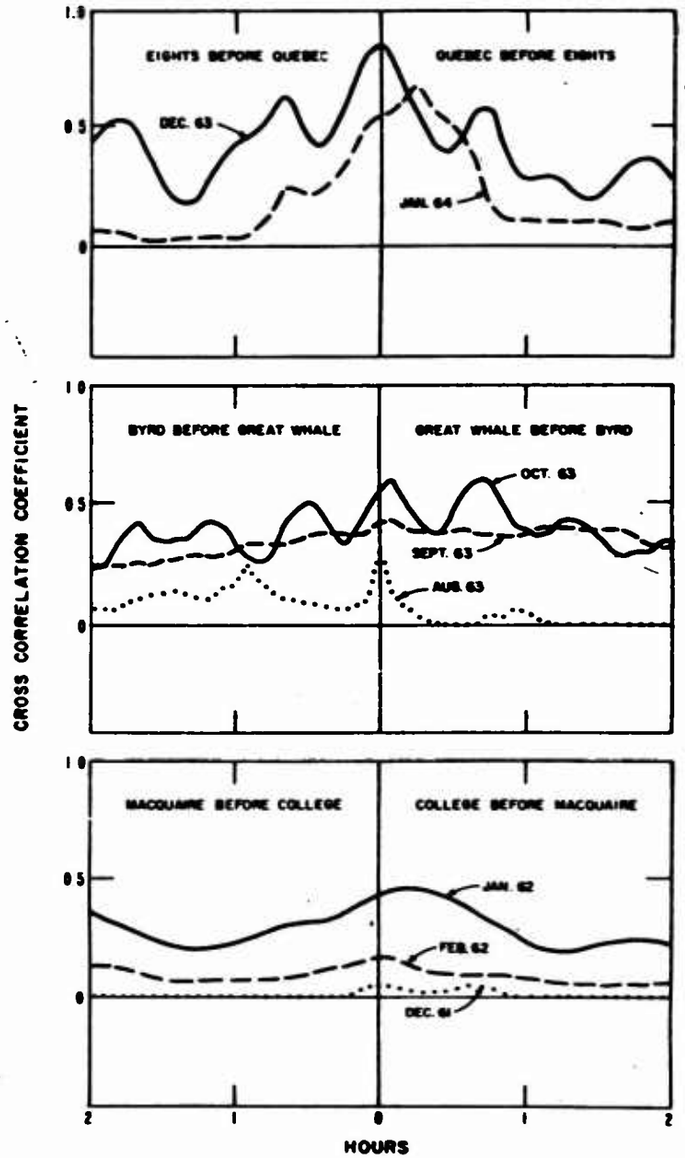

Figure 13. Monthly cross-correlation diagrams for 5-min scalings of pc 1 events at three sets of conjugate stations for lead and lag period to two hours (Campbell and Stiltner, 1965).

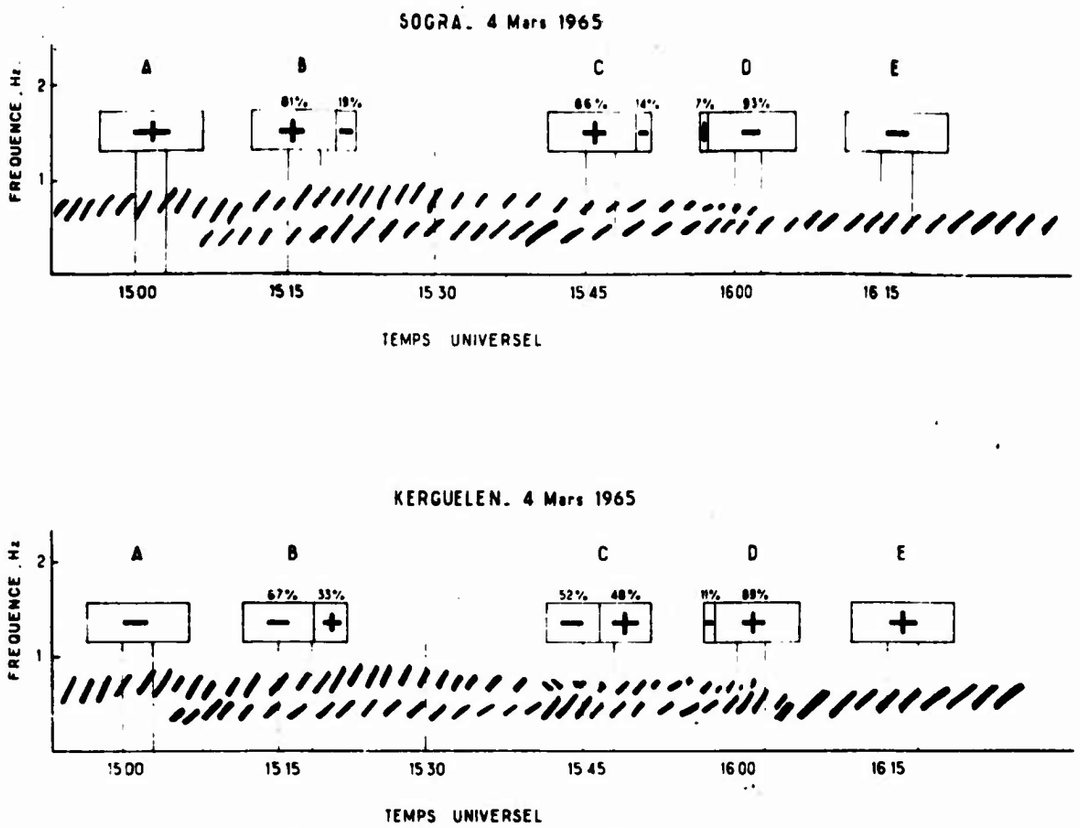

Figure 15. Average polarization sense in horizontal plane for pc 1 events measured simultaneously for the periods indicated at Sogra, USSR, and Kerguelen Islands on 4 March 1965. Percentages indicate the proportional mixture of + and - rotation sense (Gendrin et al., 1966).

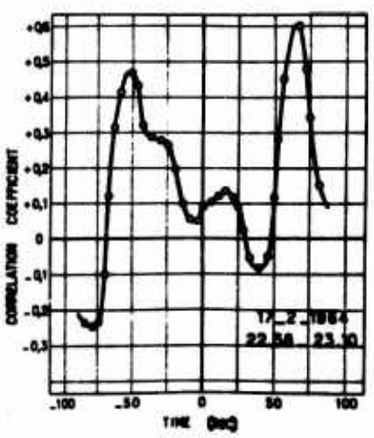

Figure 16. Correlation function for envelopes of pc 1 signals received at Borok and Kerguelen on February 17, 1964 (Borsukov and Ponsot, 1964).

Pi Events

J.A. Jacobs

Institute of Earth and Planetary Sciences
The University of British Columbia
Vancouver 8, B.C., Canada

1. Introduction

The amount of literature on irregular micropulsations (Pi) is relatively sparse, particularly when compared to that on the more regular, continuous pulsations, and very little work has been done on the characteristics of Pi activity at conjugate points. Originally such irregular micropulsations, which tend to appear during the initial stages of relatively large scale geomagnetic disturbances known as bays, were designated Pt. At the 13th General Assembly of the IUGG, Jacobs et alia (1964) proposed the present classification of impulsive micropulsation activity known as Pi; this was subdivided into the categories Pi 1 (periods 1-40 sec.) and Pi 2 (periods 40-150 sec.). Pi 1 are usually seen in the initial stages of a Pi 2 and appear as riders on the longer period pulsations.

2. Pi 2

2.1 The frequency spectrum of Pi 2's

As in the case of auroral and geomagnetic bay activity, Pi 2 micropulsations have a maximum occurrence frequency around local midnight. The relationship between the occurrence of Pi 2 and planetary magnetic activity is, however, not clear. Yanagihara (1959) has presented evidence that, while auroral and geomagnetic bay activity increase towards sunspot maximum, Pi 2 activity in low latitude regions decreases. On the other hand, he found that the probability of occurrence of a Pi 2 increases with increasing Kp index (Yanagihara, 1960). At the same time Pi 1 activity increases towards sunspot maximum, suggesting that either Pi 1 and Pi 2 have different source mechanisms or that they have different modes of propagation over the earth's surface. Rostoker (1967a) has shown that Pi 2 may be considered to consist of two separate contributions: the initial kick which is a broad band effect and the actual damped oscillation. Sometimes the initial kick may occur but insufficient energy is imparted to the mechanism of generation to cause an oscillation to take place. Such kicks appear often prior to an auroral breakup, and Rostoker has referred to these occurrences as "one pulse effects".

Spectral analysis of Pi 2 trains bear out this picture. Rostoker (1967b) found that, exclusive of Pi 1 activity, a Pi 2 may contain anywhere from one to several frequency components (see Figs. 1 and 2). None of the frequency components in the spectra he obtained were present prior to the initiation of the Pi 2 event. In his analysis of 18 Pi 2 events periods as long as 286 seconds were found. Thus it appears as though the range of Pi 2 should perhaps be extended to 300 sec.

2.2 The relationship between Pi 2 activity and the Kp index

Rostoker also found that the number of frequency components in a Pi 2 event increased approximately linearly with increasing Kp index (see Fig. 3), reminiscent of the relationship obtained by Yanagihara (1960) of the probability of occurrence of a Pi 2 as a function of the Kp index. The frequencies measured in each event were usually not harmonics of a fundamental frequency and thus each frequency may be thought of as having a separate generation from one another.

Troitskaya (1964) has given evidence that the period of a Pi 2 decreases with increasing Kp index; however, this conclusion is a result of the assignment of a single frequency

to a Pi 2 event by visual analysis of chart recordings. With the aid of power spectra of 18 Pi 2 events, Rostoker (1967b) has shown that the minimum period in a Pi 2 event decreases with increasing Kp while the maximum period increases with increasing Kp up to Kp 2o, after which it decreases slightly with further increase in Kp. Visual analysis of the 18 events reveals a decrease in dominant apparent period with increasing Kp, in accordance with the results of Troitskaya. Rostoker's results also indicate that the period of a given Pi 2 event does not change with latitude for a single event, although Eleman (1966) has shown that the average period of many Pi 2's at a given station is longer the closer the observing station is to the auroral zone.

2.3 Polarization characteristics of Pi 2's

It is generally agreed that Pi 2's are polarized in the horizontal plane in mid and low latitude regions, although there is usually a relatively strong vertical component in the vicinity of the auroral zone of an event. The results obtained at low latitude stations by Kato et alia (1956) indicate that Pi 2's are polarized in a clockwise sense before

local midnight. This is in disagreement with the results of Christoffel and Linford (1966) who found that Pi 2's were polarized predominantly, although not always, in a clockwise sense in midlatitude regions in the southern hemisphere.

Rostoker (1967a) showed that the polarization of Pi 2's in midlatitude regions in the northern hemisphere is predominantly in the anticlockwise sense, although cases of clockwise rotation are observed on occasion. He found that the sense of polarization does not depend on the position of the observing station relative to local midnight, but that its geographical location relative to the source of the Pi 2 directly influences the polarization characteristics.

The implication of the results of Rostoker and those of Christoffel and Linford is that at least the last part of the propagation of Pi 2's may be dominated by the Alfven mode of a hydromagnetic wave propagating through the ionosphere in a direction parallel to the ambient field lines. However, the fact that some clockwise pulsations are observed in the northern hemisphere and some anticlockwise pulsations in the southern hemisphere suggests that the mode of propagation of a Pi 2 is not a pure Alfven wave.

The observed polarization characteristics indicate that Pi 2 micropulsations cannot be described by a simple

equivalent current system such as that used to describe a bay. Such a current system would provide an "in phase" relationship between the H and D components which is not observed to be the case. Nor can a rotating line current such as that proposed by Wilson (1966) for Pc 4, Pc 5, and Pg-type micropulsations fully describe the source mechanism for Pi 2's, since for anticlockwise rotation of the current system all pulsations in the northern hemisphere should be polarized in an anticlockwise sense, which is not the case. The appearance on occasion of a clockwise rotation at a station while the sense of polarization at other stations for the same event is anticlockwise, together with the fact that the dominant sense of rotation is anticlockwise in the northern hemisphere, and clockwise in the southern hemisphere, suggests that the disturbance is subject to propagation effects and hence in midlatitude regions Pi 2's may be considered to propagate as a wave rather than being the effect of an ionospheric current system.

Although Pi 2 micropulsations as a whole seem to be unrelated to the bay type equivalent current system, the initial kick on the magnetogram appears to be strongly correlated with the polarity of the accompanying bay. In general the direction of the initial kick of either component on the micropulsation record has the same sign as the polarity

of the corresponding component of the bay; this effect is strongest in the D component, although it is also prominent in the H component.

It is suggested that the initial kick of a Pi 2 micropulsation may be represented by an equivalent overhead current system in the manner shown by Jacobs and Sinno (1960). The current is set up in the Hall region of the ionosphere as a consequence of the fact that the ambient ionospheric particles cannot respond sufficiently rapidly to the first hydromagnetic impulse generated in the breakup.

2. Possible source mechanisms for Pi 2 activity

The initial hydromagnetic impulse arriving in the auroral zone from the tail region of the magnetosphere is broad band, containing periods ranging from those of a Pi to a bay. Near the source all the frequency components arrive at approximately the same time, and thus the leading edge of the bay near the source is very steep. However the dispersive effect of the ionosphere on the propagation to lower latitudes causes the higher frequencies to arrive at a field point earlier than the lower frequencies; this effect results in a spreading on the time axis of the impulse, and the lead-

ing edge of the bay becomes less steep the further it is observed from the source. In this respect the bay and initial pulse of the Pi 2 may be regarded as part of the response of the ionosphere to a hydromagnetic impulse generated in the magnetosphere. Ward (1963) has endeavored to find the transfer function of the magnetosphere, that is, how the incoming solar plasma generates hydromagnetic disturbances which, when modified by the ionosphere, are received on the surface of the earth.

Rostoker (1967a) suggests that Pi 2's originate as eigen oscillations on auroral zone field lines, although the initial movement is probably due to a current system set up in the ionosphere as an impulse response to the influx of energy from the tail of the magnetosphere. That part of the Pi 2 generated by the eigen oscillations of the field lines is thought to propagate through the E region of the ionosphere, and the observed polarization at a field point is determined by the screening effect of the ionosphere over that point.

Herron (1966) observed sizeable phase shifts (of the order of seconds) in the appearance of micropulsations at stations separated by hundreds of kms along an east-west line. From Herron's results the relationship between the projected velocity of propagation of the disturbance and its period appears to be hyperbolic in nature. Rostoker (1965)

showed that Pi 2 micropulsations can be described by a weak coupling of fluid and electromagnetic disturbances in which the electromagnetic contribution is dominant. Any variation in the values of the parameters which may occur in the course of propagation of the waves over the earth's surface may cause one or other of the coupled modes to become dominant. Thus alterations in ionospheric conductivity caused by the precipitation of auroral particles will cause the waves to acquire irregular phase velocities during the course of their propagation from the source of the pulsations to the field points. In particular, in the case of pulsating auroras different phase shifts between two stations would be expected for different sets of peaks in a chain of pulsations. Rostoker observed this to be the case for the horizontal components of Pi 2's observed at Vancouver, B.C., and Ralston, Alberta.

3. Pi activity at Great Whale River and Byrd Station

When Pi activity can clearly be recognized on the records as by the abrupt commencement of polar substorms they occur within a minute or two at stations in and between the two auroral zones over large areas of the earth. The changes when sufficiently abrupt have been called psc's (polar sudden commencement or change) by analogy with the much larger commencements (ssc) of a magnetic storm. It is this system of psc events, the following impulsive Pi activity and the preceeding quiet interval that governs the general pattern of nighttime activity at the pair of conjugate auroral zone stations, Great Whale River, Quebec, and Byrd Station, Antarctica. There is a very persistent statistical occurrence of psc's and psi's between 0300 and 0400 UT at these two stations. A quiet interval which often preceeds the psc makes possible greater accuracy in the timing of the event. Negative psc's without exception move initially in the direction corresponding to a decrease in H, in contrast to the relatively few (in 1963) daytime positive psc's which all moved in the direction of increasing H.

The fact that high frequency components seem to appear on the micropulsation records only when the psc events are sufficiently abrupt is not new and it has long been known

that the sudden commencements of magnetic storms are associated with frequencies up to at least 3 cps. It is known also that abrupt psc's in the auroral zones can be recognized in the midlatitudes of Canada almost simultaneously. This behaviour suggests that there might be a layer in the ionosphere that can be shock excited at its natural frequency of about 1 cps. It is then natural to consider the sudden event as being caused by the shock of a sudden change in velocity of the solar wind, the effect of which is propagated towards the earth by hydromagnetic waves. The earlier, less abrupt event might possibly be due to a change in direction of the solar wind which probably occurred less suddenly.

A comparison of the times of individual negative psc's at Byrd and Great Whale has been made by Jacobs and Wright (1965). Examination of a series of 140 days from September 28, 1963, to February 21, 1964, yielded 72 cases judged suitable for comparison of times. Measurement was made to the nearest half minute from paper records moving at a speed of 6 inches per hour. This analysis showed 17 cases of zero difference, 29 cases of positive difference and 26 cases of negative difference (Byrd minus Great Whale). Excluding the 17 cases of zero difference the average differences were +1.1 minute and -1.1 minute. The differences do not conform to a smooth error curve and personal errors in

judging the times are not wholly responsible; instead we believe that the stations are not truly conjugate at the times of all negative psc's.

Green (1967) has carried out a detailed study of Pi 1 events recorded during the IQSY at Great Whale River, Byrd Station, College, Alaska and Kiruna, Sweden. In particular he investigated the nature of the conjugacy and the degree of similarity between Great Whale River and Byrd Station in an effort to better understand electron precipitation from the magnetospheric boundary. His study included comparisons of dynamic micropulsation spectra, the relationship with concurrent cosmic noise absorption and possible conductivity enhancement effects.

At auroral zone stations the occurrence of irregular and burst-like micropulsations is frequently observed. These are very different from the intrinsic regular and continuous micropulsations. Noise bursts include a wide range of frequencies and their wave forms are therefore irregular. They occur suddenly and die out after a short time. They are simultaneously accompanied by the sudden enhancement of DS fields such as negative bays. The main part of a noise burst decreases abruptly away from the central area of activity. Thus frequently no evidence of a noise burst is observed at

Churchill although the Great Whale records clearly show a noise burst and vice versa. (The distance between Churchill and Great Whale is about 1100 km.). At Victoria, Vancouver and Ottawa corresponding noise bursts are not found at all on records of the same sensitivity. On the other hand Pi 2 micropulsations are sometimes found at the middle latitude stations when noise bursts occur at Great Whale or Churchill (Yanagihara, 1963). The corresponding Pi 2 part of the noise bursts in the central area of activity in the auroral zone is not clearly seen because it is swamped by the higher activity. Generally speaking there is a conjugate relationship between Byrd and Great Whale or Churchill for noise bursts. Sometimes a burst at Byrd corresponds to one at Great Whale and sometimes to one at Churchill. The conjugacy is thus rather loose. The loose conjugacy can be explained by movement of the active centre provided that the dimensions of the active area of the noise burst are of the order of several hundred km.

4. Other forms of Pi activity

Tepley (1966) has found that other types of signals may be observed, particularly during stormy periods, which are less regular in appearance than the continuous emissions but are more regular than noise bursts (Pi 1). Signals referred to as SIP and IPDP by Troitskaya may possibly be placed in this transition category. The signal is characterized by a rising frequency fine structure similar to that of hm emissions but the structural elements do not repeat periodically. Tepley refers to these signals as storm time emissions since all events he has observed so far have occurred during magnetically disturbed periods, often in conjunction with magnetic bays. Less formally he has called such signals gurglers since when monitored aurally on time compressed magnetic tape with a speed up factor of 1000 to 2000, the signals are characterized by a sound similar to bubbles being blown under water. Occasionally rising frequency structural elements are superimposed on Pi emissions and a composite signal may be placed in the transition category, gurgler-Pi 1. Transition signals are characterized aurally by bubbly sounds similar to those made by gurglers. The occurrence times of gurglers and gurgler-Pi 1 transition signals at Palo Alto show a strong maximum around 2000 local time (0400 UT). Helms and Turtle (1964) found an almost identical occurrence curve

for impulsive high frequency micropulsations recorded at Byrd Station, Antarctica, and reported a strong intensification of visual auroral activity with each micropulsation burst.

IPDP events frequently have structural elements in the noiseand have been detected simultaneously at conjugate stations by Gendrin et alia (1966). On the assumption that these structural elements have been generated at the equator in the magnetosphere by an impulsive source, Knaflich and Kenney (1967) have interpreted the later arrival of the higher frequencies as the results of propagation in a dispersive medium. A dispersion analysis of structured IPDP elements observed during 1965 and 1966 showed that they were generated in a narrow range of solar magnetospheric longitude centred around 2000 LMT at L values 6$\sim$13. The broad band unstructured noise seems to originate in a zone of magnetic turbulence just outside the normal trapping region so that the structured elements could be the dispersed signal resulting from a broad-band impulse. That part of the magnetosphere where turbulence exists is also the same region where the field lines cease to be closed and become transported out to the tail region. Hence it is possible that the broad-band impulses that cause the amplitude enhancements are merely manifestations of the instabilities associated with opening and closing of field lines in a critical region.

Heacock (1967) has distinguished two subtypes of Pi. The first subtype are midnight Pi bursts. He found (1966) that most weak impulsive noise bursts occurring on summer nights showed an enhancement in the 2 to 6 sec. period range. There seems to be an annual variation in the mid-frequency of the enhancement with the lowest value occurring in summer - the mid-frequency varying from approximately 0.2 cps in daytime in summer to 0.3-1.0 cps during dark nights in fall and winter. Bursts tend to be seen clearly on the records only when Kp is less than or equal to 3. At times of high Kp, bursts seem to be superimposed on other Pi activity and cannot be clearly distinguished. Sudden commencements and sudden impulses that occur during the nighttime at College rarely coincide with the onset of micropulsation bursts (although ssc's that occur at College during the daytime usually coincide with the onset of micropulsation events).

In addition to impulsive bursts, the records of Pi activity at College contain events which have a continuous non-impulsive character, designated by Heacock as Pi (c). A subclass (elementary Pi (c)) are simple, isolated events characterized by the auroral electrojet being nearly stationary just north of College. These events are characterized by simultaneous negative bays in the magnetic H and Z components. Heacock found that every elementary Pi (c) event which

began in the interval 2300 - 0200 LMT was inaugurated with at least one Pi burst. Pi (c) can occur any time of the day, but are most intense in early morning near 0400 LMT. It was found that at high Kp values, Pi occurrence is increasingly dominated by Pi (c).

5. Theories of Pi's

Pc theories are quite different from Pi theories. Pc theories generally depend on some kind of resonance to achieve the narrow band effect. Although a number of sources for broad band geomagnetic noise have been suggested, including auroral electrojets and the action of the solar wind at the surface of the magnetosphere, the only detailed Pi theory is that of Nishida (1964). Nishida showed that the presence of a passing electron beam through the magnetospheric plasma modifies the character of hydromagnetic waves in such a way that an instability takes place. The situation is reminiscent of the hydromagnetic instability due to run-away electrons encountered in Project Matterhorn. With adequately chosen parameters for the beam and the ambient plasma, Nishida estimated the range of the period of growing waves generated in the magnetosphere and found close agreement with that of a

pulsation burst. As the bombardment of the ionosphere by the electron beam continues the electrical conductivity of the ionosphere would be enhanced and hydromagnetic waves incident from above would be shielded to an increasing degree. This might be the explanation of why pulsation bursts are observed only in the early stages of the development of a magnetic bay. It might also explain why the longer period part of the burst lasts for a longer time. Nishida suggests two mechanisms as possible causes of Pi 1 and Pi 2 in middle and low latitudes. The first is the oblique propagation of unstable hydromagnetic waves to lower latitudes. The second is the leakage of the screening current which flows in the auroral zone when the pulsation burst passes through the ionosphere to lower latitudes. The occurrence of Pi 2 is less frequent in solar active years than in quiet years although the activity of Pi 1 is higher in solar active years. Because the ionospheric conductivity would be higher and the degree of ionospheric screening and the intensity of the screening current would also be higher in solar active years it might be possible to account for Pi 2 by oblique propagation and Pi 1 by the leakage of the screening current.

Although there are many examples of good correlation between micropulsations at conjugate points, it is not obvious that there should be perfect correlation since conjugate

points are defined by the geometry of the static field. There are many important questions requiring answers, some of which are: How much of the lack of conjugacy is due to magnetic activity? How much to the magnitude of the disturbance, which we might assume determines the area of conjugate relationship and how much to the positions of the stations vis-a-vis the angle of the solar wind? To settle these questions more statistical data are required, particularly at different seasons. Limited data may give quite misleading results.

REFERENCES

1. Christoffel, D.A. and J.G. Linford. Diurnal properties of the horizontal geomagnetic micropulsation field in New Zealand. *J. Geophys. Res. 71, 891-897, 1966.*

2. Eleman, F. Studies of giant pulsations, continuous pulsations, and pulsation trains in the geomagnetic field. *Ark. Geofys. 5, 231-282, 1966.*

3. Gendrin, R., M. Gokhberg, S. Lacourly and V.A. Troitskaya. Apparition simultanée de pulsations magnétiques d'ultrabasse fréquence en phase en deux points conjugués. *Compt. Rend. Acad. Sci. Paris 262, 845-, 1966.*

4. Green, R.G. Conjugate observations of Pi 1 micropulsation events during the IQSY. (Abstract) *Trans. Amer. Geophys. Union 48, 68, 1967.*

5. Heacock, R.R. The 4 sec. summertime micropulsation band at College. *J. Geophys. Res. 71, 2763-2775, 1966.*

6. Heacock, R.R. Two sub-types of type Pi micropulsations. (Submitted *J. Geophys. Res., February 1967.*)

7. Helms, W.J. and J.P. Turtle. A cooperative report on the correlation between auroral, magnetic, and ELF phenomena at Byrd Station, Antarctica. *Stanford Elect. Lab. Tech. Rep. No. 3408-2, August 1964.*

8. Herron, T.J. Phase characteristics of geomagnetic micropulsations. *J. Geophys. Res. 71, 871-889, 1966.*

9. Jacobs, J.A. and K. Sinno. World wide characteristics of geomagnetic micropulsations. *Geophys. J. 3, 333-353, 1960.*

10. Jacobs, J.A., Y. Kato, S. Matsushita and V.A. Troitskaya. Classification of geomagnetic micropulsations. *J. Geophys. Res. 69, 180-181, 1964.*

11. Jacobs, J.A. and C.S. Wright. Geomagnetic micropulsation results from Byrd Station and Great Whale River. *Can. J. Phys. 43, 2099-2122, 1965.*

12. Kato, Y., J. Ossaka, T. Watanabe, M. Okuda and T. Tamao. Investigation on the magnetic disturbance by the induction magnetograph, Part V On the rapid pulsation, p.s.c. *Sci. Rept. Tohoku Univ. 5, Geophys. 7, 136-146, 1956.*

13. Knaflich, H.B. and J.F. Kenney. IPDP events and their generation in the magnetosphere. (Submitted *Earth & Plan. Sci. Letters, May 1967.*)

14. Nishida, A. Ionospheric screening effect and storm sudden commencement. *J. Geophys. Res. 69, 1861-1874, 1964.*

15. Rostoker, G. Propagation of Pi 2 micropulsations through the ionosphere. *J. Geophys. Res. 70, 4388-4390, 1965.*

16. Rostoker, G. The polarization characteristics of Pi 2 micropulsations and their relation to the determination of possible source mechanisms for the production of nighttime impulsive micropulsation activity. *Can. J. Phys. 45, 1319-1335, 1967a.*

17. Rostoker, G. The frequency spectrum of Pi 2 micropulsation activity and its relationship to planetary magnetic activity. *J. Geophys. Res. 72, 2032-2039, 1967b.*

18. Tepley, L.R. Recent investigations of hydromagnetic emissions, Part I Experimental observations. *J. Geomag. Geoelect. 18, 227-256, 1966.*

19. Troitskaya, V.A. Rapid variations of the electromagnetic field of the earth. *Research in Geophysics, vol. 1, edited by H. Odishaw, 485-532. The M.I.T. Press, Cambridge, Massachusetts, 1964.*

20. Ward, S.H. Dynamics of the magnetosphere. *J. Geophys. Res. 68, 781-788, 1963.*

21. Wilson, C.R. Conjugate three dimensional polarization of high latitude micropulsations from a hydromagnetic wave-ionospheric current model. *J. Geophys. Res. 71, 3233-3249, 1966.*

22. Yanagihara, K. Some characters of geomagnetic pulsation pt and accompanied oscillation spt. *J. Geomag. Geoelect. 10, 172-176, 1959.*

23. Yanagihara, K. Geomagnetic pulsations in middle latitudes - morphology and its interpretation. *Mem. Kakioka Mag. Obs. 9, 15-74, 1960.*

24. Yanagihara, K. Geomagnetic micropulsations with periods from 0.03 to 10 seconds in the auroral zones with special reference to conjugate point studies. *J. Geophys. Res. 68, 3383-3397, 1963.*

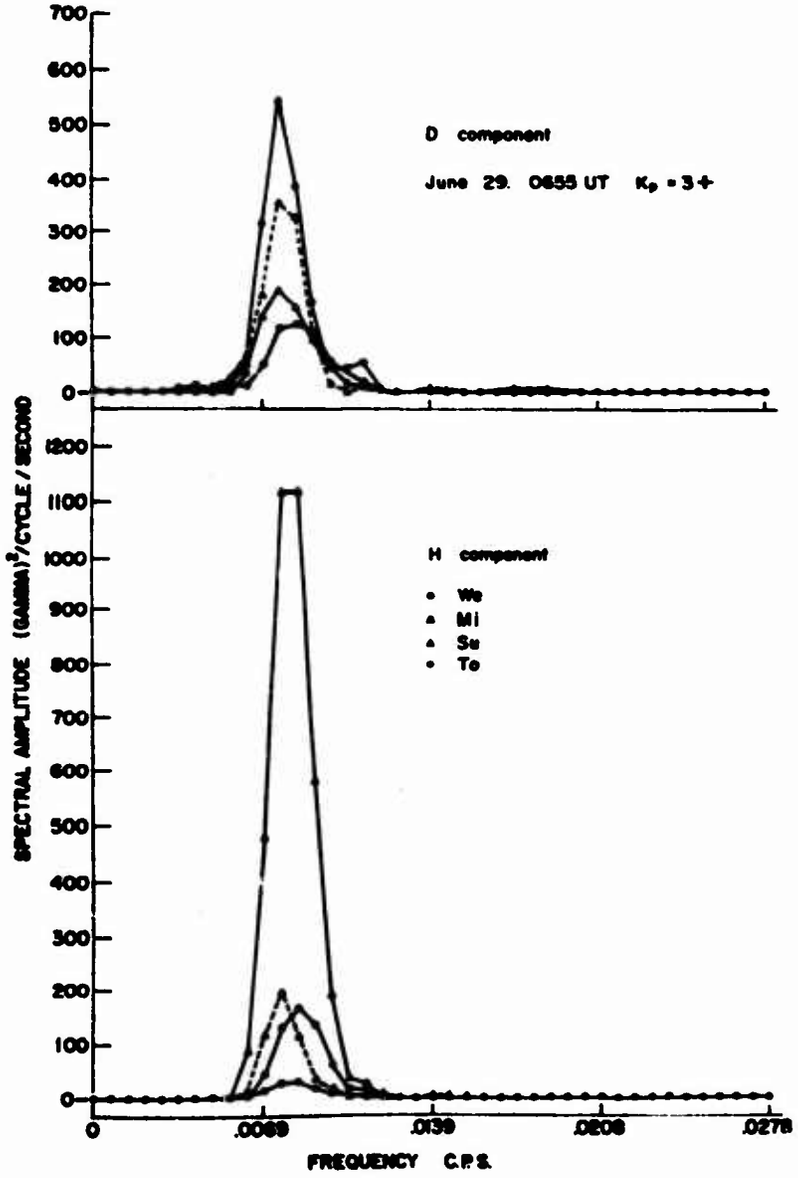

Figure 1. Example of a single-frequency Pi 2 event. (After G. Rostoker)

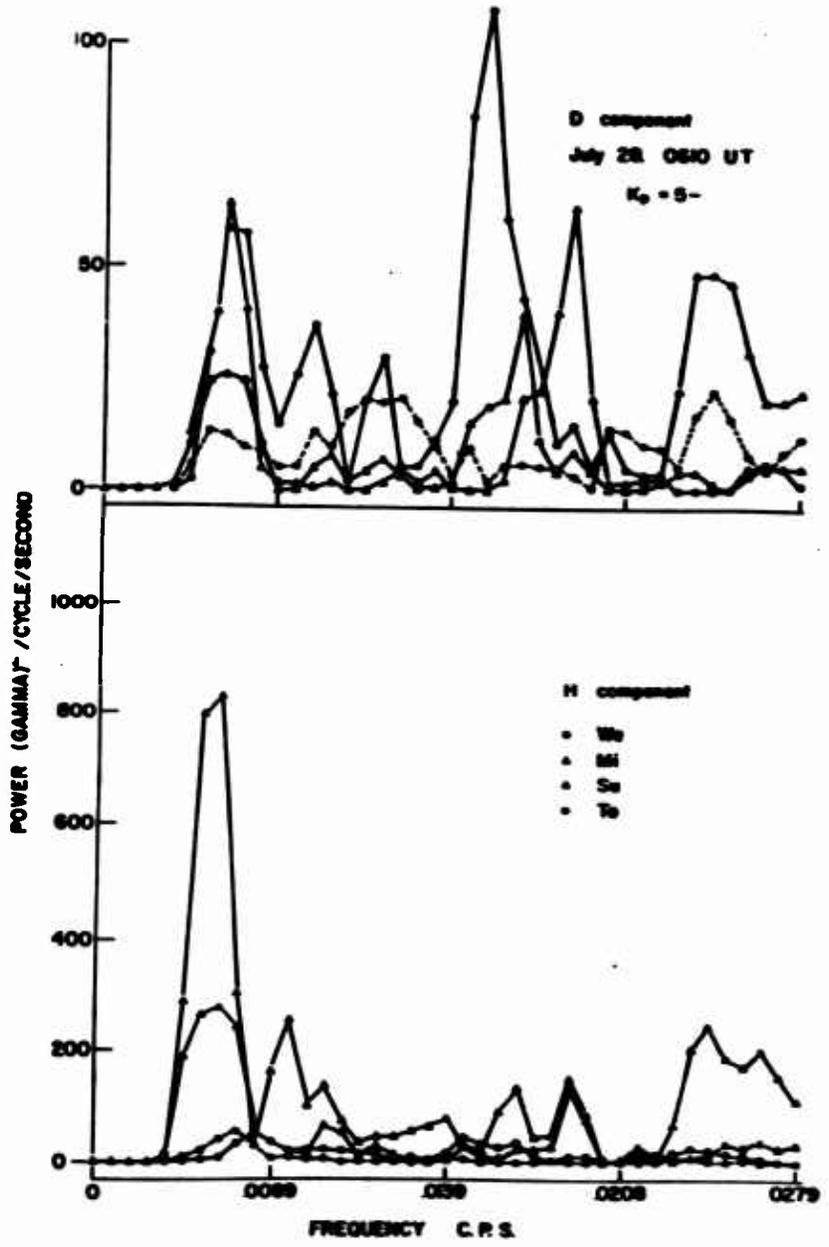

Figure 2. Example of a Pi 2 event containing several frequency components. (After G. Rostoker)

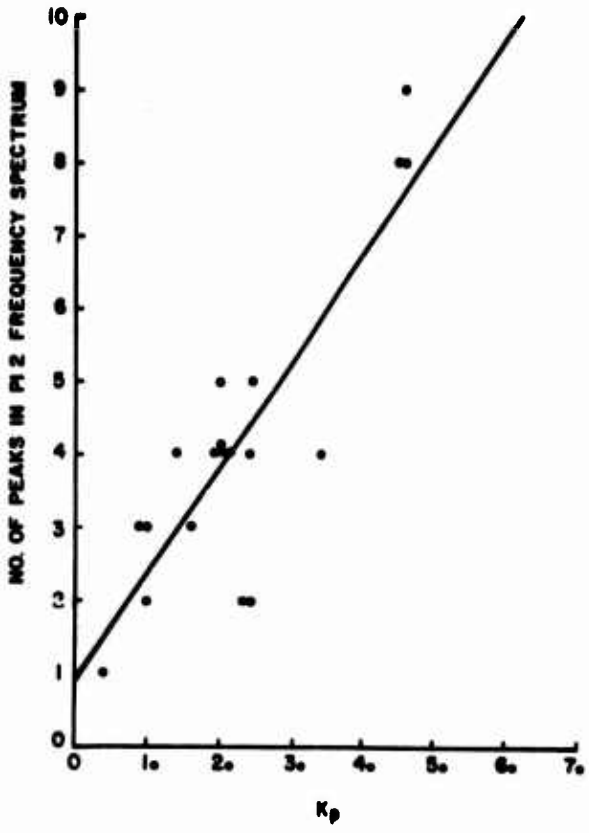

Figure 3. Number of frequency components in Pi 2 events as a function of the K_p index. (After G. Rostoker)

Conjugate Observations of the pi 1 Micropulsation Event of May 25, 1964

by

R. G. Green

Institute for Telecommunication Sciences and Aeronomy
Environmental Science Services Administration
Boulder, Colorado

1. Introduction

This is a brief account of an IQSY event that probably originated with the 108 MHz burst of May $21^{d}11^{h}46^{m}$ U.T. Conjugate ULF pulsations of irregular amplitude and period (1-40 sec) were recorded as a micropulsation storm at Baie St. Paul, Quebec, and Eights, Antarctica for several hours on May 25. These stations comprise a pair very near to the exact computed conjugacy (L = 4.0) as well as being very close to each other in local time (U.T. - 5^{h}). It is the purpose of this paper to show the nature of conjugacy between this pair of stations. Comparisons of dynamic micropulsation spectra, simultaneous amplitude spectra, and concurrent cosmic noise absorption are given.

2. Method of Analysis

For the measurements the magnetic north-south component of the magnetic flux density vector was sampled using a two meter diameter antenna of 16,000 turns. The amplified signal from the antenna was recorded with a frequency modulated, magnetic tape recording system. Sonagrams, or frequency (and intensity)-time display, are then produced for study.

3. Results

Figure 1 is such a sonagram of the entire event. There is the usual good delineation of gross features. However it should be noted that the BSP record is higher in sensitivity than the EI. Note the general impulsive behavior and broad spectrum of the frequency components. Also shown are the concurrent changes in the 30 MHz riometer ionospheric absorption in decibels above the quiet day values. Note the degree of dependence between frequency span and absorption. Figure 2 shows the event on the same time scale but with an expanded sonagraph frequency display of the portion below 0.12 cps. In quite another way, through ionospheric conductivity enhancement effects, certain features may not be at all comparable. For practically the entire event BSP was in sunlight, and EI was in darkness. There being no transitional sunlight period for either station during the storm it is not possible at this time to point out any obvious conductivity enhancement effects.

One may, upon examination of figures 1 and 2, note many groups of spectral patches concurrent at the two sites. Figure 3 is provided to show one such group.

A display of simultaneous amplitude spectra is useful to determine relative frequency enhancement. Such a display below 0.5 cps at 30^m intervals during the event is shown in figure 4.

4. Acknowledgements

This work was supported in part by the National Science Foundation. The author wishes to thank Dr. W. H. Campbell of ESSA/ITSA for suggesting this study and for many helpful discussions. Thanks are due also to F. C. Cowley of the High Latitude Physics Section of ITSA for making the riometer data available.

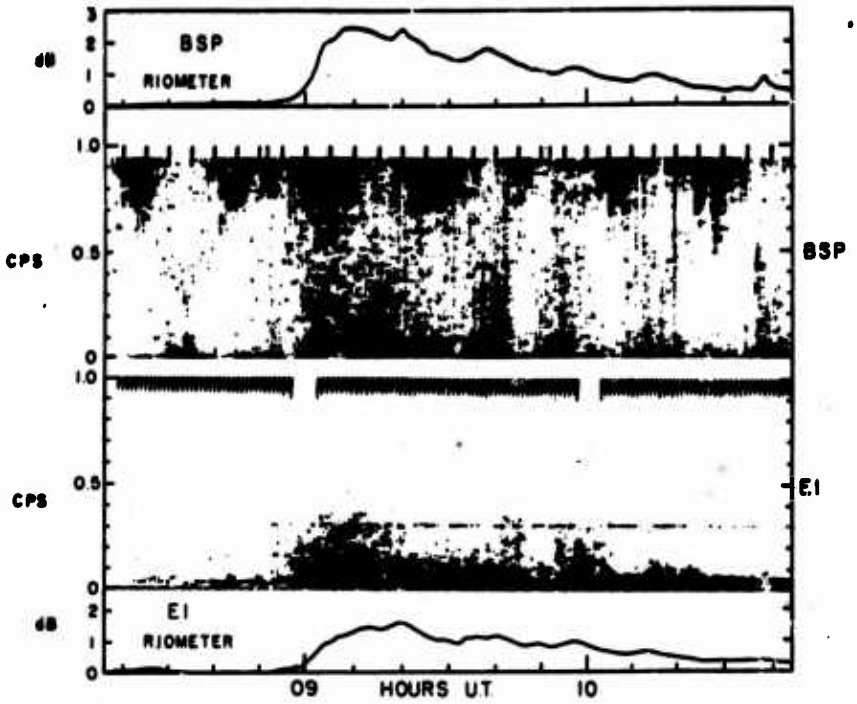

Figure 1. Sonagraph spectral display of conjugate behavior of signals at Eole St. Paul and Eights stations from 0816 to 1044 U.T. on May 25, 1964. Also shown (above and below) are the concurrent changes in 30 MHz riometer absorption above the quiet day value. On the BSP sonagram note the heavy sinusoidal noise bands occurring at 20" intervals above 0.5 cps as well as the artificially produced vertical striations elsewhere. Similarly on the EI portion noise bands are seen at 0.03, 0.1, 0.3, and 0.6 cps.

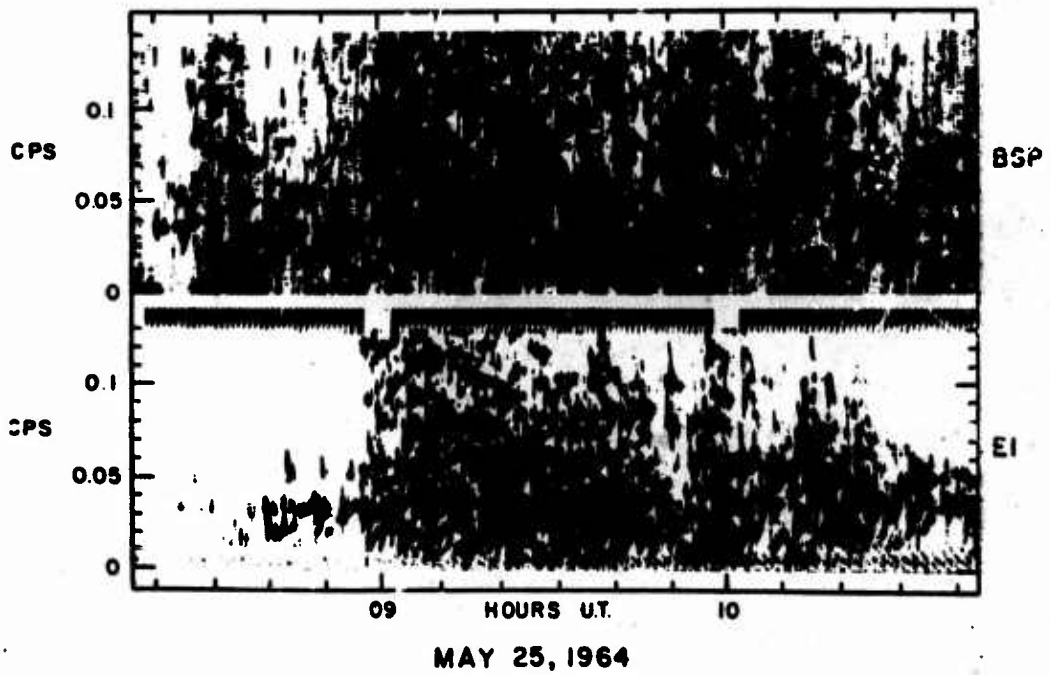

Figure 2. A portion of the previous figure expanded to show detail below 0.12 cps. On the BSP sonagram the vertical striations are artificially produced. On the EI sonagram noise bands are evident at 0.03 and 0.1 cps.

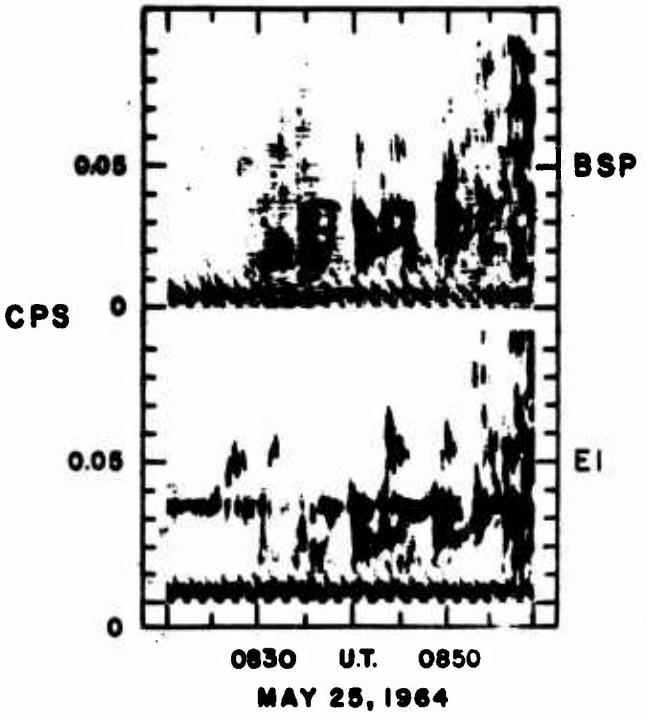

Figure 3. Some concurrent spectral patches. The vertical striations on the BSP sonagram, the noise bands at 0.03 cps, and the interference pattern near zero frequency are artificial.

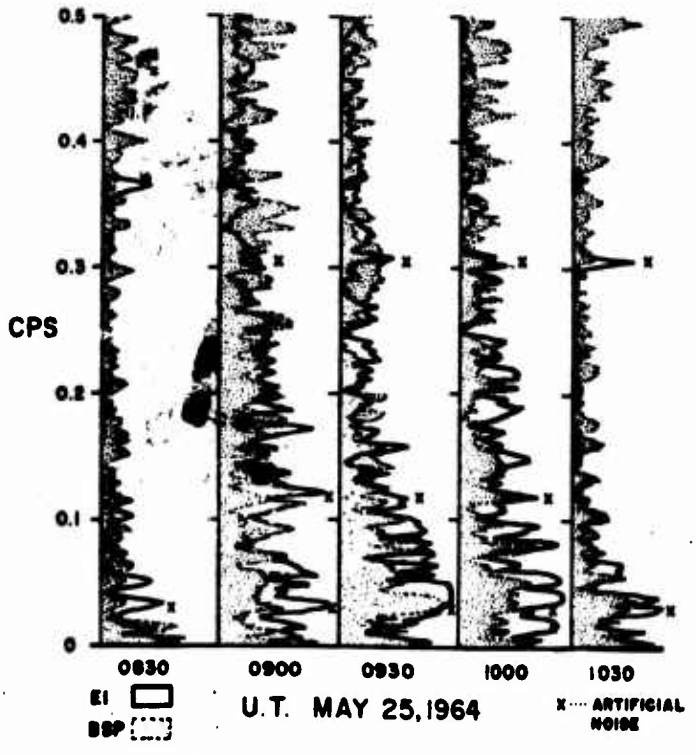

Figure 4. Simultaneous amplitude spectra at 30^{m} intervals.

Relation of Correlated Magnetic Micropulsations And Electron Precipitation to the Auroral Substorm

R. L. McPherron, G. K. Parks, F. Coroniti

Space Sciences Laboratory
University of California
Berkeley, California

Abstract

Magnetic micropulsation and energetic electron precipitation data recorded simultaneously in the auroral zone have been used to characterize distinct types of pulsation and precipitation phenomena. It is found that certain types of pulsation and precipitation are invariably associated with each other. Further, these phenomena occur only in certain limited regions of local time and are always associated with an auroral substorm. Correlated phenomena include:

Local Time 2200 - 0200, Micropulsation noise bursts and impulsive electrons, associated with auroral breakup and sudden changes in auroral electrojet.

Local Time 0200 - 1000, Band limited irregular pulsations and modulated electrons, associated with diffuse, patchy aurora and negative bays.

Local Time 1000 - 1500, Quasi-sinusoidal pulsations and modulated electrons, associated with large amplitude dayside magnetic disturbances occurring during auroral substorms.

Local Time 1400 - 1500, Magnetic impulses and microburst electrons, associated with dayside substorm disturbances.

Local Time 1500 - 2200, Micropulsation sweepers and pre-midnight pulsations, associated with no type of structured electron precipitation, but occurring only during auroral substorms.

Evidence is given substantiating the correlation between these micropulsation and energetic electron precipitation phenomena, and linking them to the auroral substorm. This evidence suggests a causal relation between modulated electron precipitation and associated micropulsation types with micropulsations playing the more fundamental role.

Introduction

Several of us from the University of California are studying the characteristics of auroral zone micropulsations and energetic electron precipitation. We have been motivated by the desire to establish two concepts. First, we believe a causal relationship exists between certain types of micropulsations and certain forms of electron precipitation. Second, we feel that both micropulsations and electron precipitation can be included in a comprehensive model of auroral zone disturbances. To demonstrate the truth of these concepts we have performed simultaneous measurements of micropulsations and electron precipitation at the auroral zone station, Flin Flon, Manitoba. Data were acquired in August and September of 1965 and 1966. Our analysis of these data supports the following conclusions:

1. Auroral zone micropulsations and energetic electron precipitation can be divided into distinct types which usually occur only in limited local time intervals.
2. Certain types of micropulsations and electron precipitation always occur together. Some of these appear to be causally related.
3. Most types of micropulsations and electron precipitation appear at their respective local times only when an auroral substorm occurs in the midnight sector.
4. Dynamical processes associated with auroral substorms are not limited to the auroral ionosphere in the midnight sector. They appear completely around the auroral zone, and throughout the magnetosphere.

The data and arguments which justify these conclusions in detail will appear in a sequence of three papers: Parks et al. (1967), McPherron et al. (1967) and Coroniti et al. (1967). In this paper we wish to illustrate the type of analysis we have carried out and to summarize our conclusions.

Instrumentation and Analysis

X-ray detectors carried by balloons to very high altitudes have provided us with precise data on the temporal characteristics of energetic electron precipitation. Various geometrical arrangements of detectors and pulse height analyzers have given information about the spatial dimensions and energy spectra of the precipitating electrons. A pair of induction coils and associated electronics at the balloon launch site detected magnetic variations. Both micropulsation and precipitation data were recorded continuously on an eight channel recorder and also on FM tape.

By visual examination of these records we identified a number of distinct types of micropulsations and precipitation. Interesting events were replayed from the FM tapes and digitized. Fourier and dynamic spectral analysis were carried out on the computer to study the frequency characteristics of pulsating signals. Numerical calculations were performed to determine source size and e-folding energy of the incident electrons.

Using riometer and earth current data from permanent auroral zone stations, we extended our electron precipitation and micropulsation data to cover, simultaneously, half of the auroral zone. Standard magnetograms from a number of auroral zone observatories demonstrated the occurrence of auroral substorms.

Experimental Results

(a) Types of Micropulsations and Electron Precipitation

Visual examination of our records shows both micropulsations and electron precipitation have a well defined diurnal occurrence pattern. We find also certain forms of electron precipitation always accompany definite micropulsation types. A summary of our results is presented in figure 1. In a paper as short as this one we shall not be able to prove in detail the truth of this picture. Detailed presentations were given at the April 1967 meeting of the American Geophysical Union in Washington, D. C. Our results are consistent with previous work which has appeared in the literature.

The region around local midnight is dominated by the most violent effects of the auroral substorms. The micropulsations are predominantly in the form of broad band noise bursts which are accompanied by impulsive electron precipitation. Fifty millisecond bursts of electrons are also observed at this time. Progressing in local time from 0200 to 1000, micropulsation activity is in the form of band limited irregular pulsations and is associated with modulated electron precipitation of 5 to 10 second period. In the region of local time from 1000 to 1500, the characteristic type of micropulsation is the quasi-sinusoidal oscillation from 15 to 40 second period. The electron precipitation is modulated at about the same period. Also, around local noon magnetic impulses are associated with microbursts. From 1500 to 2200 local time three types of micropulsations are seen. Auroral zone pearl pulsations peak around 1500. Around the dusk meridian, the so-called sweeper of I.P.D.P. events are seen. Somewhat later in local time pre-midnight pulsations occur. None of these

three micropulsation types are associated with electron precipitation.

(b) Causal Relation between Micropulsations and Electron Precipitation

We have indicated in figure 1 that micropulsations and electrons are correlated. Our analysis suggests that in some cases a causal relationship exists as well. To illustrate this point we would like to present the most convincing example we have studied so far. Figure 2 shows micropulsations of 20-40 second period beginning at 1216 (90° WMT), September 8, 1966. Modulated electron precipitation of similar period accompanies the micropulsations. This particular event was initiated by two 5-minute sequences of nearly pure 40 second pulsations at 1216 and 1220. The main pulsation event began at 1232, increasing in 20 minutes to a maximum amplitude of about 3 gammas. Thereafter, the signal amplitude decreased slowly until a new micropulsation event began at 1630. Obvious modulated electron precipitation of 20-40 second period began at the same time as the main micropulsation event and persisted throughout.

Figure 3a and b shows the results of Fourier analysis of both the X-ray and micropulsation signals. Part a contains the entire frequency spectra from DC to 10 second period plotted on a log scale. The micropulsation spectrum is made up of a number of well defined spectral peaks superimposed on a falling spectrum. The X-ray spectrum, however, falls very rapidly from DC to about 100 seconds and then appears to be made up of less well defined peaks on a more slowly decreasing background. Spectral peaks which appear to correlate have been connected by vertical dashed lines. The period of significant peaks in the micropulsation spectrum is indicated above each peak. Portions of the spectra including the 40 second peaks have been plotted on a linear scale, shown in part b of figure 3.

Visual examination of the chart records suggests that the micropulsations and X-rays are correlated at a period of 25 seconds. The spectra confirm this observation but also indicate correlation at 20, 37 and 170 seconds. It should be noted that the micropulsation peak near 40 seconds has fine structure. Furthermore, the main peak at 41 seconds does not appear to be correlated with X-rays, while the subsidiary peak at 37 seconds does.

Figure 4 illustrates the results of dynamic spectral analysis of both signals. All the features described above are clearly evident in the sonagram.

(c) Relation of Micropulsations and Electron Precipitation to the Auroral Substorm

Data obtained at one station are sufficient to determine the diurnal occurrence pattern of the auroral zone micropulsations and electron precipitation. However, these data cannot give any indication of their spatial extent. Neither can data at a single station always show the relation of these phenomena to auroral substorms. The auroral breakup and magnetic bay disturbances which characterize an auroral substorm do not generally occur in the day hemisphere. To extend our data coverage we have obtained riometer, magnetometer and earth current records from two stations east and west of Flin Flon. Kiruna, Sweden, eight hours ahead, and College, Alaska, three hours behind Flin Flon, include eleven hours in local time. The relative positions of these stations at 1500 UT are shown in figure 5. College is at 0500, Flin Flon at 0800 and Kiruna at 1600 local time.

Observations made at these three stations on the 19th of August, 1965, are shown in figure 6. The top three curves indicate the occurrence of energetic electron precipitation at these stations as detected by riometers or balloons. The fourth block contains a plot of five minute scalings of micropulsation amplitude and frequency at Flin Flon. The bottom set of curves are the horizontal magnetic field variations at the three stations. The occurrence of at least six substorms in this universal day is obvious from the characteristic bay disturbances. Comparison of the Flin Flon micropulsation and precipitation data with the magnetometer traces leads to the obvious conclusion: every major micropulsation or precipitation event occurs during an auroral substorm in the midnight sector. Although it is not evident from this figure, we find that there is one exception to this rule. Pearl pulsations do not appear to be related to substorms. All other micropulsation precipitation types mentioned above are related.

These data support a second conclusion as well. Consider the substorm which occurs over central Russia at 1500 UT as indicated by a negative bay at College. Electron precipitation begins first at College, next at Flin Flon, and later at Kiruna. By 1700 UT, precipitation is occurring simultaneously over at least half the auroral zone. By inference from our midnight data we suggest that it is also occurring over Russia. Thus, we conclude that electron precipitation appears nearly simultaneously throughout the entire auroral zone when an auroral substorm occurs in the midnight sector.

Micropulsations of the band limited irregular type occur at Flin Flon during this substorm. College earth currents also show the presence

of these pulsations. Kiruna is beyond the appropriate local time interval and no significant activity is observed. Thus, micropulsations also occur simultaneously over a more limited region during the course of an auroral substorm.

Conclusions

Before concluding, we summarize again the results of our work:

1. Auroral zone micropulsations and energetic electric precipitation can be divided into distinct types which usually occur only in limited local time intervals.
2. Certain types of micropulsations and electron precipitation always occur together. Some of these appear to be causally related.
3. Most types of micropulsations and electron precipitation appear at their respective local times only when an auroral substorm occurs in the midnight sector.
4. Dynamical processes associated with auroral substorms are not limited to the auroral ionosphere in the midnight sector. They appear completely around the auroral zone and throughout the magnetosphere.

The fact that the occurrence of an auroral substorm is present not only in auroral disturbances but also in electron precipitation and micropulsation activity throughout the auroral zone, indicates that it is the dynamical processes occurring in the magnetosphere which determine the local time characteristics of the substorm. Recent satellite observations have shown that many magnetospheric phenomena are correlated

with substorms. In order to generalize the concept of the auroral substorm to include the world-wide disturbance characteristics and to emphasize the importance of the magnetosphere in auroral zone observations, we suggest a new terminology: magnetospheric substorm.

References

Parks, G. K., F. V. Coroniti, R. L. McPherron and K. A. Anderson, Studies of the auroral substorm. I. Characteristics of Modulated Energetic Electron Precipitation Occurring during Auroral Substorms, to be submitted for publication.

McPherron, R. L., G. K. Parks, F. V. Coroniti, and S. H. Ward, Studies of the auroral substorm. II. Correlated Micropulsations and Electron Precipitation Occurring during Auroral Substorms, to be submitted for publication.

Coroniti, F. V., R. L. McPherron, and G. K. Parks, Studies of the auroral substorm. III. Concept of the Magnetospheric Substorm and Its Relation to Electron Precipitation and Micropulsations, to be submitted for publication.

Figure Captions

1. Diurnal occurrence pattern for various types of micropulsations and electron precipitations showing correlated phenomena.

2. Quasi-sinusoidal micropulsations and modulated electron precipitation of 25-40 second period, 1216 (90° WMT), September 8, 1966.

3. Fourier spectra for micropulsations and modulated electron precipitation, 1240-1440 (90° WMT), September 8, 1966.

4. Digital dynamic spectra, power spectra and computer plot of digitized data for micropulsations and modulated electron precipitation, 1240-1440 (90° WMT), September 8, 1966.

5. Locations of various auroral zone stations in local time for substorm of 1500 UT, August 19, 1965.

6. Plot showing world-wide extent and relation of electron precipitation and micropulsations to auroral substorms, August 19, 1965.

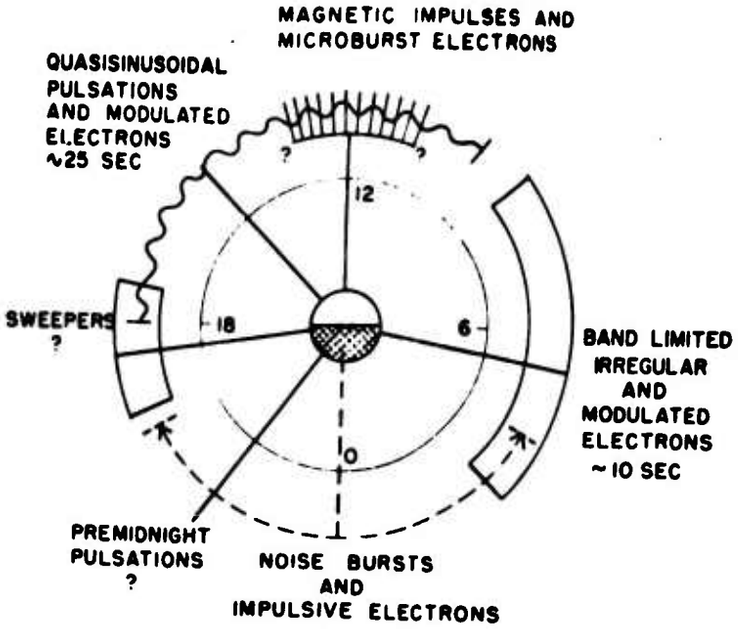

Figure 1

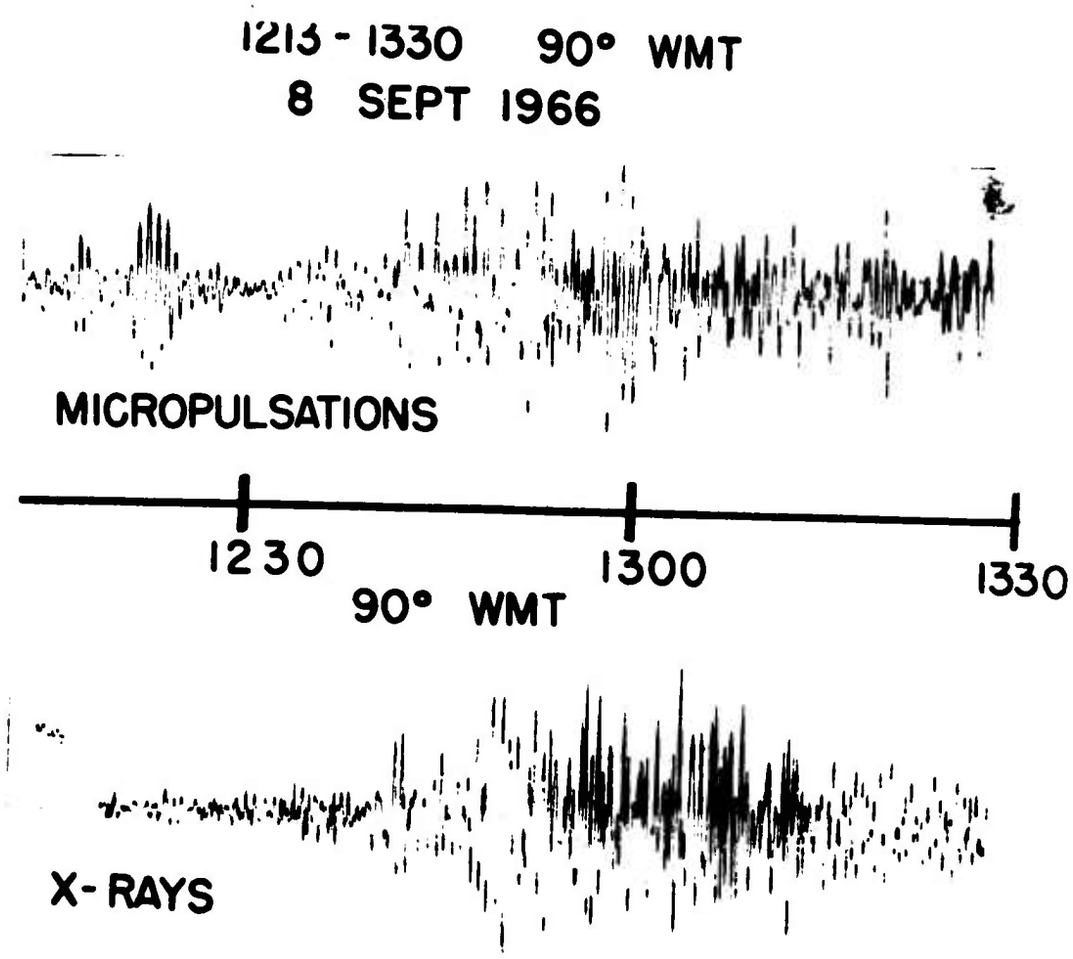

Figure 2

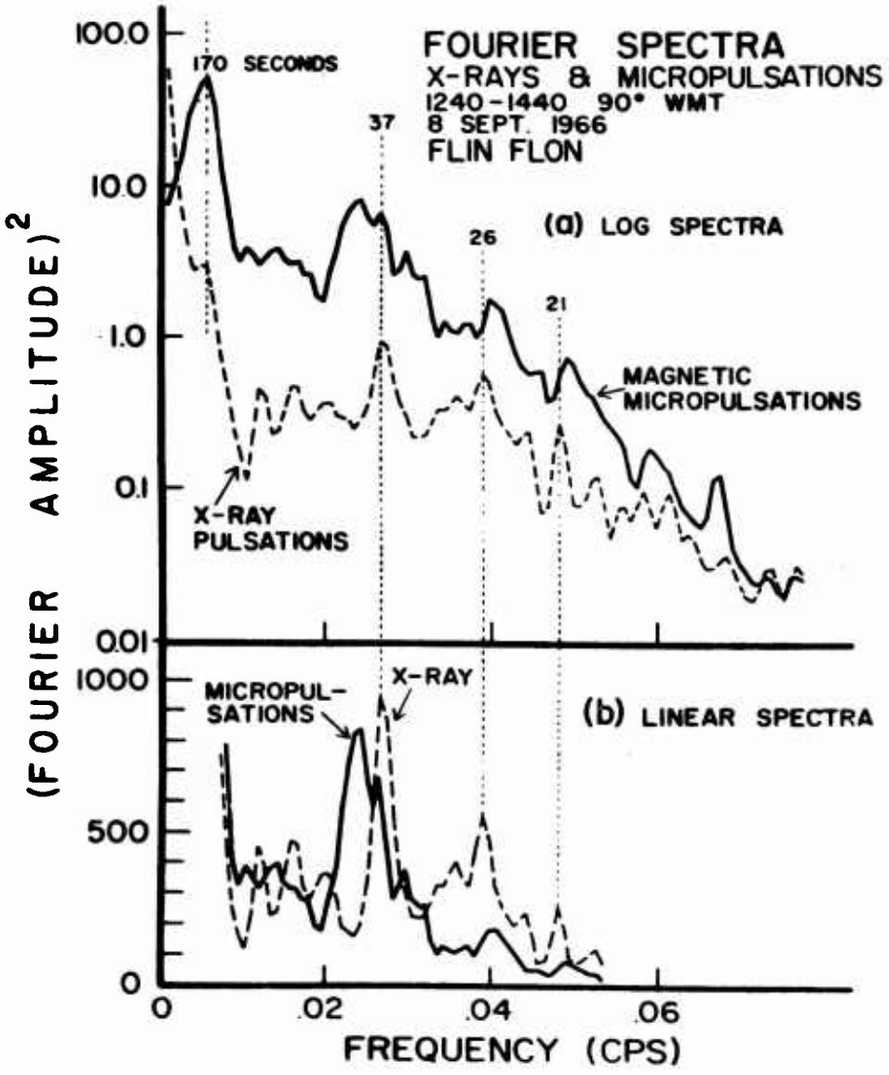

Figure 3

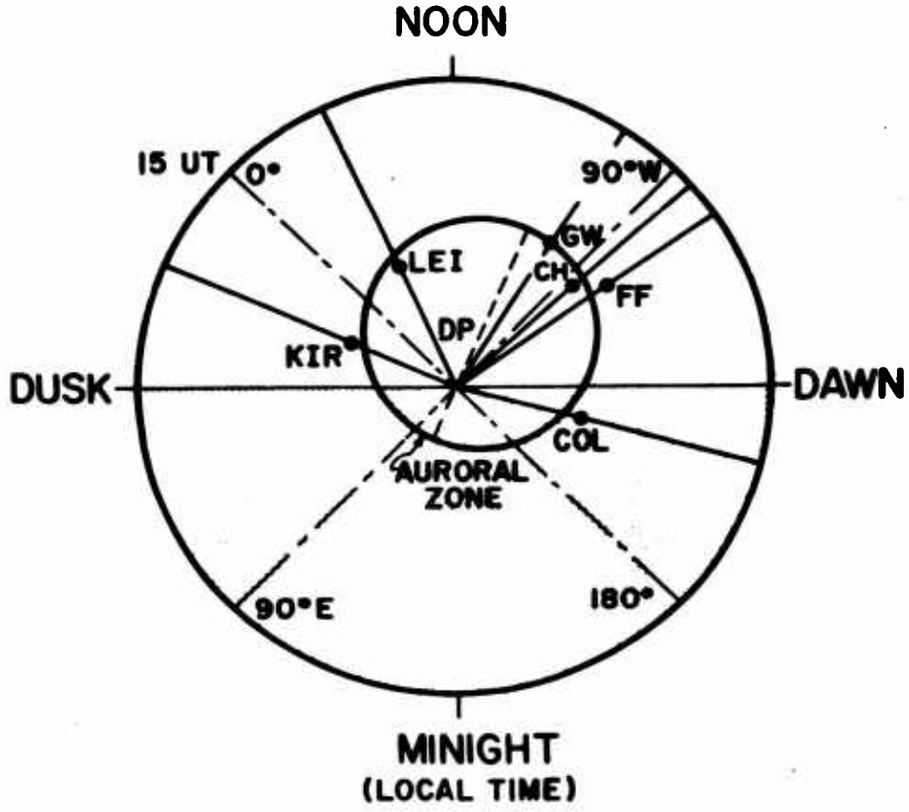

Note: Figure 4 is a color slide and not available.

Figure 5

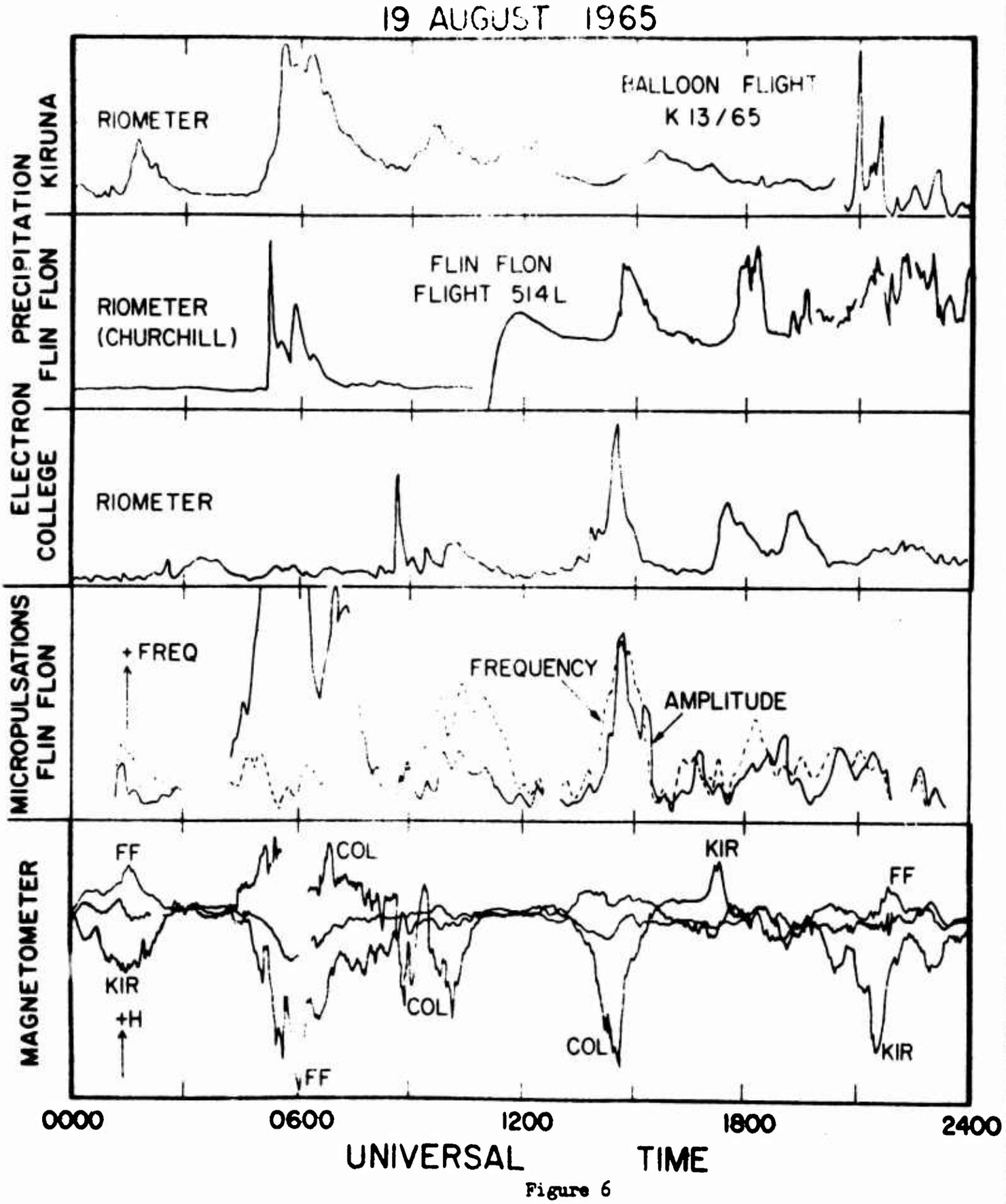
19 AUGUST 1965
ELECTRON PRECIPITATION KIRUNA
RIOMETER
BALLOON FLIGHT
K 13/65
FLIN FLON
RIOMETER (CHURCHILL)
FLIN FLON
FLIGHT 514L
COLLEGE
RIOMETER
MICROPULSATIONS FLIN FLON
+FREQ
FREQUENCY
AMPLITUDE
MAGNETOMETER
FF
COL
KIR
FF
KIR
+H
COL
COL
KIR
FF
0000
0600
1200
1800
2400
UNIVERSAL TIME

Figure 6

POLARIZATION ANALYSIS OF NATURAL AND ARTIFICIALLY INDUCED GEOMAGNETIC MICROPULSATIONS

by

R. A. Fowler
B. J. Kotick

The polarization characteristics of geomagnetic micropulsations are investigated using quasi-monochromatic wave train theory of physical optics. The polarization of a wave train is analyzed by considering the coherency matrix of the wave field. The elements of the matric are calculated over the desired frequency band and the polarization parameters evaluated. Since the determinant of the coherency matrix is zero for a totally polarized wave field, this property can be used to separate a partially polarized wave field into its polarized and unpolarized parts. The ellipticity, orientation and sense of polarization for the polarized portion are then calculated in terms of the martix elements using power and cross-power spectral analysis techniques. Based on this approach, the polarization of a number of different signals has been digitally determined. Test cases include a random number time series, a constructed signal with a predetermined polarization, and an example typical of geomagnetic micropulsations resulting from high altitude nuclear weapons tests superimposed on high natural backgrounds The results of these analyses are then compared with those from the standard hodogram technique and the effectiveness of both methods discussed in terms of the signal characteristics.

Frequency Analysis of the Geomagnetic Micropulsations Observed at the Magnetic Equator

Yoshio Kato

Geophysical Institute of Tohoku University
Sendai, Japan

The conjugate phenomena concerning geomagnetic micropulsations have been investigated by many workers and have been reported by Campbell and others in this symposium. However, at the present time characteristics of the geomagnetic micropulsations at the magnetic equator have not been so thoroughly investigated.

Prince and Bostick (1964) calculated theoretically the power spectrum of micropulsations of the extraordinary mode, propagating at 90° with respect to the earth's magnetic field from the outer boundary of the magnetosphere. Field and Greifinger (1965) calculated the transmission of micropulsations of ordinary mode which propagate parallel to the geomagnetic field.

Last year we observed the magnetic micropulsations at Huancayo, Peru whose location is near the magnetic equator. This enabled us to compare the observed power spectrum of the micropulsations at the magnetic equator with that of Maui Island, Hawaii, and Onagawa, Japan, in the middle latitude. We also compared the same magnetic micropulsations with the theoretical power spectrum of the results by the above-mentioned workers.

Before talking about these results the occurrence mechanism of pi 2 using the data of its power spectrum is proposed. Figs. 1 and 2 show examples of records of the frequency analysis of pi 2. These are reproduced through several band pass filters.

It is interesting to note that pi 2 has a broad band of periods from 1 sec to 210 sec, and it seems as if the maximum amplitude of the individual bands nearly form a series of harmonic periods as shown in the power spectrum of pi 2 in Figs. 3 and 4.

Concerning the mechanisms of the excitation of pi 2, the following were proposed by the author. We can expect a kind of instability (a neutral point instability) in the transition region of the neutral sheet of the magnetic tail (Fig. 5). The energy due to the deformation of a dipole magnetic field is stored within the magnetosphere, and the growth of the instability in the transition region is necessarily accompanied by the release of stored energy. After releasing the energy for their deformation, the magnetic lines of force around the neutral point would then be compressed toward the earth. The energy released is then used to accelerate plasma particles trapped there and to generate the hydromagnetic shock wave.

This hydromagnetic shock wave will reach the outermost side of the magnetic cavity where the hydromagnetic waves will be excited by this stress, with not only its fundamental mode but also together with its higher harmonic periods.

This ordinary wave will propagate parallel to the magnetic field line and we can observe the harmonic power spectrum on the earth's surface. Fig. 6 shows the record of pc 5, observed at Maui Island on the dayside when typical pi 2 was observed at Onagawa on the tailside.

On the other hand, the extraordinary wave will propagate to the equator and the power spectrum of pi 2 is quite different at the magnetic equator as is shown in Fig. 7 or 8 and Fig. 9 or 10, showing that the powers of short period rapidly decay (Fig. 11).

Next the results of frequency analysis of pc pulsation at Huancayo are compared with those at Maui. One of the very clear characteristics is that the polarization of micropulsations at the magnetic equator is linear, while that at middle latitudes is circular.

The frequency analysis and the power spectrum of pc at Huancayo are shown in Figs. 12 and 13. As the figures show, the power spectrum of pc at Huancayo is different from that at Maui. The slope of power spectrum in daytime at Huancayo decays rapidly and the frequency of the most resonant peak occurs in the short period at night but in the long period during the day.

This characteristic is consistent with the theoretical result presented by Prince and Bostick.

The frequency analysis and power spectrum at Maui is shown in Figs. 14 and 15. The slope of the power spectrum is not as rapid as that at Huancayo. Also the mode of the power spectrum during the day does not decay as rapidly as that at night (Fig. 16). This characteristic seems also consistent with Field and Greifinger's result, but the resonant frequency peak is not always consistent with their theory.

More detailed investigation not only of theory but also of simultaneous observations for the northern and southern hemispheres and the equatorial region at high and middle latitudes to include the day- and nightside of the earth are highly desirable.

References

Field, E. C., and C. Greifinger, Transmission of geomagnetic micropulsations through the ionosphere and lower exosphere, J. Geophys. Res., 70, 4885-4900, 1965.

Prince, Jr., C. E., and F. X. Bostick, Jr., Ionospheric transmission of transversely propagated plane waves at micropulsation frequencies and theoretical power spectrums, J. Geophys. Res., 69, 3213-3234, 1964.

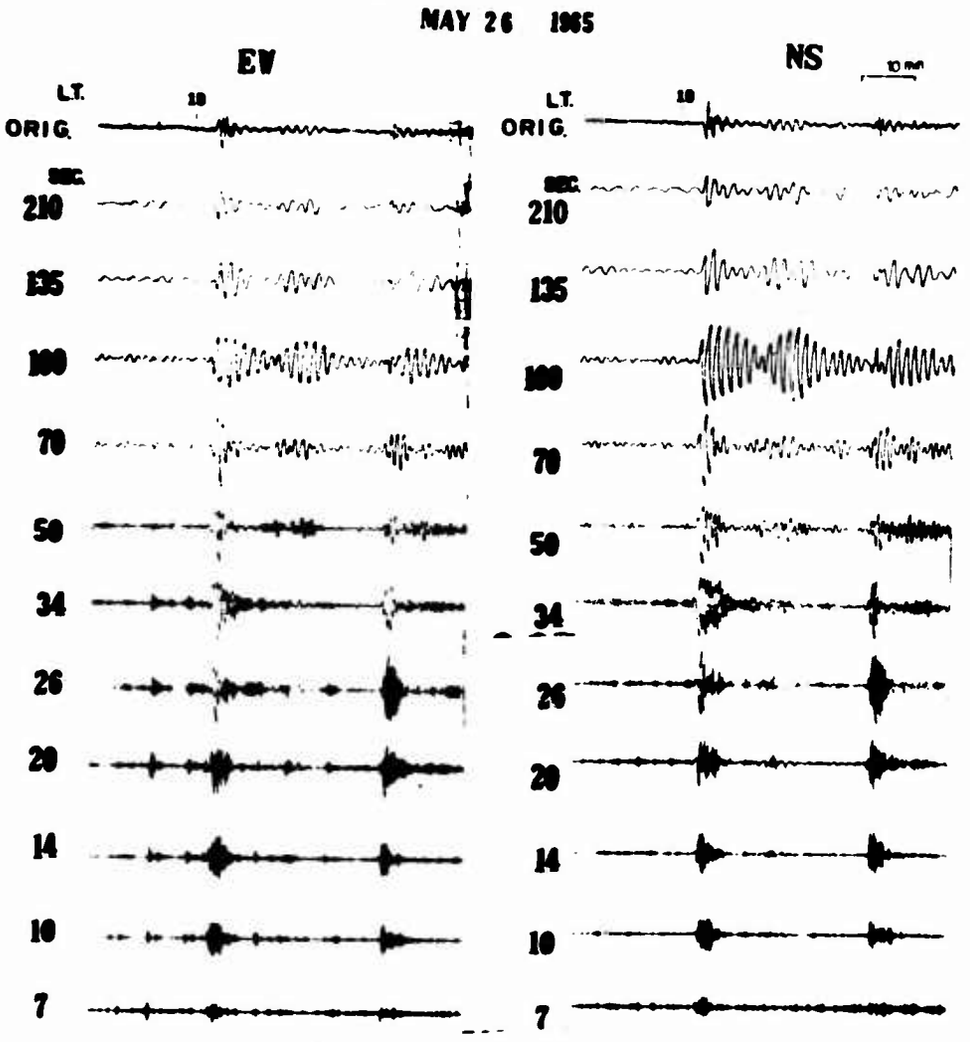

Fig. 1 Frequency analysis of pi 2.
(Observed at Maui, Hawaii)

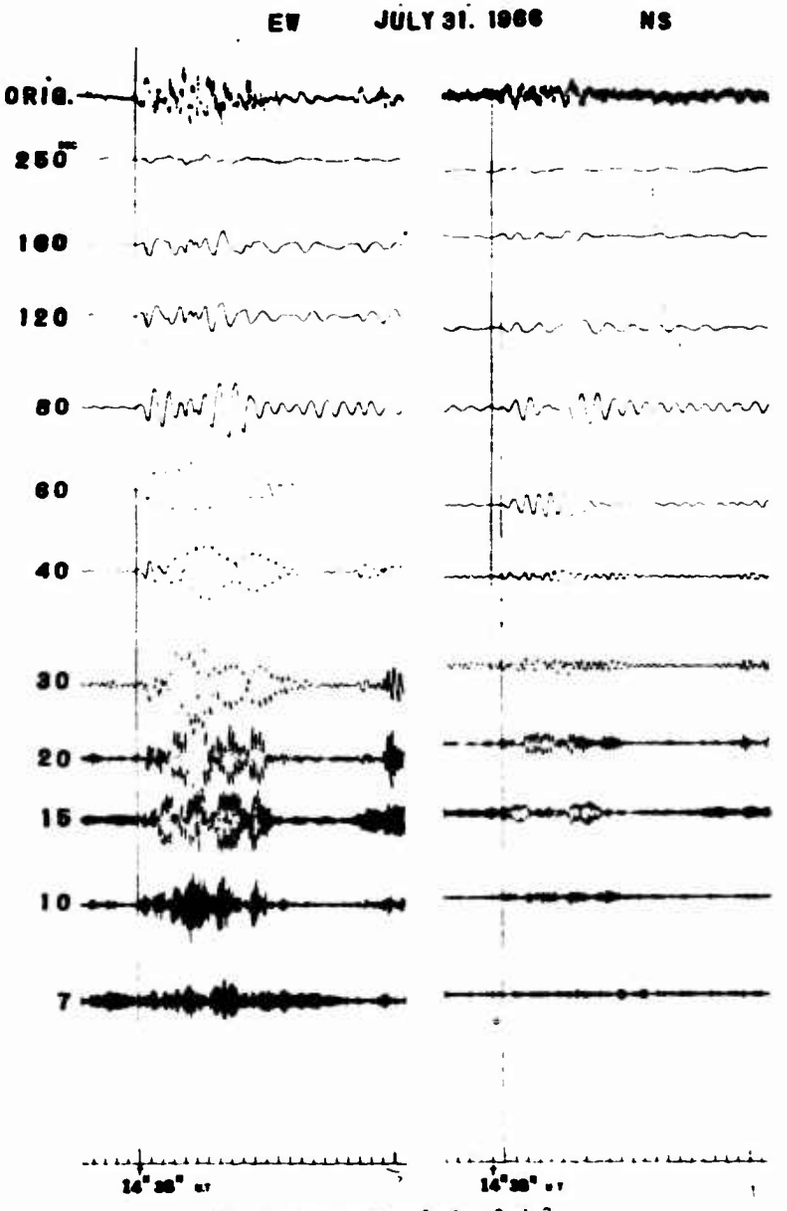

Fig. 2 Frequency analysis of pi 2.
(Observed at Onagawa, Japan)

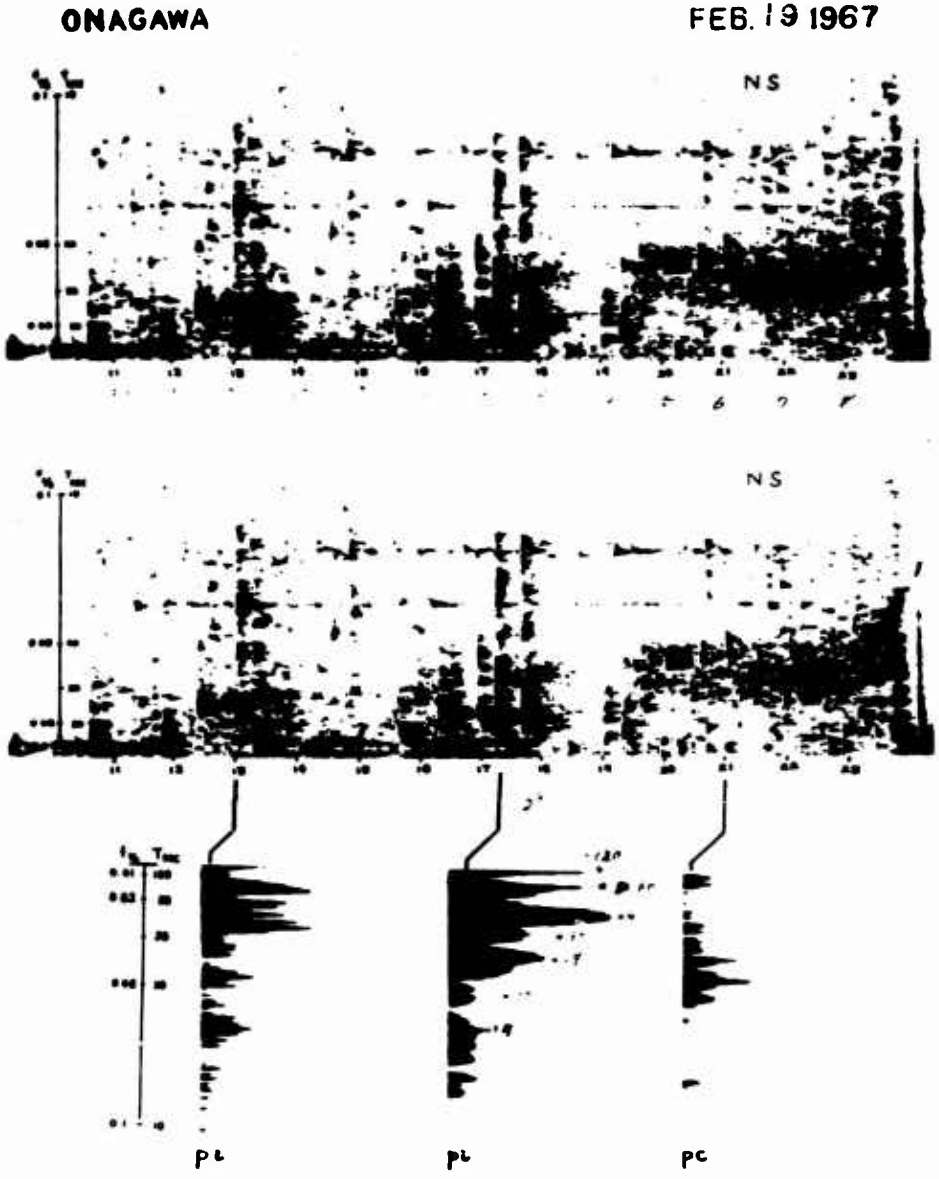

Fig. 3 Power spectrum of pi 2.

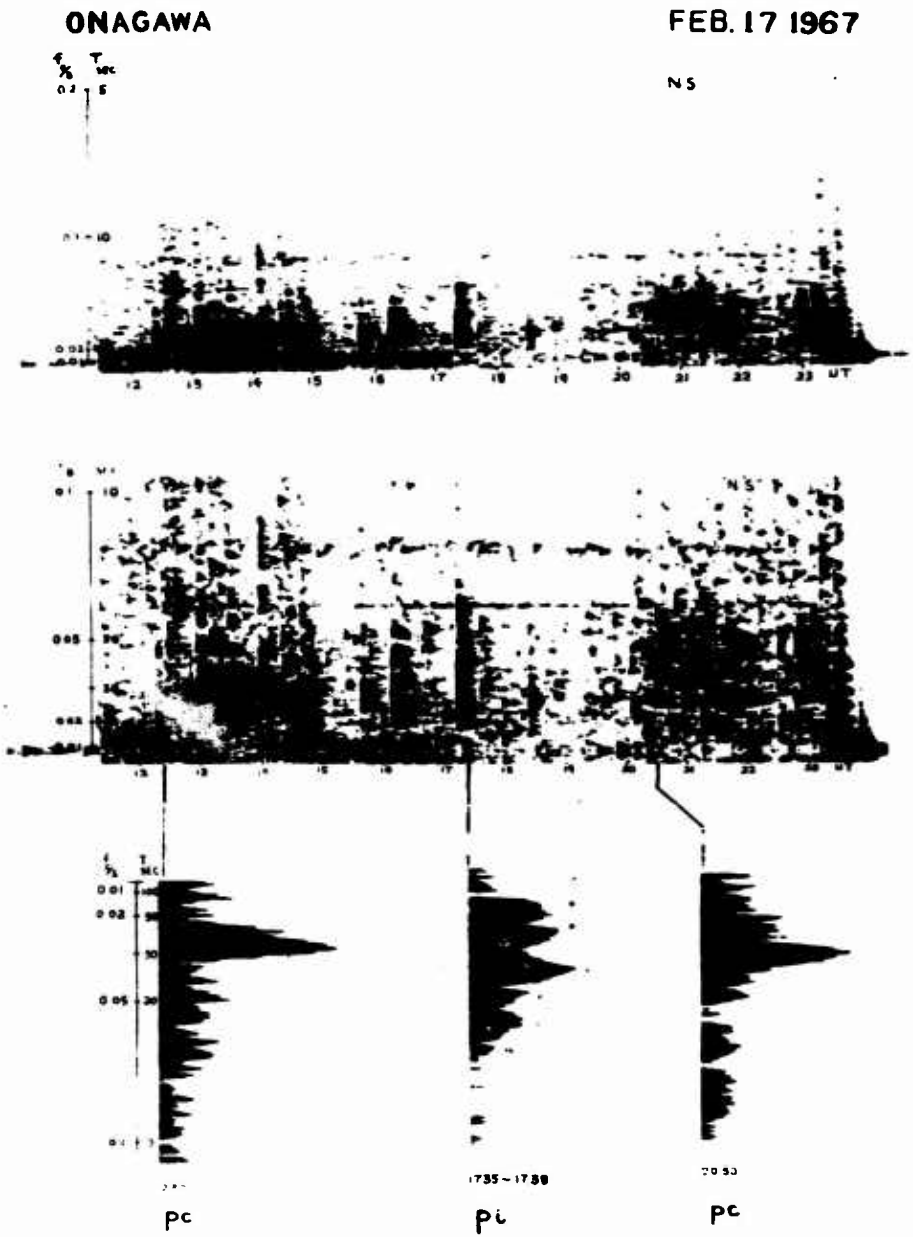

Fig. 4 Power spectrum of pi 2.

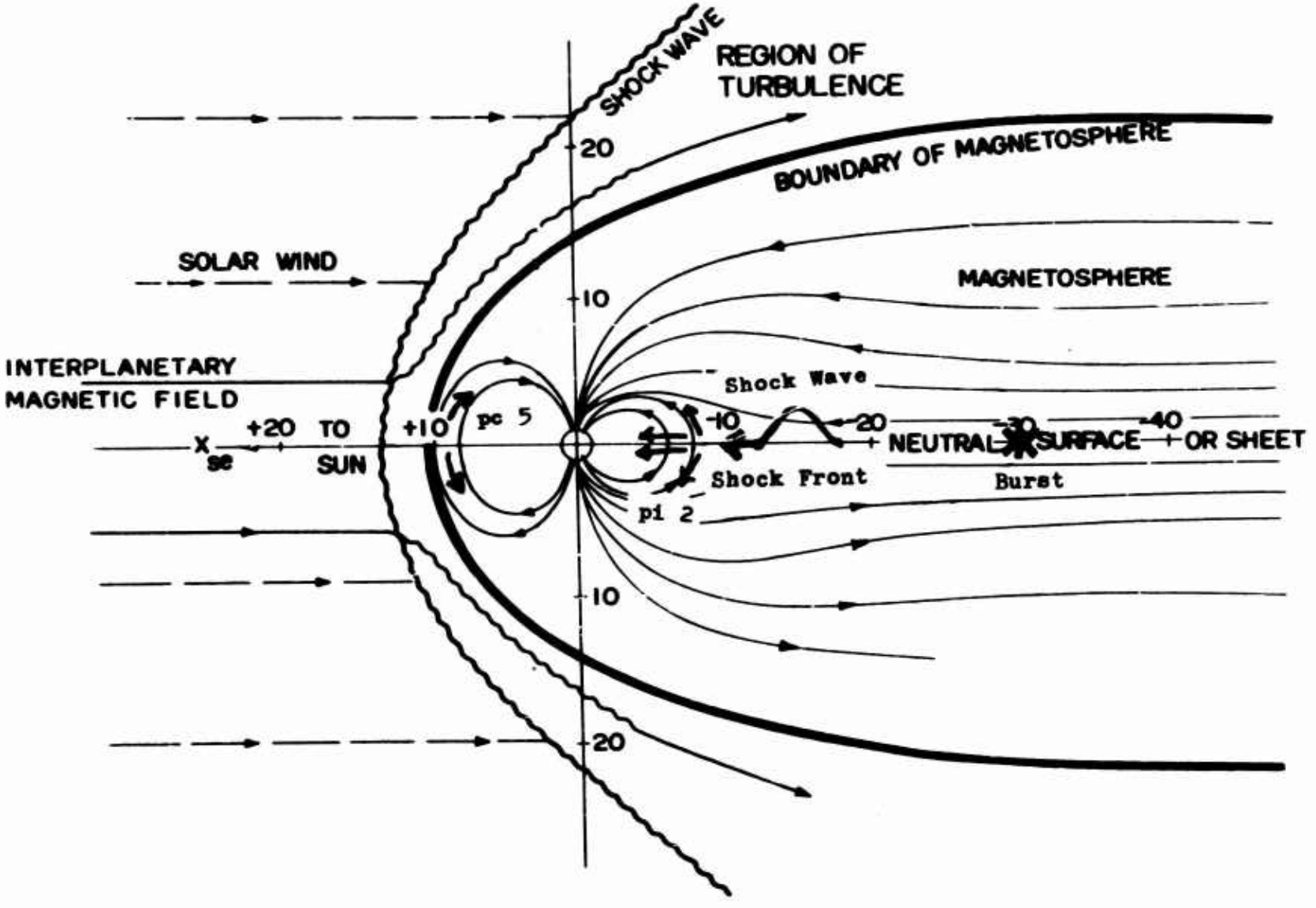
SHOCK WAVE
REGION OF
TURBULENCE
BOUNDARY OF MAGNETOSPHERE
SOLAR WIND
MAGNETOSPHERE
INTERPLANETARY
MAGNETIC FIELD
Shock Wave
+20 TO
SUN
+10
pc 5
-10
-20
-30
-40
NEUTRAL
SURFACE
OR SHEET
Shock Front
Burst
pi 2
20
10
10
20

Fig. 5

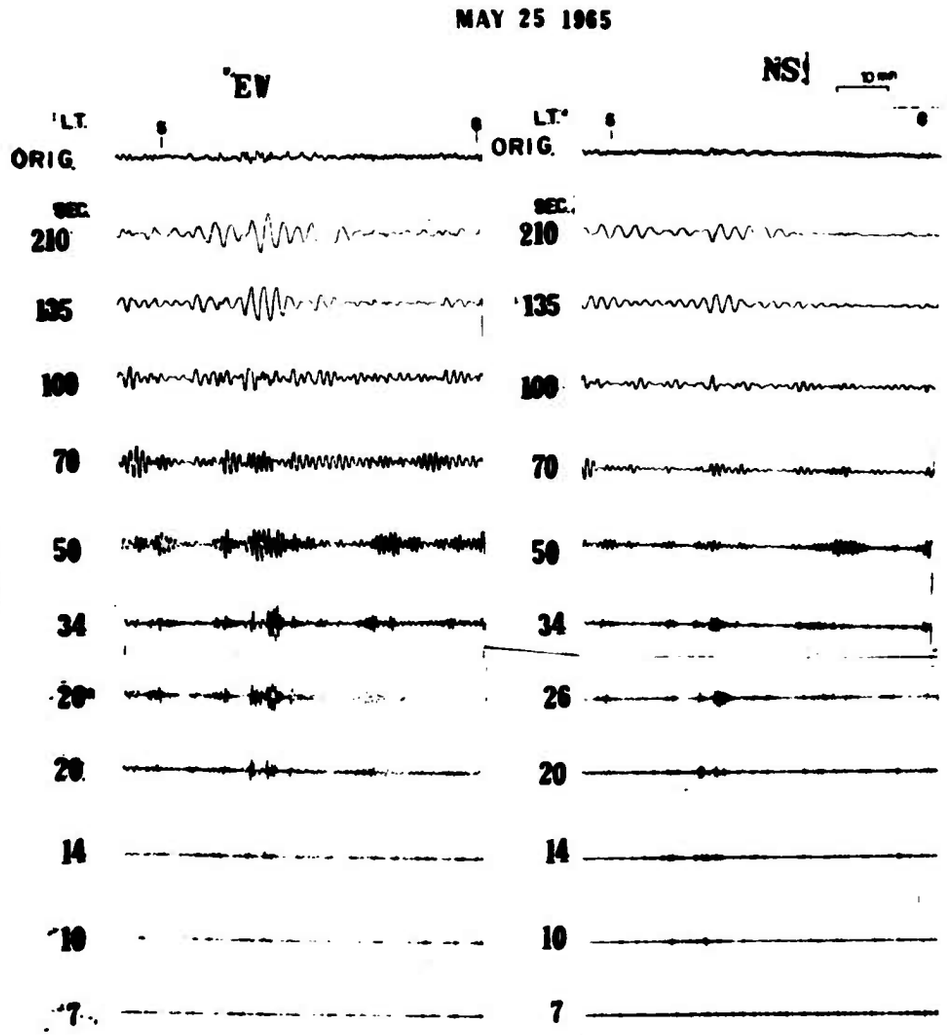

Fig. 6 One example of the results of frequency analysis of micropulsations at Maui, Hawaii on the dayside of the earth when typical pi 2 was observed at Onagawa on the nightside.

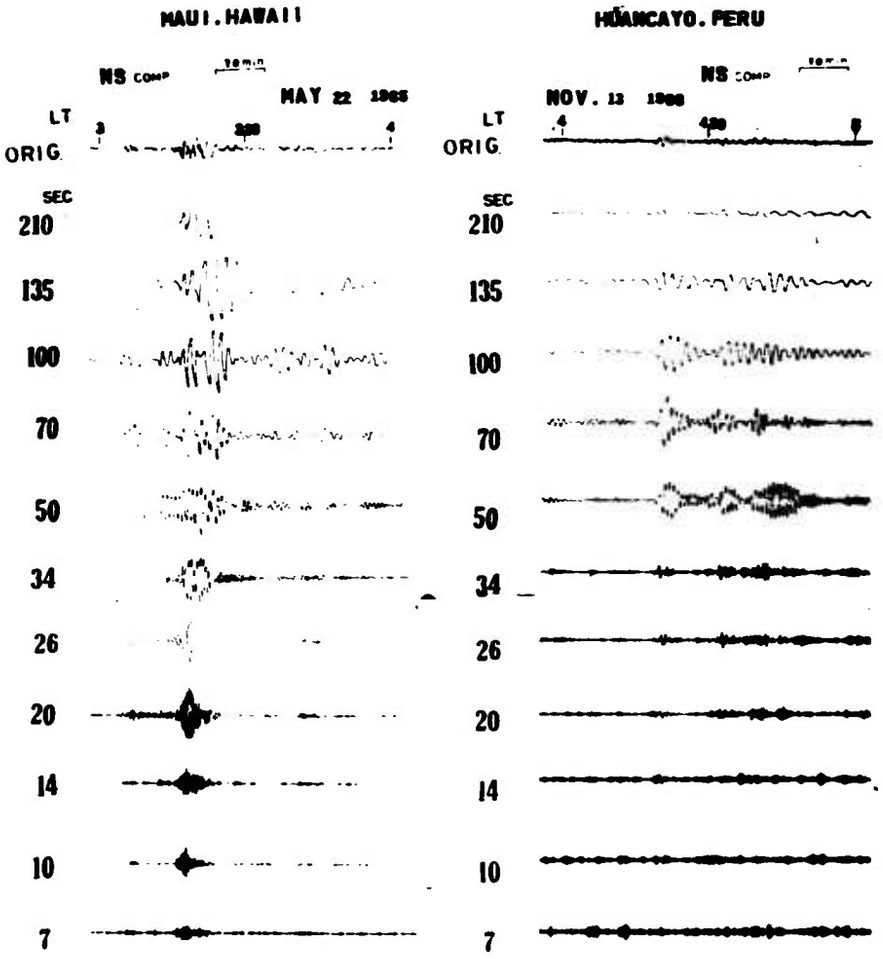

Fig. 7 Frequency analysis of pi 2 at Huancayo and Maui.

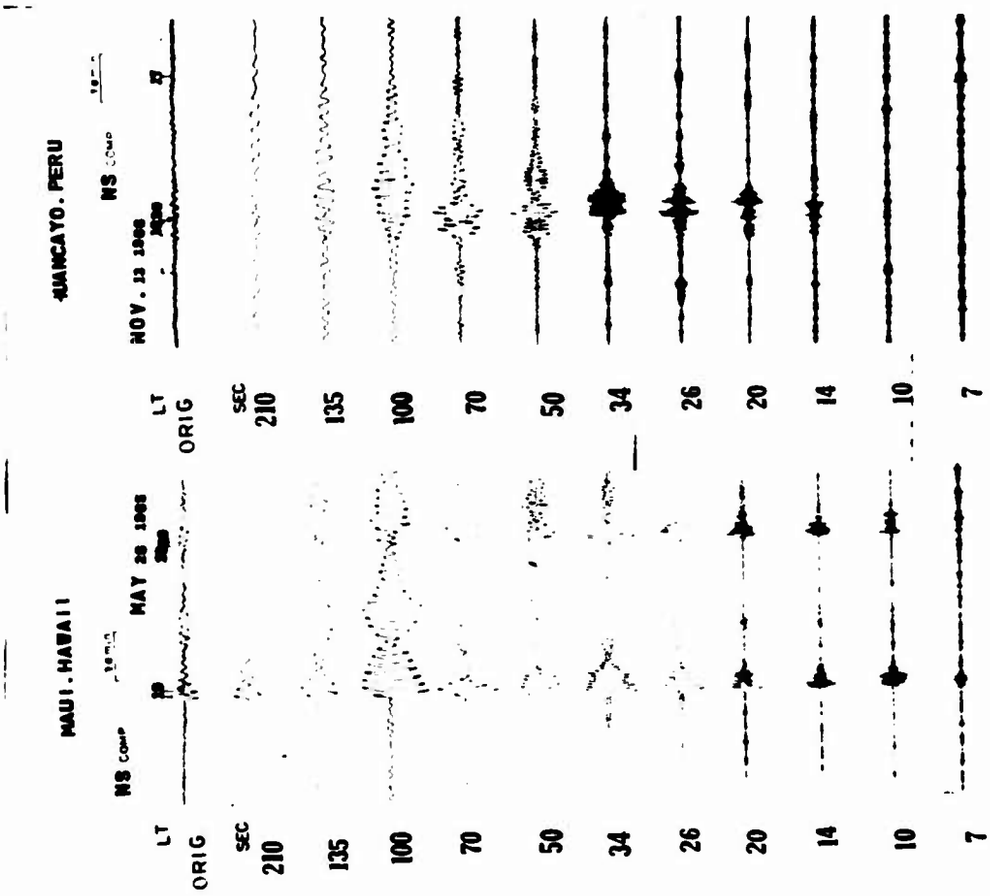

Fig. 9 Frequency analysis of pi 2 at Huancayo and Maui.

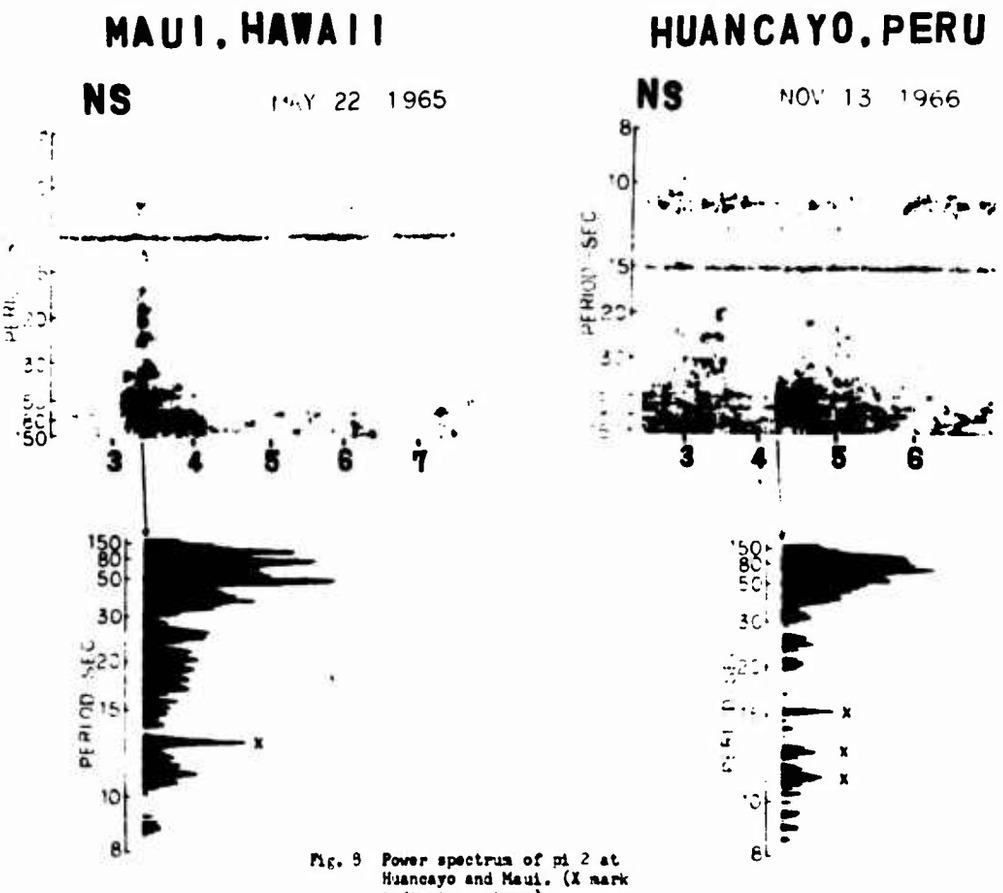

Fig. 8 Power spectrum of pi 2 at Huancayo and Maui. (X mark indicates noise.)

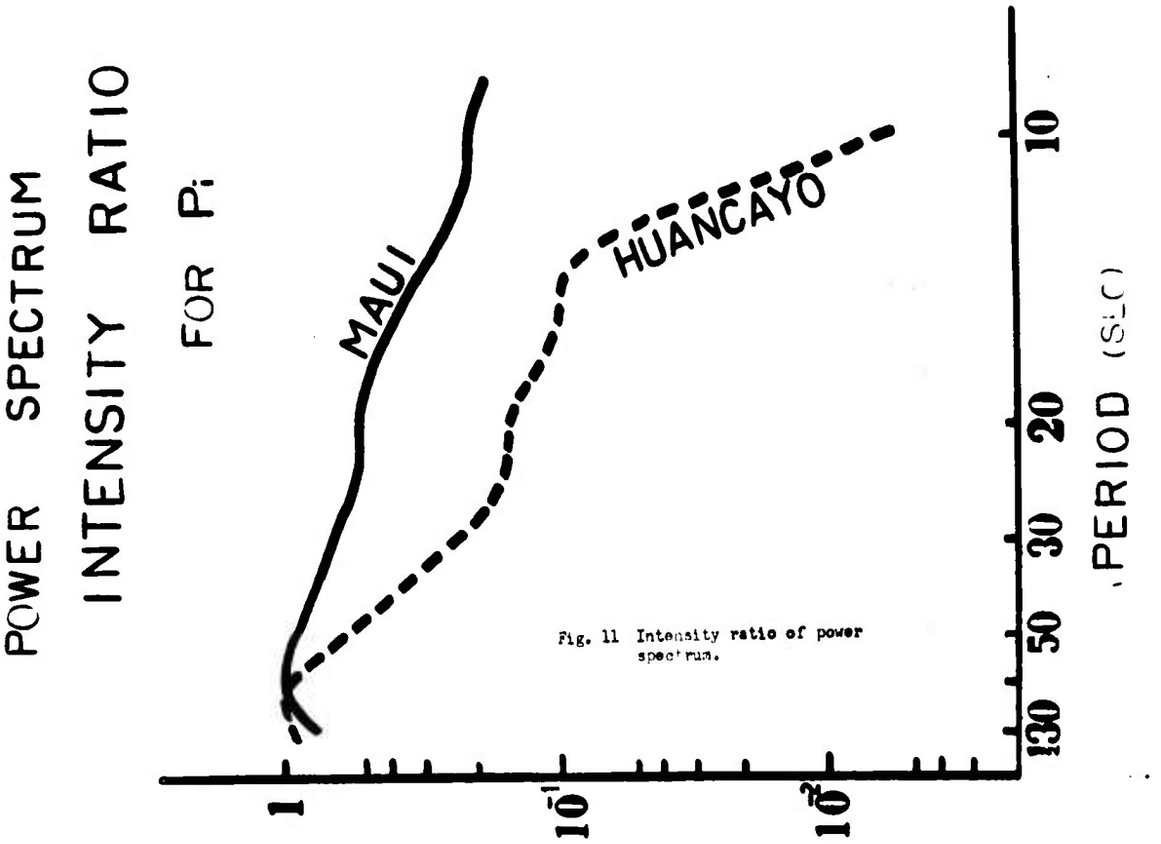

Fig. 11 Intensity ratio of power spectrum.

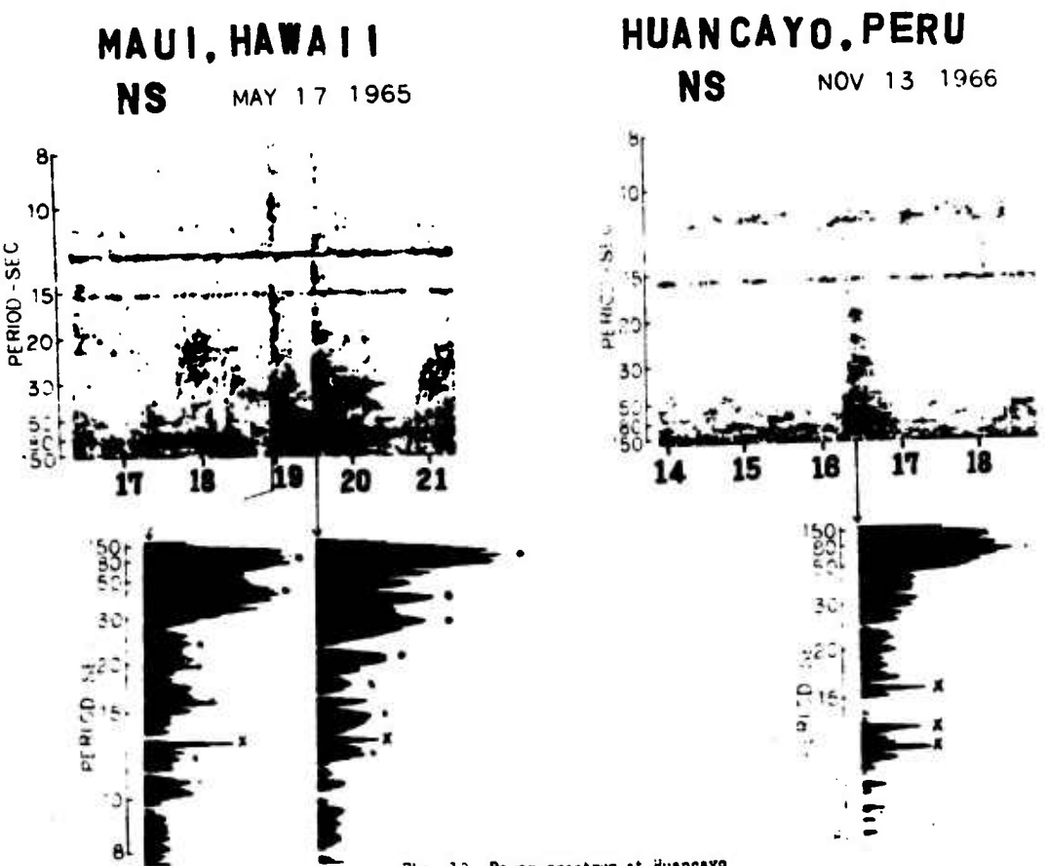

Fig. 10 Power spectrum at Huancayo and Maui. (X mark indicates noise.)

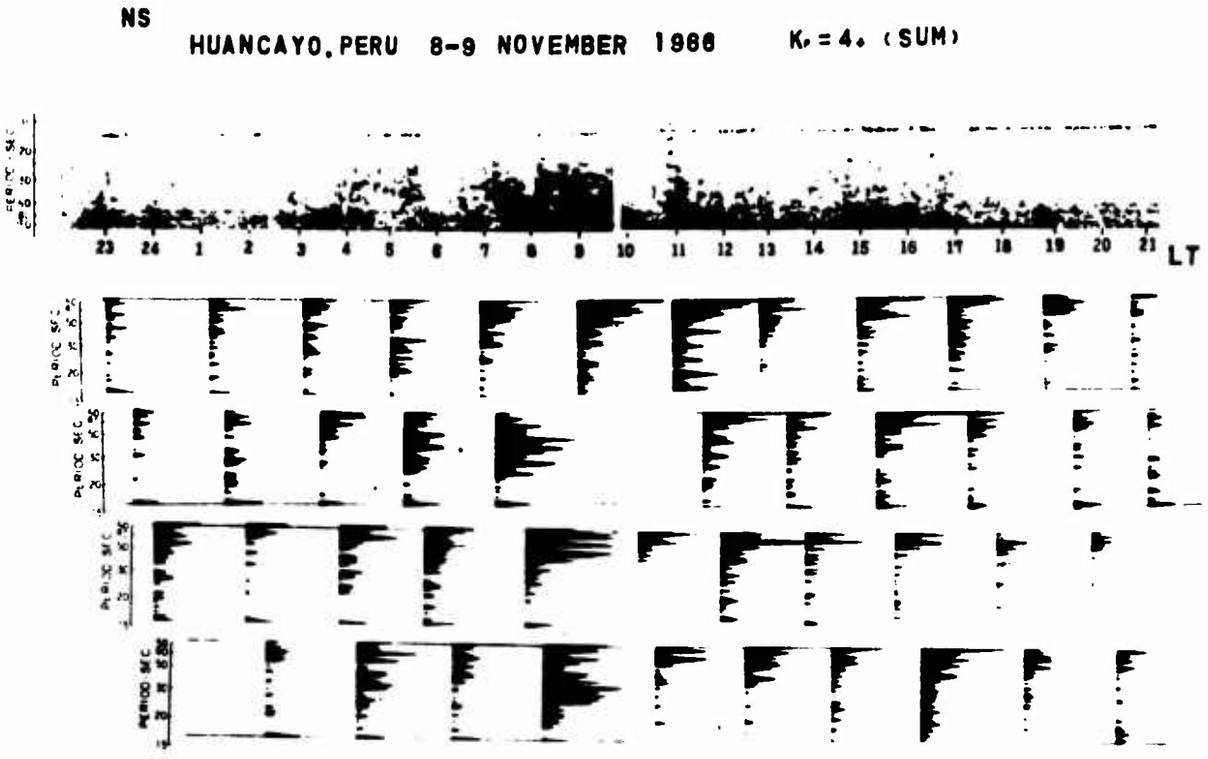

Fig. 12 Frequency analysis and power spectrum of pc at Huancayo.

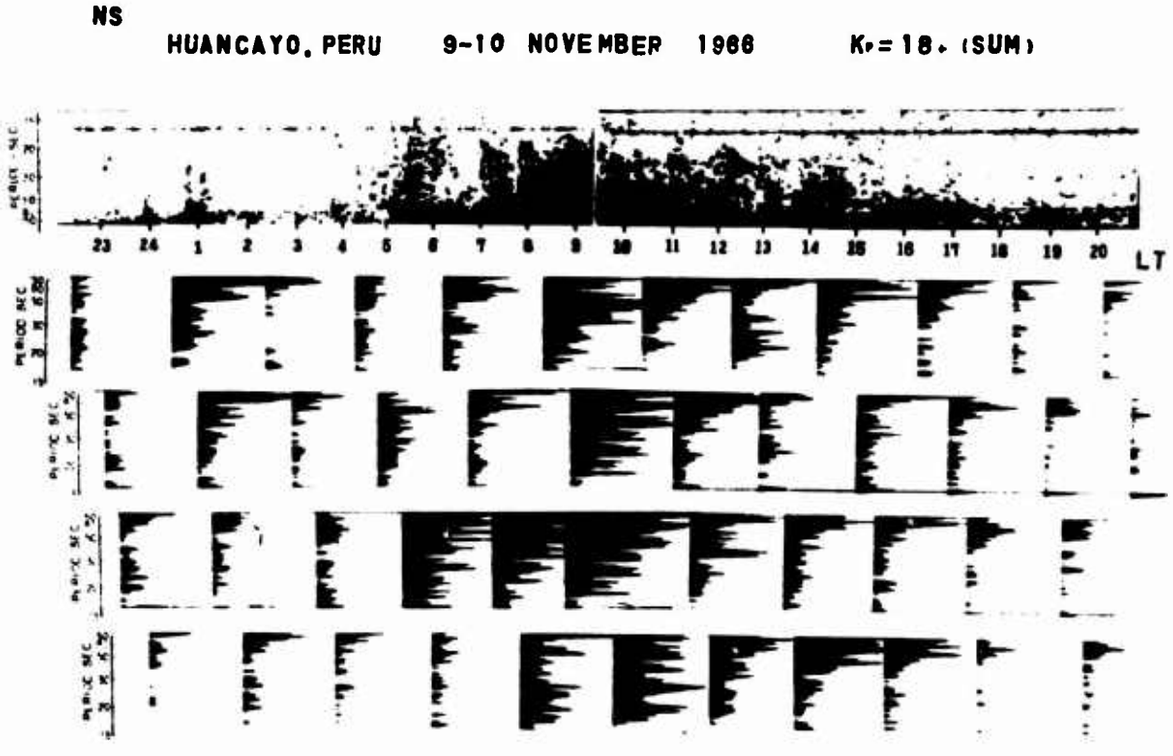

Fig. 13 Frequency analysis and power spectrum of pc at Huancayo.

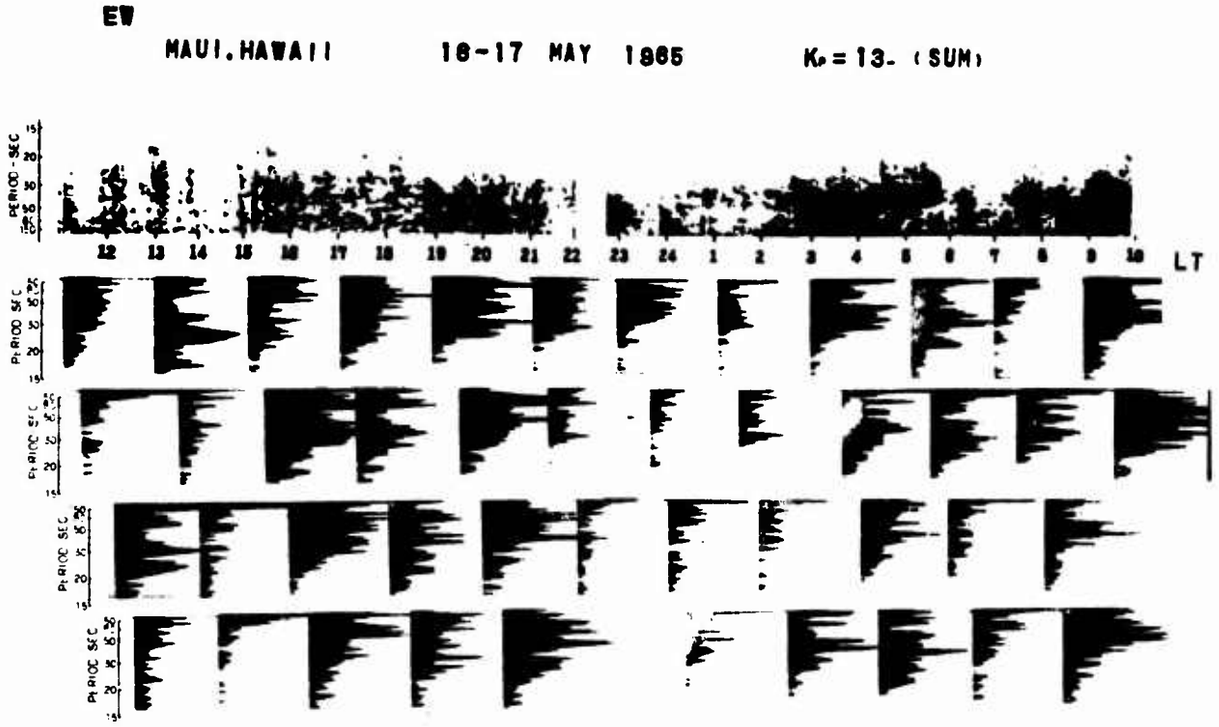

Fig. 14 Frequency analysis and power spectrum of pc at Maui.

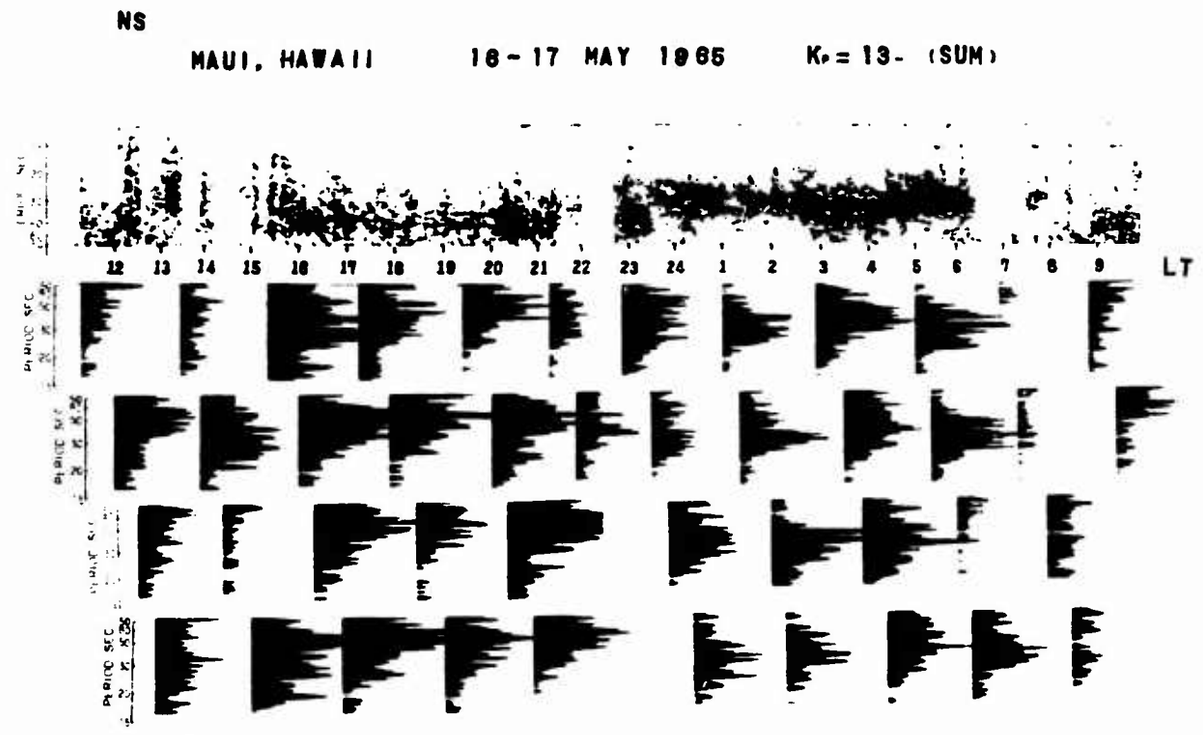

Fig. 15 Frequency analysis and power spectrum of pc at Maui.

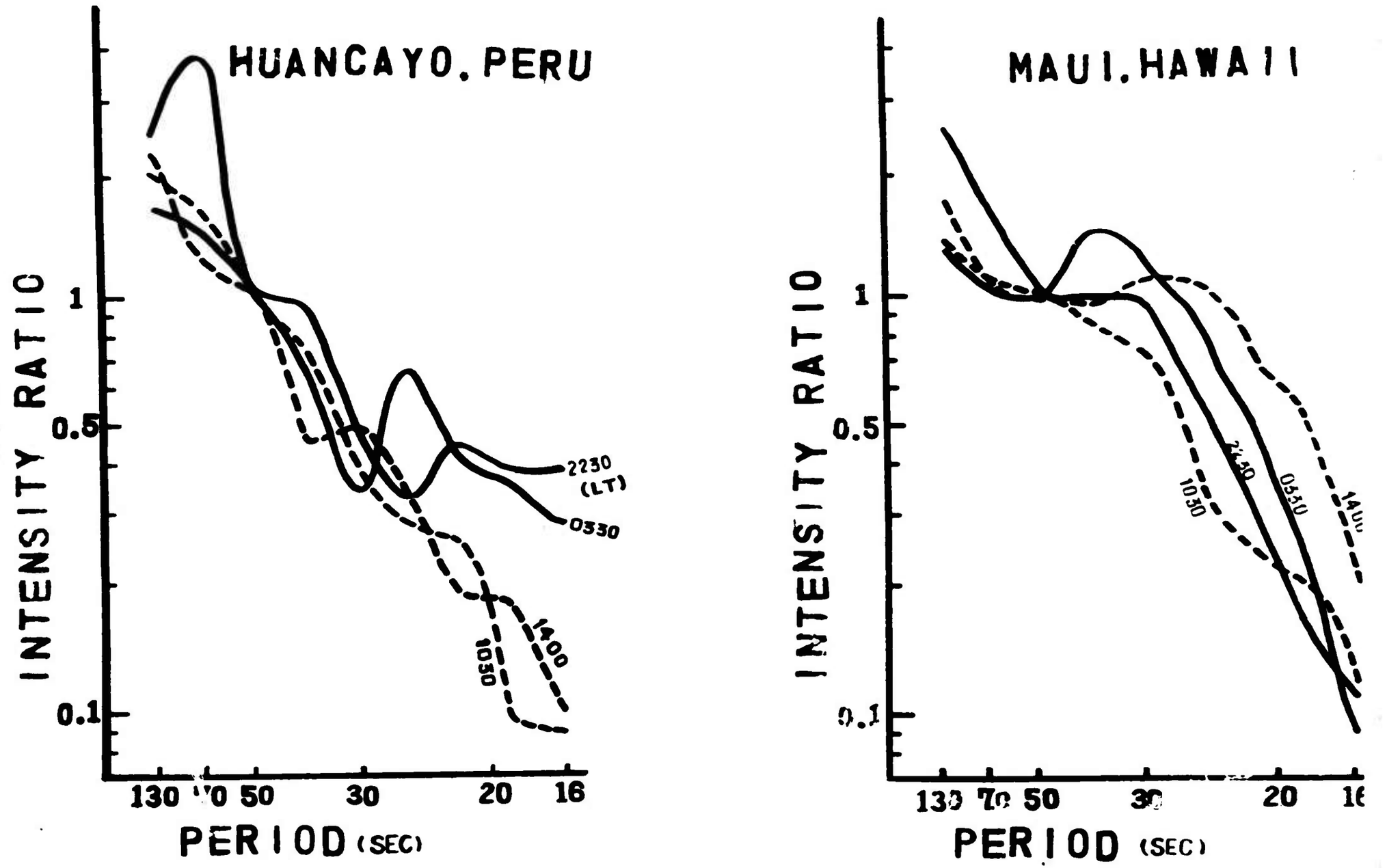

Fig. 16 Intensity ratio of power spectrum of pc.

BLANK PAGE

SIMULTANEITY OF Pc 3 MICROPULSATIONS AT CONJUGATE POINTS

A. C. Fraser-Smith
Lockheed Palo Alto Research Laboratory
Palo Alto, California 94304

Introduction Pc 3 micropulsations are small amplitude (~ gamma) oscillatory geomagnetic variations with periods in the range of 10-45 seconds. In auroral and middle latitudes they occur predominantly during the day (Campbell, 1963), and they are, therefore, sometimes called "daytime activity". Although they have been recognized as a distant class of micropulsations for a number of years, their origin is still uncertain and there are few quantitative results concerning their properties. Unlike Pc 1 micropulsations they have little apparent frequency structure.

One property of the Pc 3 micropulsations which is of importance in distinguishing between various theories of their origin, and in particular between those involving poloidal and toroidal oscillations (Jacobs & Westphal, 1964; Carovillano & Radoski, 1967) and other theories, is the closeness of their simultaneity at conjugate points. This simultaneity is difficult to measure accurately from chart records because of the nature of the waveforms and the common presence of longer period waves (Pc 4, for example). The overlay technique to be described in this paper is tedious but can in principle measure Pc 3 simultaneity between two stations to an accuracy of a few seconds.

The micropulsation data analyzed for this study were recorded during 1963 on magnetic tape at the four Lockheed Pacific geomagnetic observatories at Palo Alto, Kauai, Canton Island and Tongatapu (figure 1). The three island stations are located at approximately the same geomagnetic longitude, and Kauai and Tongatapu are also located at approximately conjugate geomagnetic latitudes. All observatories had identical recording equipment. Pc 3 signals,

which were recognizably the same, were found to occur at all four stations. However, those at Canton Island, which lies close to the geomagnetic equator, were comparatively very weak and difficult to compare in detail with the corresponding signals at the other three stations. The Kauai and Tonga signals were always closely similar when compared with those at Palo Alto, an indication of the significance of conjugacy in Pc 3 propagation (figure 2). Two periods of Pc 3 activity were analyzed in detail. These occurred during August 1-2, 1963, and August 27-28, 1963, when there were approximately seven and nine hours, respectively, of comparable activity. Altogether, a total of nearly 100 hours of recorded data from the four stations were analyzed. The results to be presented here mostly concern the two conjugate stations. Some comparison will be made, however, with the non-conjugate Palo Alto station.

Method of Analysis Following a speed-up of about 2000, the micropulsation data were frequency analyzed using a Kay Missilyzer and Scale Expander. This enabled the Pc 3 signals to be separated from other micropulsation activity. Time marks were recorded on one channel of the Missilyzer and the data on the other, a procedure enabling a close connection between the Pc 3 signals and their times of occurrence to be maintained. Only North-South component data were used, and all these data were analyzed in exactly the same way.

Frequency-time plots were made for each hour of the periods of Pc 3 activity studied, and the Missilyzer speed was adjusted using a frequency control system to give the same distance between hour marks for each station (figure 3). The hour was then divided into five sections of approximately twelve minutes each which were then photographed with polaroid transparency film. Time differences between corresponding signals at the different

stations could then be measured by overlapping and adjusting the transparencies for best fit (figure 4). In general, the two matching Tongatapu and Kauai transparencies were compared first, after which the Palo Alto transparency (which was never as good a match) was compared separately with both Tongatapu and Kauai. In this way, a double check of the time differences was possible. Once the transparencies were positioned the time differences could be measured to one second accuracy. However, since positioning of the transparencies was uncertain within small limits, measurement accuracy was effectively 2-3 seconds.

Results The results of the measurements for the two periods of Pc 3 activity studied are shown in figures 5 and 6. All time differences are measured with respect to Kauai. As was to be expected, no time differences greater than a minute were found, and on this scale of time measurement the Pc 3 micropulsations are simultaneous at Kauai, Tongatapu and Palo Alto. For time measurements on the order of seconds, however, the micropulsations may occur at different times at the three stations. On comparing the Palo Alto-Kauai (non-conjugate) results with those for Tongatapu-Kauai (conjugate), it appears that conjugacy reduces but does not eliminate the time differences between stations. The following three points are also noted:

1) There is little if any time difference between Kauai and Tongatapu at either the beginning or end of a period of activity.

2) Kauai predominantly leads Tonga in both figures 5 and 6. This is considered to be a seasonal effect and can be expected to change as the year progresses.

3) The approximate times of local noon at Palo Alto, Kauai and Tongatapu are as follows:

Palo Alto noon	~	2015 UT
Kauai "	~	2245 UT
Tonga "	~	2345 UT

While there are insufficient data to draw any general conclusions, there appears to be a connection between these times and the general trend of time differences. For example, in figure 6, the Palo Alto and Tongatapu local noontimes just precede the times of maximum time difference. Furthermore, in both figures, there is a small transition period in the Tongatapu-Kauai results preceding the Kauai noon. Some local time control is consistent with earlier observations (Troitskaya, 1964).

References

W. H. Campbell, Natural electromagnetic field fluctuations in the 3.0-0.02 cps range, Proc. I.E.E.E., vol. 51, p. 1337, 1963.

R. L. Carovillano and H. R. Radoski, Latitude-dependent plasmasphere oscillations, Phys.Fluids, vol. 10, p. 225, 1967.

J. A. Jacobs and K. O. Westphal, Physics and Chemistry of the Earth (L. H. Ahrens, F. Press and S.K. Runcorn, Editors), vol. 5, p. 158, 1964.

V. A. Troitskaya, Research in Geophysics (Hugh Odishaw, Editor), vol. 1, p. 485, 1964.

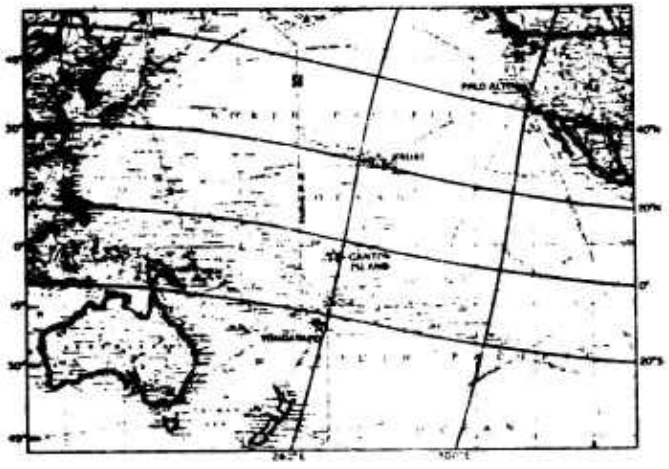

Figure 1. Location of the Lockheed Pacific geomagnetic observatories

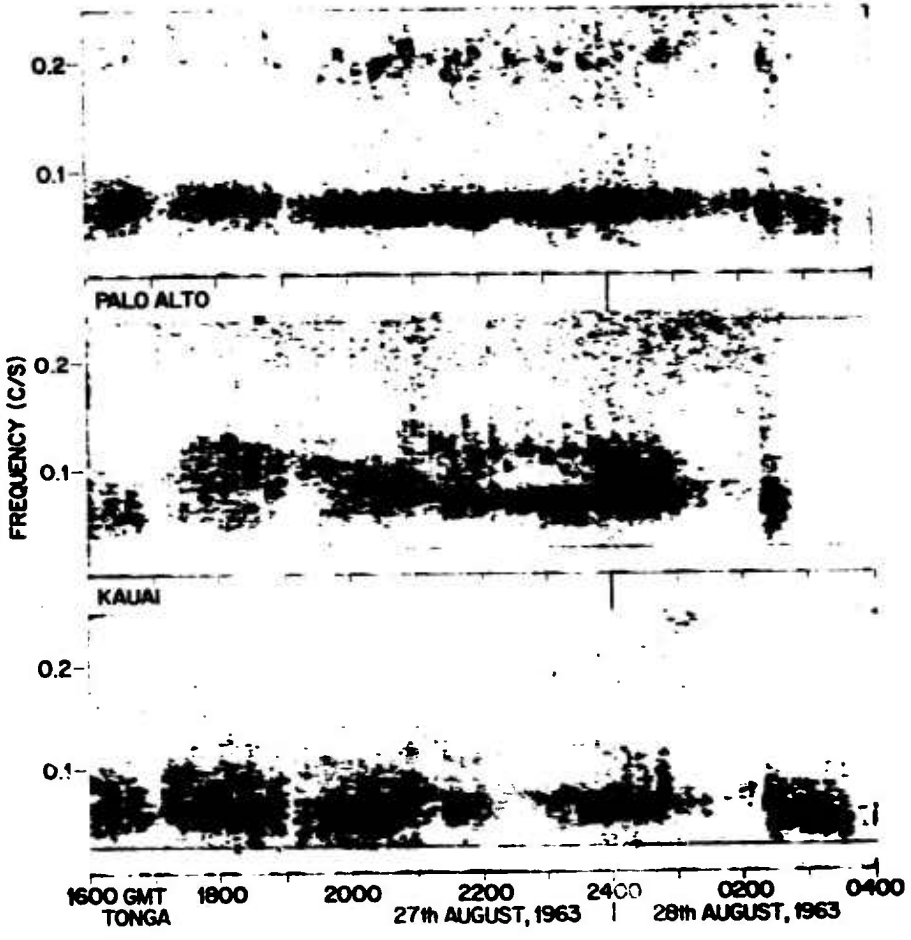

Figure 2. Pc 3 micropulsation activity at Palo Alto, Kauai and Tonga during August 27-28, 1963.

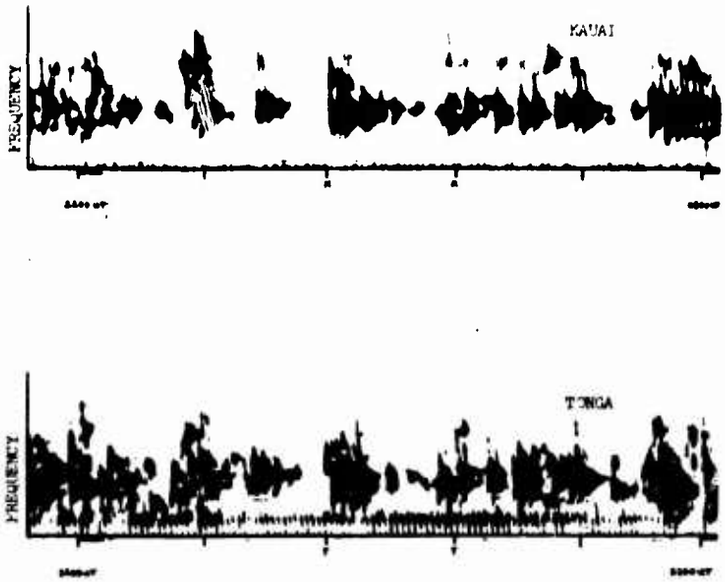

Figure 3. Detail of one hour (2200-2300 UT, August 27, 1963) of Pc 3 micropulsation activity at the two conjugate stations Kauai and Tongatapu. Note the close similarity between the individual signal bursts.

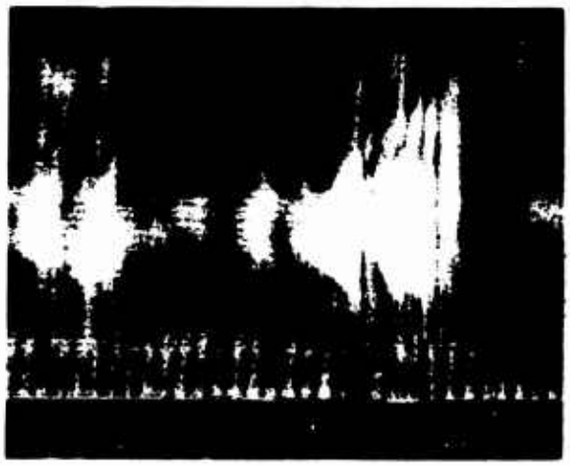

Figure 4. Two overlapped polaroid transparencies of the Pc 3 micropulsations seen in figure 3 around 2230 UT. It is difficult to reproduce the transparency patterns and a negative is shown for greater clarity.

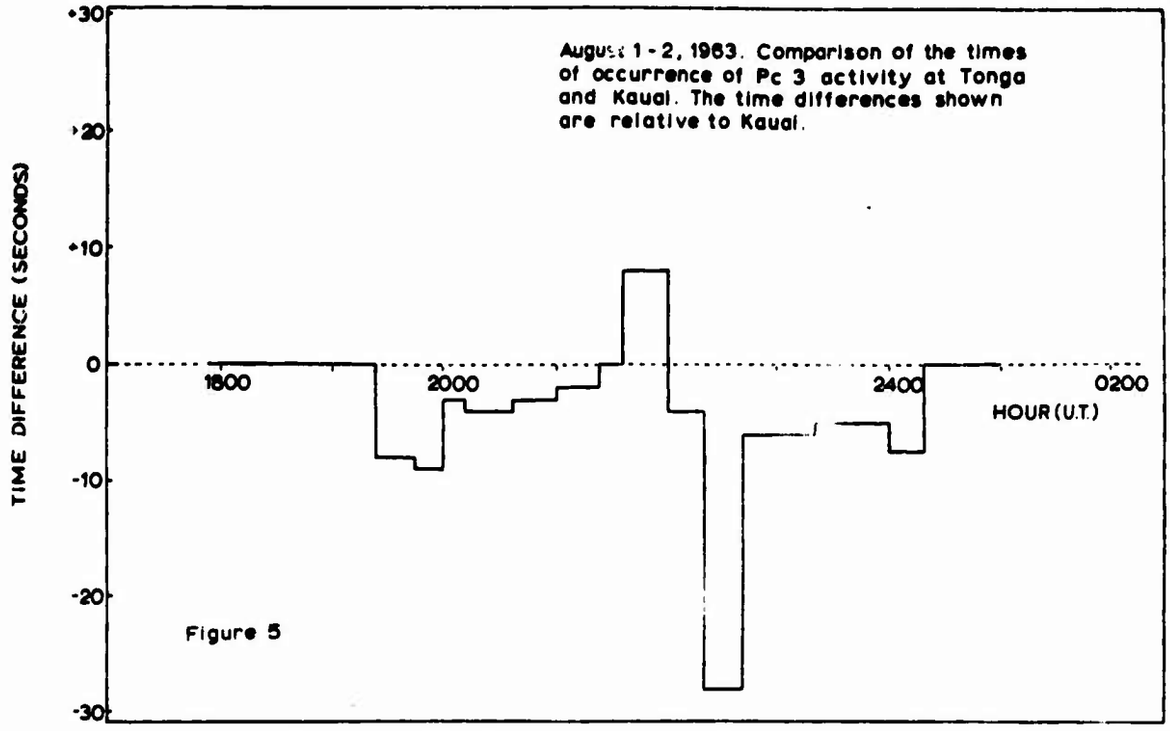

Figure 5

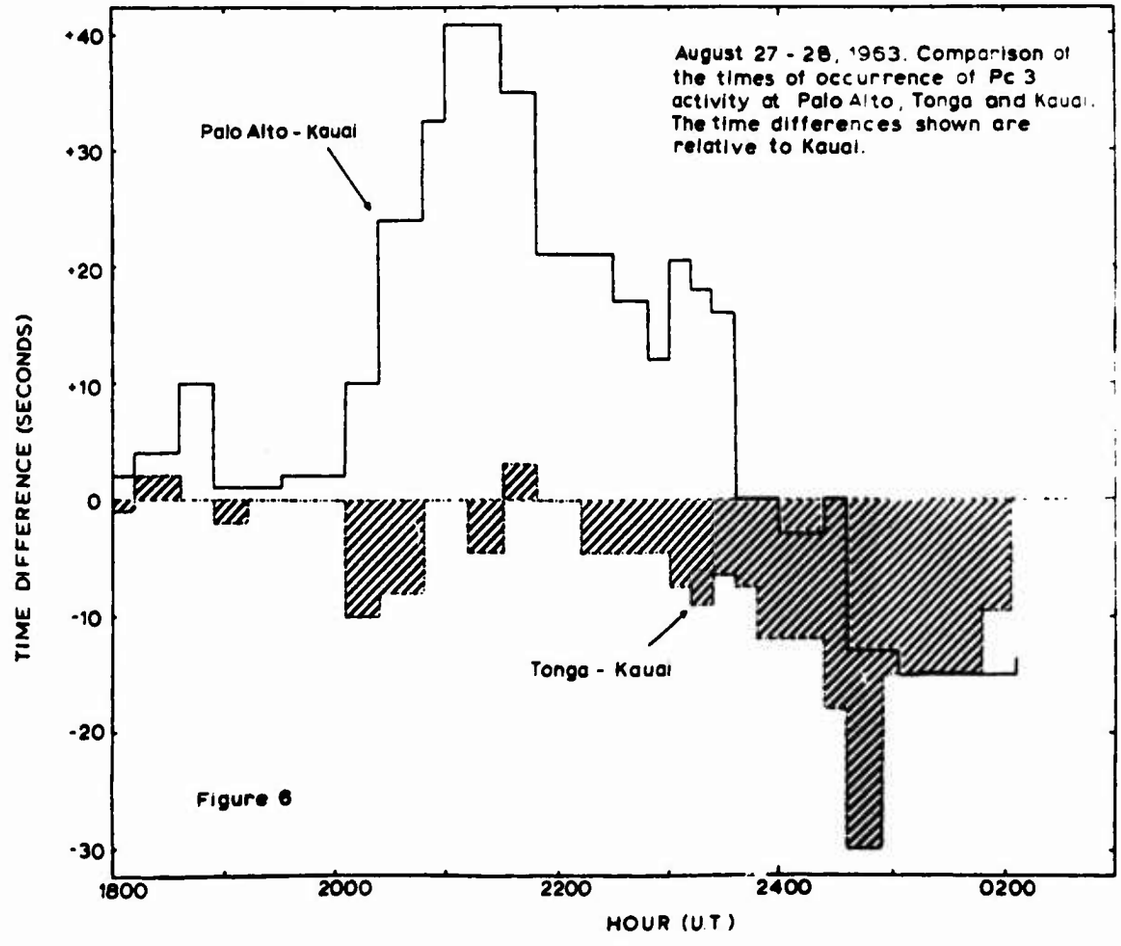

Figure 6

THE BEHAVIOR OF MAGNETOSPHERIC PROTON DENSITIES DERIVED FROM PEARL DISPERSION MEASUREMENTS*

H. B. Liemohn, J. F. Kenney and H. B. Knaflich
Boeing Scientific Research Laboratories
Seattle, Washington 98124

The dispersion characteristics of 116 pc 1 micropulsation pearls are described and analyzed using various models of the magnetosphere. Theoretical analyses have shown that the dispersion of the signals depends primarily on the plasma density distribution along the field line, and the geocentric distance measured in earth radii to the place where the field line crosses the equatorial plane. Thus measurements of experimental dispersion can be used to estimate the plasma density at various distances out in the magnetosphere. The geomagnetic field B is assumed to be a dipole so that the field-line paths are given by $R = L \cos^2\lambda$ where λ is the geomagnetic latitude and L is the geocentric distance to the equatorial intercept of the field. The plasma distribution is assumed to have the general form $N = N_0(L)P(L,\lambda)$ where $P(L,0)$ is normalized to unity so that N_0 can be interpreted as the equatorial density distribution. The different assumptions concerning the distribution of plasma along the field line will change the determination of L only a small amount while making a larger change in N_0.

---

*To be published in Earth and Planetary Science Letters, July 1967.

Figure 1 shows that pearl emissions are generated on field lines with equatorial intercepts between four and nine earth radii. The upper-frequency limit rarely exceeds 0.6 of the minimum ion cyclotron frequency, f^i_{co}, and the detectable bandwidth is about 0.1 f^i_{co}.

Figures 2 and 3 show that there is a diurnal variation in the location of the propagation paths which constitute a pearl oval with high latitude or large L-values on the dayside of the earth and small L-values or low latitude on the nightside. Figure 2 shows that in general data taken during magnetically quiet periods occur farther out in the magnetosphere than those taken at the same local time during the most disturbed periods. Figure 3 indicates no obvious seasonal shift in the location of the pearl zone.

Figure 4 shows the equatorial plasma density, $N_0(L)$, for the field-line distribution $P \sim R^{-5}$. Determinations of N_0 from pearls which are detected either simultaneously or within a short time interval are connected with straight-line segments. These straight line segments indicate that pearls which are detected essentially at the same time may have a spread of L-value in excess of 1 earth radius, but usually occur on a very steep density gradient that may coincide with the plasmapause already detected by VLF techniques.

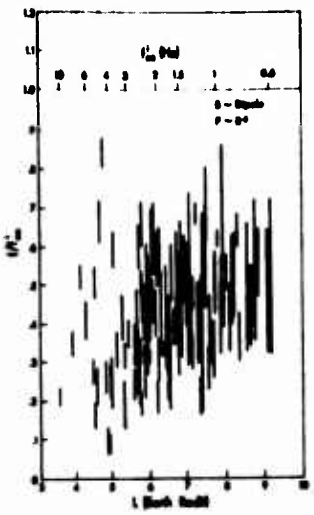

Fig. 1 - Pearl frequency bands.

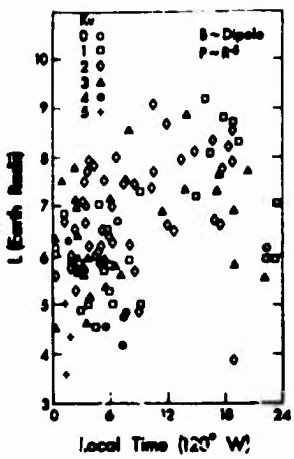

Fig. 2 – Diurnal variation of propagation paths K_v is local magnetic index.

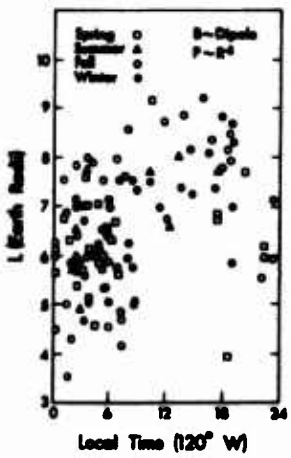

Fig. 3 - Diurnal variation of propagation paths.

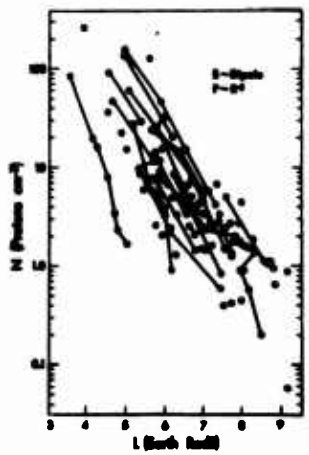

Fig. 4 - Typical plasma density distribution.

BLANK PAGE

Recent Investigation on Hydromagnetic Emissions

By Tomiya Watanabe

Institute of Earth and Planetary Sciences
University of British Columbia
Vancouver, Canada

1. INTRODUCTION

The words "hm emissions" in the title are used in a very broad sense. It is implied that hm emissions are synonymous with geomagnetic micropulsations with short periods, say, from about 0.2 sec to 5 sec, that is, the range of the shortest periods ever observed on the earth's surface for geomagnetic micropulsations. If hm emissions are defined like this, all the pc 1[1] type of micropulsations are contained in this category. Besides, some pi 1[1] type of micropulsations are also included.

There are various types of signals in hm emissions. Signals of the simplest type are hm whistlers. Figure 2 of Ref. 2 shows a typical example of hm whistlers displayed on a spectrogram. They appear as a series of rising tones which form a fan-shaped structure. An hm whistler is due to dispersion of an hm wave packet which propagates in the magnetosphere and bounces between the two hemispheres along a magnetic line of force of the earth[3 4]. In general, there are two modes of waves in a magnetoactive plasma. The mode relevant

to hm whistlers seems to be the L mode (or the slow mode, more exactly). In the hm frequency range, only the L mode of waves is likely to be guided by the ambient magnetic field[4]. The R mode (the fast mode) of hm waves is not field-guided in the hm regime. The group delay of the L mode of an hm wave is larger for a higher frequency. This explains the fan-shaped structure of hm whistlers.

Tepley and Wentworth[5] mentioned that an hm emission often starts as a weak signal and as time passes the signal intensity becomes continually stronger and in the final stage it dies out gradually. McNicol and Johnson[6] obtained an example which clearly shows such a trend (their spectrogram is cited in Ref. (15)). Tepley and Wentworth[5] also mentioned that in such an hm emission event the hm wave does not follow the dispersion process simply out that it should be amplified while propagating in the magnetosphere. Furthermore, it should be noticed that there is no fan-shaped structure in the event obtained by Johnson and McNicol, unlike hm whistlers. The emission signals are more or less parallel to each other. This also indicates that in this event there is something else to be considered besides the dispersion process. Emission signals such as this example are quite common, and it shows that there is a different group of signals from hm whistlers.

Those signals might be called hm emissions in the narrow sense. By adopting the nomenclature this way, it is implied that hm emissions should be discriminated from hm whistlers as radio emissions in the VLF range are differentiated from whistling atmospherics.

2. Some Problems about the Cyclotron Instability Process as the Triggering Mechanism of hm Emissions

2.1 Model of Periodic Emissions and Principal Results of the Linear Theory of the Cyclotron Instability Process

In 1965, Brice[7] mentioned that in hm emissions in the narrow sense mentioned above, there is a type which is similar to periodic emissions in the VLF range. One might call it hm periodic emissions. According to Brice[8], the mechanism of periodic emissions is as follows. (See Fig. 1.) Let us suppose that a wave packet is propagating along a magnetic line of force. In the case of a whistler, this wave packet is simply dispersed while propagating along the magnetic line of force. What is different in periodic emissions is that somewhere on the propagation path there is a black box, a region of triggering of hm emissions. When the initial wave packet comes back as an echo and enters the black box, it triggers a new emission. This new emission subsequently triggers the next one when it comes back to the

triggering region. In the case of VLF emissions, the triggering mechanism is believed to be the cyclotron instability process caused by nonthermal electrons[9]. In the case of hm periodic emissions, the triggering mechanism is also believed to be the cyclotron instability process. However, nonthermal protons rather than electrons are believed to be responsible for the instabilities in the case of hm emissions. The same conclusions have been obtained by some other authors[3 5 10-12] who investigated the triggering mechanism independently. According to an estimate by Jacobs and the author [11 12], the energy of each nonthermal proton is required to be from about a few kev to a few tens of kev, if the triggering region exists at a typical place in the outer magnetosphere, for example, at six earth-radii distance from the centre of the earth. On the other hand, the required energy for an electron must be relativistic to cause an instability.

Mathematical investigation of the cyclotron instability process is done by looking for solutions of growing waves in an infinite and uniform magneto-active plasma. In the case of a plane wave where the electromagnetic field varies in space and time as $\exp i(\underset{\sim}{k}\cdot\underset{\sim}{r} - \omega t)$, the wave is said to be a "growing wave" if the wave frequency ω has a positive imaginary part while the wave number $\underset{\sim}{k}$ is taken real:

$$\mathrm{Im}(\omega) > 0. \qquad (1)$$

This type of mathematical analysis concerns monochromatic waves only. In actuality, however, one has to deal with a wave packet that is a superposition of many monochromatic waves. According to Sturrock[13], a growing wave packet takes either of the following two behaviours. In one case, it is like a travelling amplifying wave. In the other case, the wave packet is like a self-exciting oscillator. When considering the model of periodic emissions, it is important to find out which of the two possible cases is relevant. If a wave packet triggered in the black box behaves as in the first case, it keeps its identity as a wave packet while propagating through the black box. However, if the triggered wave packet behaves as in the second case, it fills the whole space of the black box, stays there and grows as long as nonthermal particles supply their energy to the wave packet. The appearance of an hm emission signal on a spectrogram could be quite different for the two cases. In the case of VLF emissions, it is suggested by Brice[14] that the instability is of the second type, namely, of the self-exciting oscillator type. For hm emissions, Jacobs and the author[11 12] found that the instability process is again of the self-exciting oscillator type.

2.2 Non-linear Evolution of the Signal Strength

This result brings a difficulty to the proposed emission mechanism, because if this result is correct the appearance of an hm emission signal on a spectrogram should be a continuous line as long as the instability process goes on. This is contrary to what we have observed. Jacobs and the writer[15] are of the opinion that this difficulty can be avoided by considering non-linearities in the cyclotron instability process. Mathematically, the non-linearities arise from the Boltzmann equation which is needed to describe the particle distribution in a plasma gas. According to the linear theory of the cyclotron instability process, the wave amplitude, for instance, the strength of the wave magnetic field b changes with time as

$$\frac{db}{dt} = \Gamma b \qquad (2)$$

where Γ is the growth rate and becomes equal to the imaginary part of the wave frequency according to analysis in the complex form:

$$\Gamma = \mathcal{I}_m(\omega) \qquad (3)$$

In the linear approximation, the growth rate is constant with time, and if it is positive, the amplitude b grows indefinitely. However, the growth rate Γ is no longer constant with time in the non-linear theory. Since the wave is able to grow only by taking energy out of the nonthermal particles, the growth rate Γ should decrease with time as the nonthermal particles give up their energy. As the growth rate Γ tends to zero, the wave amplitude b must tend to a certain constant value. This is true, however, only if the temperature of the ambient plasma (excluding the nonthermal particles) is zero. If the temperature is not zero, the quasi-linear theory[15] shows that the above equation should be rewritten as follows.

$$\frac{db}{dt} = \Gamma b - Ab^3 \qquad (4)$$

where the coefficient A is a positive constant. This equation shows that the wave grows in the initial stage but as time passes it decreases to zero.

2.3 Non-linear Drift of the Emission Frequency

Concerning the model of periodic emissions, Brice[7] presented another problem of why each emission signal becomes a rising tone on a spectrogram. Brice surmised that the frequency rise might occur due, at least partly, to the

emission mechanism itself. This conjecture seems credible, particularly in the case of VLF emissions. Because the relevant mode for VLF emissions is the R mode, the emission frequency would decrease with time if the frequency change with time were due to dispersion only. In actuality, an individual signal in a series of VLF periodic emissions is a rising tone more often than a falling tone. Also in the case of hm periodic emissions, there is evidence to support Brice's idea. A series of hm periodic emissions often begins with a dim dot on a spectrogram. More often, the starting point of a series is barely defined. In such a case, there are several or more dim dots in the early stage of a periodic event. As time passes, a dot tends to extend horizontally more and more, becoming more like a line segment rather than a dot. As time goes on further, each signal becomes a rising tone, and its gradient is steeper as the signal strength becomes stronger. When a series approaches the end, the signal strength becomes weaker and weaker and subsequent signals tend to incline towards the time axis more and more, forming a fan-shaped structure. An example of an hm emission obtained by Gendrin and Stefant[16] clearly shows such a trend.

Now the idea by Brice gives rise to the question as to how the cyclotron instability process makes an emission

frequency increase with time. Regarding this problem, Jacobs and the present author[15] are again of the opinion that non-linearities in the instability process might give the answer. Suppose we are considering a wave propagating along the background magnetic field. If the medium is a cold plasma, the wave is non-attenuating and circularly polarized expressed as follows.

$$\left.\begin{aligned} b_x &= b\cos(\kappa z - \omega t - \theta), \\ b_y &= b\sin(\kappa z - \omega t - \theta), \end{aligned}\right\} \quad (5)$$

and

$$b_z = 0.$$

The linear theory gives the dispersion equation by which the wave frequency ω and the wave number κ are connected to each other. For the L (R) mode, the frequency ω is positive (negative). The amplitude b as well as the phase angle θ are constant in time. If the medium contains nonthermal particles, however, the amplitude b is no longer constant with time but gradually changes with time as shown in Eq. (2). The coefficient Γ is positive for a growing wave. The above equation can be derived in the linear approximation. The quasi-linear theory tells us how this equation must be modified, as already mentioned

(Eq. (4)). This is not the only result of the quasi-linear theory, however. It also shows that the phase angle θ is not constant with time. This means that the effective frequency ω' is different from the wave frequency ω in the linear approximation, and not only that, the effective frequency might 'drift' with time. In the case where the ambient plasma (excluding the non-thermal particles) is at zero temperature so that the nonlinear term on the right hand side of Eq. (4) vanishes, according to calculation in Ref. (17), the rate of change of the effective frequency is given as follows

$$\frac{d\omega'}{dt} = C\Gamma\left(\frac{b}{B_o}\right)^2 \qquad (6)$$

In this expression, Bo is the strength of the ambient magnetic field, and C is a constant which depends upon the linear wave frequency ω and is positive (negative) for the L (R) mode. This expression shows that the effective frequency ω' increases with time as the wave amplitude grows with time. The rate of the frequency increase is greater as the wave amplitude b and the growth rate Γ are greater.

3. Comments on an Unsolved Problem in hm Emissions

In hm emissions, there are many other unsolved problems. The author would like to mention one of those problems. (Please refer to Fig. 7 of Ref. (2).) Looking at the figure, one might wonder if this event is a periodic emission, an hm whistler, or something else. One way to look at this event is to group those dots lined up horizontally into one series and to regard it as a series of periodic emissions. According to this view, this event is an ensemble of several series of periodic emissions, although these series are not independent of each other but are somehow related. On the other hand, one could regard this event as a kind of whistler, say, a "dotted" whistler. By connecting four or five dots, one can trace out a curve along which the frequency increases with time. A series of curves traced out like this look just like signals of an hm whistler.

If one takes the second point of view, an immediate question is why a whistler signal is not smooth but dotted. An answer suggested for this question is that the "dotting" occurs due to the propagation mechanism of hm waves[18]. Considering a field-guided hm wave which propagates from a point deep in the outer magnetosphere to the earth's surface,

the transmission coefficient of the wave as a function of frequency is said to have several maxima and minima in a narrow frequency band. Whether this suggestion is correct or not might be checked by analysing the signals of this type with a high resolution sonograph or, especially, by taking the signals on a three dimensional spectrogram where the signal strength is displayed on the third dimension. On a three dimensional spectrogram like that, a dot must look like a mountain. Now, if the suggestion given above is correct, the edge-line of the mountain should run along the whistler trace. To obtain a three dimensional spectrogram of an hm emission event, one may employ a digital spectral analyser or a new experimental technique which has been developed by Kenney[19]. Kitamura has been analysing a number of hm emission events using a three dimensional spectral analyser. His investigation is still under way. However, some of the preliminary results show that the edge-line of a "dot" mountain does not necessarily run along the whistler trace: More often, it runs oblique to the whistler trace[20]. From this observation Kitamura and the author agree that due to this a dot seems more likely to be an emission rather than a segment of a whistler signal. However, why several series of periodic emissions take place simultaneously is an

unsolved problem. It may be that hm emissions of the type under consideration are something analogous to multiple emissions or a chorus in the VLF range. Since dotted structures often appear in hm emissions, they present an important problem in theoretical investigation of the emission mechanism.

ACKNOWLEDGEMENTS

The author would like to thank Drs. J.A. Jacobs and T. Kitamura for their kind help in preparing the manuscript of this paper.

NOTES

Concerning the problem on the non-linear evolution of the signal strength (raised in the section 2.2), it is worthwhile mentioning the recent result obtained by I.B. Bernstein and F. Engelmann (Phys. of Fluids 9, 937, 1966) that in the case of three dimensional electrostatic plasma instabilities in a non-magnetic electron plasma the fluctuating electric fields decay effectively to zero in a time of the order of the reciprocal of the maximum initial growth rate. It seems interesting to extend the analysis by Bernstein and Engelmann to the case of cyclotron instabilities.

REFERENCES

1. Jacobs, J.A., Kato, Y., Matsushita S. and Troitskaya, V.A. J. Geophys. Res. 69, 180 (1964).

2. Tepley, L.R., J. Geomag. Geoelear. (Society of Terrestrial Magnetism and Electricity, Japan) 18, 227 (1966).

3. Obayashi, T., J. Geophys. Res. 70, 1069 (1965).

4. Jacobs, J.A. and Watanabe, T., J. Atmosph. Terr. Phys. 26, 825 (1964).

5. Tepley, L.R. and Wentworth, R.C., Rep. Contr. NAS5-3656, Lockheed Missiles and Space Company. (1964).

6. McNicol, R.W.E. and Johnson, L., Progress Review. Boeing Sci. Res. Labs., D1-82-0380-1, p. 62, Aug. 15, 1964.

7. Brice, N., Nature, Lond. 206, 283 (1965).

8. Brice, N., Su-SEL-64-088, Radio Sci. Lab., Stanford Electronics Labs., Stanford Univ. (1964).

9. Brice, N., J. Geophys. Res. 69, 4515 (1964).

10. Cornwall, J.M., J. Geophys. Res. 70, 61 (1965).

11. Jacobs, J.A. and Watanabe, T., D1-82-0398. Boeing Sci. Res. Labs. (1965).

12. Jacobs, J.A. and Watanabe, T., J. Atmosph. Terr. Phys. 28, 235 (1966).

13. Sturrock, P.A., Phys. Rev. 112, 1488 (1958).

14. Brice, N., J. Geophys. Res. 68, 4626 (1963).

15. Jacobs, J.A. and Watanabe, T., Planet. Space Sci. 15, 799 (1967).

16. Gendrin, R. and Stefant, R., C.R. Acad. Sci. Paris 252, 752 (1962).

17. Watanabe, T., Can. J. Phys. 44, 815 (1966).

18. Fraser-Smith, A.C., 6th Western National Meeting, Amer. Geophys. Union, Los Angeles, Calif.

19. Kenney, J.F., Private communication (1966).

20. Kitamura, T., Private communication (1967).

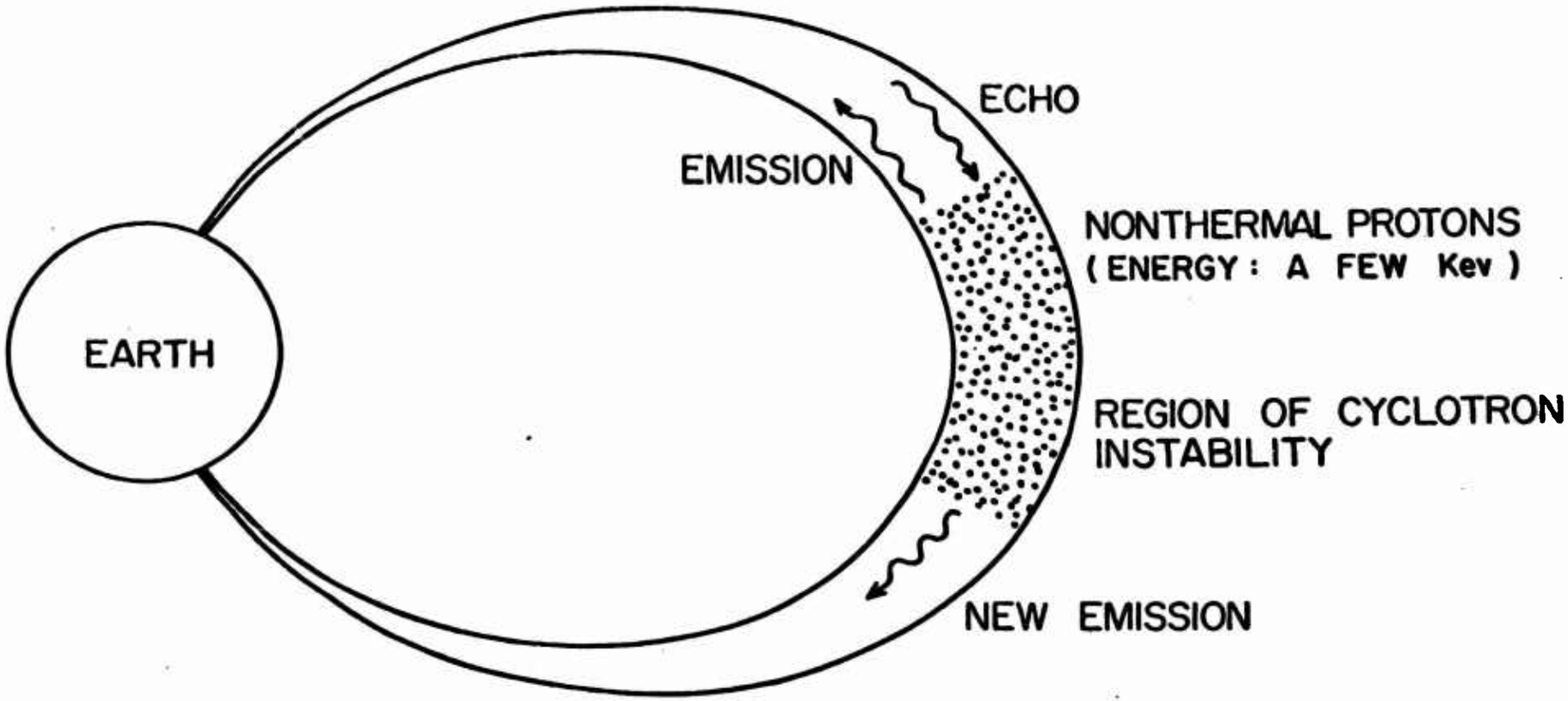

Fig. 1 Model of HM Periodic Emissions

DIFFUSION PROCESSES INFLUENCED BY CONJUGATE-POINT WAVE PHENOMENA

John M. Cornwall

Aerospace Corporation, El Segundo, California
and
Department of Physics, University of California at Los Angeles

ABSTRACT

Radial diffusion coefficients for low-energy protons in the magnetosphere are estimated for processes involving Pc 1, 2, and 3 hydromagnetic waves. These diffusion coefficients are compared to rough estimates of diffusion due to magnetic impulses and bays, to arrive at an overall diffusion rate. An effective loss rate for pitch-angle diffusion (caused by Pc 1) is developed, and combined with radial diffusion to yield a nonlinear differential equation. Some estimates of expected proton flux levels are made, on the basis of this equation.

1. INTRODUCTION

In this paper, we discuss semi-quantitatively the ways in which pitch-angle scattering caused by hydromagnetic waves can influence the inward radial diffusion of low-energy protons. The problem of radial diffusion is an extremely complicated one, with pitch-angle diffusion taken into account, and no definitive conclusions can be drawn without extensive computer studies. The results of the present work are necessarily tentative, but we hope they are sufficiently reliable to use as guideposts.

A number of authors have discussed the generation of Pc 1 micropulsations (frequencies 0.2 - 5 Hz) [Cornwall, 1965; Obayashi, 1965; Brice, 1964; Jacobs and Watanabe, 1964]. When particles of the appropriate energy have an anisotropic pitch-angle distribution, an instability results, with frequencies in the Pc 1 band for Davis-Williamson [1963, 1964] protons. (Electrons of $\gtrsim$100 kev produce a similar instability with whistlers.) Because hydromagnetic waves can bounce between conjugate points of a magnetic field line, a single wave packet can be amplified many times. The effect is reminiscent of a Q-spoiled laser. The micropulsations scatter the protons in pitch angle, which is best described as a diffusion process [Cornwall, 1966; Kennel and Petschek, 1966]. This pitch-angle diffusion is an effective loss mechanism for Davis-Williamson protons.

We are interested in the effect of pitch-angle diffusion on radial diffusion [see, e.g., Nakada and Mead, 1965, which contains further

references]. Magnetic and electric disturbances associated with the solar wind and other phenomena cause low-energy protons (and electrons) to diffuse radially inward from the magnetosphere. These disturbances act on a time scale which is long compared to the cyclotron and bounce periods of the particles, and therefore violate only the third adiabatic invariant. In addition, there are processes which act on much shorter time scales to cause radial diffusion: 1) Pc 1 micropulsations can cause radial diffusion in an axially asymmetric magnetosphere, as pointed out by Roederer [1967]; 2) longer-period micropulsations (Pc 2 or 3) can resonate with proton bounce time, violate the longitudinal invariant, and produce radial diffusion [Cornwall, 1966, has evaluated the same mechanism for electrons]. It is important to evaluate the effect of these last two mechanisms quantitatively, since the diffusion coefficients proposed by Nakada and Mead, based on long-time-scale disturbances, is much too small to explain the observed radial distribution of Davis-Williamson protons.

Probably the most important effect of all is the loss rate induced by pitch-angle diffusion, which competes strongly with radial diffusion. The loss rate is nonlinear when saturation effects set in [Cornwall, 1966; Kennel and Petschek, 1966]. When the proton flux tries to exceed a certain level, the loss rate becomes very large and limits the proton flux. When this loss rate is combined with radial diffusion, a nonlinear differential equation results.

In this paper, we estimate the strength of various radial diffusion processes, and combine this information with nonlinear pitch-angle

diffusion to estimate the proton flux at various positions in the magnetosphere. It turns out that the proton flux level at saturation depends only logarithmically on the radial diffusion constant, which is fortunate since this diffusion coefficient is very poorly known.

2. RADIAL DIFFUSION PROCESSES

The reader should consult Table I for a quick survey of the results of this section, which is partly a review of other authors' work. Certain diffusion processes are associated with electromagnetic fields which are virtually pure magnetic, and thus energy-conserving; Table I carries a column for this information.

A. Long-time-scale radial diffusion processes. These are reviewed by Dungey [1965], and important work has been done by Fälthammar [1965, 1966]. We define long time as a time long compared to the bounce period and cyclotron period of Davis-Williamson protons; thus the primary effect of these processes is to violate the third adiabatic invariant, while the first two are conserved. If these processes were the only ones acting, then the energy E of an equatorial particle should be proportional to the earth's field strength $B \sim L^{-3}$, by invariance of the magnetic moment.

Many people have discussed diffusion by magnetic impulses and sudden commencements, which have a short rise time and long decay time [e.g., Fälthammar; Nakada and Mead]. The diffusion coefficient as given by Nakada and Mead is $D \sim 3(L/10)^{10} R_e^2/\text{day}$ [R_e is the earth's radius]. The steep radial dependence, as Fälthammar has shown, comes from the very long decay time of the magnetic impulses. This has the consequence that, at $L = 6$, this type of diffusion is much too small to explain the Davis-Williamson protons.

A potentially much more important mechanism is related to magnetic bays, and their associated electrostatic potential fields [Dungey,

Fälthammar]. Magnetic bays last some 10 to 30 minutes, and are caused by ionospheric currents which are driven by electrostatic fields. Because magnetic field lines are very nearly equipotential lines, these same electrostatic fields persist to large radial distances, where they energize charged particles. The time scale (10 - 30 minutes) is short compared to proton drift periods, hence (as Fälthammar has shown) the radial diffusion coefficient goes roughly like L^6, at large ($L \geq 5$) distances. For smaller distances, this kind of diffusion is negligible, because the electrostatic potential vanishes rapidly below subauroral latitudes.

Fälthammar's expression for the diffusion coefficient is

$$D = \frac{c^2}{8B^2} \sum_{n=1} P_n \tag{1}$$

where

$$P_n = 4 \int_0^\infty d\tau \, \langle E_n(L,t) \, E_n(L,t+\tau) \rangle \cos n\omega_D \tau \tag{2}$$

is the power spectrum at the frequency $n\omega_D\tau$ of the azimuthal electric field $E(L,t)$:

$$E(L,t) = \sum_{n=0} E_n(L,t) \cos (n\omega_D t + \phi_n) \tag{3}$$

In these expressions, B is the earth's magnetic field, ω_D is the drift frequency, ϕ_n a phase angle presumably randomly distributed, and the quantity in angular brackets is the autocorrelation function of the

Fourier components of the electric field. For fields generated by magnetic bays, E points west on the night side, east on the day side, and so the term with n=1 in equations (1 - 3) is doubtless the most important. We shall in any event only keep the n=1 term. For the brackets in (2) we write

$$\langle \quad \rangle = E(L)^2 \, e^{-2\tau/T} \tag{4}$$

where T is a characteristic time for magnetic bays, say, 2×10^3 sec. It is then easy to find D:

$$D = \frac{c^2 L^6 T E(L)^2}{4B_o^2 \left[1 + \left(\frac{\omega_D T}{2}\right)^2\right]} \quad , \quad B_o = 0.31 \text{ gauss} \tag{5}$$

Little is known about E(L), but extrapolation of ionospheric potentials shows that the associated potential over several earth radii might be 1 - 10 kv. We therefore set $E(L) \approx 10^{-8} - 10^{-9}$ in cgs units, and get

$$D = (1 - 100)\left(\frac{L}{10}\right)^6 R_e^2/\text{day} \tag{6}$$

(This expression does not include the relative variation of $E(L)^2$ with L, and equation (6) should not be used below L = 4 or 5.) This kind of diffusion can easily dominate magnetic impulse diffusion. In going from (5) to (6), we have set $1 + (\omega_D T/2)^2 \approx 1$, since T is considerably

shorter than the drift period. In the opposite limit, $T\omega_D \gg 1$, we find $D \sim L^{10}$, since $\omega_D \sim L^{-2}$.

B. Short-time-scale processes. We begin by discussing very briefly certain electrostatic instabilities which can promote the fast diffusion of plasma across a magnetic field. (Such fast diffusion is known as Bohm diffusion in laboratory plasmas.) An example of the type is the universal instability [Krall and Rosenbluth, 1963]. In a plasma with a density gradient, helical electrostatic waves can propagate along a magnetic field line and be amplified by the instability. The growth rate of the instability depends on the ratio of plasma scale length to ion cyclotron radius; the smaller this ratio, the more severe the instability. For a ratio of about 10, one expects growth times on the order of minutes. Unfortunately, this ratio is liable to be about 10^3 in the magnetosphere, unless sharp spikes of enhanced (or depleted) field-aligned plasma exist. But such sharp spikes would be rapidly dissipated by drift instabilities in the thermal plasma. Our tentative conclusion is that this process is not liable to dominate radial diffusion.

Secondly, we consider processes that violate the longitudinal invariant, i.e., processes with characteristic periods near the proton bounce period of about 30 sec (for a 75-kev proton at L = 6). Pc 2-3 (5 - 45 sec) fits ideally. The formulas needed to calculate the diffusion coefficient have already been given [Cornwall, 1966], in an application to electrons interacting with Pc 1. The reader is referred to this paper

for details; the result is

$$D = 4\times10^{3}\left(\frac{L}{10}\right)^{-1/2}\left(\frac{b}{B}\right)^{2} R_e^2/\text{day} \tag{7}$$

where b is the hydromagnetic wave strength, and B is the earth's field strength. For $L \geq 4$, we might guess $b/B \simeq 10^{-2}$ ($b \simeq 5\gamma$ at $L = 4$), and thus

$$D \simeq 0.4\left(\frac{L}{10}\right)^{-1/2} R_e^2/\text{day} . \tag{8}$$

Of course, if b/B changes with L very much, formula (7) instead of (3) should be used.

Finally, Pc 1 hydromagnetic waves can cause radial diffusion in an axially asymmetric magnetosphere [Roederer, 1967]. These waves, of frequency 0.2 - 5 Hz, are thought to be generated by Davis-Williamson protons, so in a sense the protons are causing their radial diffusion. It is difficult to estimate the diffusion coefficient without extensive numerical analysis, but we can argue as follows: A Davis-Williamson proton drifts around the earth on a time scale measured in hours. During this time, strong pitch-angle diffusion may change the pitch angle by a few tenths of a radian, corresponding to a radial movement of a few tenths of an earth radius. We estimate D by

$$D \simeq \frac{1}{2}\frac{(\Delta r)^2}{T_D} \tag{9}$$

where Δr is a fraction of an earth radius, and T_D the drift time (say

one or two hours). An upper limit for D might be 1 R_e^2 day^{-1}. This sort of diffusion cannot occur below L = 5, where the magnetosphere begins to look axially symmetric.

It is clear from the crudity of the estimates of this section that it is difficult to pin down a good value for the radial diffusion coefficient. All things considered, it is probably fair to take D at L = 6 of the order of 1 R_e^2/day. It would be not at all surprising to learn that other workers have made different (and better) estimates of the diffusion coefficient, but the author knows of no published values for processes other than magnetic impulses.

3. COMBINED DIFFUSION AND NONLINEAR LOSS RATE

Scattering of Davis-Williamson protons by Pc 1 can be described as a diffusion process acting on the protons' pitch angles, which causes the protons to leak into the loss cone. Because the protons themselves produce Pc 1 waves, the pitch-angle diffusion process is nonlinear [Cornwall, 1966; Kennel and Petschek]. For a sufficiently strong source of protons, saturation occurs and the proton flux is effectively bounded. It would be virtually impossible to combine the nonlinear partial differential equations of pitch-angle diffusion and wave growth with a radial diffusion differential equation. There is, however, a simple approximation which allows us to describe pitch-angle diffusion by an effective nonlinear loss term, whose magnitude has recently been calculated [Cocke and Cornwall, 1967].

Let $f(\underset{\sim}{r},\underset{\sim}{v},t)$ be the Boltzmann distribution function for the protons. The time rate of change of f by pitch-angle diffusion can be written:

$$\frac{\partial f}{\partial t} = x^{-1}(1-x^2)^{1/2}\,\frac{\partial}{\partial x}\left[x(1-x^2)^{1/2}\,D\epsilon\,\frac{\partial f}{\partial x}\right] \tag{10}$$

where x (not to be confused with the spatial coordinate) is the sine of the pitch angle, $D \approx 75\,(L/4)^{-3}\ \text{sec}^{-1}$, and ϵ is essentially b^2/B^2 (b = Pc 1 magnetic field, B = earth's field). (See Cocke and Cornwall for details.) We propose to replace equation (10) by a much simpler form:

$$\frac{\partial f}{\partial t} = -\lambda(f) f \tag{11}$$

To do so, we need to know some average behavior of f and ϵ. We can make an empirical fit to the calculations of Cocke and Cornwall; this fit is shown in Figure 1, where the data points are computer calculations, and ϵ is inversely proportional to the omnidirectional flux J of protons. A good fit is:

$$\epsilon(J) = 1.7 \times 10^{-4} \exp\left|\frac{-2 \times 10^3}{J}\left(\frac{L}{4}\right)^{-4}\right| \tag{12}$$

where J is the omnidirectional flux in $cm^{-2}\ sec^{-1}$. The number of protons entering the loss cone per second is

$$\left|\frac{\partial}{\partial t}\int_{x_o}^{1} dx\ x(1-x^2)^{-1/2} f\right| = x(1-x^2)^{1/2} D\epsilon \left.\frac{\partial f}{\partial x}\right|_{x=x_o} \tag{13}$$

where x_o is the sine of the loss angle. Experimentally, $f \sim x^2$ (roughly), so we carry out the differentiation in (13), multiply by a factor representing the fraction of time micropulsations are present (say, 0.3), and assume it is sufficiently accurate to replace f by J. The resulting equation of the type (11) is:

$$\frac{\partial J}{\partial t} = -J\lambda(J) = -3 \times 10^2\, J\left(\frac{L}{4}\right)^{-3} \exp\left|\frac{-2 \times 10^3}{J}\left(\frac{L}{4}\right)^{-4}\right| day^{-1} \tag{14}$$

Note the saturation effect: as J becomes large, the loss rate grows exponentially.

The next step is to add to (14) an effective source term from radial diffusion. On very general grounds [Dungey; Fälthammar, 1966] the diffusion term looks like

$$r^2 \frac{\partial}{\partial r}\left(Dr^{-2} \frac{\partial J}{\partial r}\right) \tag{15}$$

(again we replace the Boltzmann distribution function f by J), where r is the radius variable: $r = LR_e$. In equilibrium,

$$0 = \frac{\partial J}{\partial t} = r^2 \frac{\partial}{\partial r}\left(Dr^{-2} \frac{\partial J}{\partial r}\right) - J\lambda(J) \tag{16}$$

This is a nonlinear equation in J, which a computer could easily handle. The important nonlinear feature means that, given the spatial dependence of J, the magnitude of J can be determined at a particular point. To illustrate, suppose $J \sim r^N$, $D \sim r^6$; equation (16) becomes

$$N(N+3)DJr^{-2} = J\lambda(J) \tag{17}$$

Take $r = 6R_e$, $D = 1\ R_e^2\ \text{day}^{-1}$, $N = -6$ to find $J(L=6) = 10^7\ \text{cm}^{-2}\ \text{sec}^{-1}$. This is quite comparable to observed fluxes. Note that the value of J depends only logarithmically on the details of the diffusion process, which is fortunate since these details are very poorly known.

Of course, there are other loss processes (e.g., charge exchange, Coulomb scattering) not considered here, but apparently in $L = 4$-6 pitch-angle diffusion is the main loss mechanism, on the basis of rough estimates.

4. CONCLUSIONS

A wide variety of physical effects contribute to radial diffusion, and these are difficult to estimate severally and collectively. However, the exponential dependence of loss rate on J minimizes the effect of this uncertainty. We are left with the task of calculating accurately the coefficient of J^{-1} in the exponent in loss rate (equation (12)). The work of Cocke and Cornwall may well contain systematic errors of a factor of 2 or 3, which might best be revealed by fitting the observed data to the solution of equation (16), or a similar, more accurate equation.

Little can be said about the radial dependence of J until equation (16) is solved numerically. It is unlikely that J can stray too far from a dependence like L^{-4}, since $J \sim L^{-4}$ means that the exponential term in (14) depends rather insensitively on L. This sort of radial dependence is reasonably consistent with experiment.

One major problem we have left untouched is that most of the processes listed in Table I give quite small diffusion coefficients at $L = 3\text{-}4$, with at least the exception of electrostatic processes, about which we know little. The Davis-Williamson protons are certainly seen in this L range, so something must be diffusing them inward. One is tempted to speculate that universal instabilities might be important near the density knee, near $L = 3\text{-}4$, where plasma density gradients are larger than elsewhere in the magnetosphere.

ACKNOWLEDGMENTS

I would like to thank Prof. C-G Fälthammar for valuable discussion on the topics of this paper.

This work was completed at Aerospace Corporation. Publication was supported by the U.S. Air Force under Contract AF 04(695)-1001.

REFERENCES

Brice, N. M., Fundamentals of very low frequency emission generation mechanisms, J. Geophys. Res., 69, 4515-4522, 1964.

Cocke, W. J., and J. M. Cornwall, Theoretical simulation of micropulsations, J. Geophys. Res., 72, 2849-2856, 1967.

Cornwall, J. M., Cyclotron instabilities and electromagnetic emission in the ULF and VLF frequency ranges, J. Geophys. Res., 70, 61-69, 1965.

Cornwall, J. M., Micropulsations and the outer radiation zone, J. Geophys. Res., 71, 2185-2199, 1966.

Davis, L. R., and J. M. Williamson, Low-energy trapped protons, Space Res., 3, 365-375, 1963.

Dungey, J. W., Effects of electromagnetic perturbations on particles trapped in the radiation belts, Space Science Reviews, 4, 199, 1965.

Fälthammar, C-G., Effects of electric fields on trapped radiation, J. Geophys. Res., 70, 2503-2516, 1965.

Fälthammar, C-G., On the transport of trapped particles in the outer magnetosphere, J. Geophys. Res., 71, 1487-1491, 1966a.

Fälthammar, C-G., Coefficients of diffusion in the outer radiation belt, Radiation Trapped in the Earth's Magnetic Field, ed. B. M. McCormac, D. Reidel Company, Holland, 1966b.

Jacobs, J. A., and T. Watanabe, Micropulsation whistlers, J. Atmos. Terrest. Phys., 26, 825-829, 1964.

Kennel, C. F., and H. E. Petschek, A limit on stably trapped particle fluxes, J. Geophys. Res., 71, 1, 1966.

Krall, N. A., and M. Rosenbluth, Low-frequency stability of non-uniform plasmas, Phys. Fluids, 6, 254, 1963.

Nakada, M. P., and G. D. Dungey, Diffusion of protons in the outer radiation belt, J. Geophys. Res., 70, 3529-3532, 1965.

Obayashi, T., Hydromagnetic whistlers, J. Geophys. Res., 70, 1069-1078, 1965.

Roederer, J. G., On the adiabatic motion of energetic particles in a model magnetosphere, J. Geophys. Res., 72, 981-992, 1967.

Table I. A survey of processes liable to be effective in promoting radial diffusion.

Type	Time Scale of Fundamental Process	Effectively Energy-Conserving?	Radial Dependence	Effective Diffusion Coeff. (R_e^2/day)
Magnetic impulses and sudden commencements (betatron effect)	Fast rise; decay over several hours to days	No	L^{10}	$3\left(\frac{L}{10}\right)^{10}$
Magnetic bays (azimuthal electric field)	10 - 30 minutes	No	L^6	$(1\text{-}100)\left(\frac{L}{10}\right)^6$
Electrostatic instabilities (Bohm diffusion)	Very short to a few minutes	No	?	?
Pc 2-3 (violation of 2nd invariant)	5 - 45 sec	Yes	Probably not as steep as L^6	~0.5
Pc 1 (splitting of drift shells in axially asymmetric magnetosphere)	0.2 - 5 sec	Yes	Ineffective below L = 5	<1

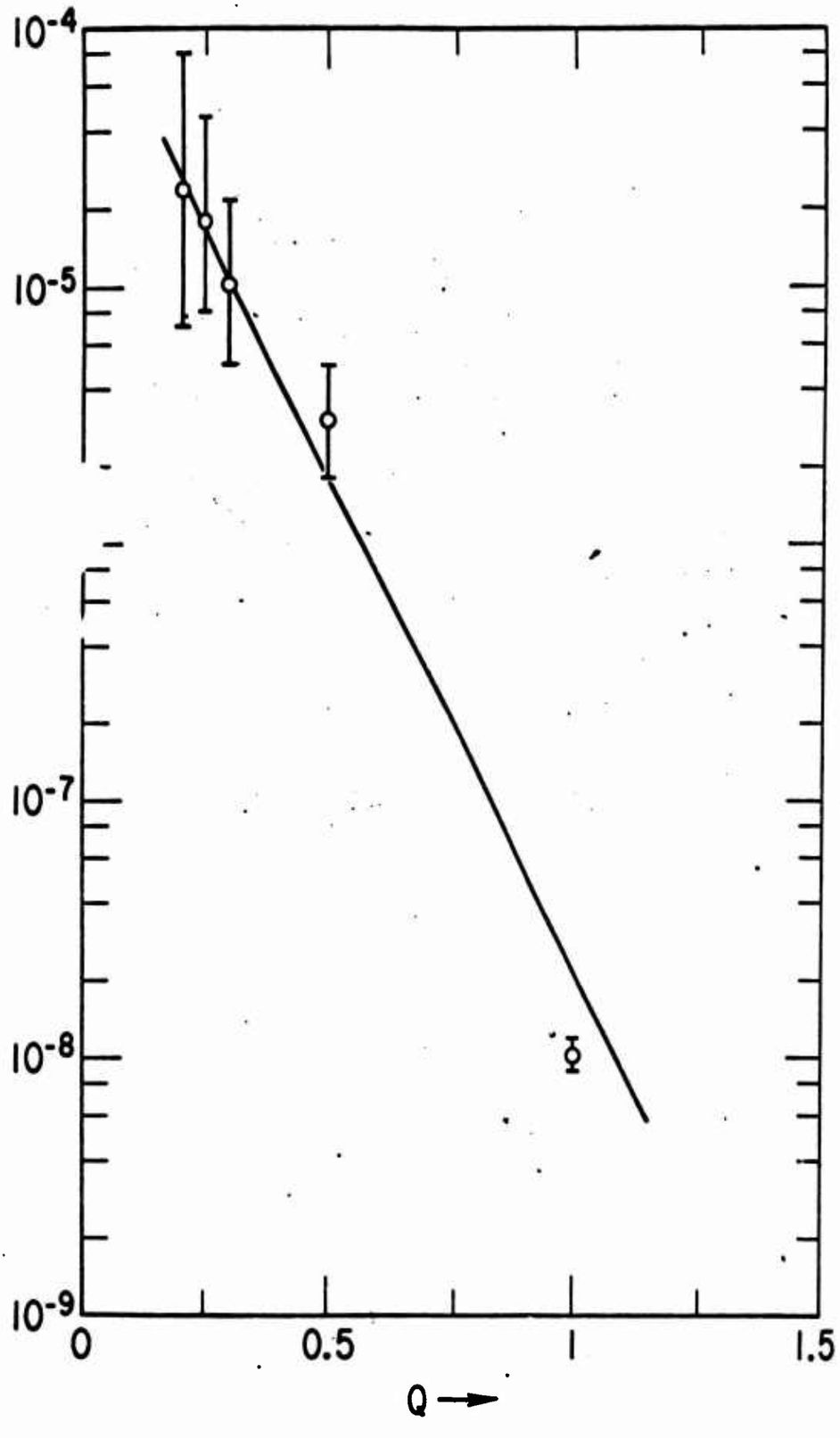

Figure 1: Effective loss rate (unnormalized) vs. Q. Q is a variable inversely proportional to the omnidirectional flux; see text for details.

MEASUREMENT AND INTERPRETATION OF ULF AND VLF POWER SPECTRA

J. F. Kenney, H. B. Knaflich and H. B. Liemohn
Boeing Scientific Research Laboratories
Seattle, Washington 98124

Recently a method was proposed for estimating the pitch angle and energy distributions of nonthermal particles in the magnetosphere based on the cyclotron-resonance amplification of VLF and ULF whistlers. The method requires measurements of the power-spectral density of two or more consecutive whistler elements which have traversed the same path. Multi-hop VLF whistler events recorded by a ground receiver (courtesy D. L. Carpenter) and by satellite (courtesy R. E. Barrington) have been analyzed for power spectra by playing a tape loop repeatedly through a swept-frequency filter. Several multi-hop ULF whistlers, otherwise known as pearl micropulsations, have been similarly analized for power spectra.

The relationship between the observed power spectra of successive whistler echoes is shown schematically in Figure 1. P_W is the initial spectrum incident on the top of the ionosphere, P_S and P_R are the observed source and response spectra and M, T, and R are linear power-transfer coefficients for the magnetosphere and ionosphere. Observed ratios give the product MR, which requires independent measurements of M or R to test the theory.

An ampligram of one of the multihop VLF events (D. L. Carpenter) which we have analyzed, and some of its fine structure is shown in Figure 2. The power spectra of elements in this event are shown in Figure 3 and their successive ratios P_R/P_S are shown in Figure 4. Using published ionospheric absorption curves to estimate R (Helliwell, Whistlers and Related Ionospheric Phenomena) the magnetospheric amplification can be estimated as shown in Figure 5. The cutoff ratio of propagation frequency ω to minimum electron gyrofrequency ω_{co}^{e} is based on conventional dispersion analysis (R-mode).

The cyclotron resonance interaction between VLF whistlers and nonthermal electrons (0.1-10 keV) gives amplification or absorption of the signal in the magnetosphere depending on the phase space distribution, F. The theory for whistler propagation in a hot plasma gives a complex propagation vector $k = k_r + ik_i$ where k_r is given by the cold plasma approximation and k_i depends strongly on F. The growth or decay along the propagation path is given by $A(db) = \text{const} \int_{path} k_i ds = 10 \log_{10} M$. The logarithmic magnetospheric power transfer has been evaluated for energy (E) and pitch-angle (α) distributions of the form $F = E^{-n} \sin^m \alpha$ (Liemohn, J. Geophys. Res. 72, 39-55, 1967) and a typical result is shown in Figure 6. The curve m = 0.5, n = 2.5 agrees fairly well with the data in Figure 5.

An ampligram of a typical multihop ULF whistler event (pearl) is shown in Figure 7. The unsmoothed power spectra of the elements in this event and their successive ratios are shown in figures 8 and 9, respectively. There appears to be a steady downward shift in the peaks

of maximum power. Since reflection can only reduce the power in successive hops it is evident that some amplification is present along the magnetospheric path. From dispersion analysis (L-mode) the propagation path is along L = 5.3 which has a minimum proton gyrofrequency 3.1 Hz.

The ionospheric reflection coefficient is not sufficiently well known to correct the observed ratios. The published reflection curves (Field and Greifinger, J. Geophys. Res. 70, 4885-4899, 1965) for propagation parallel to a vertical magnetic field (polar case) which are shown in Figure 10 are not quantitatively applicable to our data. The deep resonance spikes in $|R|$ depend on the model but may explain the large fluctuations in the power spectra that have been detected in pearl elements.

Typical theoretical power-transfer curves for the cyclotron resonance interaction between ULF whistlers and nonthermal protons (0.1-10 keV) in the magnetosphere are shown in Figure 11. Although the power transfer to individual elements cannot be determined, an estimate of $m=2$, $n=2$ has been inferred from certain general properties of pearls.

It has been demonstrated that the product MR can be determined experimentally for both VLF and ULF whistlers. For VLF, R is sufficiently well known to allow quantitative estimates of M, but for ULF, more realistic estimates of R are needed before an adequate measure of M can be attained.

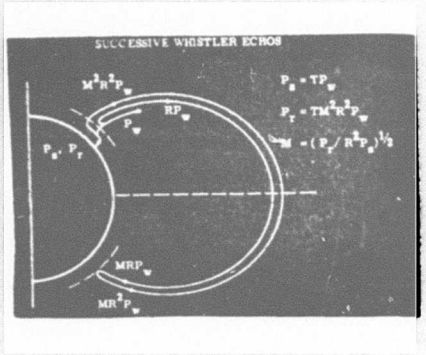

Fig. 1 - Power transfer relationships.

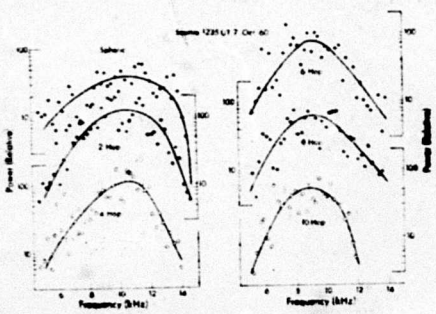

Fig. 3 - Power spectra of elements.

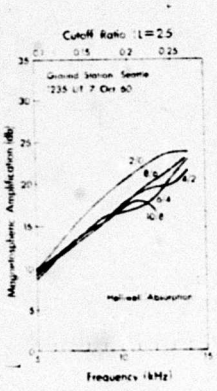

Fig. 5 - Ratios after ionospheric correction.

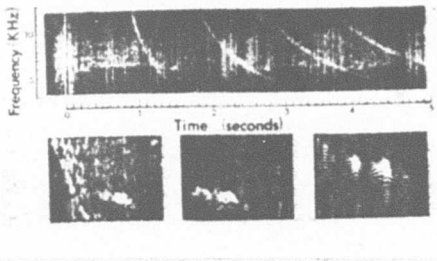

Fig. 2 - Multihop VLF event recorded at Seattle 7 Oct. 60, 1235 UT (Carpenter).

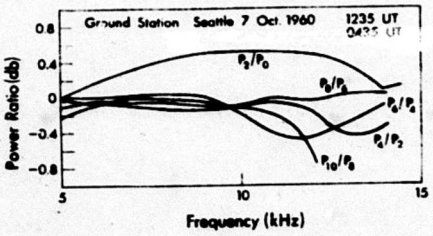

Fig. 4 - Power ratios.

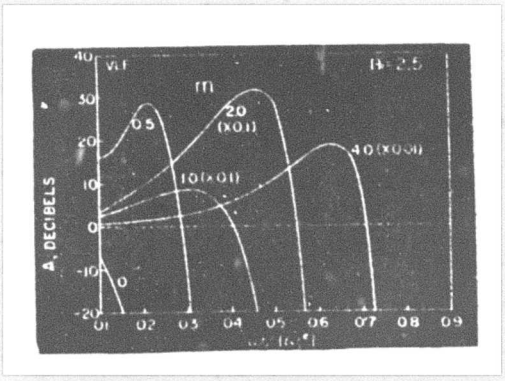

Fig. 6 - Theoretical power transfer in the magnetosphere.

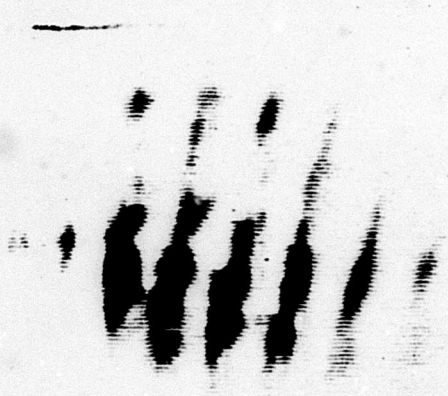

Fig. 7 - ULF pearl event recorded at Seattle 17 Jan. 67, 1330 UT.

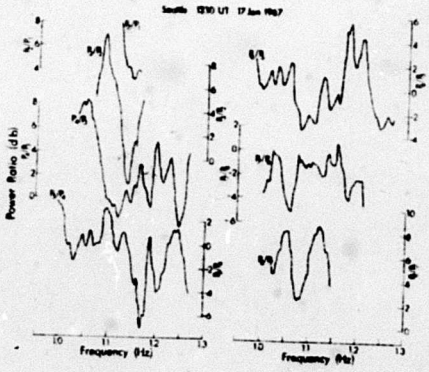

Fig. 9 - Power ratios.

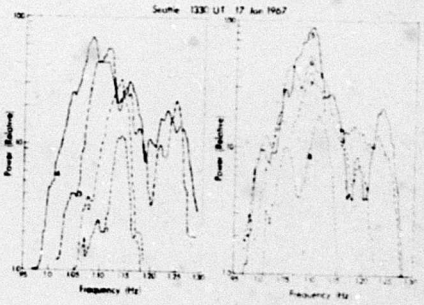

Fig. 8 - Power spectra of elements.

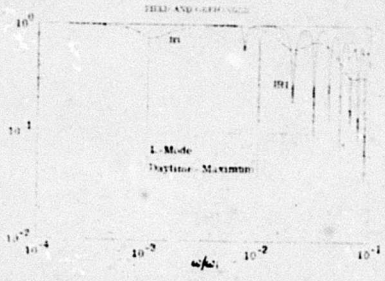

Fig. 10 - Ionospheric reflection coefficients.

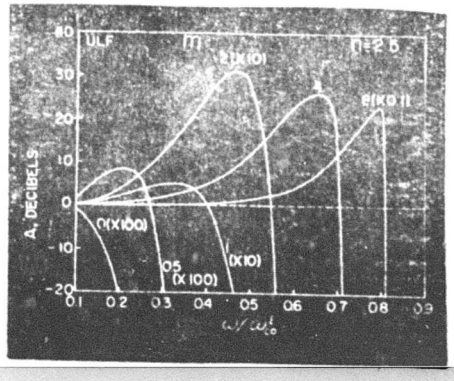

Fig. 11 - Theoretical power transfer in the magnetosphere.

BLANK PAGE

EM AND HM GUIDED WAVES IN THE EARTH'S ATMOSPHERE

Neil Brice

CENTER FOR RADIOPHYSICS AND SPACE RESEARCH
CORNELL UNIVERSITY
ITHACA, NEW YORK

In this paper I shall consider guiding of waves in the upper atmosphere and then discuss the guided waves which are of natural origin. Guiding of waves in the earth's upper atmosphere may be brought about by either inhomogeneity or anisotropy. The inhomogeneity may take the form of a discontinuity in refractive index (such as is found at the earth's surface) from which partial reflection occurs or of a gradient in refractive index. In the latter case in an isotropic medium, the curvature of the ray is given by the $\frac{\nabla n \cdot \hat{k}}{n}$ where n is the refractive index and $\hat{k}$ is a unit vector in the wave normal direction.

The general condition for trapping or ducting of waves along a surface is that the component of refractive index normal to the surface be sufficient to give the ray a curvature at least equal to the curvature of the surface. For example, the ducting of high frequency waves in the magnetosphere requires a gradient of refractive index in the meridian plane normal to the magnetic field which produces a curvature of the ray at least equal to the curvature of the magnetic field

Of greater interest to conjugate point studies is the guiding of waves due to anisotropy in the propagation which arises from the earth's magnetic field. In a homogeneous magnetoplasma such as the upper atmosphere, the group ray (or vector group) velocity W_{gr} of a wave with frequency ω and wave vector $\bar{k}$, propagating at an angle θ to the magnetic field is given by

$$\bar{W}_{gr} = \hat{k} \left.\frac{d\omega}{d|k|}\right|_{\theta} + \frac{\hat{\theta}}{|k|} \left.\frac{d\omega}{d\theta}\right|_{|k|}$$

The first term gives the component of group ray velocity in the direction of propagation while the second term, the component normal to the direction of propagation, arises from the anisotropy of the medium and produces the guiding to be discussed below. The angle, α, between the ray direction and wave normal direction is given by

$$\alpha = \tan^{-1}\left(\frac{-1}{n}\frac{dn}{d\theta}\right) = \tan^{-1}\left(\frac{1}{W}\frac{dW}{d\theta}\right)$$

where W is the phase velocity of the wave. For guiding in the magnetic field direction, we require α to be negative and hence $\frac{dn}{d\theta}$ to be positive. The magnitude of $dn/d\theta$ may be estimated from the shape of the phase velocity surface (a polar plot of phase velocity, W, versus θ). If the phase velocity surface is elliptical, $\frac{dW}{d\theta}$ (and hence $dn/d\theta$) is generally small, corresponding to a weak guiding condition. If the phase velocity surface has a "figure 8" shape, $dW/d\theta$ is generally large, corresponding to strong guiding. Thus a general idea of the conditions under which strong guiding will occur can be obtained from examination of the phase velocity surfaces for a CMA diagram. Figure 1 shows a CMA constructed for conditions appropriate to the magnetosphere, i.e., a plasma consisting of electrons and protons.[1] The vertical scale is the ratio of electron gyrofrequency squared to wave frequency squared ($Y_e^2 = \Omega_e^2/\omega^2$) and the horizontal scale is the ratio of electron plasma frequency squared to wave frequency squared ($X_e^2 = \pi_e^2/\omega^2$). For each area of the diagram, the shape of the phase velocity surface is given at the right of the figure, the vertical direction being that of the magnetic field. For strong guiding in the direction of the magnetic field we require a vertical "figure 8" phase velocity surface, which is

found in regions 7 and 8 for the right-hand polarized (whistler) mode and region 10 for the left-hand polarized (Alfven) mode. Thus the strong guiding along the field of right-hand polarized waves occurs at frequencies below the plasma frequency ($X_e > 1$) and the electron gyrofrequency ($Y_e > 1$) but above the electron-ion hybrid (or lower hybrid) resonance frequency, while for the left-hand polarized waves it occurs at frequencies below the ion gyrofrequency.

For a sufficiently dense plasma the phase velocity for the right-hand circularly polarized mode (W_R) at low frequencies is given by (ignoring ion effects)

$$W_R^2 = \frac{c^2 \Omega_e \omega}{\omega_e^2}$$

where

ω_e is the electron plasma frequency and

Ω_e is the electron gyrofrequency and

ω is the wave frequency.

For the left-hand, (L) and plasma (P) modes the phase velocities are approximately

$$W_L^2 \doteq \frac{-c^2 \omega \Omega_e}{\omega_e^2}$$

and

$$W_P^2 \doteq -c^2 \frac{\omega^2}{\omega_e^2} \doteq 0 \ .$$

For the extraordinary mode, the phase velocity is given by

$$W_x^2 = \frac{W_R^2 + W_L^2}{2} \doteq 0 \ .$$

The Astrom equation for the phase velocity, W, as a function of propagation angle, θ,

$$(W^2 - W_R^2)(W^2 - W_L^2)\cos^2\theta + (W^2 - W_P^2)(W^2 - W_X^2)\sin^2\theta = 0$$

then reduces to

$$(W^2 - W_R^2)(W^2 + W_R^2)\cos^2\theta + W^4\sin^2\theta = 0 ,$$

$$W^4(\cos^2\theta + \sin^2\theta) - W_R^4\cos^2\theta = 0 ,$$

so that

$$W = W_R(\cos\theta)^{\frac{1}{2}} ,$$

and

$$n = n_R(\cos\theta)^{-\frac{1}{2}} .$$

For this case the angle between the wave normal and the ray is given by

$$\tan\alpha = -\frac{1}{n}\frac{dn}{d\theta}$$

$$= -(1/2)\tan\theta$$

The angle between the ray and the magentic field is

$$\phi = \alpha + \theta \quad \text{so that}$$

$$\tan\phi = \frac{\tan\theta}{2 + \tan^2\theta}$$

for small values of θ, $\phi = \frac{1}{2}\theta$ and for large θ, ϕ tends to zero, i.e., perfect guiding. At frequencies well below the ion cyclotron frequency,

$$W_R^2 \doteq W_L^2 \doteq W_x^2 \doteq W_A^2$$

where W_A is the Alfven velocity and the Astrom equation reduces to

$$(W_A^2 - W^2)^2 \qquad - W^2(W_A^2 - W^2)\sin^2\theta = 0$$

so that for the slow mode

$$W^2 = W_A^2 \cos^2\theta$$

from which

$$\tan\alpha = \frac{1}{W}\frac{dW}{d\theta} = -\tan\theta$$

so that

$\alpha = -\theta$ and the ray direction is the direction of the magnetic field (i.e., perfect guiding.)

The approximations used here break down for the right-hand mode at frequencies below but comparable with the electron gyrofrequency and between the ion gyrofrequency and the electron-ion hybrid (or lower hybrid) resonance frequency, and for the left-hand mode at frequencies below but comparable with the ion gyrofrequency.

In the first of these cases ($\omega \doteq \Omega_e$), we may use

$$W^2 = \frac{c^2\omega(\Omega_e\cos\theta - \omega)}{\omega_e^2}$$

to obtain

$$\tan\alpha = \frac{-\tan\theta}{(1-\omega\sec\theta/\Omega_e)}$$

so that α is negative and larger in magnitude than θ for small θ, and increases in magnitude more rapidly than θ.

For the right hand mode at the ion gyrofrequency, we may use $W_L^2 \doteq 0 \doteq W_p^2$ in the Astrom equation and obtain

$$\tan\alpha = -\frac{\tan\theta}{2 + \tan^2\theta}$$

which provides reasonable guiding only at small angles.

For the left hand mode near the ion gyrofrequency, we may use

$$0 \doteq W_p^2 \ll W^2, \quad W_L^2 \ll W_X^2$$

to obtain

$$\tan\alpha = -\frac{\tan\theta(1+\tan^2\theta)}{2 + \tan^2\theta}$$

It is seen that in the case, $\psi = -\theta/2$ for small θ, and that $\psi = -\theta$ for large θ, so that this situation is very similar to the low frequency whistler mode case discussed above.

We turn our attention now from the guiding of waves to the waves which are guided in the direction of the magnetic field in the upper atmosphere, i.e., right-hand polarized (electromagnetic) waves at frequencies between the electron and ion cyclotron frequencies and left-hand polarized (hydromagnetic) waves at frequencies below the ion cyclotron frequency. In the upper atmosphere, the naturally occurring waves which fall into the former category are whistlers and so-called "VLF" emissions while in the latter are ion whistlers and micropulsations or "hydromagnetic" emissions. The range of frequencies encompassed in this paper extends over 7 decades from a lower limit of about 0.1 Hz (for which the wavelength in the magnetosphere is at least several earth radii) to about 1.5 MHz (the electron cyclotron frequency in the ionosphere). Since the whistlers are better understood then the emissions, I will consider them first.

Whistlers have their origin in impulses radiated by lightning discharges, these impulses being dispersed by propagation in the ionosphere and magnetosphere to produce the whistler. The energy propagates from hemisphere to hemisphere along the earth's magnetic field.[2] Whistlers have many fascinating properteis, a few of which will be mentioned. (See Helliwell[3] for a more complete description). Whistlers which make many successive traverses of the magnetosphere produce echo trains, the ratio of dispersions of successive whistlers being 2:4:6, etc. (if initiating lightning discharge was in the same hemisphere as the observer), or 1:3:5, etc. (if the lightning was in the opposite hemisphere).

Frequently whistler energy is trapped in field-aligned columns of enhanced ionization or "ducts",[4] producing whistlers with a number of discrete traces, each corresponding to a particular field-aligned outer-magnetospheric path. An example of such a multipath whistler is shown in Figure 2. Occasionally the whistler follows different paths on successive hops (mixed-path whistlers) and multiple-flash lightning produces multi-flash whistlers. Whistlers have long been used to measure electron densities in the magnetosphere.[2,4,5] More recently radial motions of the ducts have been measured using whistlers, and from these measurements the magnitude of the electric fields in the magnetosphere have been deduced.[6] An example of movement of ducts is illustrated in Figure 3.

Audio frequency receivers on board satellites have recorded proton[7] and helium[8] (ion) whistlers in which the dispersion arises primarily from the proximity of the wave frequency to the appropriate ion cyclotron frequency.[9] An example of a proton whistler is shown in Figure 4. The electron and ion whistler traces meet at the crossover frequency[10] from which the fractional abundance of hydrogen ions at the satellite may be determined.[11] The dispersion of the proton whistler is dependent on the proximity of the wave frequency to the proton gyrofrequency at the satellite and is proportional to the proton plasma frequency at the satellite. These properties of proton whistlers have been used to determine the earth's magnetic field strength at the satellite with considerable accuracy[1] and also the proton number density.[12] The proton whistler is cut off by cyclotron damping at frequencies a few cycles below the proton gyrofrequency. The difference between cut-off frequency and gyrofrequency arises from the thermal motion of the ions, and has been used to determine proton temperature.[13]

Whistlers have been recorded in the frequency range from a few tens of Hz to a few tens of kHz.

We turn now to waves which are generated in the ionized atmosphere, and generally referred to as "emissions".

A number of generalizations which may be made about these emissions[14] are illustrated in Figure 5. The scale at the top of this figure shows the range of frequencies occupied by the emissions, from a (rather arbitrary) lower limit of about 0.1 Hz to an upper limit of about 10^6 Hz. The emissions observed on the ground fall naturally into two calsses, those below about 10 Hz which we call hydromagnetic (HM) and those above 100 Hz which we call electromagnetic (EM).

At intermediate frequencies, ground-based observations of waves of upper atmospheric origin are hampered by Schumann resonances and power-line interference, and the dearth of observed emission may be due to this interference, to the opacity of the ionosphere at these frequencies (due to multiple-ion propagation effects) or to an absence of noise generation in this frequency range in the magnetosphere.

Each of these classes of emissions (EM and HM) may be further subdivided into "discrete" emissions which consist of a series of gliding (rising and/or falling) tones and "diffuse" emissions, or hiss, which most resemble band-limited white noise.

As illustrated in Figure 5, for both EM and HM emissions there are two types of diffuse emission and one type of discrete emission. The diffuse impulsive HM emissions (P_i micfopulsations) occur primarily at night[15] (N) when the energetic particle precipitation contains both electrons (e) and protons (p). The diffuse continuous HM emissions (P_c micropulsations) occur primarily in the morning[15] (M) when the

energetic particle precipitation consists primarily of electrons[16] (e). Discrete HM emissions (pearls) occur in the afternoon[17] (A), presumably in association with proton precipitation.[18]

At night one also finds a maximum for diffuse EM emissions at frequencies generally above 4 kHz (auroral hiss) while in the morning one finds diffuse EM emissions below 4 kHz (polar chorus and mid-latitude hiss) as well as discrete EM emissions (chorus).[19] The frequency ranges generally occupied by these emissions are also shown in Figure 5. The night-time diffuse emissions (EM and HM) are often associated with auroral substorms[19,20].

EM and HM discrete emissions have a number of fascinating characteristics in common. For both types, a predominance of rising tones is observed.[22,23] On occasion, periodic emissions are detected,[23,24] an example of periodic EM emissions being shown in Figure 6. The emissions are observed alternately in opposite hemispheres[25,26] and the period of the emissions is the two-hop hemisphere-to-hemisphere propagation delay,[27] the delay being that of left-hand polarized waves for HM emissions[28] and right-hand polarized waves for EM emissions.[27] This property has allowed the use of periodic emissions to determine magnetospheric electron densities by techniques similar to those used for whistlers.[28,29]

From observations of periodic emissions, it is apparent that the generation of one emission may be stimulated by the arrival in the generation region of the echo of the previously generated emission,[30] and generation of discrete VLF emissions may also be stimulated by whistlers[2] or man-made signals from VLF transmitters,[31] an example being shown in Figure 7. Multi-phase periodic EM emissions have been

observed, i.e., evenly spaced sets for which the apparent period is a subharmonic of the true period. An example of multiphase emissions is shown in Figure 8. It is found that two sets or phases represents an unstable configuration while three phases is much more stable. Discrete EM emissions sometimes show "frequency modulation", i,e., a quasi-periodic change in the center frequency of the emission,[3] an example being shown in Figure 9. The discrete emissions are generally observed at frequencies less than, but comparable with, the minimum gyrofrequency for the magnetic field line path along which they propagate. The generation mechanism for discrete emissions is not well understood. The emission certainly involves non-linear interaction between the waves and energetic charged particles, very likely in a cyclotron-resonance interaction, probably at several earth radii in the vicinity of the equatorial plane and possibly involving trapping of energetic particles in potential wells of coherent wave fields. It is believed that discrete EM emissions are generated by energetic electrons, discrete HM emissions by energetic protons.

We come now to the generation of the diffuse emissions, and here we find a substantial divergence between EM and HM emissions. Certainly some and possibly all of the diffuse HM emissions discussed here are <u>not</u> generated through cyclotron-resonance plasma instabilities with protons, whereas we believe that all the diffuse EM emissions discussed are generated through cyclotron-resonance instabilities by energetic electrons.[33,34]

The simultaneity of onset of the night-time P_i micropulsations, of the cosmic noise (riometer) absorption, of the negative bay on the

magnetometer[19] and the overhead passage of the expanding auroral bulge[35] strongly suggests that at least some and possibly all of these micropulsations arise from high frequency components of ionospheric currents. The close association between changes in amplitude of auroral hiss, auroral luminosity, cosmic noise absorption and the rate of change of vertical magnetic field is illustrated in Figure 10.

There is less certainty about the morning P_c micropulsations. The range of periods typical for these emissions is also typical for microbursts (modulation of precipitation of energetic electrons) in balloon X-ray observations and for the fading of VHF forward scatter (of A_3 and S types), all of which generally occur at about the same time of day.[16] However, whether the modulation of the magnetic field (the micropulsations) causes the electron precipitation (the microbursts) or vice versa is not known. It is probably significant that the periods found are of the same order as the mirror periods for trapped energetic electrons.

We turn now to consideration of diffuse EM emissions. In Figure 11, contours of constant average amplitude (in db) have been plotted to show the variation of average amplitude with frequency and time of day at Byrd Station. The main features of interest are two maxima, one in the late morning hours for the low frequencies (about 700 Hz) and one at night for the high frequencies (about 20 kHz. While there is little information available between about 20 kHz and 150 kHz, the ionosonde receiver on the Alouette II satellite often records intense noise at high latitudes extending from the lowest frequency of observation (about 150 kHz) up to a frequency comparable with, but somewhat less than the electron gyrofrequency at the satellite.[37] It seems likely then that

the night-time auroral hiss extends up to frequencies of the order of 1 MHz. The higher frequencies must certainly be generated in or near the ionosphere. By contrast, the morning polar chorus is confined to frequencies less than about 1.5 kHz, and is presumably generated in the equatorial plane at several earth radii.

As was mentioned above, the EM diffuse emissions are probably generated by energetic electrons through the cyclotron-resonance plasma instability. The growth rate γ of small-signal whistler-mode waves for this instability is given by[36]

$$\gamma = \pi \Omega_e (1-\omega_e)^2 \eta(V_R) \left[A(V_R) - \frac{\omega_e}{1-\omega_e} \right]$$

where Ω_e is the electron cyclotron frequency (e B/m), ω_e is the ratio of wave frequency to Ω_e, $\eta(V_R)$ is proportional to the fraction of electrons whose velocity along the magnetic field equals the resonance velocity, V_R, and $A(V_R)$ is the anisotropy factor for the resonant energetic electrons. The form of the equation is particularly interesting, the dominant factors for the growth rate being number of resonant electrons, η, and the anisotropy factor, A.

There is not sufficient time to discuss this instability in detail, but some general observations may be made. For stably-trapped electrons in the magnetosphere the anisotropy factor, A, is approximately independent of the position along a given magnetic field line. As a result, for a given ω_e, larger fluxes of electrons (i.e., larger η, and hence larger growth rates) are found in the equatorial plane. Thus the emissions generated by stably-trapped electrons will be expected to have their origin in or near the magnetic equatorial plane. Polar chorus and mid-latitude hiss are believed to be in this category.

For energetic electrons newly injected into the magnetosphere (presumably from the tail) the anisotropy factor, A, is larger in the ionosphere than in the equatorial plane. This allows generation at larger values of ω_e where the number of resonant electrons, η, is often very much larger. Thus newly injected electrons are expected to generate EM emissions primarily in the ionosphere, where, it is believed, all or most of the auroral hiss is generated.

Thus diffuse EM emissions at frequencies less than the electron gyrofrequency in the equatorial plane, i.e., the polar chorus and mid-latitude hiss, which occur in the morning, are probably generated by stably trapped electrons. The diffuse EM emission at frequencies much above the electron gyrofrequency in the equatorial plane, i.e., auroral hiss, which occurs at night, is probably generated by newly injected electrons.

This work was sponsored in part by the National Science Foundation, Division of Atmospheric Sciences under Grant NSF GA-878.

References

1. Brice, N. M., "Ion effects observed in radio wave propagation in the ionosphere" Proc. Symp. on EM wave theory, Delft Holland, Sept. 1965, D. Reidel Publishing Co., Holland, 1967.
2. Storey, L. R. O. "An investigation of whistling atmosphere", Phil. Trans. Roy. Soc. A246, pp. 113-141, 1953.
3. Helliwell, R. A. "Whistlers and related ionospheric phenomena" Stanford University Press, Stanford, California, 1965.
4. Smith, R. L., "Properties of the outer ionosphere deduced from nose whistlers" J. G. R., 66 (11), pp. 3709-3716, 1961.
5. Carpenter, D. L., "Whistler studies of the plasmapause in the magnetosphere 1. Temporal variations in the position of the knee and some evidence of plasma motions near the knee," J. G. R., 71(3), pp. 693-709, 1966.
6. Carpenter, D. L. and K. Stone, "Direct detection by a whistler method of the magnetospheric electric field associated with a polar substorm", Planet. Space Sci., 15, pp. 395-397, 1967.
7. Smith, R. L., N. M. Brice, J. Katsufrakis, D. A. Gurnett, S. D. Shawhan, J. S. Belrose and R. E. Barrington, "An ion gyrofrequency phenomenon observer in satellites," Nature 204(4955) pp. 274, October 17, 1964.
8. Barrington, R. E., J. S. Belrose and W. E. Mather, "A helium whistler observed in the Canadian satellite Alouette II," Nature 210(5031), pp. 80-81, 1966.
9. Gurnett, D. A., S. D. Shawhan, N. M. Brice and R. L. Smith, "Ion cyclotron whistlers," J. G. R., 70(7), pp. 1665-1688, April 1, 1965.

10. Smith, R. L., and N. M. Brice, "Propagation in multicomponent plasmas," J. G. R., 69(23), pp. 5029-5040, December 1, 1964.

11. Shawhan, S. D., and D. A. Gurnett, "Fractional concentration of hydrogen ions in the ionosphere from VLF proton whistler measurements," J. G. R., 71, pp. 47-57, 1966.

12. Gurnett, D. A. and S. D. Shawhan, "Determination of hydrogen ion concentration, electron density, and proton gyrofrequency from the dispersion of proton whistlers," J. G. R. 71, pp. 741-754, 1966.

13. Gurnett, D. A. and N. M. Brice, "Ion temperature in the ionosphere obtained from the cyclotron damping of proton whistlers," J. G. R. 71(15), pp. 3639-3652, August 1, 1966.

14. Brice, N. M., "Generation of VLF and Hydromagnetic Emissions", Nature 206(4981), p. 283, April 17, 1965.

15. Jacobs, J. A. and C. S. Wright, "Geomagnetic micropulsation results from Byrd station and Great Whale River," Can. J. Phys. 43, p. 2099 1965.

16. Hartz, T. R. and N. M. Brice, "The general pattern of auroral particle precipitation," Planet. Space Sci. 15(2), p. 301-329, 1967.

17. Wentworth, R. C., "Evidence for the maximum production of hydromagnetic emissions above the afternoon hemisphere of the earth 1. Extrapolation to the base of the exosphere," J. G. R. 69(13), pp. 2689-2698, 1964.

18. Brice, N. M., "Bulk motion of the magnetosphere," Cornell-Sydney University Astronomy Center report CSUAC 78, Center for Radiophysics and Space Research, Cornell University, Ithaca, New York, 14850.

19. Morozumi, H. M., and R. A. Helliwell, "A correlation study of the variation of upper atmospheric phenomena in the southern auroral zone," Technical report number SU-SEL-66-124, Stanford Electronics Laboratories, Stanford, California, 1966.

20. Campbell, W. H., and S. Matsushita, "Auroral-zone geomagnetic micropulsations with periods of 5 to 30 seconds", J. G. R. 67(2), pp. 286-298, 1957.

21. Allcock, G. McK., "A study of the audio-frequency radio phenomenon known as 'dawn chorus'," Austral. J. Phys., 10(2), pp. 286-298, 1957.

22. McInnes, B. A., "A study of ionospheric at Macquarie Island," Austral. J. Phys. 14(2), pp. 218-233, 1961.

23. Tepley, L. R., and R. C. Wentworth, "Hydromagnetic emissions, X-ray bursts and electron bunches, J. G. R. 67(9), pp. 3317-3343, 1962.

24. Gallet, R. M., "The very low frequency emissions generated in the earth's exosphere," Proc. I.R.E. 47(2), pp. 211-231, 1959.

25. Lokken, T. E., J. A. Shand and Sir S. C. Wright, K. C. B., O. B. E. and L. H. Martin, N. M. Brice and R. A. Helliwell, "Stanford-Pacific Naval Laboratory conjugate point experiment," Nature 192 (4800), pp. 319-320, October 1961.

26. Tepley, L. R., "Low latitude observations of fine structured hydromagnetic emissions," J. G. R. 69(11), pp. 2273-2290, 1964.

27. Helliwell, R. A., and N. M. Brice, "VLF emission periods and whistler-mode group delays," J. G. R. 69(21), pp. 4704-4708, November 1, 1964.

28. Watanabe, T., "Determination of the electron distribution in the magnetosphere using hydromagnetic whistlers," J. G. R. 70(23), pp. 5839-5848, December 1, 1965.

29. Brice, N. M., "Electron density and path latitude determination from VLF emissions," J. Atmos. Terr. Phys., 27(1), pp. 1-6, January 1, 1965.

30. Helliwell, R. A., "Very-low-frequency discrete emissions received at conjugate points," Nature 195(4836), pp. 64-65, 1962.

31. Helliwell, R. A., J. Katsufrakis, M. Trimpi and N. M. Brice, "Artificially stimulated VLF radiation from the ionosphere," J. G. R. 69(11), pp. 2391-2394, June 1964.

32. Brice, N. M., "Multiphase periodic very low frequency emissions," Radio Science 69D(2), pp. 257-265, February 1965.

33. Brice, N. M., "Fundamentals of VLF emission generation mechanism," J. G. R., 69(21),pp. 4515-4522, November 1, 1964.

34. Brice N. M., "Discrete VLF emissions from the upper atmosphere," Technical Report Number 3412-6, A. F. Contract AFOSR 62-372, Stanford Electronics Labs., Stanford University, Stanford, California, August 1964.

35. Akasofu, S.-I., "The development of the auroral substorm", Planet. Space Sci., 12(4), pp. 273-282, 1964.

36. Kennel, C. F., and H. E. Petschek, "Limit on stably trapped particle fluxes," J. G. R., 71(1), pp. 1-28, 1966.

37. Hartz, T. R., and R. E. Barrington, "Simultaneous occurrence of ionospheric noise at mid-and very low frequencies," paper presented at URSI Meeting, Ottawa, Canada, May 23-25, 1967.

Figure Captions

Figure 1. A CMA DIAGRAM FOR ELECTRONS AND PROTONS. The horizontal scale (X_e) is the ratio of electron plasma frequency squared to wave frequency squared and the vertical scale (Y_e^2) the ratio of electron cylotron frequency to wave frequency squared. Lines indicate zeros or infinites of refractive index for the right-handed (R) or left-handed (L) waves propagating along the magnetic field or the extraordinary (X) or ordinary (P) modes propagating normal to the field. Sketches of the phase velocity surfaces (the magnetic field direction is vertically upwards) appropriate to the various areas of the diagram are given to the right of the figure. (After Brice[1]).

Figure 2. A NOSE WHISTLER RECORDED AT EIGHTS STATION. The zero on the time scale indicates the approximate location of the causative atmospheric. (After Brice[34]).

Figure 3. THE CHANGE OF LOCATION OF WHISTLER PROPAGATION PATHS IN THE MAGNETOSPHERE ASSOCIATED WITH A POLAR SUBSTORM. The whistler paths begin to move in toward the earth at about 0620 U.T., while the Byrd Station magnetometer and riometer and Great Whale River magnetometer show a sudden onset of activity at 0645. (After Carpenter and Stone,[6]).

Figure 4. A FREQUENCY-TIME SPECTRUM OF A PROTON WHISTLER (below) AND ILLUSTRATIVE DIAGRAM (above). The proton whistler rises from the crossover frequency and asymptotically approaches the proton gyrofrequency until cyclotron damping cuts off the whistler (After Gurnett and Brice[13]).

Figure 5. THE FREQUENCY RANGES OCCUPIED BY VARIOUS TYPES OF EM AND HM EMISSIONS. The emissions are also classified as diffuse (for broad-band emission) or discrete (for narrow band), the times of maximum occurrence, (A for afternoon, M for morning and N for night) are given, and the type of energetic particle precipitation (electron (e) or proton (p)) with which the emissions are associated. HM emissions are also called "micropulsations" and EM emissions "VLF emissions".

Figure 6. SIMULTANEOUS RECORDINGS OF SINGLE-PHASE PERIODIC EMISSIONS AT TWO PAIRS OF MAGNETICALLY CONJUGATE RECORDING STATIONS. (After Brice[34]).

Figure 7. RECORDINGS FROM GREENBANK SHOWING THE GROUND-WAVE SIGNAL FROM STATION NAA AT 14.7 kc, AND TRIGGERED EMISSIONS RECORDED ON THE RESEARCH SHIP ELTANIN. (After Helliwell et al[31]).

Figure 8. SINGLE-PHASE AND SYMMETRICAL THREE-PHASE EMISSIONS RECORDED AT GREAT WHALE RIVER, SHOWING A PRECISE THREE-TO-ONE RELATIONSHIP BETWEEN THE APPARENT PERIODS OF THE EMISSIONS. (After Brice[34]).

Figure 9. QUASI-PERIODIC EMISSIONS RECORDED AT EIGHTS STATION, SHOWING SLOWLY RISING FREQUENCY BANDS, EACH CONSISTING OF A NUMBER OF SETS OF PERIODIC EMISSIONS. (Recorded at Eights Station, 1930-34 UT and 1940-42 UT on 13 Dec. 1961.) (After Brice[34]).

Figure 10. AVERAGE AMPLITUDES OF VLF AURORAL HISS, AURORAL 5577Å LINE, COSMIC NOISE ABSORPTION AND ULF Z (i.e. the rate of change of vertical magnetic field) RECORDED AT THE ONSET OF A POLAR SUBSTORM DISTURBANCE AT BYRD STATION, ANTARCTICA. (After Morozumi and Helliwell[19]).

Figure 11. AVERAGE RELATIVE AMPLITUDE IN d.b. OF EM EMISSION AT BYRD STATION AS A FUNCTION OF FREQUENCY AND TIME FOR THE MONTH OF JUNE, 1962. (After Morozumi and Helliwell[19]).

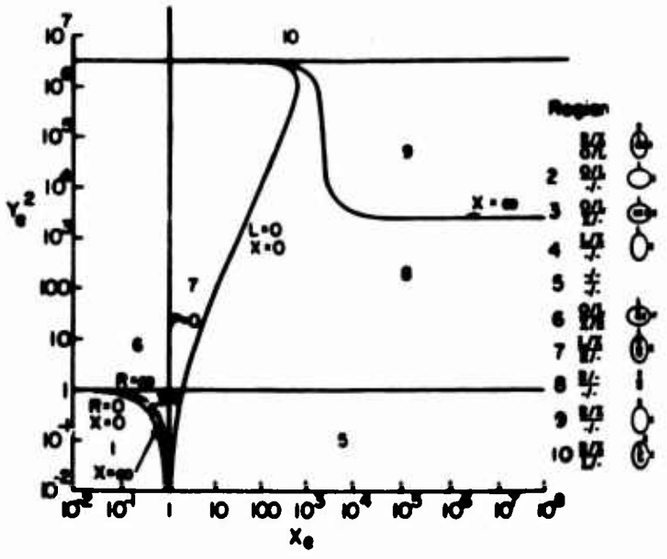

Figure 1

Figure 2.

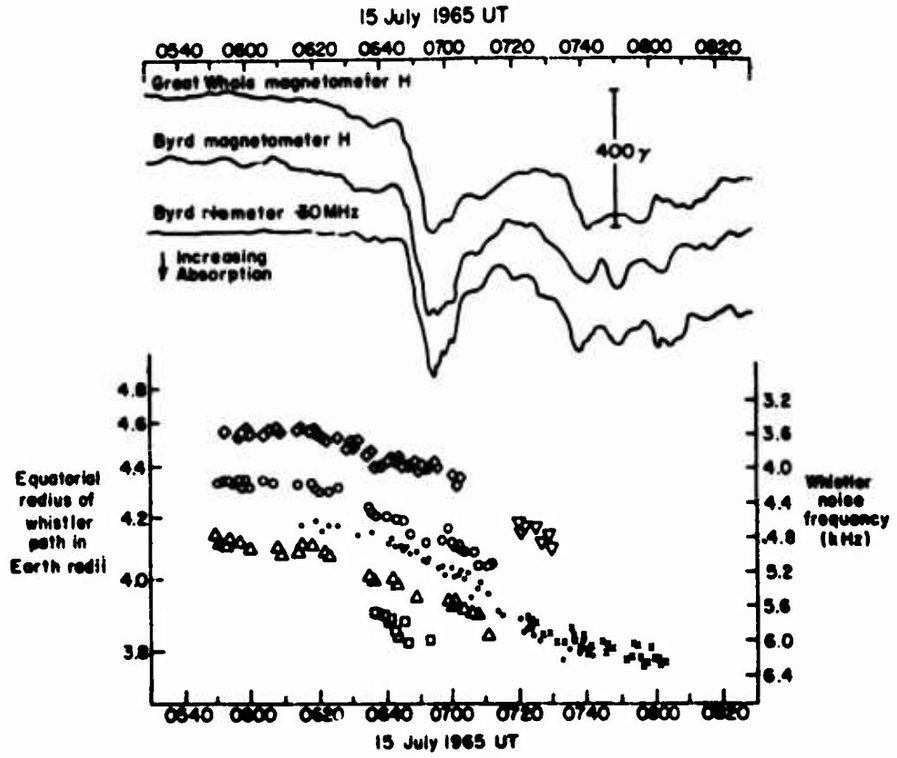

Figure 3

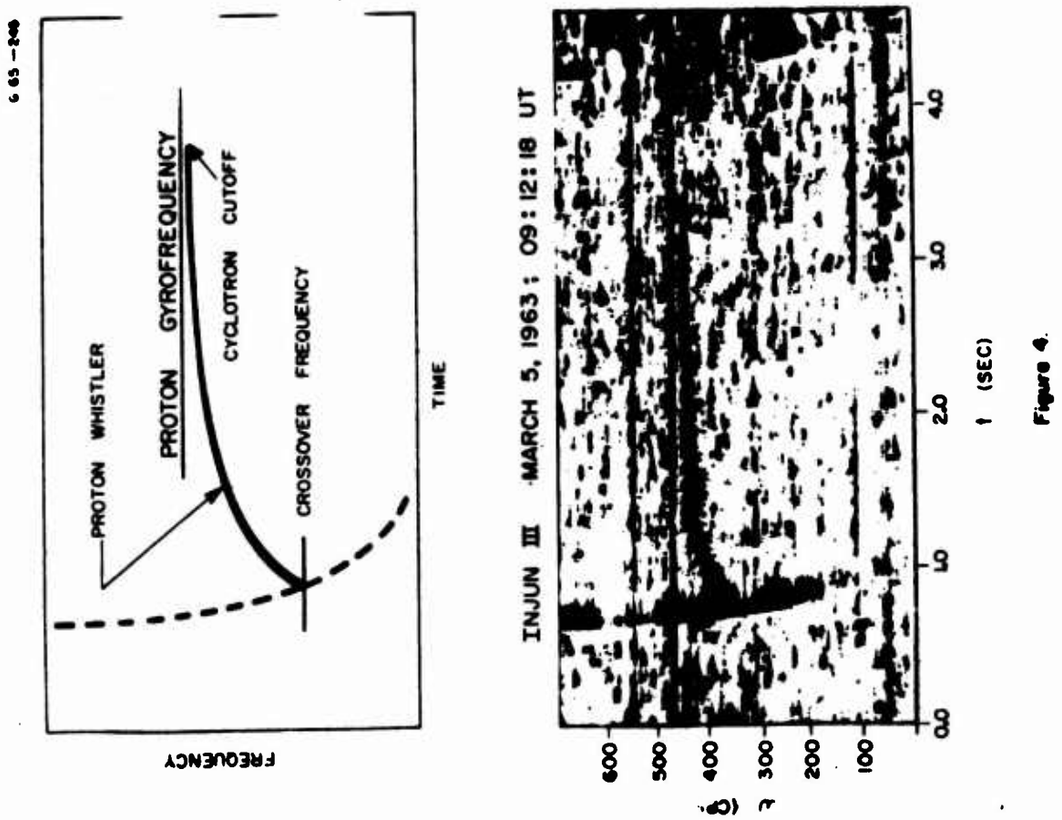

Figure 4.

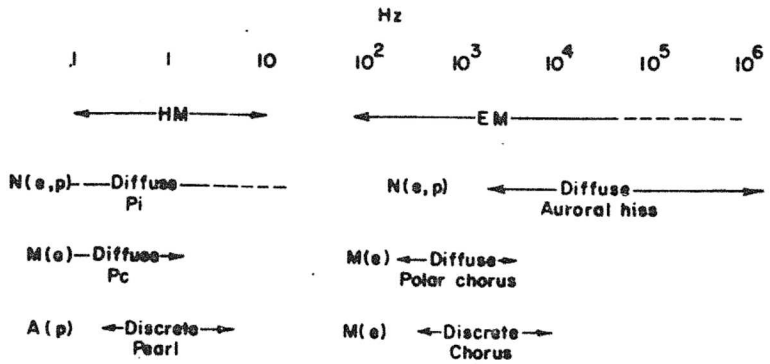

Figure 5

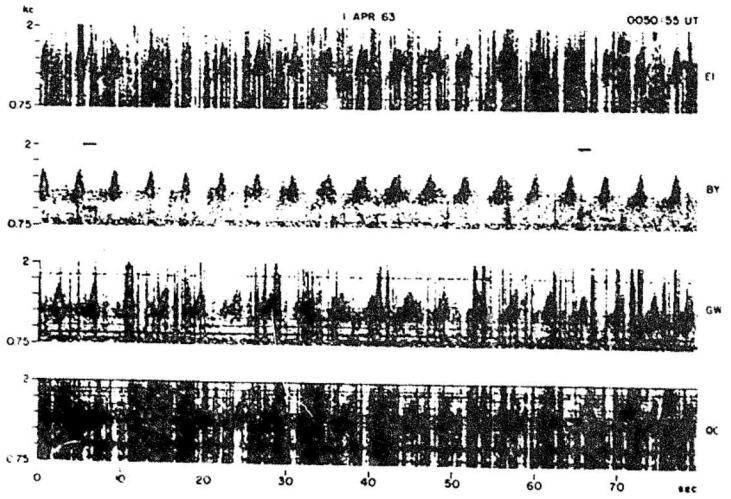

Figure 6

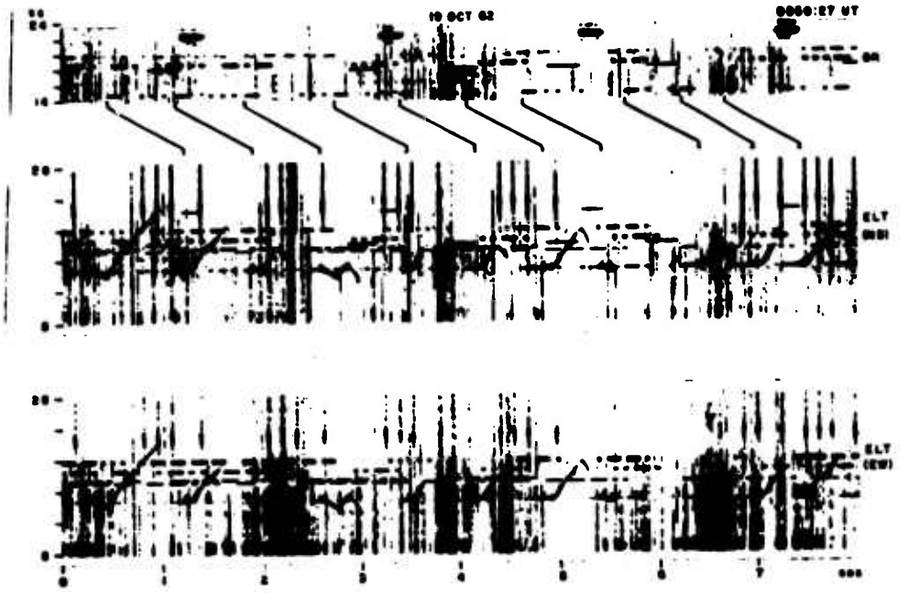

Figure 7.

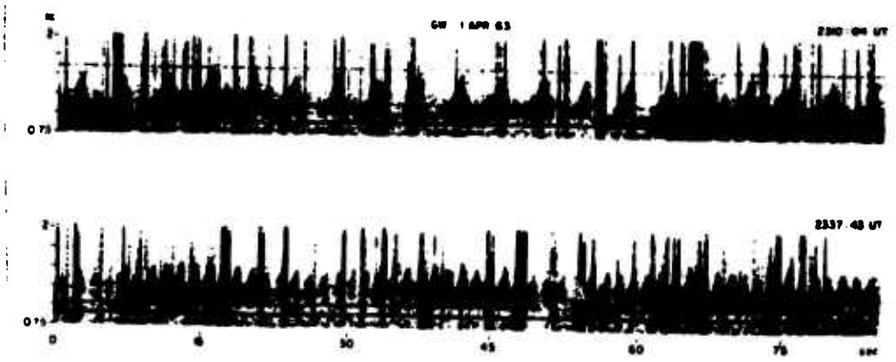

Figure 8.

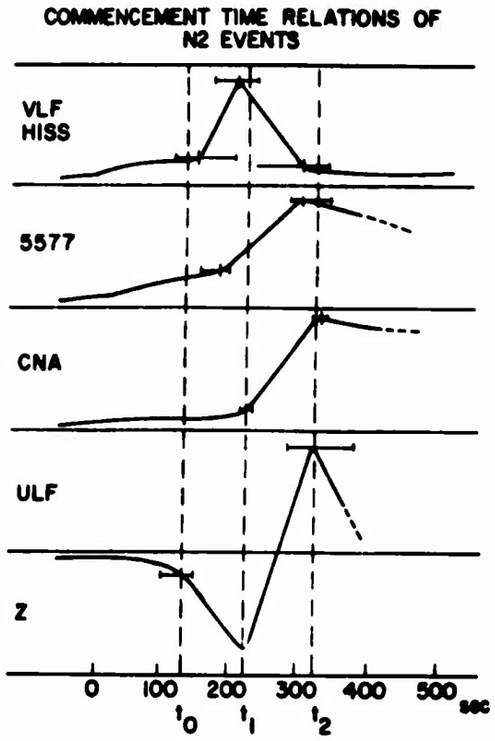

Figure 10

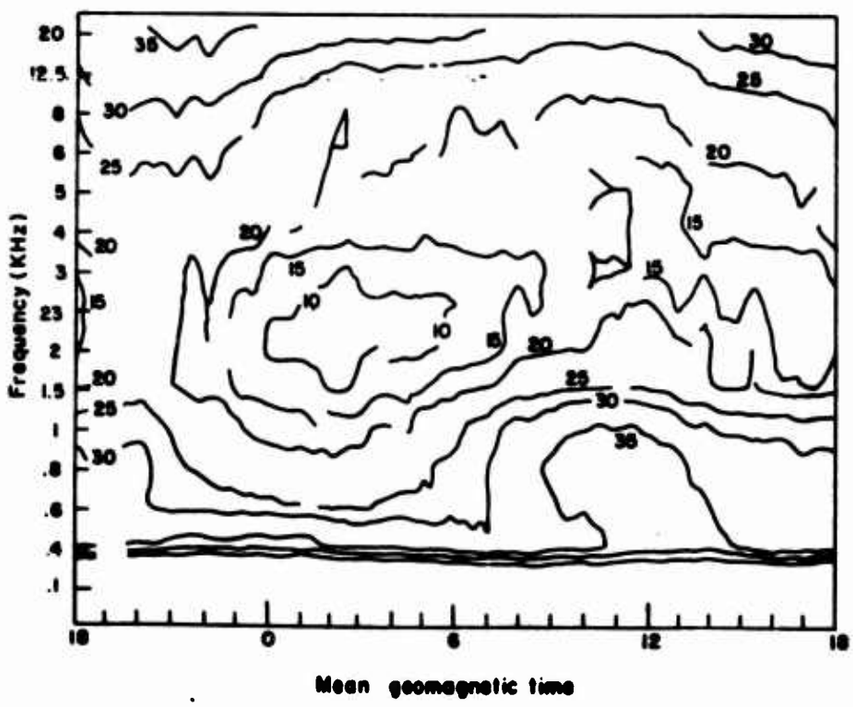

Figure 11

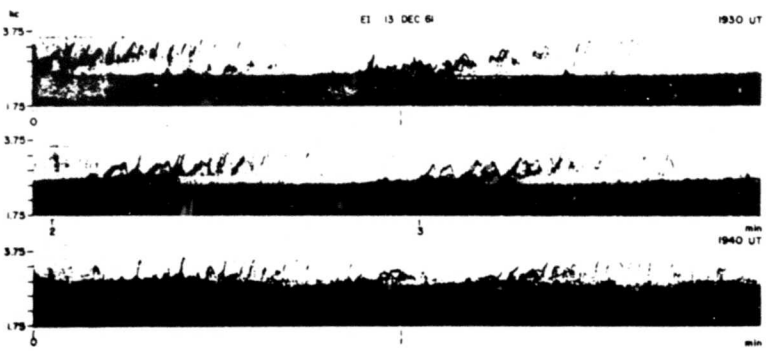
nc
E1 13 DEC 64
1930 UT
3.75
1.75
0
3.75
1.75
2
3
min
1940 UT
3.75
1.75
0
min

Figure 9.

Selected Problems in Wave-Particle Interaction, from Conjugate Point Observations

R. M. Gallet

Institute for Telecommunication Sciences and Aeronomy
Environmental Science Services Administration
Boulder, Colorado 80302

Organized examples of observations simultaneously made at conjugate points, concerning both whistlers and some types of VLF emissions, will serve as a review of the observational knowledge of natural VLF phenomena in the magnetosphere. This however will be restricted to questions touching the subject of this symposium, namely conjugate point studies. Of particular interest are types of interactions between a whistler and a triggered VLF emissions which could be disentangled only by means of conjugate point observations.

BLANK PAGE

POLAR EMISSIONS

Leif Owren
Radiophysics Laboratory
Dartmouth College

The natural ELF (0.3 - 3 kHz) and VLF (3 - 30 kHz) emissions occurring in the polar regions have been observed at Vostok, Antarctica and Thule (Qanaq), Greenland since 1964. The stations are located one degree from the South and the North Geomagnetic Poles respectively. Recordings were started at Vostok (gm. lat. 89.1° S) in February 1964 and at Thule (gm. lat. 88.9° N) in October 1964. The Thule-Qanaq station lies about 100 km north of Thule Air Force Base. The Technical University of Denmark maintains ionospheric stations including VLF equipment at Narssarssuaq (gm. lat. 71.2° N) and at Godhavn (gm. lat. 79.9° N). The chain of stations Narssarssuaq, Godhavn and Thule spans the polar cap region from the auroral zone to the geomagnetic pole at about 9° intervals of geomagnetic latitude within a 40° sector of geomagnetic longitude.

Initially the ELF-VLF recordings at the geomagnetic pole stations were made with Stanford-type IGY whistler recorders using the standard two-minute per hour sampling schedule. Later hiss recorders were installed in addition to the tape recorders. At Thule a panoramic receiver covering the 0.5 - 20 kHz frequency range was put in operation

in February 1965. The amplitude vs. frequency oscilloscope display is photographed every six minutes. At Vostok continuous hiss recordings covering the 0.2 - 8 kHz range were started in January 1966 using a dual-channel strip-chart system which displays the integrated rms amplitude and the spectral intensity distribution for each one-second frequency sweep.

One problem arising when recording phenomena observed from stations near the geomagnetic poles is the definition of local magnetic time. In view of the fact that auroral and related ionospheric phenomena appear to be centered on the eccentric dipole axis, we base local magnetic time on the eccentric rather than the earth-centered dipole. With this definition magnetic noon at Vostok corresponds to about 1300 UT and at Thule occurs at about 1500 UT, so while the geomagnetic longitude difference is about 180 degrees the local magnetic time relative to the eccentric axis poles differs by only two hours for the two stations.

For an understanding of the ELF-VLF emissions observed in the polar regions it is important to take account of the propagation characteristics of the earth-ionosphere waveguide. The basic properties may be inferred from a paper by Wait (1957) in the 1957 VLF-issue of Proc. IRE. According to the results of this paper VLF propagation over long distances can take place with little attenuation in the fundamental mode for frequencies below 2 kHz and in the first mode for frequenices above 8 kHz.

In the 2 - 8 kHz band the VLF waves are subject to strong absorption. Typically, the attenuation is of the order of 3 db per 1000 km at 1 kHz and 2 db per 1000 km at 10 kHz but exceeds 10 db per 1000 km at 4 kHz. Thus the propagation conditions tend to divide the ELF-VLF emissions observed in the highest latitude zone of the polar regions into three categories characterized by the three frequency bands 0.3 - 2 kHz, 2 - 8 kHz and 8 - 20 kHz. Phenomenologically there is a natural division between the emissions observed below and above about 2 kHz at any polar cap station.

Polar Chorus

The natural emissions occuring between 0.5 and 2 kHz are generally referred to as polar chorus although in fact they consist of a mixture of chorus-type emissions and hiss. The term polar chorus was introduced by Ungstrup and Jackerott (1963) to distinguish the chorus observed below 1.5 kHz at Godhavn, Greenland during 1957-1961 from the middle latitude chorus occurring mainly in the 2 - 4 kHz range. The proportion of chorus and hiss in the polar chorus varies with the sunspot cycle, the chorus component being more prominent near sunspot maximum and receding into the hiss background with declining solar activity.

The polar chorus observed at Vostok during 1964 showed the same diurnal and seasonal variation as that found for Godhavn and other polar stations with a diurnal maximum at

10 - 11 local magnetic time and a yearly maximum during the local summer. The polar chorus at Vostok in 1964 consisted mainly of the hiss component. A comparison of the occurrence and intensity of polar chorus at the three Greenland stations Narssarssuaq, Godhavn and Thule strongly suggests that the polar chorus is generated in the auroral zone and propagated to higher latitudes in the earth-ionosphere waveguide. This conclusion was reached by Jackerott et al. (1964) from a detailed study of the Narssarssuaq and Godhavn recordings and is further strengthened when the Thule data are taken into account.

Auroral Hiss

Wide-band hiss occurring in the 4 - 16 kHz frequency range and associated with auroral activity was first observed at Byrd Station, Antarctica by Martin et al. (1960). The hiss activity typically follows in the wake of magnetic storms and has a diurnal maximum shortly before local magnetic midnight. The hiss observed at Vostok during 1964 at frequencies above 4 kHz showed a similar diurnal variation and a similar relation to magnetic activity.

Jørgensen (1966) has studied the hiss events occurring at Narssarssuaq, Godhavn and Nord (gm. lat. 80.8° N), Greenland during November and December 1964 using continuous recordings at 8 kHz. He concludes that the auroral hiss is a rather local phenomenon. Drawing on observations in the 4 - 9 kHz frequency range from a number of high and middle latitude stations,

Jørgensen derived contour maps of spectral density for wide-band hiss bursts showing a zone of maximum occurrence. This zone has the shape of a horseshoe with its opening toward the magnetic noon meridian. The highest occurrence rate and spectral density of hiss events is observed in the auroral zone at about 70° invariant latitude an hour before magnetic midnight. In the morning and afternoon hours there is more hiss activity at 80° latitude than at 70°. The auroral hiss observed in middle latitudes appears to be propagated from the auroral zone in the earth-ionosphere waveguide as indicated by a decrease in maximum spectral density by approximately 10 db per 1000 km and the simultaneity of the hiss bursts recorded at different stations.

Local Hiss Events at the Geomagnetic Poles

The continuous hiss recordings at Vostok during 1966 provided an opportunity for a systematic study of hiss events observed near one of the geomagnetic poles. The 0.2 - 8 kHz frequency range of the hiss recorder favors the detection of local hiss events over hiss propagated from the auroral zone. Two main types of hiss bursts are observed: (1) band-limited events with a bandwidth of about 3 kHz and (2) wide-band events having an essentially uniform intensity over the 8 kHz range. The band-limited bursts occur predominantly in the lower half of the recorded frequency range but sometimes in the upper half. Both types may be represented during a single burst.

Storm bursts often show a drift of the maximum intensity from low to high or from high to low frequencies in the course of a few minutes. Spot checks of the 0.3 - 20 kHz Vostok tape recordings coinciding in time with hiss events indicate that the activity in the 2 - 8 kHz range is the dominant feature.

The highest level of hiss activity tends to follow moderate or moderately severe magnetic disturbances. Intense hiss storms lasting from 6 to 9 hours occurred on 27 May, 1 June and 31 August 1966 in the wake of the magnetic storms of 26 May, 31 May, and 30 August. The severe magnetic storm of 3 - 4 September was not followed by increased hiss activity at Vostok. This simply reflects the well-known migration of the major magnetic disturbances to lower latitudes. On the other hand, an intense hiss storm lasting 11 hours occurred on 22 July preceded only by a weak magnetic disturbance which apparently must have been associated with a polar storm.

Short periods of high hiss activity, occassionally reaching hiss storm levels, occur frequently in the evening hours, particularly during the local winter season. These evening "flashes" between 18 and 24 hours magnetic time typically last 1 or 2 hours but may extend over periods of 4 - 5 hours. It is the cumulative effect of these flashes which give rise to the diurnal evening maximum in the statistics of hiss activity.

Turning then to the Thule six-minute samplings of the VLF hiss, the hiss recorded during 1965 appeared mostly in the 8 - 20 kHz range and was of the wide-band variety. This

situation changed in 1966. The hiss storm activity now became most noticeable in the 2 - 8 kHz range with a significant occurrence of band-limited emissions. The hiss activity at the two geomagnetic pole stations Vostok and Thule thus showed similar overall trends during 1966.

Origin of Local Hiss Events

It is generally accepted that ELF-VLF emissions are caused by an interaction of charged particle streams flowing along the lines of force of the earth's magnetic field with the ionosphere, although the detailed mechanism for the generation of the emissions is not understood (Helliwell, 1965). The Injun 3 observations (Gurnett and O'Brien, 1964) demonstrated the direct relationship between electron precipitation, VLF hiss and aurora in the magnetic shell near the boundary of the outer radiation zone associated with the auroral zone. The occurrence of locally generated hiss in the polar cap regions therefore suggests an occassional occurrence of localized electron streams in the regions of the magnetosphere beyond the boundary of the outer radiation zone. Evidence of such electron streams has been presented by Gringauz and Khokhlov (1965) using data from the Russian satellite Electron-2 and the spacecraft Mars-1. These data showed the occurrence of high fluxes of 100 ev - 40 kev electrons in high latitudes. Similarly, McDiarmid and Burrows (1965) have reported from Alouette observations on the incidence

of high fluxes of electrons with energy above 40 kev in the form of narrow spikes occurring in high latitudes (70 - 85° invariant latitude) outside the outer radiation zone. Jørgensen (loc. cit.) found a good time correlation between the spikes observed from Alouette in 1963 over the north polar cap region and the occurrence of strong hiss activity at Godhavn, Greenland.

Magnetic Storm Events During 1965

The VLF emission activity at Thule and Vostok associated with the sudden commencement magnetic storms of 1965 has been studied in order to determine the "conjugacy" aspects of the VLF emissions at the two stations during incidences of low energy solar particles on the magnetosphere. For each storm and post-storm period the available tape and . m recordings were examined for enhancements in hiss or chorus activity over the pre-storm days. The results are shown schematically in the figure which indicates for each magnetic storm: (1) the time and position on the sun's disk of the solar flare responsible for the storm, (2) the 3-hour K_p-figures for the storm period, and (3) the occurrence and intensity of VLF emission enhancements at Thule (labelled Kanak) and Vostok.

It will be seen that in 4 of the 5 cases only one of the two stations gave evidence of increased VLF activity. During the two June storms, designated as moderately severe and comprising the strongest magnetic disturbance period of the year, both

Thule and Vostok recorded VLF emissions. It may be mentioned that a comparison of the local K-figures for the two stations during each storm indicates the same trend as the VLF emissions. The station showing VLF activity also had relatively the higher local K-figures. The observations therefore suggest an asymmetrical particle distribution and magnetic disturbance field over the two polar regions.

Consideration of the position of the solar flare provides no obvious clue to the difference in response to the solar particles in the two regions. This is perhaps not surprising since the particle ejection from the sun is not necessarily in a radial direction. Moreover, the inclination of the geomagnetic axis to the sun-earth direction might be expected to be a more important cause of an asymmetrical response, but the observations at hand give no clear indications to this effect. More detailed and comprehensive information, including spacecraft data, will be required to resolve the problem.

Acknowledgements

The ELF-VLF observations used in this paper were obtained with the cooperation of the Arctic and Antarctic Research Institute, Leningrad, U.S.S.R. which maintains Vostok Station, Antarctica and the Ionosphere Laboratory, Technical University of Denmark which operates Thule Station, Greenland. The research is sponsored by the Office of Antarctic Programs, National Science Foundation.

REFERENCES

Gringauz, K.I. and M.Z. Khokhlov, The outermost zone of charged particles. Transactions of the All-Union Conference on Space Physics, Moscow June 1965. NASA TTF-389, May 1966.

Gurnett, D.A. and B.J. O'Brien, High-latitude geophysical studies with satellite Injun 3. 5. Very-low-frequency electromagnetic radiation. J. Geophys. Res., 69, 65, 1964.

Helliwell, R.A., Whistlers and related ionospheric phenomena. Stanford University Press, Stanford, Cal., 1965.

Jackerott, Inger M., T.S. Jørgensen and J. Taagholt, Observations of whistlers and VLF emissions at Godhavn and Narssarssuaq, Greenland and at Tromsø, Norway in 1962, Ionosphere Laboratory Report No. 18, Technical University of Denmark, January 1964.

Jørgensen, T.S., Morphology of VLF hiss zones and their correlation with particle precipitation events. J. Geophys. Res. 71, 1367, 1966.

Martin, L.H., R.A. Helliwell and K.E. Marks, Association between auroras and VLF hiss observed at Byrd Station, Antarctica. Nature, 187, 751, 1960.

McDiarmid, I.B. and J.R. Burrows, Electron fluxes at 1000 kilometers associated with the tail of the magnetosphere. J. Geophys. Res. 70, 3031, 1965.

Ungstrup, E. and Inger M. Jackerott, Observations of chorus below 1500 cycles per second at Godhavn, Greenland from July 1957 to December 1961. J. Geophys. Res., 68, 2141, 1963.

Wait, J.R., The attenuation vs. frequency characteristics of VLF radio waves. Proc. IRE, 45, 768, 1957.

VLF ACTIVITY AT THE GEOMAGNETIC POLES ASSOCIATED WITH MAGNETIC STORMS IN 1965

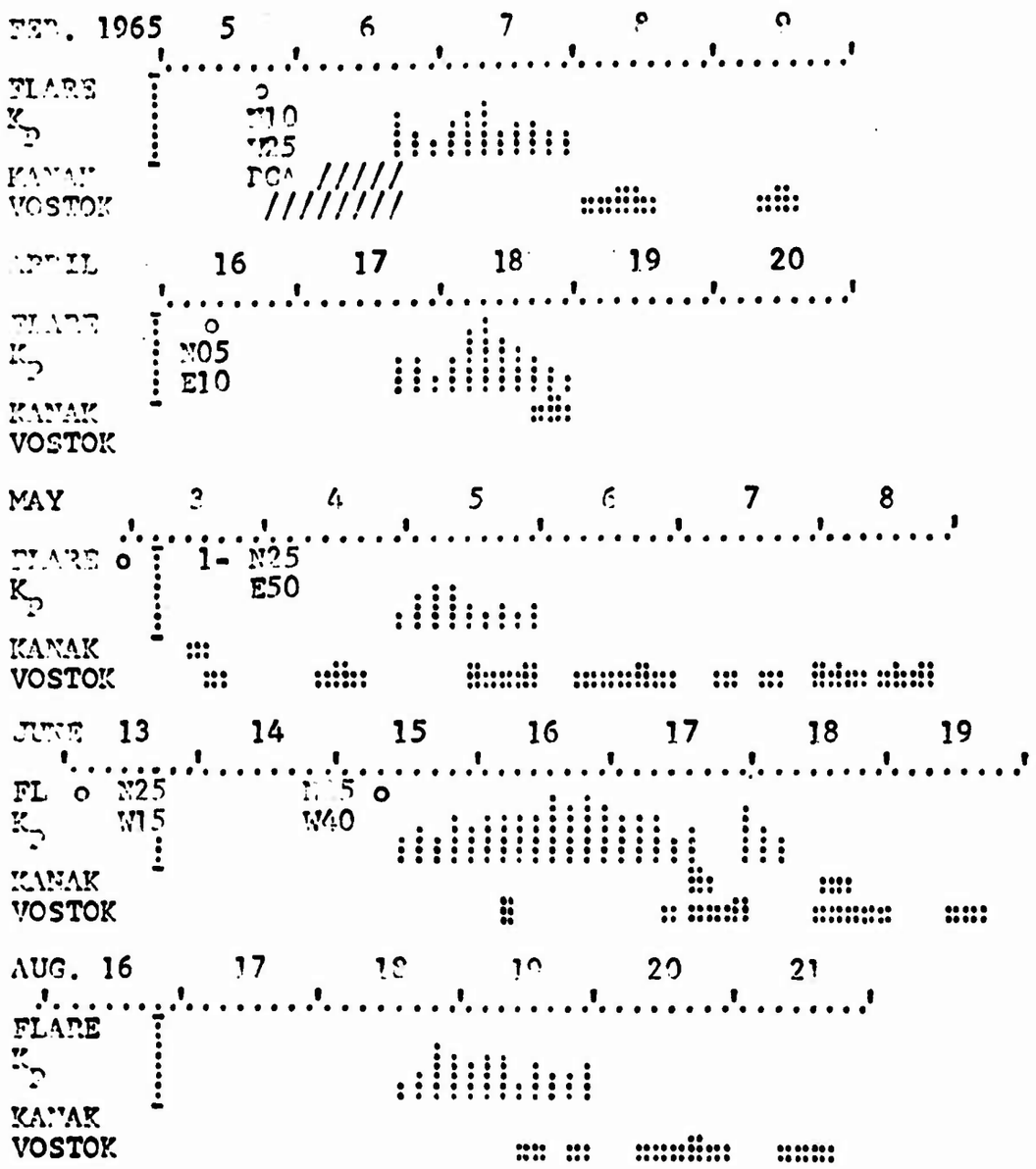

BLANK PAGE

RECENT RESEARCH ON THE MAGNETOSPHERIC PLASMAPAUSE

by

D. L. Carpenter
Radioscience Laboratory
Stanford University
Stanford, California

ABSTRACT

The plasmapause is a three-dimensional field aligned boundary that divides the closed field-line portion of the earth's magnetosphere into two physically distinct regions. The boundary is asymmetric, usually exhibiting a minimum geocentric range near dawn and a maximum near dusk under conditions of moderate but steady geomagnetic agitation (K_p=2-4). The mean equatorial radius of the plasmapause is typically about $4R_E$, but it may vary from about $5.5R_E$ during periods of extreme quiet to the range $2\text{-}3R_E$ during great storms. The approximately corotating thermal plasma within the boundary exhibits two types of radial drift motions. These may be visualized as: 1) slow "breathing" motions that follow the radial variations in a fixed, asymmetric boundary, 2) more rapid, transient (1-2 hour) motions that occur when the boundary position varies, as is the case during a polar substorm.

The asymmetry of the boundary and the nighttime drifts of tubes of ionization probably cause the mid-latitude daytime and nighttime ionospheres to be decoupled from one another insofar as the balance of upward and downward fluxes of thermal protons is concerned.

The plasmapause involves an abrupt change in electron density, in tube electron content above 1000 km, and possibly in plasma bulk velocity and mean thermal energy. To the ionosphere, the protonosphere inside the plasmapause appears as a large reservoir of thermal protons, while the region outside appears virtually empty. At the plasmapause, equatorial values of electron density change by a factor of 10 - 100 within less than 0.15 earth radii. Satellite vlf experiments suggest that the change may be far more abrupt than this, possibly on a scale of a few kilometers. Studies of the distribution of electron density along the field lines in the plasmasphere have shown that earlier empirical models of the type $N \propto R^{-3}$ are not in fact compatible with recent satellite data on topside electron concentrations. Instead, the theoretically palatable diffusive equilibrium model has been found to be an appropriate description for most of the plasmasphere, while a more rapidly varying model appears necessary to describe the tenuous outer region. Details of the latter distribution may vary in important ways as a function of local time.

Many wave propagation phenomena of conjugate interest are strongly affected by the presence of the plasmapause. For example, satellites moving poleward through the boundary observe: a cutoff in whistlers propagating from the conjugate hemisphere, a decrease in the intensity of fixed-frequency vlf signals propagating upward, and dramatic changes in vlf noise such as the LHR resonance noise. In ground recordings made at Eights ($L \sim 4$) and Byrd ($L \sim 7$) in the austral winter, four distinct magnetospheric regions of propagation may be identified: (I) the outer part of the plasmasphere; (II) the outer "surface" of the plasmapause; (III) a belt-like region extending 1-2R_E outward from the near vicinity

of the plasmapause; (IV) a region beginning $\sim 1.5R_E$ beyond the plasmapause and extending several earth radii outward. Each region exhibits special properties with respect to the occurrence and spectral behavior of vlf noise, and in particular noise triggered by whistler components. The occurrence of one-hop whistlers propagating in the outer regions III and IV is relatively low, and is particularly low near midnight and in region III at all times except in the mid-afternoon. Whistlers propagating in regions I, III and IV exhibit an abrupt half-gyrofrequency upper cutoff, while whistlers propagating in region II do not. The ground data on the occurrence of whistlers and noise are broadly consistent with recent surveys of magnetospheric noise carried out on satellites.

REVIEW OF MAJOR FEATURES OF THE PLASMAPAUSE

The plasmapause is a three-dimensional field-aligned boundary that divides the closed field-line portion of the earth's magnetosphere into two physically distinct regions. The purpose of this paper is to review some of the features of the plasmapause and to describe a few of the vlf wave phenomena whose characteristics appear to be strongly influenced by the boundary.

The boundary during moderately disturbed conditions. Under conditions of moderate but steady planetary geomagnetic agitation (K_p=2-4), the plasmapause exhibits an equatorial radius similar to that shown by the dark curve in Figure 1. The curve is based on whistler observations near the prime geomagnetic meridian in July-August, 1963 [Carpenter, 1966a]. Important features of the asymmetric plasmapause are a broad minimum in geocentric radius near dawn and, near the dusk meridian, a bulge with equatorial radius 1 to 2 earth radii larger than that of the dawn minimum.

Variation in the plasmapause boundary with magnetic activity. The plasmapause is known to move inward with increasing magnetic agitation, but relatively little is known about the details of the process by which the accretion or erosion of ionization takes place. The statistics are clear, however, in support of a boundary that is typically at 4 earth radii, reaches as little as 2 earth radii during great storms, and extends to 5 or more earth radii during very quiet conditions. Satellite measurements using a mass spectrometer on OGO-I [Taylor, et al, 1965] and a Faraday cup on IMP-II [Binsak, 1967] have provided excellent documentation of this effect.

An illustration of the boundary position during 4 successive days

is shown in Figure 2, where the plasmapause radius is plotted on an hourly basis in the upper part of the figure and the K_p index, with values increasing downward, is shown below (from [Carpenter, 1966a]). Following a period of quieting there is a weak gradual-commencement magnetic storm, during which the boundary moves inward and assumes the type of diurnal behavior illustrated in the previous figure. Some details of the variation of the plasmapause during periods of increasing disturbance and of quieting are shown, respectively, by the dotted and dashed curves in Figure 1. The dashed curve in Figure 1 is a smoothed representation of the data in the interval marked 'Q' in Figure 2.

Statistics on the geocentric radius of the plasmapause as a function of planetary magnetic activity are shown in Figure 3, where the geocentric radius near dawn on 48 days in July-August 1963 is plotted versus maximum K_p in the preceding 24 hours (from [Carpenter, 1967]). For radii less than $4R_E$, there appears to be a grouping of the data into 2 bands separated by about 0.7 earth radius. This appears to be a real effect associated with the as yet unknown time sequence of events during the development of a weak storm. During the first 2 days of a storm, points tend to lie in the right hand band, and then appear to concentrate on the left side during the latter stages.

Plasma motions and the role of the substorm. There appear to be two basic types of drift motions of the plasma inside the boundary. The first type is slow breathing motions, during which the boundary may be thought of as fixed in space, with the plasma inside approximately co-rotating with the earth and also drifting inward and outward in conformity with the asymmetries of the boundary (with the possible exception of the

1800-0000 LT region) [Carpenter, 1966a]. The other type of motion is of short duration (~ 1 hour), and appears to involve changes in the boundary itself. At such a time, the plasmapause and the dense plasma within it are observed to move radially at speeds of the order of $0.4R_E$/hr. The more pronounced inward displacements appear to take place during polar substorms and to occur on the nightside of the earth near the longitudes where the substorm bay is observed [Carpenter and Stone, 1967]. The extent to which the overall plasmapause boundary is modified is not yet known, but it appears that some substorm activity occurs on nearly all but the most quiet days. Due to the rotation of the plasmasphere, the temporal sequence of compressions in the post-midnight region may lead to longitudinal variation in the boundary radius, and possibly to spatial variations in ionospheric parameters that depend on magnetospheric drift motions.

An example of a substorm effect is shown in Figure 4 (from [Carpenter and Stone, 1967]). In the upper part of the record are shown transcriptions of the magnetic bay observed at conjugate stations Byrd, Antarctica, and Great Whale River, Canada (L ~ 7), with additional information on the Byrd riometer, the magnetometer at Eights (L ~ 4, one hour ahead of Byrd in local time), and the elf envelope at Eights (0.2-0.8 Hz). The substorm was isolated, in that the magnetic records showed very little activity in the previous 20 hours. Planetary magnetic conditions were relatively quiet, with K_p near 2. The inward motion of the plasma is demonstrated by the whistler data at the bottom of the record. At the left is a scale for the geocentric radius of a whistler path, at the right a corresponding scale for measured whistler nose frequency. A

series of arrows shows various important features of the event, including an inward drift of plasma that began prior to the bay. For a period of 1-2 hours, the plasma drifted inward at a velocity on the order of 700 m/sec, corresponding to a $\vec{v} \times \vec{B}$ electric field of some 2-3 kV/earth radius at 4 earth radii in the magnetosphere. The plasmapause boundary was not itself observed during the event, but was subsequently found to have shifted inward to about 4 earth radii (further details of the event are presented in the original reference).

Asymmetry of the plasmapause as a function of magnetic activity. During very quiet planetary magnetic conditions, the plasmapause appears to assume a more nearly circular configuration at its larger radius. This is supported strongly by the recent data of Binsak [1967] from a Faraday cup on IMP-II. During great storms the degree of asymmetry probably becomes more pronounced, although details are not yet known. Corcuff and Delaroche [1964] reported knee effects between 2 and 3 earth radii during great storms, and the present author has observed depressions in the magnetosphere during the August 16-19, 1959 storm which are consistent with a knee at less than 2 earth radii [Carpenter, 1962].

Further description of the plasmapause is divided into two sections, one on the changes in the medium across the boundary and another on vlf wave phenomena that are apparently affected by the presence of the plasmapause.

CHANGES IN THE MEDIUM AT THE BOUNDARY

At the plasmapause, there is an abrupt change in plasma density, and possibly corresponding changes in plasma bulk velocity and mean

thermal energy. A satisfactory description of these variations is not yet available, although much is already known about the two regimes near the boundary, if not precisely at the boundary itself.

The change in tube electron content at the boundary. At nighttime, inside the plasmapause, the electron content in a tube of force extending from a square centimeter at 1000 km to the equatorial plane may be as much as an order of magnitude larger than the total content in a cm^2- column in the ionosphere below. From low latitudes the tube content rises steadily, reaching a maximum at the plasmapause and then falling to extremely low values in the tenuous region outside. This is illustrated in Figure 5 from the work of Angerami [1966]. The solid curve shows the content measured on a very quiet day, when the boundary was presumably beyond the observing range of Eights Station. The open and filled circles show individual data points from moderately disturbed days (K_p=2-4). It is clear that the nighttime levels of $2\text{-}4.10^{13}$ el/cm^2- tube inside the plasmapause provide at least numerically a substantial reservoir for an ionosphere of say, 4.10^{12} el/cm^2- column, while the values of $1\text{-}2.10^{12}$ el/cm^2- tube for the outer region are low by comparison. The possible insufficiency of the protonosphere as a reservoir for the nighttime ionosphere at middle to high latitudes may be relevant to the mid-latitude trough phenomena described by a number of investigators, e.g. [Muldrew, 1965; Sharp, 1966; Stanley, 1966].

The change in field-line distribution of ionization at the boundary. Until the recent work of Angerami [1966], whistler data were believed to support an $N \propto R^{-3}$ or 'gyrofrequency' model of the distribution of electrons along the field lines of the magnetosphere [Smith, 1961a].

Meanwhile, theoretical considerations favored the much more slowly decreasing hydrostatic model (e.g. [Johnson, 1960]). The convenient R^{-3} model, still useful in many essentially model-independent calculations, was developed using what are now known to be unrealistic assumptions about the latitudinal distribution of electrons in the upper F-region. Using extensive new sources of whistler data and satellite information on ionospheric electron density at 1000 km, Angerami demonstrated that the hydrostatic model is in fact the best choice for describing the region inside the plasmapause. In the same investigation, he found that the tenuous outer region or 'trough' cannot usually be described by the hydrostatic model, but in fact appears to require a distribution varying roughly as R^{-4}. Thus the gyrofrequency-type model may again be invoked, with the supporting physical argument that the outer region is describable by a 'collisionless' model in which particles move in ballistic orbits (see [Eviatar, et al, 1964]), and in which forbidden, collision-associated orbits become populated only gradually. Much remains to be learned about electron density in the outer region, in particular the manner in which the field-line distribution varies with time from after midnight to late afternoon. At night the distribution may be essentially 'collisionless,' while by afternoon it may approach a collision-dominated model.

Change in the equatorial profile of electron density at the boundary. Fine details of the electron-density profile at the boundary are not yet known, and perhaps may not be known until high-time-resolution experiments are flown on satellites. From whistler data, it was found that the electron density decreases by between one and two orders of magnitude within a distance of less than .15 earth radius [Angerami and Carpenter, 1966].

The satellite data of Taylor, et al [1965] and Binsak [1967] indicate that plasma density at the plasmapause decreases by a factor greater than 10, but these experiments do not provide fine details, say on a scale of 10 km. There are some indications from satellite vlf experiments that the boundary may at times be only a few km in thickness. Abrupt changes in whistler rate and vlf noise phenomena are observed over distances of the order of 10 km on Alouette I at 1000 km [Carpenter, et al, 1967] and over distances of 20-100 km on OGO-III at 20,000 km (K. Howell, private communication).

A summary of the variation in electron density across the 'knee' is shown in Figure 6, which is based on whistler data for June-July 1963 [Angerami, 1966]. Outside the knee nighttime densities (filled points) are extremely low, so low that during moderately severe storms near sunspot minimum, the plasma frequency in the trough may fall below the local gyrofrequency over a large portion of the path. As pointed out by Bell [1966] this condition will permit the propagation of the left-hand mode, and may give rise to enhanced Landau damping of whistler waves.

The density outside the knee is sensibly higher on the afternoon side of the earth than at night, and appears to reflect the filling from below of the tubes of ionization. As noted above, the manner in which the tubes are filled has not yet been studied, and could provide good research opportunities. An example of a problem would be to check on models of high-latitude convective motions in which the daily cycle of filling of tubes at high L values is interrupted in specific ways (e.g. [Nishida, 1966, Brice, 1967]).

Attention will now focus upon a number of wave phenomena that are apparently affected by the presence of the plasmapause.

WAVE PHENOMENA AFFECTED BY THE PRESENCE OF THE PLASMAPAUSE

Satellite observations of a whistler cutoff and vlf noise effects at the boundary. It has been known for some time that the probability of observing a whistler component propagating in the tenuous region outside the plasmasphere is relatively low by comparison to the probability of observation in the dense inner region [Carpenter, 1963]. A recent statistical study of the occurrence of whistlers as a function of observing station latitude and magnetic activity supports this conclusion [Allcock, 1966]. It has recently been shown that the whistler rate observed on satellites Alouette I and II drops abruptly as the vehicle moves to invariant latitudes beyond the plasmapause [Carpenter, et al, 1967]. Frequently associated with this whistler cutoff are abrupt changes in the structure and intensity of vlf noise, one such change being an apparent 'breakup' in the lower hybrid resonance (LHR) noise band. A summary of 12 case studies comparing ground whistler data on the plasmapause position with the invariant latitude of the whistler cutoff and noise breakup effect is present in Figure 7 (from [Carpenter, et al, 1967]). The cases are ordered according to maximum K at Byrd Station in the preceding 12 hours (4th column), and for the group corresponding to K = 5, according to plasmapause position. There is clearly a close spatial relation between the plasmapause and the whistler cutoff and noise breakup (when the latter is observed). The agreement persists over a wide range of variation in magnetic activity and a corresponding invariant latitude range of 52° - 66°. The apparent tendency for the whistler cutoff and noise breakup to occur slightly equatorward of the plasmapause is not yet understood, but may be attributable to uncertainties

in the model of the earth's field used in the calculations (the plasmapause position at 1000 km was calculated in dipole coordinates). In particular, use of a model in which the field at several earth radii is dilated by plasma currents (see [Mead and Cahill, 1966; Heppner, et al, 1967]) would tend to reduce the offset shown in the figure.

Reviewing this initial study, it appears that broadband vlf measurements on satellites may provide one of the most precise methods of determining the location of the plasmapause and of identifying the range over which the transition from the inner to the outer regime takes place in a physical sense.

Ground observations of propagation from the conjugate hemisphere. The probability of observing a whistler trace propagating to a ground station from the conjugate hemisphere is a complicated function of latitude, local time, and magnetic activity (e.g. [Laaspere, et al, 1964; Yoshida, 1965; Allcock, 1966]). To partially clarify this picture, there is offered in Figure 8 a crude summary of whistler occurrence in four field-aligned regions inside and outside the plasmapause. The figure is based on a visual survey of spectrographic records from Eights, Antarctica ($L \sim 4$) for 15 days in July-August, 1963. On these days the plasmapause was typically near $L = 4$, and planetary magnetic agitation was moderate and steady (K_p=2-4). The four regions of propagation are:

(I) in the plasmasphere, the field-aligned region within about one earth radius of the boundary in L space;

(II) the outer 'surface' of the plasmapause;

(III) in the plasma trough, the field-aligned region extending outward roughly 1 earth radius in L space from the plasmapause;

(IV) in the plasma trough, the field-aligned region beginning roughly 1 earth radius beyond the boundary, and extending possibly several earth radii beyond.

Approximate local-time periods represented are 2300-0100, 0500-0700, and 1400-1600. For each period, three 2-minute synoptic recordings were available. The numbers on the graph represent the number of periods (of a possible 15) during which at least one whistler component was identified as propagating from the conjugate hemisphere. Major features of the pattern are: 1) generally low values beyond the plasmapause, but high ones in the plasmasphere and on the outer 'surface' of the plasmapause; 2) extremely low values in the plasma trough near local midnight; 3) relatively low values in a belt-like region outside the boundary (region III).

Propagation in region I is frequently characterized by periodic emissions, low decrement whistler echoing, and strong vlf noise activity near local dawn. Triggering of vlf 'chorus' by whistlers is often observed in region II, and the noise may persist for from a fraction of a second to tens of seconds following the whistler. Region III appears to be the'quietest' region, and is described by whistler traces only rarely, the most probable time of occurrence being mid-afternoon. Region IV, which may possibly be associated with the relatively low-frequency 'polar chorus' band, is a region of active noise and frequent strong triggering of noise by whistlers.

Certain spectral properties of whistlers may be identified with the various regions. In all but region II, whistlers observed on the ground tend to exhibit a well-defined half-gyrofrequency upper cutoff frequency,

at which the wave intensity drops by 10 db or more within a fraction of a kHz [Carpenter, 1966b]. Such a cutoff appears to be related to the predictions of ray theory for propagation in ducts of enhanced ionization [Smith, 1961b]. In region II, the traces do not usually exhibit the abrupt half-gyrofrequency effect, but instead show more gradual cutoff effects and a wide range of upper limiting frequencies, sometimes extending to within 10 per cent of the minimum gyrofrequency.

The occurrence pattern in Figure 8 is broadly consistent with other types of observations, including the Alouette cutoff effects described above. The lack of whistler activity in region III may be related to some observations of Heyborne [1966], who made a satellite study of the field strength of fixed-frequency signals (~18 kHz) from vlf transmitters. Digital data from the polar-orbiting satellite OGO-II showed that as the satellite moved poleward near $L \sim 4$, there occurred field-strength decreases of about 25 db in less than 5^{o} in daytime (1600 LT) and about 20 db in less than 10^{o} at night (0400 LT). Heyborne considered it likely that increased absorption in the lower ionosphere accounted for the effect. A problem in interpreting the whistler cutoff in terms of ionospheric effects is the observation on satellites of continued upward propagation of short fractional hop (0_{+}) whistlers at latitudes poleward of the cutoff of whistlers from the conjugate hemisphere (R. E. Barrington, private communication). These persisting short-path whistlers have not yet been studied for intensity changes at the plasmapause. Certainly much remains to be done before the propagation characteristics of the outer region are well understood.

ACKNOWLEDGMENTS

This research was supported in part by the Atmospheric Sciences Section of the National Science Foundation under grant GA-775, in part by the Office of Antarctic Programs of the National Science Foundation under grant GA-214, and in part by the Air Force Office of Scientific Research under grant AF-AFOSR-783-67.

REFERENCES

Allcock, G. McK., Whistler propagation and geomagnetic activity, J. Inst. of Telecom. Engrs., 12(4), 158-175, 1966.

Angerami, J. J., A whistler study of the distribution of thermal electrons in the magnetosphere, Tech. Rept. SU-SEL-66-017, Radioscience Lab., Stanford Electronics Labs., Stanford University, Stanford, Calif., May 1966 (PhD Thesis).

Angerami, J. J. and D. L. Carpenter, Whistler studies of the plasmapause in the magnetosphere, 2, electron density and total tube content near the knee in magnetospheric ionization, J. Geophys. Res., 71(3), 711-726, Feb. 1, 1966.

Binsak, J. H., Observations of the plasmapause by the M.I.T. experiment of Imp 2, Paper presented AGU Meeting, Washington, D.C., April 1967. Abstract in Trans. AGU, 48(1), 176, March 1967.

Brice, N. M., Bulk motion of the magnetosphere, Cornell-Sydney University Astronomy Center, CSUAC No. 78, April 1967.

Carpenter, D. L., New experimental evidence of the effect of magnetic storms on the magnetosphere, J. Geophys. Res., 67(1), 135-45, Jan. 1962.

Carpenter, D. L., Whistler evidence of a 'knee' in the magnetospheric ionization density profile, J. Geophys. Res., 68(6), 1675-1682, March 15, 1963.

Carpenter, D. L., Whistler studies of the plasmapause in the magnetosphere, 1, temporal variations in the position of the knee and some evidence on plasma motions near the knee, J. Geophys. Res., 71(3), 693-710, Feb. 1, 1966a.

Carpenter, D. L., The upper cutoff frequency of ducted whistlers in the magnetosphere, Paper presented URSI Meeting, Washington, D.C., April 1966b.

Carpenter, D. L., Relations between the dawn minimum in the equatorial radius of the plasmapause and D_{st}, K_p, and local K at Byrd Station, J. Geophys. Res., June 1967 (in press).

Carpenter, D. L. and Keppler Stone, Direct detection by a whistler method of the magnetospheric electric field associated with a polar substorm, Planet. Space Sci., 15, 395-97, 1967.

Carpenter, D. L., F. Walter, R. E. Barrington, and D. J. McEwen, A cutoff at the plasmapause in whistlers observed on Alouette I and II, Paper presented URSI Meeting, Ottawa, Ontario, Canada, May 1967.

Corcuff, Y. and M. Delaroche, Augmentation du gradient d'ionisation dans la proche magnetosphere en periodes de forte activite magnetique, C.R. Acad. Sc. Paris, 258, 650-53, Jan. 13, 1964.

Eviatar, A., A. M. Lenchek, and S. F. Singer, Distribution of density in an ion-exosphere of a nonrotating planet, Phys. of Fluids, 7(11), 1775-79, Nov. 1964.

Heppner, J. P., M. Sugiura, T. L. Skillman, B. G. Ledley, and M. Campbell, OGO-A magnetic field observations, NASA/GSFC Rept. No. X-612-67-150, Greenbelt, Maryland, March 1967.

Heyborne, R. L., Observations of whistler-mode signals in the OGO satellites from vlf ground station transmitters, SU-SEL-66-094, Radioscience Lab., Stanford Electronics Labs., Stanford University, Stanford, Calif., Nov. 1966 (PhD Thesis).

Johnson, F. S., The ion distribution above the F_2 maximum, J. Geophys. Res., 65(2), 577-584, Feb. 1960.

Laaspere, T., M. G. Morgan, and W. C. Johnson, Chorus, hiss, and other audio-frequency emissions at stations of the whistlers-east network, Proc. IEEE, 52(11), 1331-49, Nov. 1964.

Mead, G. D. and L. J. Cahill, Jr., Explorer 12 measurements of the distortion of the geomagnetic field by the solar wind, NASA/GSFC Rept. No. X-640-66-527, Greenbelt, Maryland, Nov. 1966.

Muldrew, D. B., F-layer ionization troughs deduced from Alouette data, J. Geophys. Res., 70(11), 2635-50, June 1, 1965.

Nishida, A., Formation of plasmapause, or magnetospheric plasma knee, by the combined action of magnetospheric convection and plasma escape from the tail, J. Geophys. Res., 71(23), 5669-79, Dec. 1966.

Sharp, G. W., Midlatitude trough in the night ionosphere, J. Geophys. Res., 71(5), 1345-56, March 1966.

Smith, R. L., Properties of the outer ionosphere deduced from nose whistlers, J. Geophys. Res., 66(11), 3709-3716, Nov. 1961a.

Smith, R. L., Propagation characteristics of whistlers trapped in field-aligned columns of enhanced ionization, J. Geophys. Res., 66(11), 3699-3707, Nov. 1961b.

Stanley, G. M., Ground-based studies of the F region in the vicinity of the midlatitude trough, J. Geophys. Res., 71(21), 5067-75, Nov. 1, 1966.

Taylor, H. A., Jr., H. C. Brinton, and C. R. Smith, Positive ion composition in the magnetoionosphere obtained from the OGO-A satellite, J. Geophys. Res., 70(23), 5769-82, Dec. 1, 1965.

ILLUSTRATIONS

Figure 1. Equatorial radius of the plasmapause versus local time. The solid curve represents average behavior during periods of moderate, steady geomagnetic agitation (K_p=2-4). The observations were made in July and August 1963 at Eights, Antarctica. The dots show a particular example involving increasing magnetic agitation, the dashes an example of decreasing agitation (see Figure 2) (from [Carpenter, 1966a]).

Figure 2. Comparison of the equatorial radius of the plasmapause and the K_p index during the 4-day period July 28-31, 1963. The quieting interval of outward displacement in the plasmapause radius, marked 'Q' on July 28-29, is shown on a polar plot in Figure 1 (from [Carpenter, 1966a]).

Figure 3. The geocentric equatorial distance to the plasmapause near local dawn versus maximum 3-hour K_p value in the 24 hours preceding the distance measurement. The whistler data were recorded in the Antarctic at Byrd and Eights, and represent a roughly 30^o range of longitudes near the prime geomagnetic meridian. Centered dipole coordinates were employed in the calculations of geocentric distance (from [Carpenter, 1967]).

Figure 4. Some features of a 15 July 1965 polar substorm and associated whistler path motions. See text and original reference for details (from [Carpenter and Stone, 1967]).

Figure 5. Scatter plot of day and nighttime data on total tube electron content above 1000 km versus dipole latitude. The whistler

observations were made at Eights, Antarctica in July-August, 1963, during periods of moderate, steady geomagnetic agitation (K_p=2-4). The continuous curve corresponds to $K_p \sim 0$ (from [Angerami, 1966]).

Figure 6. Scatter plot of day and nighttime data on equatorial electron density versus geocentric distance in earth radii. The data points correspond to those in Figure 5 (from [Angerami, 1966]).

Figure 7. Summary of case studies in which the whistler cutoff on Alouette I is compared to simultaneous ground measurements of the plasmapause position. The K-values in the 4th column at the left are for Byrd Station. See original reference for details (from [Carpenter, et al, 1967]).

Figure 8. Crude statistics on the frequency of observation of whistler components propagating to Eights Station from the conjugate region, versus local time and path location in the magnetosphere.

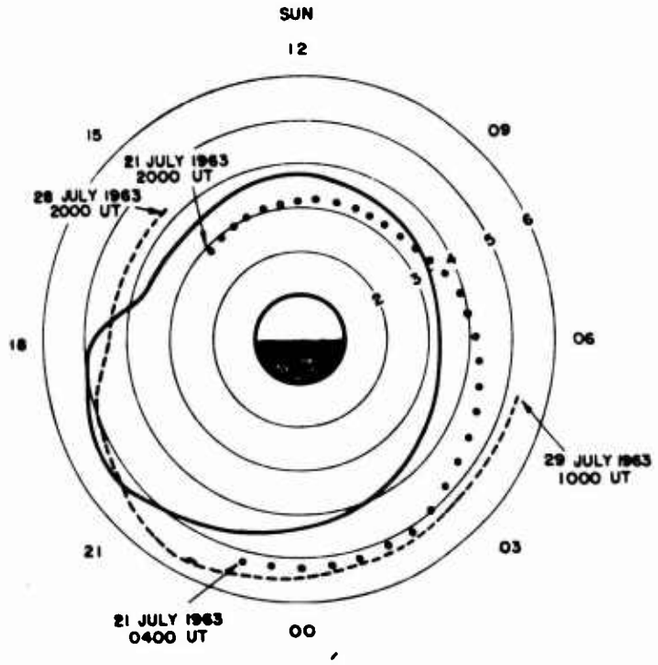

Figure 1

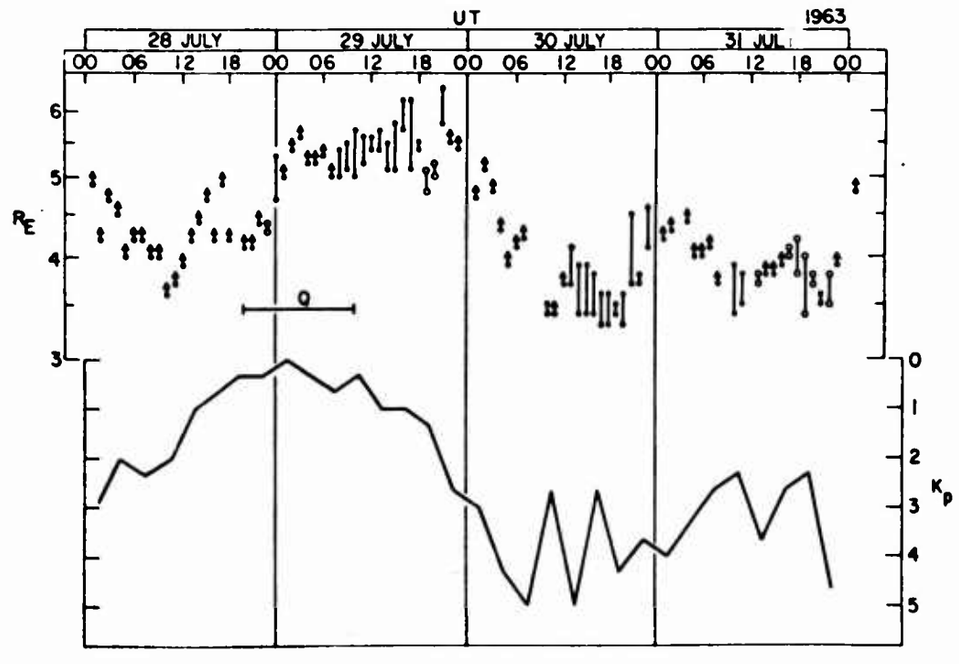

Figure 2

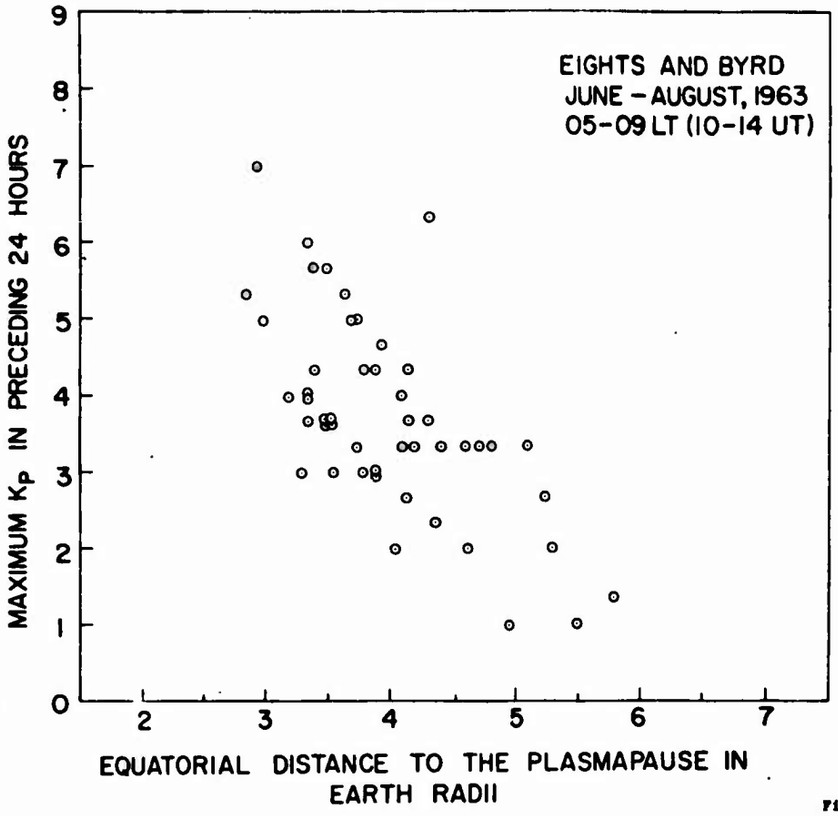

Figure 3

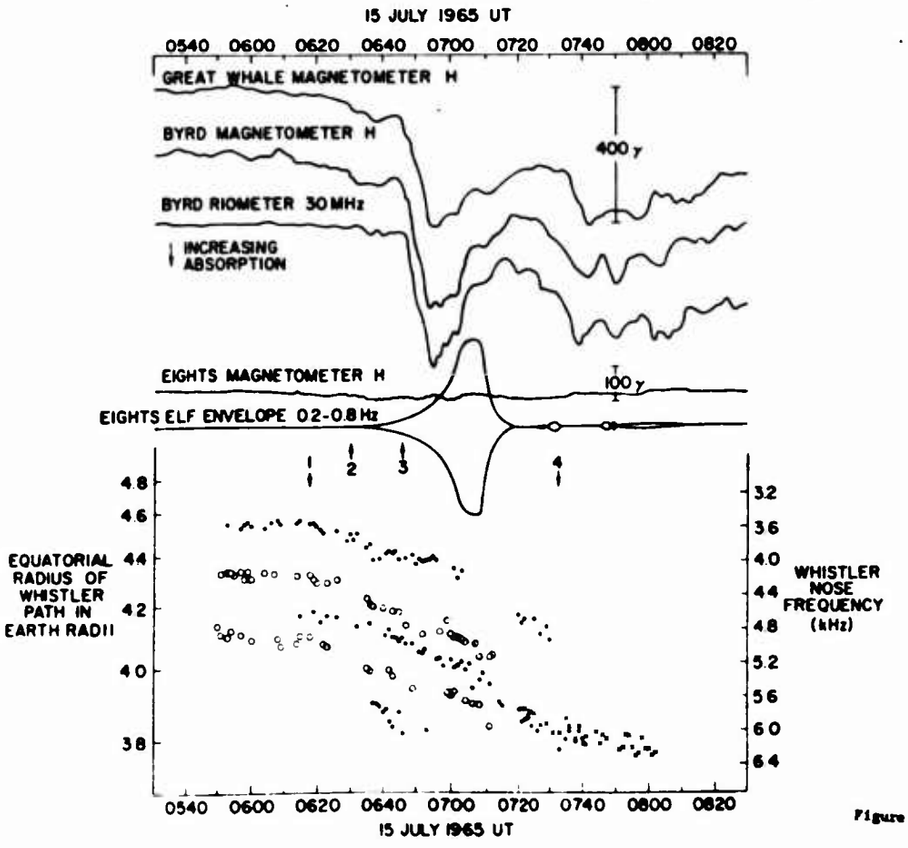

Figure 4

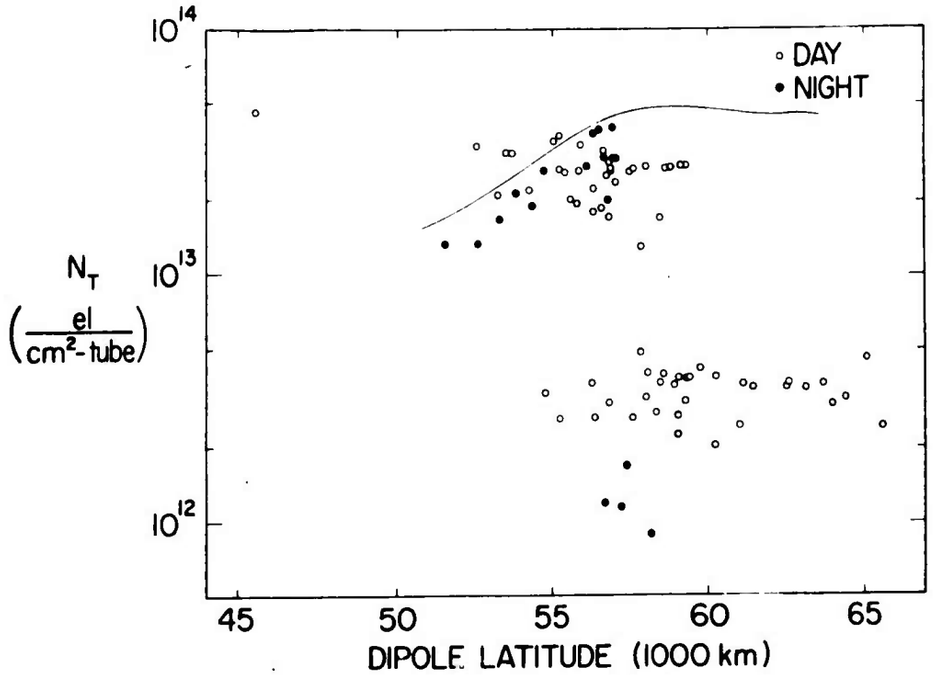

Figure 5

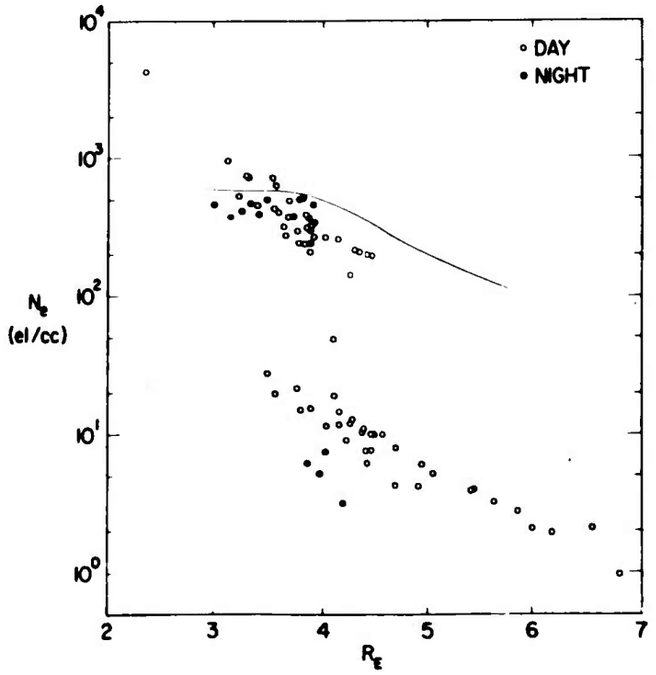

Figure 6

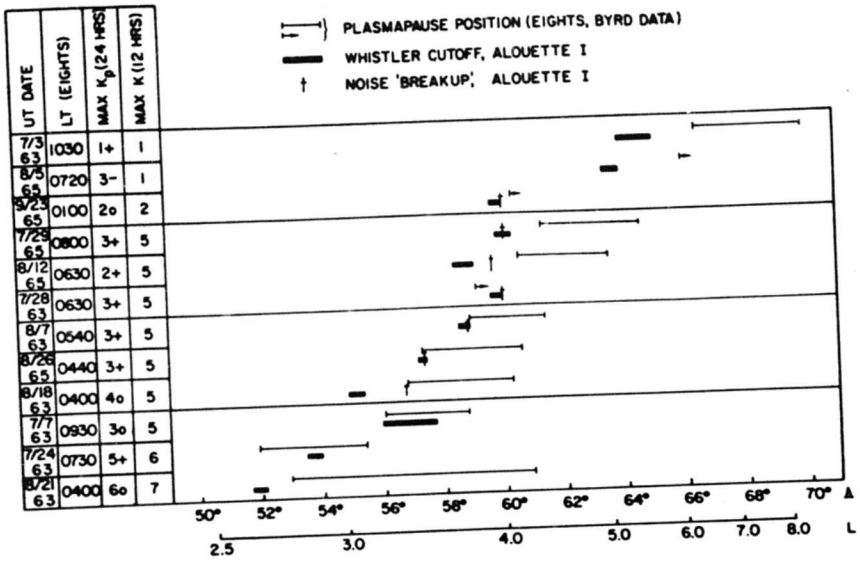

Figure 7

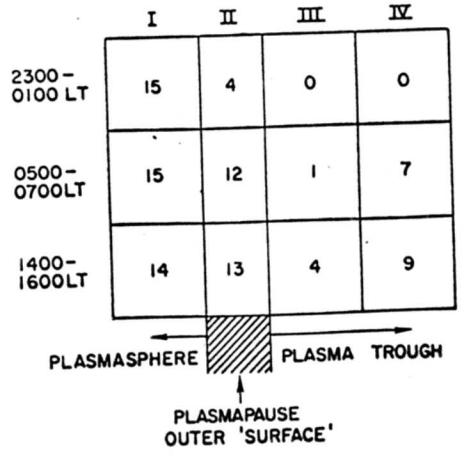

Figure 8

WHISTLER PROPAGATION IN MAGNETOSPHERIC DUCTS *

by

R. L. Smith and J. J. Angerami
Radioscience Laboratory
Stanford University

In this paper we will review some of the theories of propagation of whistlers in field aligned ducts and their relation to recent observations. A number of the features of propagation deduced from the ray theory approach have been verified by recent ground and satellite observations. These observations in turn have led to further ray tracing studies which explain some interesting high frequency leakage effects and suggest an indirect experimental determination of duct dimensions and enhancement factors.

Whistlers observed by ground stations have been explained as the result of the propagation of energy from lightning along field-aligned ducts of enhanced ionization. The theory of propagation in a smooth magnetosphere without ducts was inadequate to explain many of the features of whistlers observed on the ground, such as the multiplicity of discrete components and the integral relationships between whistler echoes.

The theory of propagation in ducts can be approached in many ways. The simplest (and the most productive so far) is through the use of ray tracing techniques. By using Poverlein's construction and by making ray tracing calculations in a medium with a uniform magnetic field and a variation of electron density across the field lines, one may deduce the following:

1) Whistlers are more readily trapped in ducts of enhanced (rather than reduced) ionization.

2) Frequencies below the lower hybrid resonance may be trapped only in enhancements.

3) The upper cutoff frequency for trapping in enhancements is approximately one half of the minimum gyrofrequency.

4) If the electron density varies slowly across the duct, the energy below one half the minimum gyrofrequency can be completely trapped.

5) On the other hand, if the duct has sharp sides, so that the gradients of ionization across the duct are quite large, then the duct will usually become "leaky," and some of the energy will escape.

6) The average group velocity of the trapped whistler energy is nearly the same as that for a whistler traveling strictly along the direction of the static magnetic field.

Another approach has been used by several workers who applied to the magnetosphere the mode theory of propagation as developed for tropospheric ducting. One of the results of this approach is a trapping condition which is a function of the curvature and gradient of the duct. Another result gives a discrete set of trapped modes and a minimum size ("track width") of the duct. We note two points on which some care must be taken: 1) the anisotropy of the medium must be taken into account, and 2) one must choose the proper phase of the reflected wave relative to the incident wave.

Still another approach is a full wave treatment using Maxwell's equations directly. However, in order to make the problem tractable, the duct is usually considered to have a discontinuous boundary. Because of this, authors following this approach deduce that only depressions of ionization are suitable for trapping the whistler energy, or that, if one must study trapping in the enhancements, that the ducts are very leaky. We see that both results depend directly on the sharp boundary assumption and hence do not necessarily represent the physical case.

The ray theory of duct propagation has been applied to ground-based whistler observations with considerable success. The most easily tested prediction of the ray theory approach is that the upper cutoff of whistlers observed on the ground should be approximately one-half of the minimum

gyrofrequency along the path. Carpenter has measured the upper cutoff of hundreds of nose whistlers, and his results show a very strong tendency for upper cutoff frequency to equal one-half the minimum gyrofrequency.

One might ask what happens to the whistler energy which is not trapped in ducts of enhanced ionization. The answer to this question has been found in OGO satellite observations of a new type of whistler which is described as "magnetospherically reflected." The wave normal of this non-ducted whistler rapidly approaches 90°, and consequently it cannot propagate through the lower ionosphere to be observed on the ground.

Ducted whistlers are also seen in satellites, mainly at L values greater than about 3. At high altitudes (several thousand km), they exhibit frequency-time spectra which are characterized by discrete changes in shape, corresponding to the motion of the satellite through successive ducts. It is therefore possible to identify the different ducts and to measure their size and spacings.

The best example of these ducted whistlers is found in records from an inbound, nearly equatorial pass of OGO-III on 15 June 1966. The whistlers are classified as short fractional hop (0^{+}). We note the following results:

1) In the region between 4.2 and 4.8 earth radii (inside the plasmapause), the satellite traversed five ducts, their sizes ranging from 200 km to 400 km measured radially. The spacings between ducts range from a few tens of km to 1000 km. Such density of occurrence of ducts is quite comparable to the duct occurrence inferred from ground observations of whistlers, under similar conditions of magnetic activity (very quiet). This has led us to suggest that the ducts are E-W elongated, rather than circular.

2) The measured nose frequencies agree (within a measurement uncertainty of 3%) with the predictions based on purely longitudinal propagation,

hydrostatic distribution of ionization along the magnetic field, and the measured intensity of magnetic field at the satellite (about 6% lower than the Jensen and Cain field). This comparison provides further support for the electron density model and the longitudinal approximation discussed above.

3) Whistlers are observed to have an upper cutoff as high as 0.75 times the gyrofrequency at the satellite even inside a duct. This result, which might be thought to be contradictory to the ray theory of ducting, is actually very consistent with it. The frequencies above half the gyrofrequency become untrapped (as seen below). As the propagation changes from a trapped mode to an untrapped mode, the energy nevertheless is close to the original enhancement for some distance. This is confirmed by ray tracing. Since frequencies above half the gyrofrequency are observed in situ but not on the ground, it is suggested that the upper cutoff frequency of whistlers is not due to Landau damping effects, as proposed by Scarf and Liemohn.

4) The high frequency portions of whistlers (lying roughly between 0.5 and 0.75 of the local gyrofrequency) become unducted as the gyrofrequency decreases along the propagation path. They propagate then from the outer (high L-value) ducts toward the inner region. We can predict the behavior of these unducted components from previous ray tracing experience: the wave normals will tend to rotate away from the magnetic field in an outward direction, and the ray will tend to rotate inward. (Recall that the medium is highly anisotropic.) As a consequence, as the satellite moves inward, not only are signals from a given duct observed but also the high-frequency unducted components escaping from ducts at higher L values.

The original proposals concerning the untrapping of whistler energy were based on a simple application of Poverlein's diagram. A more convincing

demonstration of the transition from the trapped to the untrapped mode can be made by tracing rays in a more realistic magnetosphere including at least a dipole magnetic field and a small field-aligned enhancement of ionization superimposed on a reasonable background ionization model. Such ray tracings have shown at least qualitative agreement with the observations. The frequencies at which untrapped signals from an outer duct are observed in an inner duct may be used to set an upper limit for the density enhancement factors in the intervening ducts. Preliminary results based on such procedure indicate an upper limit of 60%.

*This research was supported in part by the National Aeronautics and Space Administration under grant NsG 174-SC/05-020-008 and contract NAS 5-2131 and in part by the National Science Foundation through the Office of Computer Sciences in the Mathematical Division under grant NSF GP-948.

FIGURE CAPTIONS

Figure 1. Ray tracing of waves initially trapped in a duct of enhanced (10%) ionization. Frequencies above half the minimum gyrofrequency (7.55 kHz) leave the duct (become untrapped or non-ducted). The points where the local gyrofrequency are twice the wave frequencies are indicated by the small circles.

Figure 2. (a) - (d). Ducted whistlers and related untrapped components (leakages) as observed on OGO-III. Figure 2a shows whistlers observed while the satellite is in duct no. 1. Figure 2b shows the whistlers observed in duct no. 2. Figures 2c and 2d show the leakage signals from duct no. 2 observed in the region between ducts no. 2 and 3. Note that as the satellite moves inward the observed low frequency cutoff of the leakage signals increases.

Figure 2. (e) - (h). Figure 2e shows observations in duct no. 3, where the related ducted whistler is seen as well as the leakages from duct no. 2. The leakage signals from ducts no. 2 and 3 are observed in the interval between ducts no. 3 and 4 as seen in Figure 2f. Similarly we observe in Figures 2g and 2h the ducted whistlers in ducts no. 4 and 5, as well as the leakages from the prior ducts.

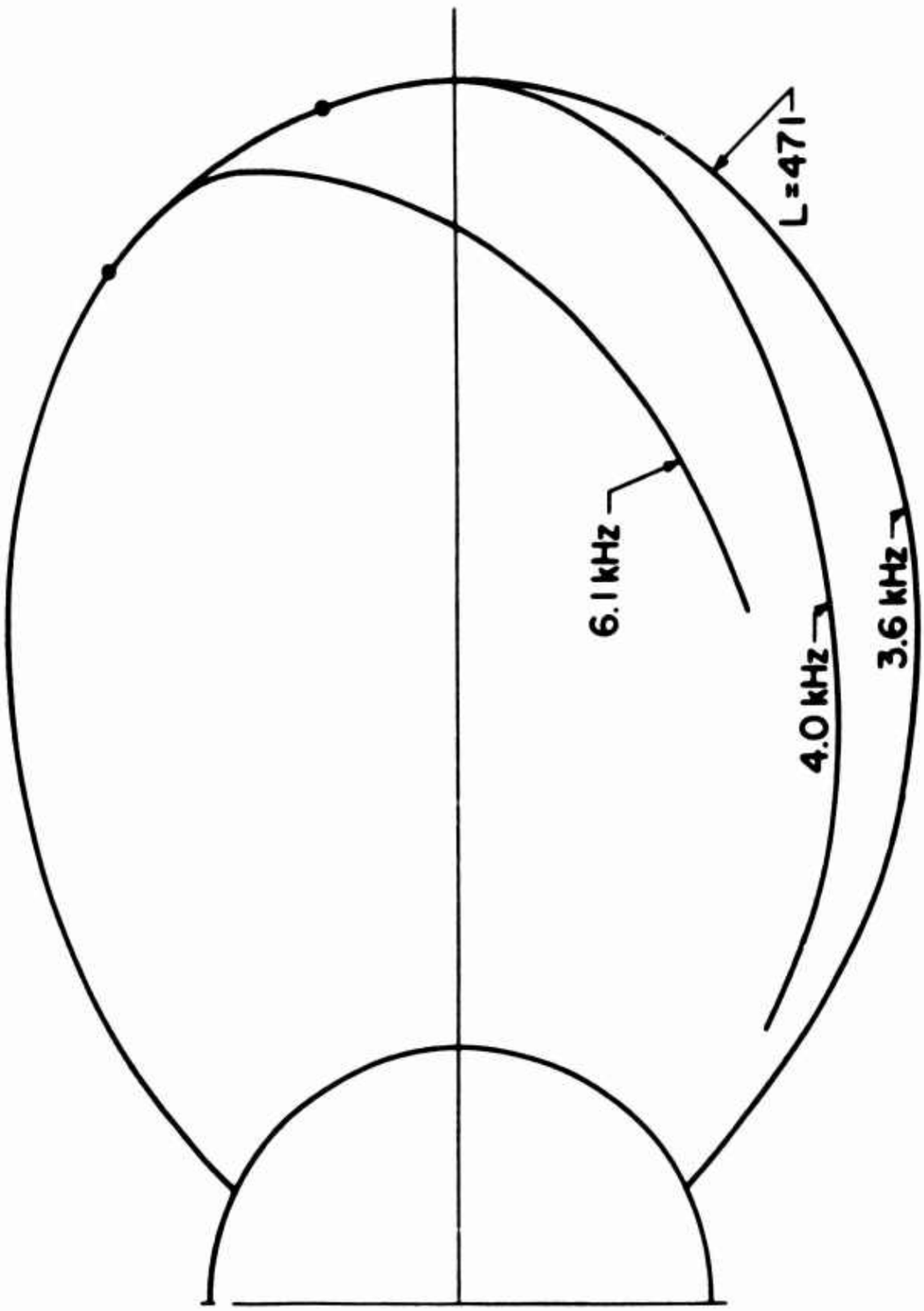

Figure 1

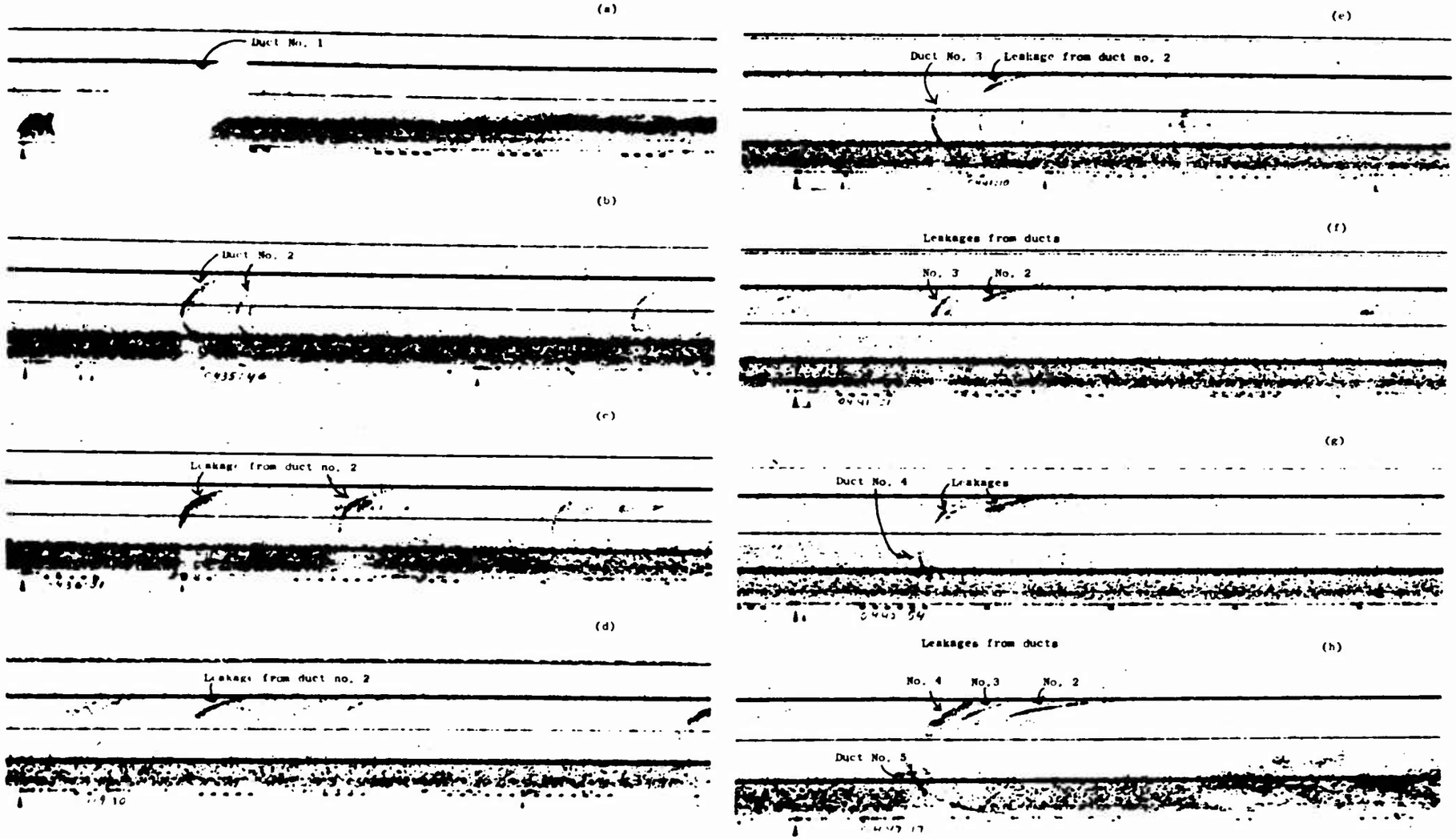
(a)
Duct No. 1
(b)
Duct No. 2
(c)
Leakage from duct no. 2
(d)
Leakage from duct no. 2
(e)
Duct No. 3
Leakage from duct no. 2
(f)
Leakages from ducts
No. 3
No. 2
(g)
Duct No. 4
Leakages
(h)
Leakages from ducts
No. 4
No. 3
No. 2
Duct No. 5

Figure 2

WAVEGUIDANCE IN THE MAGNETOSPHERE ALONG FIELD-ALIGNED IRREGULARITIES

Nicholas Gothard
Texas A&M University, College Station, Texas

ABSTRACT

A study is made of waveguidance along an inhomogeneous field-aligned plasma stratum. A time invariant model of the ionosphere imbedded in the earth's dipole field is postulated. Along the lines of flux of the earth's magnetic field bell shaped plasma strata are aligned. The theory presented here is based on the mode of theory of propagation in an inhomogeneous medium and is modified to account for anisotropy. The two dimensional problem is reduced to a one dimensional integral equation, the mode condition, by using Booker's q parameter.

The results of the solution are given in terms of mode angles and track widths.

The numerical results are calculated for the locked modes only, although the theory is capable of handling the leaky modes as well.

The numerical results indicate the existence of total guidance between the conjugate points for some frequencies, for others only partial guidance exist.

CONJUGATE HF DUCTING

J. A. Thomas
Physics Department (RAAF Academy)
University of Melbourne, Australia

Many attempts have been made to observe conjugate ducting of HF radio waves from the ground. Some long range signals of more or less the correct radar range have been detected by Obayashi (1959), Gallet and Utlaut (1961) and Du Castel (1965), but they were not definitely established as having travelled the field line paths involved. Muldrew (1963) established the nature of certain long delay echoes observed by Alouette I above the ionosphere - they were attributed to multi hop ducted propagation between the conjugate reflection levels for the frequencies involved. Such echoes have since been detected by the fixed frequency topside sounder Explorer XX and by Alouette II. I wish to briefly outline certain aspects of investigation into such propagation, with particular emphasis on Explorer XX observations.

Loftus, VanZandt and Calvert (1966) have made an analysis of HF conjugate ducted echoes occurring during two 3-month periods of 1964 and 1965, and established the latitudinal variation, diurnal variation, NS duct thicknesses and separations and, (following Booker (1962)), minimum relative enhancements of electron density required for trapping the observed signals. Subsequently (in conjunction with I.T.S.A.), work was commenced on follow-up problems related to the E-W thickness and lifetime of the ducts.

It should be pointed out that observations of a related phenomenon have given some estimate of minimum E-W duct widths for what are believed to be the lower ends of ducts which may on occasion extend to the conjugate point. Ducts may be detected not only when the satellite is directly within the duct but more often by means of "combination mode" propagation (Muldrew

(1963), Calvert and Schmid (1963)). Dyson (1967) has shown that field aligned sheet-like irregularities with $\Delta N/N$ of about 2% and thickness perpendicular to the field of 1 km, can trap downward signals from a satellite well above the duct and return a small portion of the signal to the vicinity of the satellite. Assuming meridional propagation, the sequential observation on a number of Alouette ionogram frames of traces due to a duct on the same L shell, gives an estimate of the E-W extent of the duct since the sub-satellite path is usually inclined to the magnetic meridian. Typical maximum widths are 20-30 km, but these should not be regarded as maximum values, both because of steepness of field-lines, and because the possibility of non-meridional entry into a duct should be considered. It seems likely that signals entering an elliptical duct from E or W of the meridian plane should also be trapped under appropriate conditions but detailed ray tracing still has to be carried out for suitable models and estimates made of the power returned to the vicinity of the satellite. This problem also arises when such a duct is at or near the satellite height - i.e., if ducts are elliptical in sections, how far to the E or W of the duct can it be detected by the observation of radio propagation to the near or far end reflection levels?

Two experimental observations have been attempted:

(a) Attempts have been made to identify the same duct at both ends of a line of force when the satellite passes nearly along the magnetic meridian (or at least close to the conjugate points).

and (b) Attempts were made to identify the same duct observed by both Explorer XX and Alouette I at times when they passed through the same area close in time or longitude.

If such identification can be made then valuable information is available concerning the E-W extent, drifting and/or lifetime of conjugate and "near-end" ducts. No positive identification has yet been achieved, partly because of time and space difficulties but mainly because of difficulties associated with the accuracy of both the satellite location and magnetic field models together with the methods of tracing field lines to the conjugate point. Fortunately, we are concerned with L values of not more than 2 and generally rather less than this, so Main Field models might be expected to give a sufficiently accurate picture.

Some indication of the problem can be gained from the set of observations of Table 1 which show the departures of the magnetic field determined by gyrofrequency plasma resonance of observations on Alouette I in the Australian Area from the values computed from the GSFC 12/66 set of coefficients (Cain (1967)). The significant feature is that for south-going passes the departures are negative whereas for north-going passes the departures are positive. It is to be hoped that the satellite locations are not in error by amounts sufficient to account for these differences. In order to establish the duct identity we would like to be able to locate the satellite(s) to within 2 or 3 km and also trace a field line from the satellite to its conjugate point (or at least to the level at which the satellite passes) with the same accuracy. It is probable that this is beyond the presently available techniques. It may be that the problem should be turned around and a detailed comparison of the duct structure used to establish a better knowledge of conjugate point locations in mid and low latitude regions.

Some attempt has been made to investigate the reason for the dawn peak of conjugate duct observations reported by Loftus et al. (1966).

If one examines the CRPL prediction maps of f_xF_2, for 1964 and 1965 the pre-dawn period is seen to be one of extremely low critical frequencies (2.5 to 3.0 Mc/s) and this is followed by a situation lasting an hour or more in which the critical frequencies vary very little with latitude but steadily increase with local time. This suggests that either (a) propagation along ducts at 1.5 - 4 Mc/s is more easily maintained under such ionospheric conditions, or (b) that ducts are more readily formed and maintained then. Preliminary tests with model ionospheres varying realistically with dip latitude and time of day indicate that while some latitude zones tend to have more observable ducts crowded into them than others, and these zones change with time of day, such changes are not sufficient to account for the observed diurnal variation of conjugate ducting. The curves of figure 1 show the numbers of possible conjugate echoes (O & X) detectable in the first four "windows" of Explorer XX records at 2 MHz assuming ducts are uniformly present at all satellite locations. The vast majority of ducted echoes observed are propagated in the X-mode and all the computed ducts for 1400 LMT are in fact O mode (as the electron density at the satellite is then too high to support X mode propagation). This result is then in agreement with the observed midday minimum of conjugate ducted propagation but the midnight propagation conditions are not too dissimilar to those at 0700 LMT and on the basis of propagation changes alone one would not expect a dawn peak of occurrence. The second alternative is in many ways more attractive since a given fractional enhancement of the electron density is achieved around dawn with a smaller absolute value of electron density enhancement, e.g., a 2.5% relative enhancement at a plasma frequency of 2.5 MHz requires an absolute enhancement of 2,000 el/cc, but at 5 MHz requires 8,000 el/cc. Singleton (1962) has commented to some extent on this feature in spread F data.

Finally, it is worth bringing to notice a feature which is occasionally observed on Explorer XX records. At times when the electron density at the satellite is just below that required for the X-mode propagation cut off, the virtual range of the signal (at a fixed frequency) is a very sensitive indicator of the electron density - greater ranges corresponding to smaller electron densities close to the satellite. Occasionally, when such a condition holds for the 1.5 Mc/s frequency of the sounder, near-end ducts and conjugate ducts are observed on the other frequencies, and these occur most strongly at times of relative minimum electron density at the satellite.

References

Booker, H. A. : - J.G.R. 67, 4135 (1962).

Calvert, W. and Schmid, C. W.: - J.G.R. 69, 1839 (1964).

Dyson, P. L.: - J.A.T.P. (in press) (1967).

Du Castel, F.: - C. R. Acad. Sci. Paris 261, 1057 (1965).

Gallet, R. M., and Utlaut, W. F.: - Phys. Rev. Letters 6, 591 (1961).

Loftus, B. T., VanZandt, T. E. and Calvert, W.: - Ann. de Geophys. 22, 530, (1966).

Muldrew, D. B.: - J.G.R. 68, 5355 (1963).

Obayashi, T.: - Rep. Iono. Res. Japan 13, 177 (1959).

Singleton, D. A.: - Aust. J. Phys. 15, 242 (1962).

TABLE I - Alouette I Gyrofrequency Measurements

Comparison of GSFC 12/66 Field Model with Field Values Deduced from Gyrofrequency Harmonics - Australian Region 1962-3

nf_H	No. of Observations	N or S going	Model - Exptl B
2	70	S	-111 ± 192 γ
3	617	419S, 198N	- 70 ± 174 γ
4	349	271S, 78N	- 31 ± 169 γ
5	52	26S, 26N	+ 33 ± 138 γ
6	25	5S, 10N	+ 60 ± 163 γ
7	15	N	+231 ± 20 γ
All	1118	791S, 329N	- 50 ± 176 γ
All	791	791S	- 99 ± 158 γ
All	327	327N	+ 68 ± 163 γ

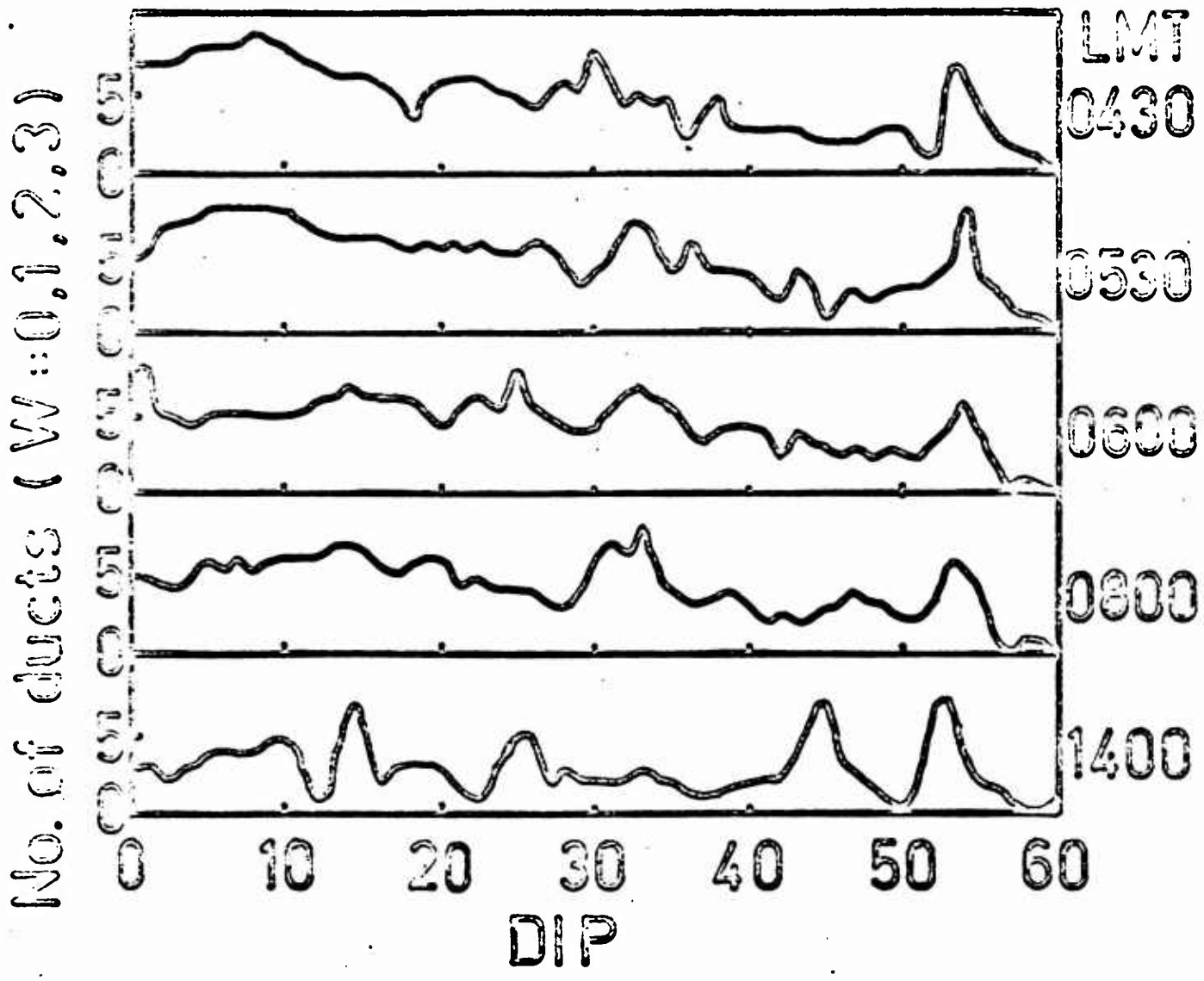

Fig. 1. Predicted conjugate echoes observable in Explorer XX "Windows" 0, 1, 2, and 3 for both O- and X-mode propagation at 2 MHz. (Satellite ht. 1000 km) Ducts are assumed to be available at all satellite locations.

MEDIUM-FREQUENCY CONJUGATE ECHOES OBSERVED ON TOPSIDE-SOUNDER DATA

D.B. Muldrew

Radio Physics Laboratory
Defence Research Telecommunications Establishment
Ottawa, Canada

Introduction

Medium-frequency conjugate echoes (or ducted echoes) were first observed on the Alouette I sweep-frequency topside-sounder ionograms. An example of an Alouette I ionogram containing conjugate-echo traces and a sketch illustrating the propagation paths corresponding to the different traces are given in Figure 1. Combinations of the paths along the magnetic field to the north and to the south of the satellite for the extraordinary and ordinary waves are labelled using the symbols N_X, N_O, S_X, S_O. Conjugate echoes were also observed on the Explorer XX fixed-frequency topside-sounder ionograms; an example, from the paper by Loftus, VanZandt and Calvert (1966), showing two distinct ducted echoes at 1009:13 and 1009:14 U.T. at apparent ranges of 300 and 1200 km is shown in Figure 2. The time interval over which each of these echoes was received indicates that the radio energy is ducted in a region which has a thickness, in a direction normal to the magnetic field, of about one kilometer.

An example of an Alouette II ionogram containing conjugate echoes is given in Figure 3. The Alouette II sounder is better suited to the study of conjugate echoes than that of Alouette I because of the lower low-frequency limit of the sounder. The results of a statistical study of about 60,000 Alouette II equatorial ionograms, of which about 3,000 (5%) contain conjugate echoes, will be presented in this paper.

All the available ionograms from eight equatorial stations were classified into five groups depending on the value of fxS, that is, the frequency of the extraordinary wave which has zero refractive index at the satellite height. The five classes are: $0.2 < fxS < 0.9$ MHz, $0.9 < fxS < 1.25$ MHz, $1.25 < fxS < 1.6$ MHz, $1.6 < fxS < 2.0$ MHz and $fxS > 2.0$ MHz. There were no conjugate echoes observed in the last class and consequently it was excluded in the statistical study. The fxS was chosen for the classifications because it gives a rough indication of the electron density at the satellite height and is readily obtained from the ionograms. Conjugate echoes tend to occur at frequencies slightly above fxS so this parameter also gives an indication, on the average, of the frequency of the conjugate echoes. For each class the recording time was noted for those ionograms containing conjugate echoes as well as for those ionograms not containing conjugate echoes. The percentage occurrence of conjugate echoes on ionograms was then calculated as a function of Kp index, L value, local time and calendar date.

There are two important factors which must be considered in an interpretation of the results:

1. The orbital plane of the satellite precesses 1.78 degrees per day with respect to the sun so that for north-to-south (or south-to-north) passes of the satellite the local time at a given latitude changes slowly with the date (day of year). Thus, a plot of percentage occurrence of conjugate echoes as a function of local time can also be interpreted as a plot of occurrence as a function of date.

2. The argument of perigee rotates 1.89 degrees per day which is almost the same as the precession of the orbital plane with respect to the sun. Hence, the local time at perigee (or apogee) changes less than 3 hours per year. About one year of data is presented here and for these data perigee occurs near noon and apogee near midnight. Thus the satellite intersects the lowest L shells near noon.

Conjugate Echoes as a Function of Kp Index

The percentage occurrence of conjugate echoes on ionograms as a function of Kp index for all the data with $0.2 < fxS < 2.0$ MHz is presented in Figure 4. The error bars are a measure of confidence for the points; they give the standard error of the mean assuming, although it is not strictly true, that all the data are independent and random. It can be seen that the occurrence is independent or decreases very slightly as the Kp index increases from 0 to 6. Muldrew (1963)

and Loftus et al (1966) also concluded that the occurrence of conjugate echoes was not correlated with Kp index.

At geomagnetic latitudes less than 30° Calvert and Schmid (1964), using Alouette I data, found a weak negative correlation between Kp and topside spread F (below the satellite height) attributed to aspect-sensitive scatter. This agrees with the low latitude results of Shimazaki (1959). Shimazaki found that the correlation between occurrence of spread F and geomagnetic activity is strongly negative for geomagnetic latitudes less than 20° and strongly positive for latitudes between 20° and 60°. In the present study 94% of the conjugate echoes occur at L values greater than 1.25 and the geomagnetic latitude corresponding to L = 1.25 at 300 km height is about 21°. Thus, assuming L value to be a more appropriate parameter than geomagnetic latitude, the relationship between the occurrence of conjugate echoes and Kp does not agree with the positive correlation between spread F and Kp found by Shimazaki from ground-based stations at latitudes greater than 20°. However, the characteristics of spread F are dependent on the epoch of the solar cycle (Shimazaki, 1959) and Shimazaki's correlation results were for high sunspot activity (IGY) whereas the data presented here is for lower sunspot activity (1966).

Conjugate Echoes as a Function of L Value

The percentage occurrence of conjugate echoes between 21 hours and 04 hours local time is plotted as a function of L in Figure 5. This period of local time was chosen because the percentage occurrence of conjugate echoes remains fairly constant

throughout the period (see Figure 6) and, as mentioned in the introduction, the satellite height remains near apogee.

To date, the highest L value for a conjugate echo observed with Alouette II is 3.8. This is not a real cut-off however since the sweep-frequency receiver is no longer tuned to the frequency of the echoes that arrive after the long delay for propagation along a duct with an L value of about 4 or greater.

The occurrence of conjugate echoes increases with decreasing L down to about L = 1.4. There is an apparent rapid drop in occurrence for L less than about 1.35. It is not certain at present whether this drop is real since, due to the characteristics of the satellite orbit, the data at these lower L values may not be representative. If it is real the distribution is not unlike the distribution of energetic electrons (energy $>$ 1 meV) with L value (Katz, 1966).

In Figure 5 plots for $0.2 < fxS < 0.9$ MHz and for $0.9 < fxS < 1.25$ MHz are given; plots for other classifications are not given because of insufficient data. For L less than 2.5 the occurrence of conjugate echoes for $0.9 < fxS < 1.25$ MHz is about twice the occurrence for $0.2 < fxS < 0.9$ MHz. This could be due to the lower efficiency of the antennas at lower frequencies; however, because of the high echo signal strength of conjugate echoes this seems unlikely. For ducting, the transverse thickness of field aligned ionization irregularities would likely need to be in the order of a wavelength or more. Thus, the two distributions in Figure 5 could be explained if

for L values between about 1.3 and 2.5, thin field-aligned ionization irregularities of thickness less than about 300 meters were more numerous than those of thickness greater than about 300 meters.

Conjugate Echoes as a Function of Local Time (Two-Hour Averages)

The percentage occurrence of conjugate echoes for $0.2 < fxS < 1.6$ MHz (solid line) and for $1.6 < fxS < 2.0$ MHz (dashed line) as a function of local time is given in Figure 6. The data in the three classifications between $0.2 < fxS < 1.6$ MHz were similar and for simplicity were included together. The data were averaged in two hour intervals of local time. It can be seen that the occurrence of conjugate echoes is less than about 1% from about 10 to 16 hours local time, starts to increase before sunset and reaches a maximum of about 11% just before sunrise. In this plot the noon values are for heights near perigee (500 km) and the midnight values are for heights near apogee (3000 km). The Alouette I analysis (Muldrew, 1963) indicated maxima at both midnight and noon; the disagreement at noon might be due to the lower height of Alouette II for noon data (500 kilometers vs 1000 kilometers).

The occurrence distribution of conjugate echoes for the case $1.6 < fxS < 2.0$ MHz is quite different than that for $0.2 < fxS < 1.6$ MHz. Although there are not many data during the night with $1.6 < fxS < 2.0$ MHz, it appears that the occurrence of conjugate echoes begins to increase sometime after 21 hours local time, reaches a peak somewhere near 07 hours and drops off to near zero at 13 hours. This type of distribution is

similar to that obtained by Loftus et al (1966) from the fixed-frequency topside-sounder data. They obtained conjugate echoes on 1.50, 2.00, 2.85 and 3.72 MHz. There thus appear to be two quite different distributions for the occurrence of conjugate echoes as a function of local time; one for frequencies below, and one for frequencies above, about 1.5 MHz.

Conjugate Echoes as a Function of Local Time or Date (Half-Hour Averages)

The percentage of conjugate echoes for $0.2 < fxS < 1.6$ MHz as a function of local time is given in Figure 7 (north-to-south passes of the satellite) and Figure 8 (south-to-north passes). The class for $1.6 < fxS < 2.0$ MHz was excluded because there are too few conjugate echoes in this class to make a significant contribution to the graphs. The data for Figures 7 and 8 were averaged in half-hour intervals of local time. It was mentioned in the introduction that a plot of this type can also be interpreted as a plot of occurrence as a function of date; the day of the year is thus given along the top of the figures, increasing from right to left.

In Figures 7 and 8 it is seen that the occurrence of conjugate echoes with date or local time does not vary smoothly but tends to have a considerable fluctuation. An attempt was made, using all of the data of Figures 7 and 8, to determine a regular period for the fluctuations. The best fit gives a period of 1.75 hours in local time or 14.8 days in date. This periodicity is illustrated in Figures 7 and 8 by the arrows.

It can be seen that, in general, the peaks in the occurrence distribution lie near the arrows. There are some exceptions however, notably the large maximum in Figure 7 at 2130 hours local time where a minimum might have been expected.

If it is assumed that the percentage occurrence of conjugate echoes oscillates in local time, then this can be interpreted as shown in Figure 9. The shaded regions are fixed relative to the sun as the earth rotates beneath them and are separated by 1.75 hours of local time. The shaded areas represent regions in the earth's magnetosphere which are most favourable for the formation of conjugate ducts.

A different interpretation results if it is assumed that the periodicity of the percentage occurrence of conjugate echoes is one in date. Twice the period of 14.8 days is very nearly the synodic period of the moon (29.53 days). For the data presented in Figures 7 and 8 it appears that conjugate ducting is most likely to occur when the position of the moon, relative to the sun and earth, is in either of the two positions shown in Figure 10. This is not a simple tidal effect since the location of Alouette II is not of primary importance in determining when the occurrence of conjugate echoes is a maximum.

Further studies, using both Alouette I and Alouette II data should determine whether or not the occurrence of conjugate echoes oscillates with a regular period and whether the oscillation is with respect to local time or with respect to date.

Summary

The percentage occurrence of conjugate echoes on Alouette II data from November 1965 to about October 1966:

1. is either independent of Kp or decreases slightly with increasing Kp for Kp between 0 and 6,

2. increases for night-time data, from about 1% at L = 3 to 18% (0.2 < fxS < 0.9 MHz) or 32% (0.9 < fxS < 1.25 MHz) near L = 1.35 and then may decrease rapidly for L less than this,

3. increases from a minimum of less than 1% near noon (possibly affected by low satellite heights) to a maximum of about 11% before sunrise for 0.2 < fxS < 1.6 MHz and for 1.6 < fxS < 2.0 MHz increases from very low values between 13 and 21 hours local time to a maximum near 07 hours,

4. appears to have an oscillation in either local time or calendar date with periods of either 1.75 hours or 14.8 days.

References

Calvert, Wynne; Schmid, C.W., Spread-F observations by the Alouette topside sounder satellite, J. Geophys. Res., 69, 1839-1852, 1964.

Katz, Ludwig, Electron and proton observations, Radiation Trapped in the Earth's Magnetic Field, D. Reidel Publishing Company, Dordrecht, Holland, 1966.

Loftus, B.T., T.E. VanZandt and W. Calvert, Observations of conjugate ducting by the fixed-frequency topside-sounder satellite, Ann. de Geophys., 22, 530, 1966.

Muldrew, D.B., Radio propagation along magnetic field-aligned sheets of ionization observed by the Alouette topside sounder, J. Geophys. Res., 68, 5355-5370, 1963.

Shimazaki, T., A statistical study of world-wide occurrence probability of spread F, J. Radio Res. Labs., Japan, 6, 688-704, 1959.

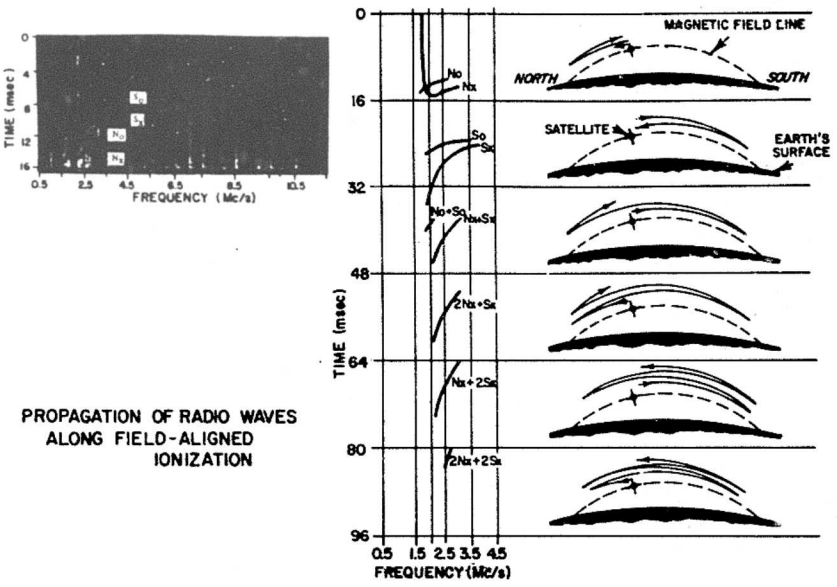

Figure 1 After Muldrew (1963). An Alouette I ionogram recorded at 1725 U.T. on Dec. 18, 1962. The propagation paths of the various conjugate echoes are illustrated.

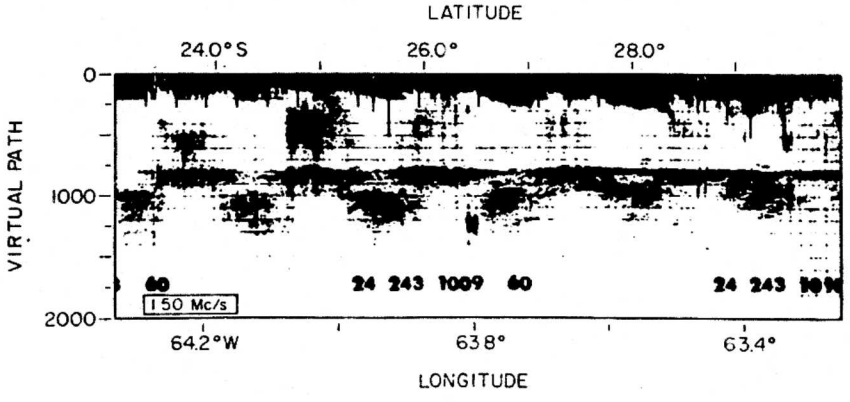

Figure 2 After Loftus, VanZandt and Calvert (1966). An Explorer XX ionogram, for a frequency of 1.50 MHz, recorded on Aug. 30, 1964. Conjugate echoes can be observed at 1009:13 and 1009:14 U.T.

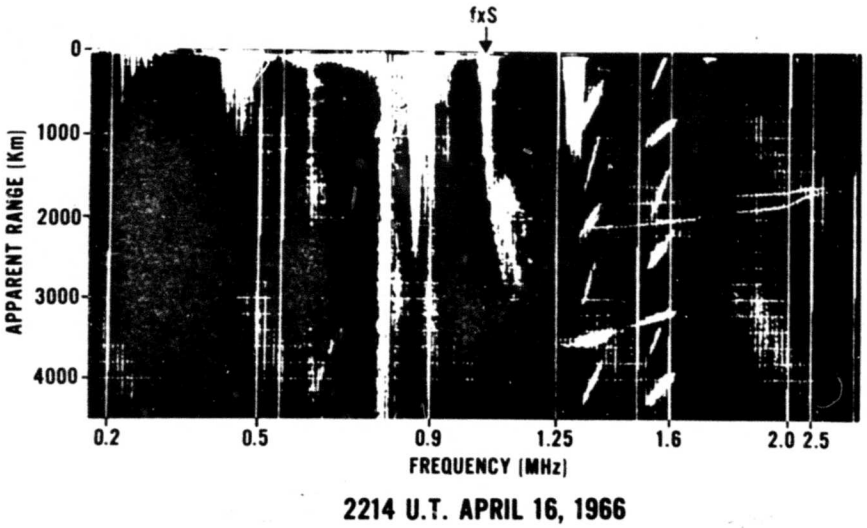

Figure 3 An Alouette II ionogram, showing two sets of conjugate echoes, recorded at 2214 U.T., April 16, 1966.

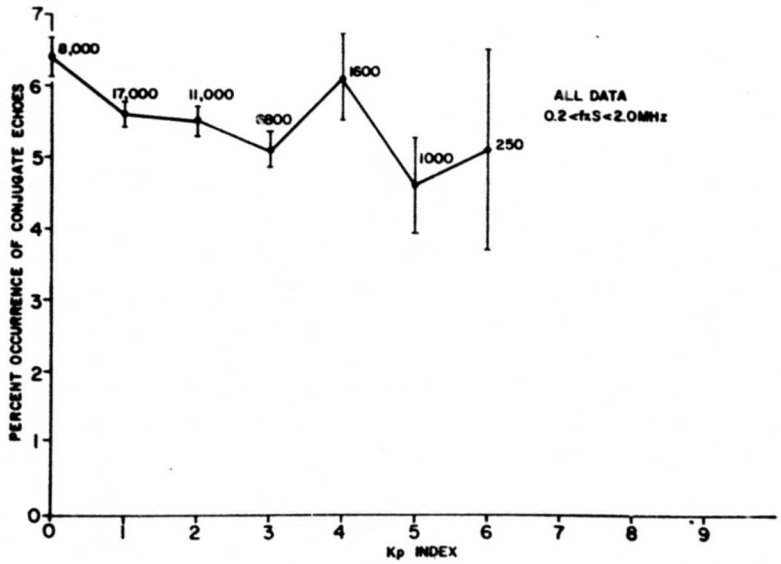

Figure 4 Distribution of conjugate echoes with Kp index. The total number of ionograms used in calculating each point is given. The standard error of the mean is given by the bars.

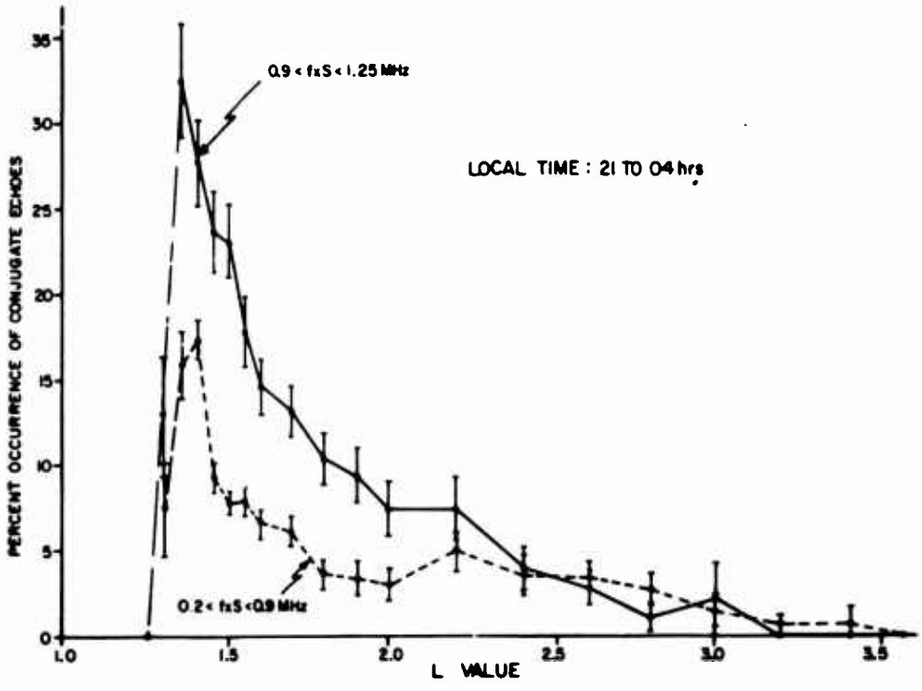

Figure 5 Distribution of conjugate echoes with L value for 21 to 04 hours local time (see Figure 6).

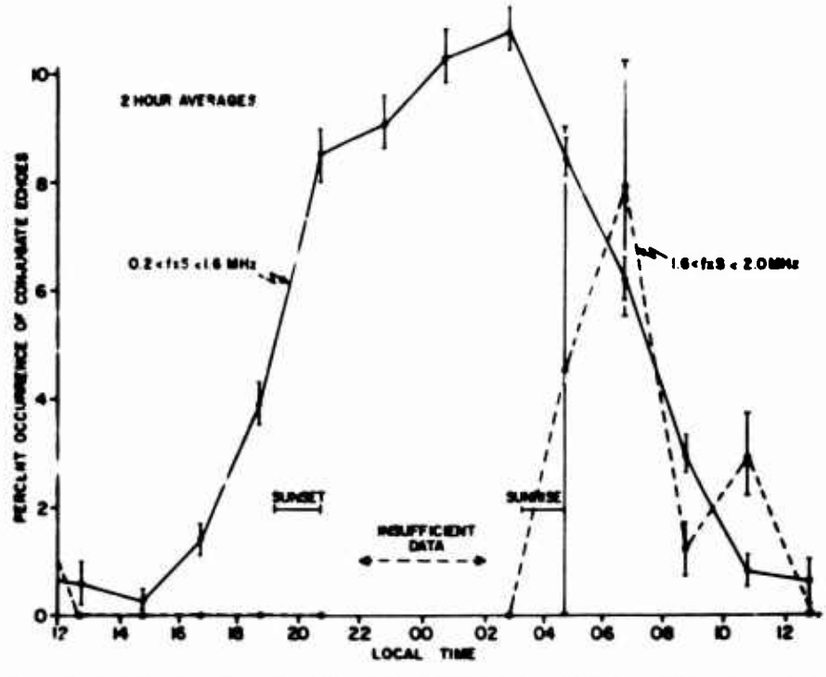

Figure 6 Distributions of conjugate echoes with local time when averaging is done over relatively long intervals of local time (two hours). All data are grouped into a single 24 hour local-time period.

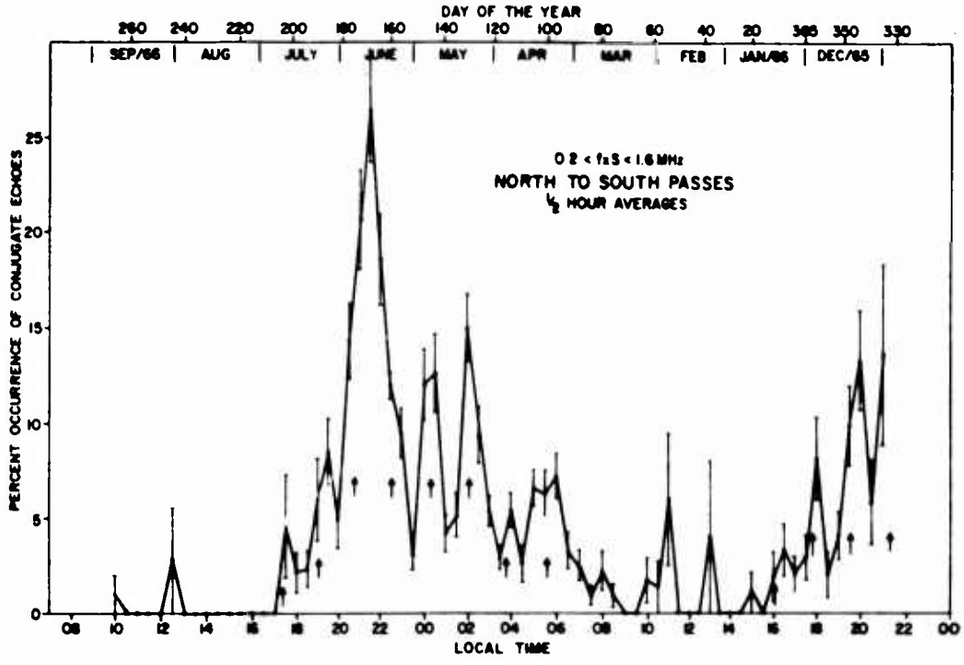

Figure 7 Distribution of conjugate echoes with local time or day of the year for north-to-south satellite passes. The averaging is done over relatively short intervals of local time (half hour).

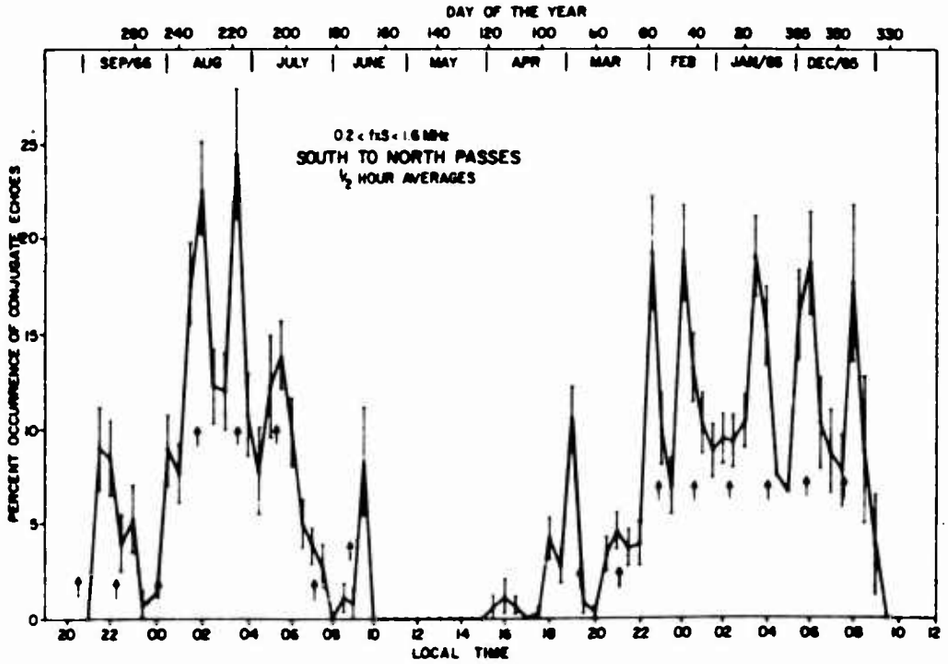

Figure 8 Distribution of conjugate echoes with local time or day of the year for south-to-north satellite passes.

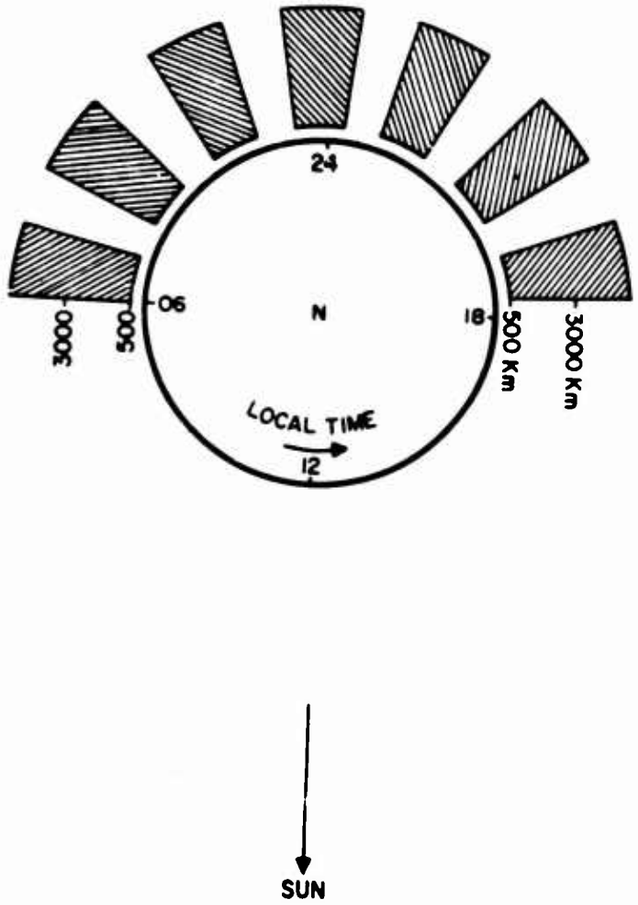

Figure 9 Sketch of the regions in which conjugate ducts are most likely to occur assuming the occurrence of conjugate echoes oscillates with local time.

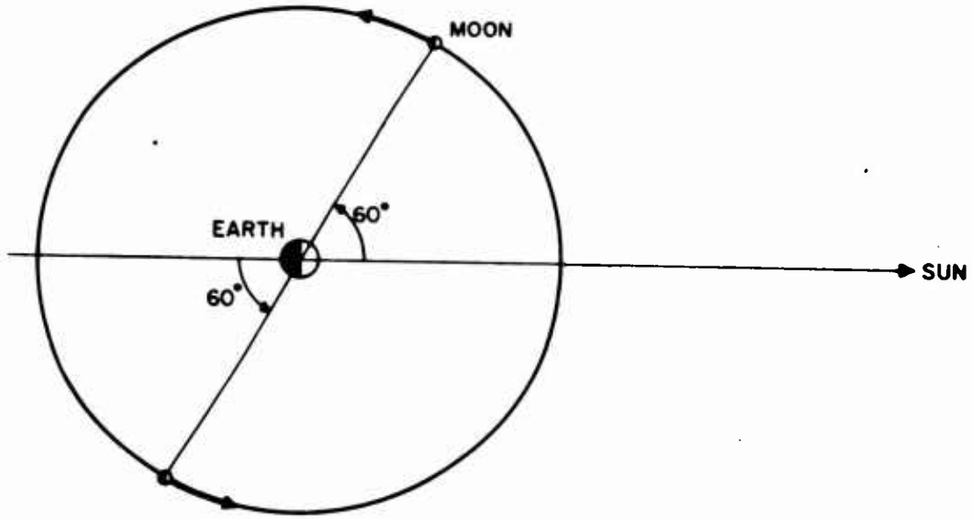

Figure 10 Sketch of the two locations of the moon relative to the earth and sun for which conjugate ducts are most likely to occur assuming the occurrence of conjugate echoes oscillates with date.

PROPAGATION CHARACTERISTICS OF THE EQUATORIAL IONOSPHERE AS MEASURED BETWEEN MAGNETICALLY CONJUGATE POINTS AT VHF

by E. D. Bowen
Smyth Research Associates
3555 Aero Court
San Diego, California 92123

A transequatorial propagation experiment was conducted in the Far East in which an anomalous propagation mode appeared. This anomalous mode has been interpreted as a field guided mode as suggested by the experimental evidence.

The program for studying the propagation characteristics of the equatorial ionosphere was conducted from December 1965 to June 1966. In the experiment, transmissions at 34, 45, 54 and 77 MHz from Okinawa were monitored at receiving sites at Darwin, Australia and at Fiji. The Okinawa-Darwin terminals are very nearly magnetically conjugate and separated by 4300 km. They occupy positions on the same L shell ($L \approx 1.10$), but are separated by about two degrees in latitude. The Okinawa-Fiji path of 7200 km is skewed to about 40° with the magnetic equator. Horizontally polarized yagi antennas were placed three wavelengths above a smooth foreground at each experimental site and at each frequency. Phase locked receivers with narrow tracking loops received the emmissions from the stable frequency, 300 Watt, CW transmitters. These transmissions were on occasion pulsed at a 25 cps rate and with a 100 microsecond pulse width for travel time measurements.

Figure 1 shows the signal levels of received frequencies at Darwin (upper half of figure) and at Fiji (lower half) for a characteristic day near the equinox. Thirty-four MHz and occasionally 45 MHz occur throughout much of the day at both Fiji and Darwin, but a propagation mode with markedly different characteristics occurs at Darwin in the late evening hours (2200). The incidence of this mode is displayed by a significant increase in frequency support, with the lowest frequency appearing first and the higher frequencies progressively.

The diurnal occurance of the guided mode is limited to the nighttime hours with a maximum at 2300 local path midpoint line. The seasonal variation

maximizes at the equinox, but the biannual peaks in activity are broadened to include the magnetic equinox which follows the vernal equinox by fourteen days. This skewing of the seasonal dependence carries over to the solsticial periods as a higher activity at northern summer than at northern winter.

Nearly free space signal levels (≈ -70 dBm) are produced by the guided mode on occasion. Generally a frequency independence for path loss is shown that persists up to some cut off frequency. This cut off frequency varies with each occurance of the mode, and severe path loss is noted beyond. An average of all the guided mode occurances yields a $\lambda^{4.5}$ dependence for the path loss.

Figure 2 shows three fading distributions of the received signal at Darwin. The lower histogram is the fading distribution obtained from a sample of the normally propagated F layer modes. The fading frequency is 0.25 Hz. By contrast the fading distributions shown in the upper two histograms from the guided modes have more than an order of magnitude higher fading frequency. The fading frequency was found to be transmission frequency independent and near five Hertz.

Experimental evidence for the field guided mode was obtained from elevation angle and relative travel time measurements. The experimental travel time difference measurements agree with differences between the calculated travel time for the numerous modes occuring over the trans-equatorial path and the calculated travel time for the field guided mode. Figure 3 shows a field guided path and two trapazoidal paths and several dipole magnetic field lines along the experimental magnetic meridian. The trapazoidal mode occured regularly over the transequatorial path but did not display the high fading frequencies of the field guided mode.

The occurance of this mode at 2300 local time coincides with equatorial topsite spread F which displays magnetic field aligned irregularity structure and occurs at a time when $h_m F_2$ (dotted line in the figure) is decreasing to below the height of the field guided path.

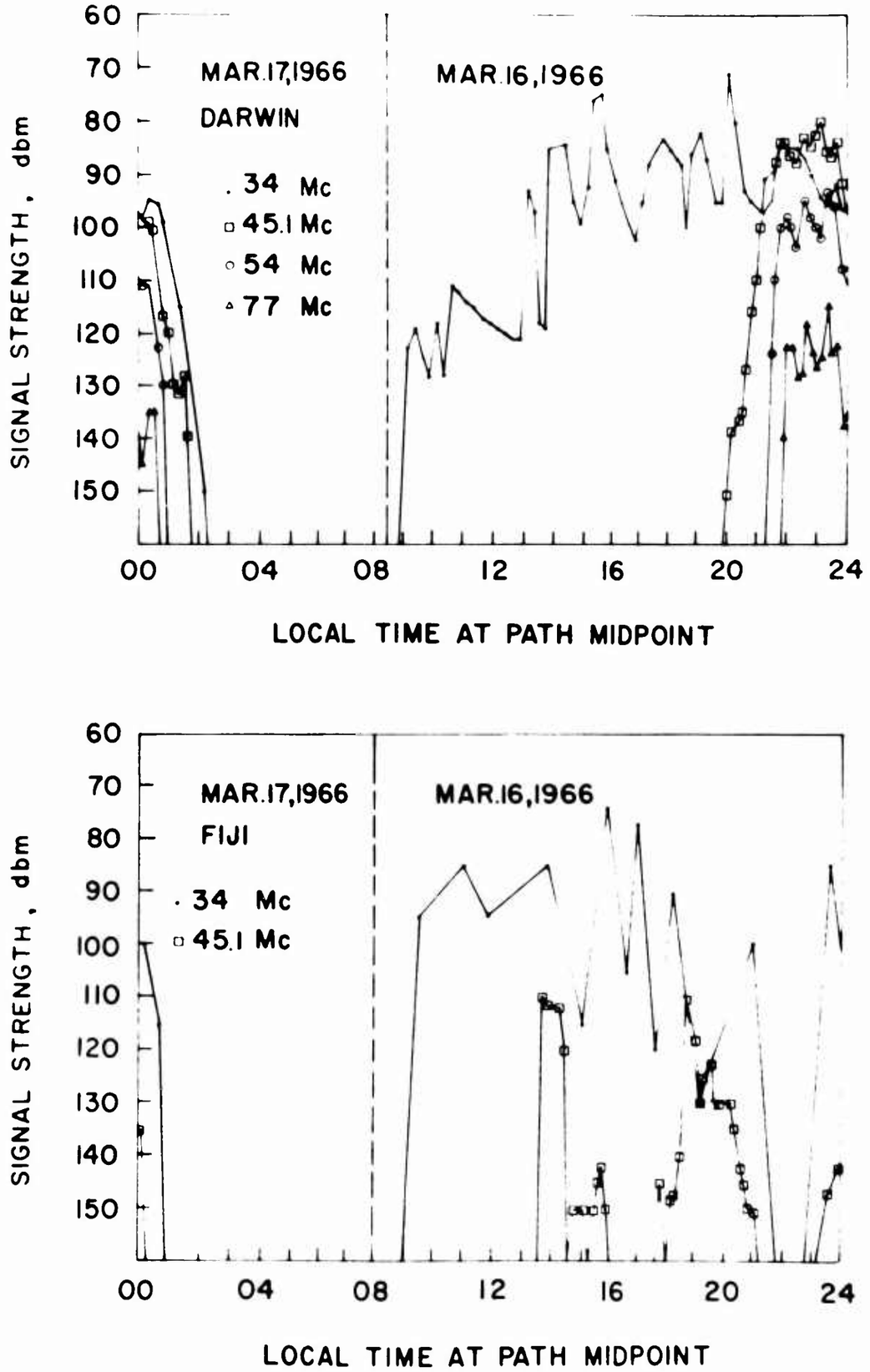

Figure 1. Diurnal variation of signal level at Darwin and Fiji for the period 0800 March 16 to 0800 March 17.

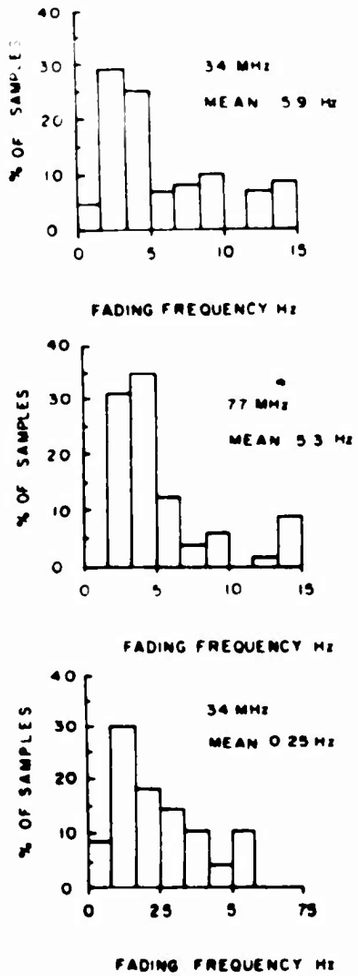

Figure 2. Characteristic fading frequency histograms.

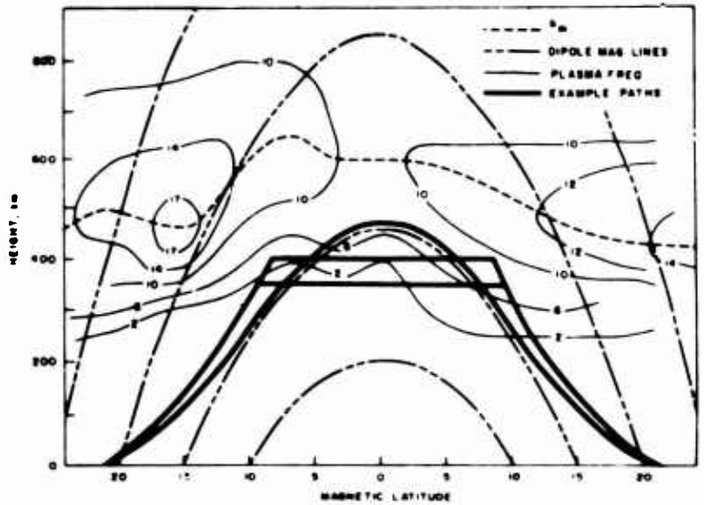

Figure 3. View of magnetic meridian showing the field guided path.